Enterohaemorrhagic *Escherichia coli* outer membrane vesicles: The influence of the colonic milieu and their interaction with host cells

Daniel Alejandro Yara, B.Sc. (Hons), M.Sc.

A thesis submitted in fulfilment of the requirements of the University of East Anglia for the degree of Doctor of Philosophy (PhD)

Norwich Medical School

University of East Anglia

September 2020

Abstract

Enterohaemorrhagic *Escherichia coli* (EHEC) is a major foodborne pathogen which can cause bloody diarrhoea and potentially fatal haemolytic uremic syndrome (HUS). HUS is associated with the release of Shiga toxin (Stx) by EHEC, leading to the damage of globotriaosylceramide (Gb3) expressing cells located in the vascular system, kidneys and the central nervous system. In addition to release following bacterial cell lysis, Stxs can be secreted via outer membrane vesicles (OMVs). While OMVs are constitutively produced by Gram-negative bacteria, specific growth conditions can influence vesiculation.

To successfully colonise, EHEC must survive the various hostile conditions present in the gastrointestinal tract. The production of OMVs can facilitate bacterial survival as OMVs are known to constitute a defence mechanism against harsh environmental conditions. Thus, in this investigation, the effect of various colonic environmental factors on EHEC OMV vesiculation was examined by quantifying OMV yield through different techniques. This study concluded that while simulated colonic environmental medium, which mimics various abiotic factors of the colonic milieu, and the presence of bile salts increased OMV vesiculation, no significant differences in OMV yields were detected when EHEC was grown in physiologically relevant levels of carbon dioxide and in the presence of host colonic T84 cells.

In addition to their defensive role, OMVs can also contribute to pathogenesis by transferring virulence proteins into host cells. Since EHEC is not an invasive pathogen and the colonic epithelium does not express Gb3, OMVs may provide a mechanism which allows trafficking of Stx and other virulence factors across the colonic epithelium. Therefore, the ability of the colonic epithelium to internalise and translocate EHEC OMVs was investigated. This study determined that while OMVs are internalised and subsequently trafficked to late endosomal/lysosomal compartments in non-polarised Gb3-positive colonic-derived Caco-2 cells, OMVs are transported to the basolateral membrane and subsequently released by polarised

Caco-2 cells. Nevertheless, using the more physiologically relevant Gb3-negative colonic-derived T84 cell line, little OMV internalisation was exhibited. To evaluate this discrepancy in a more biologically relevant context, EHEC OMV trafficking was evaluated in human colonic organoids which demonstrated OMV translocation across the polarised cell monolayer. The trafficking of EHEC OMVs was also elucidated to be similar in renal Vero cells as that in non-polarised Caco-2 cells. Furthermore, it was elucidated that upon OMV internalisation, encapsulated Stx2 dissociates from OMVs and follows retrograde trafficking to the Golgi apparatus and the endoplasmic reticulum, eventually leading to cell death.

In summary, this PhD study has shown that different conditions of the colonic milieu can affect EHEC OMV vesiculation in different ways. Moreover, the colonic epithelium can internalise and translocate EHEC OMVs, with cytotoxic effects in target cells. This study underlines the potential role OMVs have in the development of HUS.

Table of Contents

List of figures

List of tables

List of abbreviations

A/E - Attaching and effacing

AMP - Antimicrobial peptide

AIEC - Adherent invasive *E. coli*

AI-3 - Autoinducer 3

APS - Ammonium persulfate

AR - Acid resistance

ArcA - Aerobic respiration control protein

ARP 2/3 - Actin related protein 2/3

BSA - Bovine serum albumin

cAMP - Cyclic adenosine monophosphate

CDC - Centres for Disease Control and Prevention

Cdt - Cytolethal distending toxin

cfu - Colony forming units

Cif - Cystic fibrosis transmembrane conductance regulatory inhibitory factor

CL - Containment level

CMGF - Complete media with growth factors

DAEC - Diffusely-adherent *E. coli*

DAPI - 4', 6-diamino-2-phenylindole

DAEC - Diffusely-adherent *E. coli*

d.H_20 - Distilled water

DLS - Dynamic light scattering

DMSO - Dimethyl sulphoxide

DMEM - Dulbecco's modified Eagle's medium

DMEM/F-12 - Dulbecco's modified Eagle's medium/Nutrient Mixture F-12

DGC - Density Gradient centrifugation

EAEC - Enteroaggregative *E. coli*

EDCD - European Centre for Disease Prevention and Control

EDTA - Ethylenediaminetetraacetic acid

EEA - European Economic Area

EHEC - Enterohaemorrhagic *E. coli*

EIEC - Enteroinvasive *E. coli*

EPEC - Enteropathogenic *E. coli*

ER - Endoplasmic reticulum

Esp - *E. coli* secreted protein

ETEC - Enterotoxigenic *E. coli*

FA - Formaldehyde

FBS - Foetal bovine serum

FITC - Fluorescein isothiocyanate

Fnr - Furmarate and nitrate reduction regulator

Fus - Fucose sensing

Gb3 - Globotriaosylceramide

GM1 - Monosialotetrahexosylganglioside

Grl - Global regulator of Locus of enterocyte effacement encoded regulator

Grv - Global regulator of Virulence

hBD - Human beta-defensins

HBMEC - Human brain microvasculature endothelial cells

HC - haemorrhagic colitis

HCl - Hydrochloric acid

HlyA - Haemolysin A

Hp90 - Host epithelial protein 90

HRMEC - Human renal microvasculature endothelial cells

HUS - Haemolytic uraemic syndrome

IRSp53 - Insulin receptor tyrosine kinase substrate p53

IL - Interleukin

IVOC - *In vitro* organ culture

kb - Kilobase

LB - Luria Bertani

LEE - Locus of enterocyte effacement

Ler - Locus of enterocyte effacement encoded regulator

Lpf - Long polar fimbraiae

LPS - Lipopolysaccharide

LT - Heat-labile enterotoxin

MUC-2 - Mucin-2

MWCO - Molecular weight cut-off

N/A - Not applicable

Nle - Non-Locus of enterocyte effacement-encoded effector

NTA - Nanoparticle Tracking Analysis

N-WASP - Neuronal Wiskott-Aldrich syndrome protein

OD - Optical density

OM - Outer membrane

Omp - Outer membrane protein

OMV - Outer membrane vesicle

PI - Pathogenicity island

PBS - Phosphate buffered saline

PHE - Public Health England

PQS - Pseudomonas quinolone signal

Qse - Quorum-sensing *E. coli* regulator

rpm - Revolutions per minute

RSB - Reducing sample buffer

SCFA - Short-chain fatty acids

SCEM - Simulated colonic environment medium

SD - Standard deviation (of the mean)

SDS-PAGE - Sodium Dodecyl Sulphate Polyacrylamide Gel Electrophoresis

STEC - Shiga toxin-producing *E. coli*

Stx - Shiga toxin

TBST - Tris buffered saline with 0.05% (v/v) Tween-20

TCA - Trichloroacetic acid

TEER - Transepithelial electrical resistance

TEM - Transmission electron microscopy

TEMED - Tetramethylethylenediamine

Tir - Translocated intimin receptor

TJ - Tight junction

TNF - Tumour necrosis factor

tRNA - Transfer ribonucleic acid

TSB - Tryptic soy broth

TTSS - Type three secretion system

UK - United Kingdom

UPEC - Uropathogenic *E. coli*

USA - United States of America

VacA - Vaculating cytotoxin A

wt - wild type

Acknowledgements

I would like to thank my primary supervisor Stephanie Schüller, who has provided much guidance throughout my PhD. Thank you for your training and your patience. I would also like to thank Tom Wileman for being my secondary supervisor. I am also very thankful to Regis Stentz for his support, training and motivation. Your OMV enthusiasm has really kept me going. Thank you in advance to my *viva voce* examiners Mark Jepson and Arjan Narbad for taking the time to read this thesis. I also want to thank the BBSRC for funding this project.

Many thanks to past members of the Schüller group and a special thank you to Conor McGrath for his invaluable encouragement and friendship. Thank you for all the great conversations on scientific and non-scientific matters. I will miss our great conversations in the microscopy room (aka confessional). Also, thanks for the 'crisis room', very much appreciated.

Thank you to the Gastrointestinal bacteria reference unit (GBRU) at Public Health England for hosting me during my PIPS placement, especially Claire Jenkins, Tim Dallman and David Grieg. I thoroughly enjoyed my time there and learnt a great deal.

A special thanks to Stephanie Bates, Joseph Donleavy and Dale Taylor for your immense encouragement, support and help. Really, I cannot thank you three enough! I would also like to thank Ann Marie Keane for all the pints, movie nights, games, outings and great craic! My time in Norwich really would have been uneventful without you! Thank you for keeping me sane for the last four years. I would also like to thank everyone at the Bob Champion Research and Education building who made me feel so welcome after the move from the Quadram Institute. A special thank-you to Jayna Mistry and Adam Pattinson for the support and great banter.

I would also like to thank everyone who has supported me throughout my PhD and who have helped me with my journey. I would also like to express my appreciation

to everyone who video called and checked-up on me during lockdown! I would also like to give a particular thanks to Magdalena Kujawska, Paul Dickinson, Luke Theobald, Joseph and Amy Miller (and Sarah of course!), Gregory Wickham, Ariadna Miquel Clopés and Dimitra Lamprinaki for always encouraging me, helping me maintain a life outside of the PhD and for supporting me when I really needed it. Really there are so many people I would like to thank, but you all know who you are!

Above all, I want to thank my loving family - Viviana, Severiano and Valeria - for your unwavering support in all I do. I really could not have done this without your care! Thank you for all the food packages, for always being there for me and for your constant encouragement and love.

Magnificat anima mea Dominum

Chapter One: Introduction

1.1 *Escherichia coli*

In 1885, Theodor Escherich isolated the bacterial species *Bacterium coli commune* from the faecal content of healthy infants and infants suffering from diarrhoeal disease (Escherich, 1885). In 1958, in honour to his work, *Bacterium coli commune* was renamed *Escherichia coli* (Judicial Commission of the International Committee on Bacteriological Nomenclature, 1958). Part of the Gammaproteobacteria class and the Enterobacteriaceae family, *E. coli* is a Gram-negative bacterium which colonises the large intestine of warm-blooded animals, including humans (Berg, 1996, Penders *et al.*, 2006).

The first *E. coli* strains to colonise the gastrointestinal tract of a new-born infant can be sourced from both the maternal faecal flora and the nursing maternity staff (Fryklund *et al.*, 1992, Adlerberth and Wold, 2009). During an individual's life, such colonising *E. coli* strains reside within the mucus layer which covers the host gastrointestinal epithelium. During adulthood, *E. coli* is one of the predominant facultative anaerobes, reaching a density of over 10^9 colony forming units per gram of faeces yet a gradual decrease in numbers follows during senior years (Smati *et al.*, 2015, Tenaillon *et al.*, 2010). Residential gastrointestinal *E. coli* strains can partake in various roles including nutrient processing, colonisation resistance and contributing to the development and maintenance of the immune system (Deriu *et al.*, 2013, Geva-Zatorsky *et al.*, 2017, Maltby *et al.*, 2013, Conway and Cohen, 2015). Nevertheless, the strains which colonise the gastrointestinal tract can change during a person's lifetime (Conway and Cohen, 2015).

E. coli can also be isolated from the natural environment, including soil, sand and sediment (Ishii and Sadowsky, 2008). Initially, the presence of *E. coli* in such environments were thought to be introduced through faecal contamination from animal-hosts, as studies had shown that *E. coli* could not survive outside of the host (Winfield and Groisman, 2003). However, subsequent studies have reported that *E. coli* can be an active member of microbial communities in the natural environment (Ishii *et al.*, 2006). Currently, it is not clear whether such environmental strains are

from animal-origin which have adapted to the new environment or are from an ancestral lineage which evolved to reside in soil and sediment (Ishii and Sadowsky, 2008, Jang *et al.*, 2017).

By far, *E. coli* is the most studied bacterial organism, making it a 'model' organism. Due to the high plasticity of the genome, *E. coli* has been exploited for biological engineering and molecular biological studies. Furthermore, various *E. coli* strains such as K-12, have been adapted to the laboratory environment, thus facilitating genetic manipulation and allowing the expression of recombinant therapeutic proteins (Heimesaat *et al.*, 2013), including human insulin and monoclonal antibodies (Lih *et al.*, 2010, Huang *et al.*, 2012).

As a species, *E. coli* is genotypically and phenotypically diverse due to the high plasticity of the *E. coli* genome. Genetic studies of representative *E. coli* strains have demonstrated that the core-genome of *E. coli* consists of less than 20% of genes in a 'typical' genome, with the remaining genes constituting the flexible genome (Hao *et al.*, 2012, Touchon *et al.*, 2009, Lukjancenko *et al.*, 2010). The plasticity of the genome allows different *E. coli* strains to acquire prophages, transposable elements and accessory genes which can give rise to pathogenic *E. coli* strains.

Serotyping is often employed to identify different *E. coli* strains. The importance of strain identification is key to tracking and following pathogenic *E. coli* strains during outbreaks. Serotyping is a method based on the characterisation of different strains based on the O-antigen (lipopolysaccharide), H-antigen (flagella) and K-antigen (capsule; Orskov *et al.*, 1977, Orskov F., 1984). To achieve this, strains are tested against various antibodies which work against specific antigens, with matching antibody-antigen complexes causing solute agglutination. Yet, the application of serotyping methods to classify and track of *E. coli* outbreaks is shifting to whole genome sequencing technology due to reduced cost and time, and the greater ability to track isolates allowing for efficient trace back investigation (Lindsey *et al.*, 2016, Abdalhamid *et al.*, 2019, Jenkins *et al.*, 2019).

1.2 Pathogenic *E. coli*

E. coli was first recognised as a pathogenic microorganism by John S. B. Bray in the 1940s (Bray, 1945, Bray and Beavan, 1948). Following an outbreak of diarrhoea in infants, Bray and Beaven examined the faecal material of both healthy and ill infants. Antisera raised against isolates from both groups revealed that even though *Bacterium coli commune* was part of the normal faecal flora, it was also the causative agent to the diarrhoeal disease arising in infants (Bray, 1945, Bray and Beavan, 1948).

Based on the location of the disease, pathogenic *E. coli* can be classified into two distinct groups: intestinal and extraintestinal *E. coli*. Furthermore, according to the defined set of virulence factors and the main site of infection, both groups can be further subdivided into pathotypes (Fig. 1.1). Currently, the pathotypes associated with extraintestinal disease are uropathogenic *E. coli* (UPEC), which infect the urinary tract; neonatal meningitis-associated *E. coli* (NMEC) which can infect the brain, and sepsis-associated *E. coli* (SEPEC) which is a group made up of strains that infect open wounds and cause sepsis.

Within the intestinal pathogenic *E. coli* classification, pathotypes include Shiga toxin-producing *E. coli* (STEC), enteropathogenic *E. coli* (EPEC), enterotoxigenic *E. coli* (ETEC), enteroinvasive *E. coli* (EIEC), enteroaggregative *E. coli* (EAEC) and diffusely adherent *E. coli* (DAEC; Guignot *et al.*, 2009, Croxen and Finlay, 2010). The adherent invasive *E. coli* (AIEC) pathotype can also be included with the intestinal pathogenic *E. coli* classification, however, unlike the other members of the group, AIEC is associated with inflammatory bowel disease such as Crohn's disease and ulcerative colitis rather than diarrhoeal disease (Palmela *et al.*, 2018). Currently, such pathotypic grouping is under debate as pathogenic *E. coli* do not always obey the pathotype alignment due to genomic plasticity. Pathotypic combinations have arisen and caused outbreaks, such as the 2011 European outbreak caused by a Shiga toxin (Stx)-producing EAEC strain (Navarro-Garcia, 2014, Robins-Browne *et al.*, 2016).

A STEC subgroup termed enterohaemorrhagic *E. coli* (EHEC) is distinguished by its ability to cause severe disease in humans, including haemorrhagic colitis (HC) and haemolytic uremic syndrome (HUS). Two primary virulence factors are associated with the ability of EHEC to cause disease; (i) the locus of enterocyte effacement (LEE) pathogenicity island which encodes for a type three secretion system (TTSS) and (ii) Shiga toxin (Stx) encoding prophages which enable the production of toxins such as Stx1 and Stx2. Nevertheless, LEE negative STEC strains have emerged in the last decade and have been associated with the development of severe disease such as HUS (Franz *et al.*, 2015, Fruth *et al.*, 2015, Herold *et al.*, 2009a). Currently, the molecular mechanism by which such LEE-negative STEC strains adhere to the host intestinal epithelia is largely unknown.

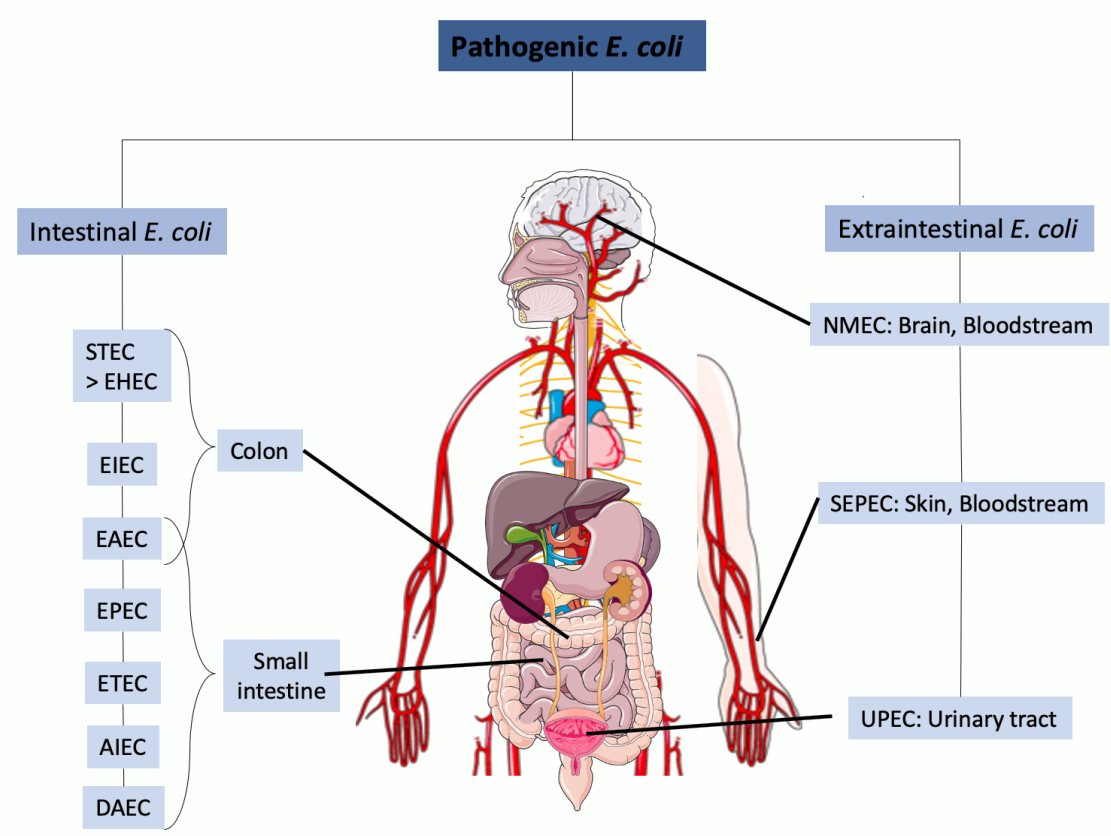

Figure 1.1: Sites of pathogenic *E. coli* colonisation.

1.3 Enterohaemorrhagic *E. coli*

1.3.1 Emergence and evolutionary origin

The ability of EHEC to cause human disease was first associated in 1982 by Riley *et al.*, following an outbreak of haemorrhagic colitis (HC) which affected 47 individuals in the states of Michigan and Oregon, USA (Riley *et al.*, 1983). The source of this outbreak was identified to be from undercooked hamburgers contaminated with the then 'rare' EHEC serotype O157:H7. Prior to 1982, EHEC O157:H7 had only been isolated once from a patient who developed HC in 1975 (Riley *et al.*, 1983). Following the first isolation of EHEC O157:H7, an *E. coli* strain with the serotype O26 was isolated from an infant suffering from a diarrheagenic disease. Investigations on this O26 strain deduced that some *E. coli* strains could produce a toxin which was termed verocytotoxin since it had cytotoxic effects on African green monkey kidney 'Vero' cells (Konowalchuk *et al.*, 1977). Successively, it was discovered that this toxin was structurally similar to Stx synthesised by *Shigella dysenteriae* type 1 and that both toxins could elicit the same biological activity, thus verocytotoxin is also known as Stx (O'Brien *et al.*, 1982, O'Brien and LaVeck, 1983). Furthermore, following investigations into sporadic cases of HUS, Karmali *et al.* demonstrated that the development of HUS was associated with EHEC infections, with further investigations linking Stx produced by EHEC to the development of HC and HUS (Karmali *et al.*, 1983b, Karmali *et al.*, 1983a).

In the UK, EHEC O157:H7 was first isolated in 1983 from faecal samples of three children during a HUS outbreak in the West Midlands involving 35 children (Taylor *et al.*, 1986). Following this, the first documented community outbreak of HC caused by EHEC O157:H7 in the UK arose in 1985 in East Anglia, with 49 people falling ill, and 19 individuals being admitted to hospital (Morgan *et al.*, 1988).

It is currently accepted that EHEC O157:H7 diverged from *E. coli* O55:H7, with current models suggesting that the first evolutionary step was the seroconversion from O55

to O157 (Feng *et al.*, 1998). Subsequently, a split occurred in the O157 lineage which resulted in two populations, (i) a lineage which lost flagella (O157: H^-) giving rise to ancestral lineages commonly known as 'German clones'; and (ii) a lineage which lost the ability to ferment sorbitol, giving rise to the common ancestor of all EHEC O157:H7 strains.

EHEC O157:H7 does not fall under a single phylogenetic group, instead there are three main lineages (I, II and I/II) and eight sub-lineages (Ia, Ib, Ic, IIa, IIb, IIc, I/IIa and I/IIb), all of which are genetically distinct (Dallman *et al.*, 2015). Such variation may have arisen as a result of the geographical spread of an ancestral clone and subsequent regional expansion. Distinctions which have arisen between the lineages have come about due to differences in the insertion sites of Stx-encoding bacteriophages, the difference in Stx subtype being carried by strains and lineage-specific polymorphisms.

1.3.2 Epidemiology

In 2015, the World Health Organization (WHO) estimated that in 2010, more than 600 million people fell ill due to foodborne disease (Codex Alimentarius Commission, 2015, The World Health Organization and Food and Agriculture Organization, 2018). EHEC infection is a moderately rare cause of gastrointestinal illness, with estimates of 2.5 million acute illnesses developing (Majowicz *et al.*, 2014). Indeed, the number of confirmed cases falls short of the estimated number of total cases, as patients will usually seek medical attention once the development of bloody diarrhoea occurs.

Thus far, EHEC is the fourth most reported bacterial zoonotic pathogens in the European Union/European Economic Area (EU/EEA), following members of the *Campylobacter* species (spp.), *Salmonella* spp. and *Yersinia* spp. (European Food Safety Authority, 2018). Between 2014 and 2018, both the UK and Germany reported the highest number of EHEC cases within the EU/EEA, with a total of 4115 reported cases (46.7%) out of 8811 reported cases reported in the EU/EEA in 2018 (Fig. 1.2;

European Centre for Disease Prevention and Control, 2020). Beyond Europe, the highest rates of EHEC infections can be found in the USA, Canada, Australia, New Zealand, Argentina and Japan (Croxen *et al.*, 2013).

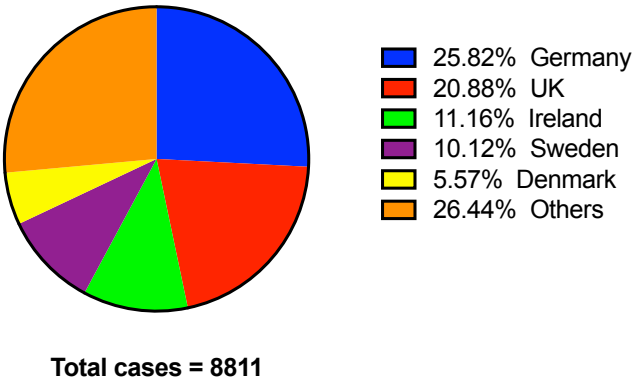

Figure 1.2: Proportion of total EHEC cases reported by countries in the EEA in 2018. Based on data from European Centre for Disease Prevention and Control, 2020.

Data collected by Public Health England (PHE) has reported that more than 40% of EHEC incidents occur in children under the age of 15, with the highest incidence occurring in 1- to 4-year-olds (Byrne *et al.*, 2015). Interestingly, other foodborne pathogens such as *Campylobacter* spp., do not follow this pattern. The suggested reasons for this unique occurrence include: (i) the low infectious dose of less than 100 EHEC bacteria and (ii) infant behaviour which increases the chances of environmentally acquired EHEC infection.

In the UK, the largest recorded outbreak of EHEC O157:H7 occurred in 1996, where 512 cases were reported, along with 20 associated deaths (Cowden *et al.*, 2001). Investigations into the source of the outbreak was traced to a local butcher selling contaminated meat products.

Between 2009 and 2012, EHEC O157:H7 was attributed to 98.8% of all EHEC infections in England and Wales (Byrne *et al.*, 2015), with only 89 cases of non-O157 STEC being reported. Nevertheless, in 2018 a total of 1,219 cases of EHEC infection were reported in England and Wales, of which 607 (50%) were O157:H7 (Public Health England, 2020). This increase in infections by non-O157 EHEC strains is likely

due to increased awareness of non-O157 serotypes after the 2011 outbreak caused by Stx-producing EAEC O104:H4, which affected over 4000 people and caused 855 cases of HUS, thus representing the highest incidence of EHEC-related HUS reported thus far (World Health Organization, 2011, Wu *et al*., 2011, Karch *et al*., 2012). As such, from 2013 there has been an increased level of screening for non-O157 EHEC strains through molecular-based assays such as PCR and genomic sequencing (Byrne *et al.*, 2014, Byrne *et al.*, 2015, Public Health England, 2020, Greig *et al.*, 2019). In 2018, the five most common non-O157 serogroups detected in England were: O26, O91, O146, O128ab and O117 (Public Health England, 2020), with O26 representing the most commonly reported non-O157 STEC serogroup.

Globally, whilst EHEC O157:H7 is the utmost recognised serotype to cause disease, over 150 non-O157 serotypes have been associated as causative agents of several outbreaks and sporadic cases of EHEC infection (Mellor *et al.*, 2016, Fan *et al.*, 2019). Lately, the number of non-O157 EHEC infection cases have increased globally, among which serotypes, O26, O45, O103, O111, O121, and O145, referred to as “the big six”, being major non-O157 STEC serotypes eliciting human disease (Karch *et al.*, 2009, Scallan *et al.*, 2011, Brooks *et al.*, 2005). Disease which arises with an infection with one of these serotypes can range from mild non-bloody diarrhoea to HUS and death, with the young, the elderly and immunocompromised being most at risk (Brooks *et al.*, 2005). The regions of which the rate of incidence for these non-O157 EHEC serotypes have increased includes the USA, Canada, Western Europe, Australia, Japan, and Argentina (Valilis *et al.*, 2018).

Both cattle and sheep can carry EHEC, with cattle representing the primary reservoir. In cattle, EHEC preferentially colonises the recto-anal junction, yet carriage remains asymptomatic (Cobbold *et al.*, 2007, Naylor *et al.*, 2003). In cattle, the intestinal vasculature lacks the Stx receptor glycolipid globotriaosylceramide (Gb3) thus explaining why asymptomatic carriage in cattle arises (Pruimboom-Brees *et al.*, 2000). Another reason for asymptomatic carriage is due to Gb3 isoforms present in bovine epithelial cells located in intestinal crypts, lacking association to lipid rafts,

resulting in inhibition of the cytotoxic activity of Stx in host cells (Falguieres *et al*., 2001, Hoey *et al*., 2003).

Global levels of EHEC O157:H7 carriage in dairy cattle varies with estimates of 0.2% to 48.8%. Furthermore, carriage levels increase in calves and during the summer months (Hussein and Sakuma, 2005, Elder *et al.*, 2000). By far, beef has been identified as the most common food source for EHEC infection by the WHO (The World Health Organization and Food and Agriculture Organization, 2018). It is acknowledged that EHEC contamination of bovine food products arises when faecal shedding and spreading occurs in slaughterhouses (Omisakin *et al.*, 2003). Most EHEC infections result from the consumption of undercooked meats, with a higher proportion being attributed to the summer months due to undercooked barbecued foods such as burgers (Chapman *et al.*, 2000, Chapman *et al.*, 2001, Tuttle *et al.*, 1999, Barlow *et al.*, 2006, Lansbury and Ludlam, 1997, Keenswijk *et al.*, 2017).

Direct contact with animals such as in a petting zoo is another route of EHEC transmission, particularly in children (Gould *et al.*, 2009). In the UK, the largest petting zoo outbreak of EHEC O157:H7 occurred in 2009 (Public Health England, 2011), when 93 individuals were infected after visiting Godstone petting farm. Of those infected, 82% were children under age 10 years, of which a total of 17 (18%) developed HUS (Public Health England, 2011). Other transmission routes include close contact with other infected patients such as in day-care centres and healthcare settings (Wheeler *et al.*, 1999, Carter *et al.*, 1987).

A meta-analysis study which examined various case control and surveillance studies identified contact with animals or their habitat, and the consumption of raw meat as the main sources of EHEC infections (Kintz *et al.*, 2017). In Kintz *et al*. (2017), 62.5% of studies associated the consumption of undercooked/raw meat as a significant source of EHEC infection and 70.4% of studies acknowledged contact with animals or their environment as a source of EHEC infection. Interestingly, this meta-analysis identified contact with animals as the major risk factor for EHEC infection in British investigations, with the consumption of raw meat as a lower associated risk factor to

contracting an EHEC infection. The risk factors associated with contracting an EHEC infection were also similar for European case studies, yet Northern American studies identified the consumption of raw meat as the main source of EHEC infection, with less than 42% of studies identifying animal contact as a source (Kintz *et al.*, 2017).

Another source of EHEC infection is through the consumption of contaminated bovine produce such as milk and other unpasteurised dairy products (Armstrong *et al.*, 1996). The use of cattle faeces as a fertiliser can also lead to the contamination of other produce such as vegetables and unpasteurised fruit drinks (Cody *et al.*, 1999, Ackers *et al.*, 1998, Kintz *et al.*, 2019, Gobin *et al.*, 2018). In the USA, surveillance data from the Centers for Disease Control and Prevention for the period between 2000 and 2009 identified leafy greens as the most frequently linked source to outbreaks of EHEC O157:H7 among fresh produce (Anderson *et al.*, 2011). In the US, various multistate fresh produce associated outbreaks have occurred such as the 2006 outbreak of EHEC O157:H7 which arose due to the consumption of contaminated spinach, consequently causing approximately 200 cases and three deaths (Grant *et al.*, 2008, Wendel *et al.*, 2009). The largest recorded outbreak caused by EHEC O157:H7 arose in Sakai city, Japan, in 1996 (Michino *et al.*, 1999). During this outbreak, more than 7000 were infected, with over 98% of the infected being children. The source of the outbreak was identified to be white radish sprouts, contaminated with bovine faecal matter containing EHEC O157:H7 (Michino *et al.*, 1999). Overall, Japan recorded approximately 10,000 EHEC O157:H7 cases that year (Watanabe *et al.*, 1999). The largest global outbreak of HUS occurred in 2011, with the source of the outbreak being traced to fenugreek seeds contaminated with Stx-producing EAEC O104:H4 (King *et al.*, 2012).

1.3.3 Clinical disease

It has been estimated that the EHEC infectious dose required to cause human illness is less than 100 organisms (Tuttle *et al.*, 1999). Typical symptoms of an EHEC infection includes gastroenteritis and watery diarrhoea, with vomiting developing in some

cases (Holtz *et al.*, 2009). In 60% to 90% of patients, 2 to 3 days after symptoms start to appear, diarrhoea becomes bloody, an indication of the development of HC (Holtz *et al.*, 2009, Byrne *et al.*, 2015). While most patients recover within 8 days, a subset of patients (5 to 15%), develop HUS which arises due to the action of Stx released by EHEC (Tarr *et al.*, 2005, Trachtman *et al.*, 2012, Byrne *et al.*, 2015). Interestingly, the development of HC and HUS is strongly linked with EHEC strains which produce Stx2a over other Stx2 subtypes and Stx1 (Werber *et al.*, 2003, Orth *et al.*, 2007, Kawano *et al.*, 2008).

HUS is typically characterised by a triad of ailments: (i) the development of haemolytic anaemia, (ii) thrombocytopenia, and (iii) severe kidney injury which can result in renal failure (Trachtman *et al.*, 2012). Furthermore, HUS may cause cardiac and neurological complications which can lead to coma, seizure and cortical blindness (Trachtman *et al.*, 2012). In approximately 5% to 10% of cases, HUS is fatal, usually due to neurological complications (Trachtman *et al.*, 2012). Other sequelae include hypertension, stroke, gallstone formation and diabetes mellitus (Byrne *et al.*, 2015). Furthermore, rectal prolapse, massive lower gastrointestinal tract bleeding, toxic megacolon, colonic necrosis and perforation have been reported in children with HUS. EHEC induced HUS is the major cause of renal failure in children globally (Tarr *et al.*, 2005).

1.3.4 Treatment

Antibiotic use during EHEC infection is generally not recommended as it may increase the incidence of HUS (Wong *et al.*, 2000, Mor and Ashkenazi, 2014, Smith *et al.*, 2012). This occurs as EHEC exposure to certain antibiotics activates the SOS-response, prompting the activation of the stress-induced Stx-phage lytic cycle, which consequently triggers the expression and synthesis of Stx (Waldor and Friedman, 2005). Various studies have shown an increased risk of developing HUS when patients are given antibiotics such as ciprofloxin, fluoroquinolones, trimethroprim-sulfamethoxazole and furazolidone (Kimmitt *et al.*, 2000, Zhang *et al.*, 2000,

McGannon *et al.*, 2010). A study, investigating a cohort of children under 10 years of age exhibiting diarrhoea due to infection with EHEC O157: H7, concluded that antibiotic treatment increases the risk of HUS (Wong *et al.*, 2000). Nevertheless, a systematic review concluded that antibiotics such as fosfomycin, erythromycin and rifaximin, which target protein and cell wall synthesis, do not activate the SOS-response, thus they have been recommended in EHEC infected patients (Agger *et al.*, 2015). In contrast, antibiotics which affect DNA synthesis such as β-lactams should be avoided (Agger *et al.*, 2015). As of late, several EHEC strains, including some O157:H7 isolates can harbour antibiotic resistance genes, hence furthering the question on whether antibiotic use is appropriate (Um *et al.*, 2018).

Currently, hydration and supportive management are given to HUS patients. Administration of intravenous fluids has been shown to prevent electrolyte imbalance and reduce the risk of HUS-associated damage (Hickey *et al.*, 2011). Platelet and erythrocyte transfusions may also be administered to counter the effects of thrombocytopenia and haemolytic anaemia, respectively (Tarr *et al.*, 2005, Mody *et al.*, 2015). In cases of renal failure, haemodialysis and peritoneal dialysis are usually administered (Rizzoni *et al.*, 1988, Grisaru *et al.*, 2011). Other ways to manage HUS include plasma infusion and exchange; and antihypertensive therapy (Rizzoni *et al.*, 1988, Slavicek *et al.*, 1995, Allford *et al.*, 2003, Van Dyck and Proesmans, 2004). Ultimately, such therapies are administered in order to avoid chronic renal damage which may require life-long dialysis or renal transplantation.

Currently, a clinical trial is being undertaken to elucidate the benefits of the complement protein C5-targeting monoclonal antibody known as Eculizumab (ECULISHU, NCT02205541). Eculizumab has been shown to be an effective therapy, which helps patients recover from HUS-associated neurological complications (Lapeyraque *et al.*, 2011). Eculizumab has been used in patients who developed HUS and acute kidney injury during the 2011 EHEC O104:H4 outbreak. However, retrospective studies concluded that Eculizumab did not provide greater benefit than supportive care or hydration therapy (Kielstein *et al.*, 2012, Loos *et al.*, 2012, Loos *et al.*, 2017). Following this, smaller studies have concluded that early treatment should

be considered once patients are infected with EHEC, in order to avoid neurological complications from arising (Pape *et al.*, 2015, Gitiaux *et al.*, 2013). Another potential monoclonal antibody based therapeutic known as Urtoxazumab, targets Stx2 and is currently in randomised placebo-controlled studies (Lopez *et al.*, 2010, Moxley *et al.*, 2017). Stx competitive inhibitors are also being examined and are currently waiting to be introduced into clinical trials (Bernedo-Navarro *et al.*, 2014, Li *et al.*, 2016).

Currently, various vaccines are in development, with vaccines which elicit protection against the action Stx being developed for human administration and vaccines eliciting protection against EHEC colonisation being developed for administration in cattle. Vaccine candidates include attenuated bacterium based vaccines made up of EHEC mutant strains lacking virulence factors or attenuated bacteria from different species such as *Salmonella* Typhimurium, expressing recombinant EHEC-related virulence factors (Liu *et al.*, 2009, Fujii *et al.*, 2012, Oliveira *et al.*, 2012); bacterial ghost-based vaccines which consist of EHEC cell envelope preparations lacking cytoplasmic contents (Cai *et al.*, 2015); and DNA based vaccines which contain EHEC virulence genes (Bentancor *et al.*, 2009, Riquelme-Neira *et al.*, 2015). In addition, the use of outer membrane vesicles (OMVs) as a tool to develop EHEC vaccines has been explored (Rojas-Lopez *et al.*, 2019). In Rojas-Lopez *et al.* (2019), inoculation of OMVs from *E. coli* K12 strains expressing EHEC lipid A deacylase into mice, resulted in antibodies being generated which recognises this antigen and consequently reduced EHEC colonisation.

1.4 EHEC pathogenesis

1.4.1 EHEC colonisation

For disease to develop, EHEC colonisation of the gastrointestinal tract is essential. Colonoscopy examinations of EHEC infected individuals have shown the development of erythema, oedema, inflammation, bleeding and ulceration in the caecum and the

ascending colon (Griffin *et al.*, 1990, Shigeno *et al.*, 2002, Kelly *et al.*, 1987). Histological examination of biopsies attained from EHEC infected individuals has revealed destruction of the surface epithelium and of the lamina propria (Griffin *et al.*, 1990), indicating that the integrity of the epithelial barrier is compromised during EHEC infection. Due to the potential life-threatening sequalae of EHEC infection, human volunteer studies are unethical, therefore animal and *in vitro* models have been used instead.

In gnotobiotic piglets, EHEC infection can cause watery and bloody diarrhoea (Tzipori *et al.*, 1986, Francis *et al.*, 1986, Moon *et al.*, 1983), with EHEC colonisation and mucosal damage in the caecum and colon (Tzipori *et al.*, 1989). Similar to humans, piglets develop renal endothelial damage and complications in the central nervous system develop due to the effects of Stx produced by colonising EHEC (Tzipori *et al.*, 1987, Gunzer *et al.*, 2002, Pohlenz *et al.*, 2005).

Watery diarrhoea also develops in young New Zealand white (NZW) rabbits upon EHEC colonisation of the colon (Farmer *et al.*, 1983, Pai *et al.*, 1986, Ritchie *et al.*, 2003). Similar to the sequelae observed in humans, histological examination of the infected colon of NZW rabbits displays haemorrhage, inflammation and cellular apoptosis (Potter *et al.*, 1985, Pai *et al.*, 1986). The deletion of genes which encode for intimin and translocated intimin receptor (tir) needed for EHEC intimate adhesion with host cells (described in more detail in section 1.4.2.1), inhibited colonisation (Ritchie *et al.*, 2003). No renal manifestations such as HUS arise upon EHEC colonisation in young NZW rabbits due to the lack of Gb3 in the kidneys (Zoja *et al.*, 1992). Yet, Stx2 has been implicated in increasing the severity and duration of intestinal disease in infant NZW rabbits (Ritchie *et al*., 2003). In contrast, Garcia *et al.* (2006) have demonstrated that infection of EHEC O157:H7 in Dutch Belted (DB) rabbit can cause diarrhoea and due to the action of Stx, renal vascular and glomerular lesions appear. Indeed, Gb3 homologs have been identified in the kidneys of DB rabbits, yet a study which examined EHEC infection in NZW and DB rabbits did not identify significant difference of disease outcome with renal pathology not being a major feature in DB rabbits (Panda *et al.*, 2010). In addition, while suckling and young

rabbits are susceptible to oral administration of EHEC, older rabbits tend to be more resistant to EHEC (Keenan *et al.*, 1986, Agin *et al.*, 1996).

In both piglet and rabbit models, EHEC adheres to the intestinal epithelium by forming characteristic attaching and effacing (A/E) lesions (Tzipori *et al.*, 1995, Ritchie *et al.*, 2003). A/E lesions were first described in piglets following infection with EPEC (Staley *et al.*, 1969). As shown in Fig. 1.3, A/E lesions are characterised by the presence of intimately adherent bacteria, the loss (effacement) of microvilli and the formation of actin-rich pedestals beneath adherent bacterium (Knutton *et al.*, 1989).

The development of A/E lesions by EHEC and EPEC has been demonstrated in various cultured cell lines such as cervical HeLa cells and colonic Caco-2 cells (Fig. 1.3). Furthermore, to detect actin polymerisation, fluorescent actin staining was initially used to detect such lesions and quickly became employed as a standard diagnostic test for A/E bacteria (Knutton *et al.*, 1989).

Figure 1.3: Transmission electron micrograph showing EHEC A/E lesion on host enterocyte. Arrow indicates A/E lesion (Wong *et al.*, 2011).

By using EPEC, the formation of A/E lesions were first demonstrated in human *in vitro* organ culture (IVOC) models (Knutton *et al.*, 1987). Following this, similar studies also demonstrated that EHEC could form A/E lesions at the follicle associated epithelium (FAE) of Peyer's patches in the terminal ileum but not at other regions of the small intestines and colon (Phillips *et al.*, 2000). Further investigations elucidated that

priming EHEC on FAE aided colonic colonisation, yet bound EHEC exhibited a non-intimate adherence phenotype inconsistent with A/E lesions (Chong *et al.*, 2007). With little intimate adherence to the colon, these results did not explain why pathology was most pronounced in the colon and why animal studies revealed adherence to the large intestine. Interestingly, Lewis *et al.* (2015), discovered that EHEC could in fact colonise the human colon when oxygen levels were lowered in IVOC experiments. With this evidence, a model has been proposed where upon ingestion, EHEC colonises both the terminal ileum and the colon.

1.4.2 Virulence factors of EHEC O157:H7

The ability of EHEC to cause disease is attributed to its genetic makeup. EHEC O157:H7 contains three major genetic elements which are associated with the development of disease: (i) the locus of enterocyte effacement pathogenicity island (LEE PI), (ii) the *stx* genes found within Stx-encoding bacteriophages and (iii) the pO157 plasmid.

1.4.2.1 The LEE pathogenicity island

Initial adherence between EHEC and the intestinal epithelium arises through the action of various proteins. These include a type four pilus known as haemorrhagic coli pilus (Xicohtencatl-Cortes *et al.*, 2007); and other fimbrial and afimbrial adhesins, such as the *E. coli* common pilus, long polar fimbriae, flagellin, *E. coli* secreted protein (Esp) A and outer membrane protein (Omp) A (Rendon *et al*., 2007, Farfan *et al*., 2011, Erdem *et al*., 2007). There is evidence to suggest that the synthesis of these initial adherence proteins is downregulated upon the expression of LEE genes such as *tir* (Mahajan *et al*., 2009).

The ability of EHEC to intimately adhere to the intestinal epithelium and form A/E lesion is mainly mediated by genes within the LEE pathogenicity island (PI; Nguyen and Sperandio, 2012). PIs are large DNA regions of foreign origin which carry virulence genes and are made up of remnants of transposons and phage genes, flanked by tRNA genes and regions of direct repeats (Schmidt and Hensel, 2004). The LEE PI was first described in EPEC, and all the genes encoded in the EPEC LEE PI are also found within the EHEC LEE PI, with a sequence homogeny of 94% (McDaniel *et al.*, 1995, Perna *et al.*, 1998). Yet, the EHEC LEE PI is larger than that of EPEC due to remnants of a lysogenic bacteriophage being present (Perna *et al.*, 1998). Additionally, the LEE PI is also found in *Citrobacter rodentium*, albeit with a higher difference with respect to EPEC and EHEC (Deng *et al.*, 2001, Petty *et al.*, 2010).

The EHEC LEE PI is 35 kb in size and is made up of 41 genes which are arranged across five transcriptional units, ordered LEE1 to 5. Encoded within the LEE1 operon, the LEE-encoded regulator (Ler) is the global regulator for the transcription of LEE1 to 5 (Elliott *et al.*, 2000, Mellies *et al.*, 1999). Ler activates the transcription of all the LEE operons by antagonising the repressing activity of histone-like nucleotide structuring protein. The regulators of Ler known as GrlA (activator) and GrlR (repressor) are encoded at the *grlRA* operon located between the *rorf3* gene and the LEE2 operon in the LEE (Iyoda *et al.*, 2006). GrlA binds to the LEE1 promoter and positively regulates Ler expression. Moreover, Ler can control the grlRA operon, thus forming a positive regulatory loop that ensures the appropriate level of Ler for LEE gene expression. Furthermore, other non-LEE encoded regulators of Ler exist, such as quorum sensing in *E. coli* (Qse) signalling proteins (described in more detail in section 1.7). The regulatory, structural and chaperone components of the type three secretion system (TTSS) are encoded in operons LEE1 to 3, with genes encoding for *E. coli* secreted proteins (Esps) making up the LEE4 operon. Genes involved in intimate adherence of EHEC such as *tir* and *eae* are located in the LEE5 operon (Wong *et al.*, 2011, Elliott *et al.*, 1998).

The TTSS encoded in the LEE PI, is a syringe-shaped structure which protrudes from the bacterial surface into the eukaryotic cell, with a central channel allowing for

protein translocation (Gaytan *et al.*, 2016, Slater *et al.*, 2018). The TTSS is made up of three parts: (i) the cytoplasmic components, (ii) the basal body which consists of three membrane rings which cross the inner and outer bacterial membrane, and (iii) the extracellular translocon, entailing of the translocation pore, filament and needle (Slater *et al.*, 2018).

The LEE PI also contains the *eae* and *tir* genes which encode for intimin protein and the translocated intimin receptor (Tir), respectively. The mechanism by which EHEC implements intimate attachment was first discovered by studying how EPEC attaches onto HeLa cells (Rosenshine *et al.*, 1992, Kenny *et al.*, 1997, Rosenshine *et al.*, 1996). Initial work elucidated that for intimate attachment, EPEC virulence protein intimin binds onto a 90 kDa protein (Hp90) expressed on the host surface membrane (Rosenshine *et al.*, 1992, Rosenshine *et al.*, 1996). Further investigations deduced that Hp90 was actually a protein injected by EPEC through the TTSS (Kenny *et al.*, 1997). This discovery was the first record of a bacterium injecting its own receptor into a host cell. Upon this finding, Hp90 was renamed translocated intimin receptor (Tir). Following Tir injection into the host cell, Tir integrates into the host membrane and binds to the EPEC outer membrane protein intimin thus achieving intimate attachment (Kenny *et al.*, 1997). Further studies have deduced that EHEC achieves intimate attachment through a similar mechanism involving Tir translocation and intimin binding (Deibel *et al.*, 1998). Binding of Tir to intimin achieves an intimate attachment to within 10nm of the host cell membrane for both EPEC and EHEC (Deibel *et al*., 1998, DeVinney *et al*., 1999, Frankel *et al*., 2001).

The importance of intimin for *in vitro* intestinal colonisation has been confirmed in neonatal calves, infant rabbits and gnotobiotic piglet models (Kenny *et al.*, 1997, Ritchie *et al.*, 2003, Deibel *et al.*, 1998, Dean-Nystrom *et al.*, 1998, Donnenberg *et al.*, 1993, DeVinney *et al.*, 1999, Ritchie and Waldor, 2005). In addition, IVOC experiments using human intestinal biopsies have demonstrated that intimin is essential for EHEC A/E lesion formation on human intestinal epithelium (Schüller *et al.*, 2007). IVOC studies have identified A/E lesions upon EHEC colonisation, with such models regarded as the gold-standard in the study of EHEC adherence. This is because such

models contain all of the cell types which make up the intestinal lining and include mucus (Phillips *et al.*, 2000, Chong *et al.*, 2007, Schüller *et al.*, 2007, Lewis *et al.*, 2015).

A characteristic of A/E lesion is the effacement of microvilli around the site of bacterial adherence. It is speculated that the loss of microvilli contributes to the development of diarrhoea as the loss of cellular surface area reduces the amount of nutrients being internalised, consequently increasing the osmolarity of the gut lumen (Lai *et al.*, 2011). The mechanism by which microvillus effacement occurs after EHEC adherence is not fully understood and requires further study.

The mechanism to explain how the pedestal structures in A/E lesions form was first elucidated in EPEC. It was deduced that once the translocated Tir protein is phosphorylated by host tyrosine kinases, Nck adaptor proteins are recruited (Kenny, 1999). Following this, Nck activates the Neural Wiskott-Aldrich syndrome protein (N-WASP), consequently stimulating actin-related protein-2/3 (ARP 2/3), leading to actin reorganisation (Campellone *et al.*, 2002). Unlike EPEC, EHEC Tir is not tyrosine-phosphorylated and therefore does not recruit NcK for actin pedestal formation (Campellone *et al.*, 2002). As shown in Fig 1.4, in order to recruit N-WASP, EHEC utilises the non-LEE encoded effector protein EspFu (also known as TccP), which links to Tir via the host protein insulin receptor tyrosine kinase substrate, also known as the insulin receptor tyrosine kinase substrate p53 (Campellone *et al.*, 2004, Garmendia *et al.*, 2004, Vingadassalom *et al.*, 2009). Activation of EspFu recruits N-WASP which subsequently activates ARP 2/3, consequently rearranging actin and forming pedestals (Rohatgi *et al.*, 2001, Sallee *et al.*, 2008).

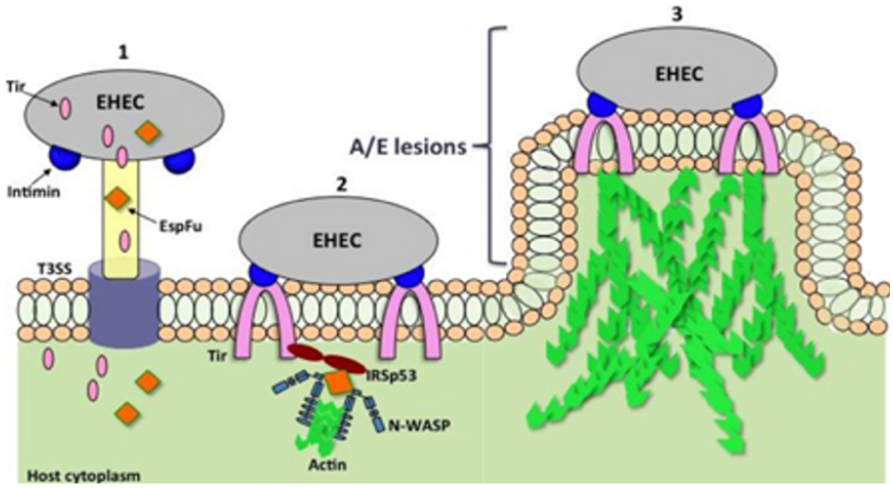

Figure 1.4: A/E lesion formation by EHEC. (1) EHEC injects Tir and EspFu into the host through the TTSS. (2) Tir localises to the host membrane and binds to intimin to intimately attach EHEC to the cell. (3) Tir and EspFu recruits host factors to subvert host cytoskeleton and actin polymerisation. IRSp53 = the insulin receptor tyrosine kinase substrate p53, N-WASP = Neural Wiskott-Aldrich syndrome protein (Nguyen and Sperandio, 2012).

Whether A/E lesions are associated with actin pedestals *in vivo* has been a matter of debate, since EHEC O157:H7 mutants which lack EspFu have shown impaired actin recruitment, yet intimate adherence and microvillus effacement occurs in IVOC infections (Garmendia *et al.*, 2004). Furthermore, atypical EPEC which can cause diarrhoea can form A/E lesions despite the lack of actin recruitment (Bai *et al.*, 2008), thus suggesting that actin recruitment is not needed for the formation of A/E lesions. Nevertheless, animal studies have concluded that actin pedestals stabilise adherence to the intestinal epithelium as the ability of EspFu EHEC deletion mutants to colonise and spread in gnotobiotic piglets and rabbits was reduced, compared to the wild type (Ritchie *et al.*, 2008).

It is estimated that EHEC secretes over 60 proteins though its TTSS into host cells (Tobe *et al.*, 2006). Many of these effector proteins are encoded within the LEE PI, however some proteins are non-LEE encoded (termed Nle proteins). These proteins contribute to EHEC colonisation and subsequent development of disease as they mimic eukaryotic proteins and consequently subvert cellular function. The consequences of such effector proteins include the weakening of tight junctions due to the reallocation of occludin away from tight junctions by EspFu (Viswanathan *et*

al., 2004); the modulation of actin and tight junction through the action of EspM (Arbeloa *et al.*, 2008, Simovitch *et al.*, 2010); and the inhibition of cell apoptosis by NleH and NleD (Newton *et al.*, 2010). For further information on the action of EHEC effector proteins in host cells the reviews by Wong *et al*., (2011) and Pinud *et al*., (2018) are recommended.

1.4.2.2 Plasmid mediated virulence factors

EHEC O157:H7 carries a non-conjugative plasmid referred to as pO157 (Burland *et al.*, 1998). This plasmid contains 100 open reading frames, encoding a type II secretion system and various virulence proteins such as pore-forming haemolysin, the zinc metalloprotease StcE, the adhesin ToxB, the catalase-peroxidase KatP and serine protease EspP which affects colonic epithelial ion and water transport (Schmidt *et al.*, 1995, Schmidt *et al.*, 1997, Brunder *et al.*, 1996, Tatsuno *et al.*, 2001, Lathem *et al.*, 2002).

1.4.2.3 Shiga toxins

The development of HUS is dependent on the release of Stxs. Stxs belong to the AB_5 toxin family, characterised by the presence of two components: (i) a single 30 kDa 'A' subunit eliciting the toxin catalytic ability, and (ii) five 'B' 7 kDa subunits, which mediate binding to host cells (Fraser *et al.*, 2004, Stein *et al.*, 1992, Ling *et al.*, 1998). Other members of AB_5 toxins include ricin toxin synthesised by the castor oil plant *Ricinus communis*, cholera toxin from *Vibrio cholerae* and heat labile enterotoxin (LT) from ETEC (Odumosu *et al.*, 2010).

Stxs were first described by Kiyochi Shiga, who isolated Stx from *Shigella dysenteriae* type 1 during a dysentery outbreak in 1897 (Shiga, 1898). EHEC can produce two structurally and antigenically distinct toxins; Stx1 and Stx2 (O'Brien and LaVeck, 1983,

Strockbine *et al.*, 1986, Melton-Celsa, 2014). Stx1 shares a 99% sequence homology to Stx synthesised by *S. dysenteriae*, whereas Stx2 shares a 56% sequence homology to Stx1 (Calderwood *et al.*, 1987, Jackson *et al.*, 1987, Takao *et al.*, 1988, Strockbine *et al.*, 1988). EHEC can carry either Stx1, Stx2 or both Stx1 and Stx2, yet Stx2 carriage is more commonly associated with the development of HUS upon EHEC infection (Werber *et al.*, 2003, Orth *et al.*, 2007, Kawano *et al.*, 2008). In addition, several variants of Stx1 and Stx2 exists (Stx1a, c and d, and Stx2a to g; Pacheco and Sperandio, 2012, Melton-Celsa, 2014), with the Stx2a subtype being highly associated with severe disease (Karch *et al.*, 2006, Orth *et al.*, 2007). In contrast, EHEC strains which synthesise Stx2b and Stx2e do not cause severe symptoms.

1.4.2.3.1 Stx prophage

Stx are encoded within lysogenic bacteriophages which are integrated into the EHEC chromosome (O'Brien *et al.*, 1984, Schmidt, 2001). Upon entering a bacterial cell, lysogenic bacteriophages integrate their genomes into the bacterial chromosome, whereby the integrated genomes are known as prophages. When lysogenic bacteriophages are silent, prophage replicate along with the bacterial chromosome consequently passing the genetic material onto daughter cells (Penadés *et al.*, 2015). Stx prophage genes remain silent, due to the action of the cI repressor which binds to operator sites (Neely and Friedman, 1998, Waldor and Friedman, 2005).

In Stx2 prophage, upon the exposure of DNA-damaging agents such as hydrogen peroxide, UV radiation, mitomycin C and DNA damaging antibiotics, the bacterial SOS-response is triggered (Grif *et al.*, 1998, Kimmitt *et al.*, 2000, Osawa *et al.*, 2000, Zhang *et al.*, 2000, Aertsen *et al.*, 2005, McGannon *et al.*, 2010, Loś *et al.*, 2010, Zhang *et al.*, 2019). This occurs due to the expression and activation of RecA which consequently removes the cI repressor upon the initiation of the SOS-response (Mühldorfer *et al.*, 1996, Aertsen *et al.*, 2005). This process ultimately results in the transcription of Stx as well as phage genes which allow the synthesis of new phage particles (Fig 1.5). Upon phage mediated bacterial lysis, bacteriophage particles and

Stx are released. In contrast to regulation of Stx2 expression, Stx1 is mainly induced by low iron concentrations in the environment. Since this trigger does not initiate the expression of late phage lysis genes, bacterial lysis does not occur. Ultimately, Stx1 accumulates in the periplasm and is released upon activation of the phage lytic cycle (Wagner *et al.*, 2002).

Interestingly, both Stx1 and Stx2 have been detected in outer membrane vesicles (OMVs), therefore demonstrating that an alternative pathway of Stx release exists, independent of bacterial lysis as (described in more detail in section 1.6).

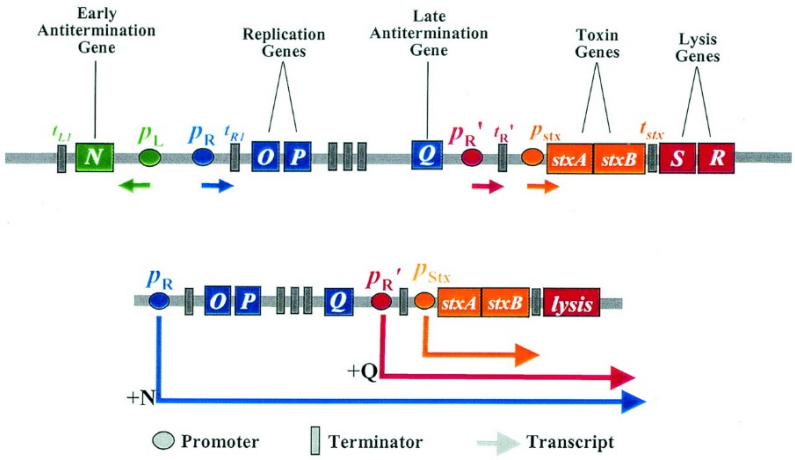

Figure 1.5: Regulation of the expression of Stx encoding genes in EHEC. Phage promoter transcription is restricted by (i) cI phage repressor activity at *pL* and *pR*, and (ii) transcriptional terminators. Upon prophage induction, (i) cleavage of cI permits transcription from *pL* and *pR* and (ii) synthesis of antiterminator proteins N and Q which facilitate transcription instigated at *pR* and *pR'* sites, respectively, by permitting terminator read-through. Both *pR* and *pR'* promoters, as well as the toxin-associated promoter (*pStx*; encoded in Stx1 prophage only) contribute to *stx* transcription. Phage lysis gene products set a limit on the duration of Stx production and encode for new phage particles which causes bacterial lysis and Stx release (Wagner *et al.*, 2002).

1.4.2.3.2 Mechanism of Stx cytotoxicity

During HUS, Stx is transported around the body via the vascular system which ultimately leads to cell damage in the kidneys and central nervous system. Stx is internalised by host cells through the binding of the Stx 'B'-subunit to glycolipid

globotriaosylceramide (Gb3; also known as CD77) which are associated to lipid rafts (Falguieres *et al.*, 2006, Lingwood *et al.*, 1987, Waddell *et al.*, 1988, Waddell *et al.*, 1990). Gb3 is highly expressed in the microvasculature of the kidneys and of the brain (Trachtman *et al.*, 2012, Chaisri *et al.*, 2001, Obata *et al.*, 2008, Hagel *et al.*, 2015), however Gb3 is also expressed by neuronal cells and various renal cells such as podocytes and mesangial cells (Obata *et al.*, 2008, Obrig, 2010).

Interestingly, free Stx has not been detected in blood, but has been found to be associated to platelets, monocytes, erythrocytes and polymorphonuclear leukocytes (Te Loo *et al.*, 2001, Stahl *et al.*, 2009, Bitzan *et al.*, 1994, van Setten *et al.*, 1996, Brigotti *et al.*, 2011). Binding of Stx to the Gb3 receptor expressed in blood cells and subsequent Stx internalisation initiates the release of microvesicles (MVs) which can contain Stx2 (Stahl *et al.*, 2009, Arvidsson *et al.*, 2015, Ståhl *et al.*, 2011). Indeed, patients who have developed HUS have elevated levels of MVs derived from blood cell (Ståhl *et al.*, 2015, Arvidsson *et al.*, 2015). The examination of kidney biopsies taken from patients who developed HUS and of EHEC infected mice, have detected MVs containing Stx (Karpman *et al*., 2017). Furthermore, it has been demonstrated that MVs are internalised by various cells which express and lack Gb3 such as renal peritubular capillary endothelial cells and glomerular endothelial (Ståhl *et al.*, 2015). Ultimately, cytotoxicity is only exhibited in cells expressing Gb3, with internalised MV-associated Stx2 following retrograde transport and inhibiting protein synthesis (Johansson *et al.*, 2020).

Neutrophils have also been identified to carry Stx, thus facilitating the distribution of Stx around the body (Brigotti *et al.*, 2013). Indeed, Stx association with neutrophils in the blood circulation of patients suffering HUS has been detected (Brigotti *et al.*, 2006). Although neutrophils do not express Gb3, Stx can binds to Toll-like receptor 4 (TLR4) through the A-subunit of the toxin, therefore allowing the transportation of Stx to Gb3 expressing cells (Brigotti *et al.*, 2019). The affinity between Stx and TLR4 is lower than that between Gb3 and Stx, hence allowing Stx transferal to Gb3 expressing cells (te Loo *et al*., 2000). In monocytes, this similar binding does not trigger Stx internalisation but rather induces the release of pro-inflammatory cytokines which

can upregulate the expression of Gb3 in renal epithelial cells (Brigotti *et al.*, 2013, Brigotti *et al.*, 2018, Te Loo *et al.*, 2001).

Internalisation of soluble Stx by Gb3-positive target cells arises through clathrin-dependent and clathrin-independent endocytosis, resulting in Stx internalisation into endosomal compartments (Lauvrak *et al.*, 2004, Sandvig *et al.*, 2008, Torgersen *et al.*, 2005). Nevertheless, the clathrin-dependent pathway is considered to be the most common mode of uptake (Bergan *et al.*, 2012). Interestingly, if Gb3 receptors lack association with lipid rafts, internalised Stx is trafficked to lysosomal compartments and is consequently degraded without any cytotoxic effect (Falguieres *et al.*, 2001). This is the reason for the resistance of bovine intestinal Gb3 expressing epithelial cells to Stx (Hoey *et al.*, 2003). In Gb3 expressing cells, internalised Stx evades the late endocytic pathway and lysosomal degradation by following the retrograde sorting pathway by entering the trans-Golgi network (Fig. 1.6).

During retrograde transport, the endoprotease furin, located in the trans-Golgi network, cleaves the Stx A-subunit into an enzymatically active A1-fragment (27.5 kDa) and an A2-fragment (4.5 kDa) which are linked by a disulphide bond (Garred *et al.*, 1995, Kurmanova *et al.*, 2007). Reduction of the disulphide bond in the endoplasmic reticulum (ER) liberates the A1 fragment which is subsequently released into the cytoplasm via the ER-associated degradation pathway (Tam and Lingwood, 2007, Yu and Haslam, 2005, LaPointe *et al.*, 2005). Due to the absence of lysine residues, the A1-fragment avoids ubiquitination and degradation, consequently allowing the A1 fragment to exercise its N-glycosidase activity by depurinating a conserved adenine residue of 28S ribosomal RNA molecules. This action subsequently blocks binding of the elongation factor 2, thus inhibiting protein translation and triggering the ribotoxic stress response (Smith *et al.*, 2003, Endo *et al.*, 1988, Ogasawara *et al.*, 1988).

The ribotoxic stress response activates mitogen-activated protein kinase (MAPK) signalling pathways, which regulates cellular proliferation and apoptosis. Specifically, Stx triggers the p38 MAPK pathway, the c-Jun N-terminal pathway and the

extracellular signal-regulated kinase pathways, ultimately leading to cell apoptosis (Ikeda *et al*., 2000, Iordanov *et al*., 1997, Foster and Tesh, 2002, Smith *et al*., 2003). The ribotoxic stress response also leads to production of pro-inflammatory cytokines (Thorpe *et al.*, 1999, Cameron *et al.*, 2003, Cherla *et al.*, 2006). Stx also induces apoptosis through the activation of caspase 8, subsequently causing the condensation of chromatin and DNA fragmentation (Tesh, 2012).

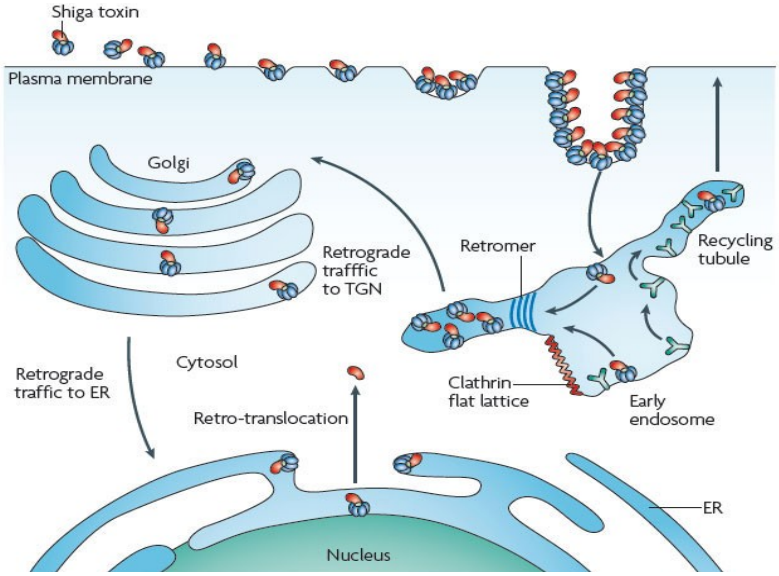

Figure 1.6: Intracellular trafficking of soluble Stx. Binding of soluble Stx to Gb3 induces the formation of endocytic invaginations. Stx then undergoes retrograde sorting in early endosomes, in which retrograde tubules are formed in a clathrin-dependent manner. Stx evades the late endocytic pathway and is transferred to the trans-Golgi network (TGN) and, into the ER. The active Stx subunit is translocated into the host cell cytosol via the ER-associated degradation machinery (Johannes and Romer, 2010).

Despite similar molecular structure and function, the toxicity of Stx1 is more potent than that of Stx2 in African green monkey Vero cell models (Fuller *et al.*, 2011, Strockbine *et al.*, 1986, Kulkarni *et al.*, 2010). This could be due to the higher binding affinity of Stx1 to Gb3 receptor than Stx2 (Nakajima *et al.*, 2001). Nevertheless, intravenous administration of soluble Stx has demonstrated that Stx2 is 400 times more toxic than Stx1 in murine models (Tesh *et al.*, 1993, Fuller *et al.*, 2011). Similar results have also been attained using primate models (Siegler *et al.*, 2003, Stearns-Kurosawa *et al.*, 2010). Furthermore, Basu *et al.* (2016), have reported that in mouse and human cells, the A1 subunit of Stx2 has a higher affinity for the target ribosomal

unit and a higher catalytic activity than Stx1 (Basu *et al.*, 2016). Interestingly, EHEC strains which produce Stx2 have been more commonly associated with the development of HUS than strains which only produce Stx1 (Werber *et al.*, 2003, Orth *et al.*, 2007, Kawano *et al.*, 2008).

1.4.2.3.3 Stx translocation across human intestinal epithelium

Upon the release of Stx from EHEC, the human intestinal epithelium represents the first point of contact between Stx and the host. As Gb3 is not expressed in human intestinal epithelium, it remains unknown how Stx crosses the colonic epithelium and enters the vasculature (Schuller *et al.*, 2004). Conversely, the expression of Gb3 is associated with cancerous malignancies, with commonly used cell lines such as Caco-2 and HCT-8 expressing Gb3 (Kovbasnjuk *et al*., 2005).

Interestingly, studies have shown that colonic T84 cells lack Gb3 yet can internalise Stx1 and Stx2 (Schuller *et al.*, 2004, Philpott *et al.*, 1997). Upon internalisation, Stx is trafficked to the Golgi apparatus and then to the ER, similar to Stx trafficking in Gb3-expressing cells (Philpott *et al.*, 1997, Schuller *et al.*, 2004). Yet, it is speculated that Stx translocation from the ER to the cytosol is inhibited as there is no effect of Stx on protein synthesis or cell viability in T84 cells upon Stx internalisation (Schuller *et al.*, 2004). Furthermore, Stx translocation across polarised T84 monolayers has been demonstrated without any cytotoxic effect on T84 cells (Philpott *et al.*, 1997, Maluykova *et al.*, 2008, Tran *et al.*, 2014, Tran *et al.*, 2018). Macropinocytosis has been proposed to explain this phenomenon in T84 cells (Malyukova *et al.*, 2009, Maluykova *et al.*, 2008). Furthermore, studies have demonstrated that EHEC can stimulate macropinocytosis, with EspP being sufficient to cause actin rearrangement and Stx1 transcytosis (Lukyanenko *et al.*, 2011, In *et al.*, 2013). Yet different investigations have shown that incubation with macropinocytosis inhibitors do not decrease the level of Stx2 translocation across polarised T84 cell monolayers suggesting an alternative route of Stx internalisation by Gb3 negative cells (Tran *et al.*, 2014).

Another proposed route to explain how Stx translocation across the epithelium occurs is via a paracellular pathway. Due to the actions of effector proteins (such as EspF and EspFu) EHEC infection leads to the disruption of tight junctions in T84 cells (Viswanathan *et al.*, 2004, Philpott *et al.*, 1997). However, no difference in Stx translocation has been observed when polarised T84 cells are exposed to soluble Stx with or without EHEC infection (Philpott *et al.*, 1997). A prominent feature of EHEC infection is the infiltration of neutrophils at the site of infection (Slutsker *et al.*, 1997, Bielaszewska and Karch, 2005). Furthermore, *in vitro* studies have demonstrated that neutrophil transmigration across polarised T84 cell monolayers can occur during EHEC infection (Hurley *et al.*, 2001). As Hurley *et al.* (2001) demonstrated an increase in Stx1 translocation across epithelial barriers upon EHEC infection and neutrophil transmigration, it is postulated that neutrophil transmigration opens a path for free Stx to translocate into the vascular system.

Currently, there is no consensus on the mechanism by which Stx crosses the intestinal epithelial barrier for subsequent spread in the host. Nevertheless, another proposed route that has recently gained attention, stems from findings of Stx released within EHEC outer membrane vesicles (OMVs; Kolling and Matthews, 1999). Thus, OMVs may provide an alternative pathway for Stx trafficking across the intestinal epithelium.

1.5 Outer membrane vesicles

The secretion of membrane vesicles is conserved throughout all the domains of life (Deatherage and Cookson, 2012). In bacteria, both Gram-negative and Gram-positive bacteria are known to secrete vesicles. Due to the structural differences of the cell envelope between Gram-negative and Gram-positive bacteria, the nature of the vesicles between the two groups differs. For gram-positives, such vesicles have been dubbed “membrane vesicles”, whereas for gram-negatives the term “outer membrane vesicles” (OMVs) is used (Brown *et al.*, 2015).

In 1965, secreted lipopolysaccharide complexes were first identified in cell-free supernatants after *E. coli* cultures were grown in lysine-limiting medium (Bishop and Work, 1965). Following this, such complexes were visualised by electron microscopy, both in free medium suspensions and associated with bacterial cells (Work *et al.*, 1966, Knox *et al.*, 1966). Originally thought to be only produced under nutrient-limiting conditions only, it is now accepted that many Gram-negative bacteria continuously produce such complexes which are now termed OMVs (Hoekstra *et al.*, 1976, Beveridge, 1999). OMVs were first isolated from humans in 1982 during the examination of cerebrospinal fluid of a child infected with *Neisseria meningitidis* and since then the role of OMVs in bacterial infection has been investigated (Stephens *et al.*, 1982).

OMVs are spherical bi-layered membrane structures, typically 50 to 250nm in diameter, and are made up of components from the outer membrane of the parental bacterium such as phospholipids, proteins and lipopolysaccharide (LPS; Mashburn-Warren and Whiteley, 2006). OMVs are constitutively released by Gram-negatives, however, external stresses such as amino acid limitations, the presence of antibiotics and high temperatures can lead to higher OMV release (Sampath *et al.*, 2018, Bauwens *et al.*, 2017a, McBroom and Kuehn, 2007). Additionally, the components encapsulated within OMVs can change upon exposure to different environmental stimuli, thus allowing OMVs to participate in many roles which can aid in the survival of the parental bacterium (McBroom and Kuehn, 2007, Manning and Kuehn, 2011, Urashima *et al.*, 2017, Lindholm *et al.*, 2020, Augustyniak *et al.*, 2018, Li *et al.*, 1998, Ciofu *et al.*, 2000, Schaar *et al.*, 2014).

In the past, there has been confusion in the literature, as some studies have used the term “OMVs” to refer to entities artificially formed by detergent treatment of bacterial cells (Ferrari *et al.*, 2006, van de Waterbeemd *et al.*, 2010). In this investigation, the term “OMVs” will be used only to refer to the naturally produced structures released during bacterial growth.

1.5.1 OMV biogenesis

Since OMVs originate through a bulging out and pinching off process from the outer membrane (OM), it is understood that portions of the OM need to be released from the underlying peptidoglycan structure. Accordingly, to understand how OMVs form, the structure of the Gram-negative cell wall needs to be considered.

The cell wall of Gram-negative bacteria consists of two membrane bilayers known as the cytoplasmic membrane and the outer membrane. The space between the two membrane bilayers is termed the periplasm which contains the peptidoglycan, several proteins, and various crosslinks which maintain the stability of the cell wall (Fig. 1.7). Such crosslinks include: (i) the covalent crosslinks between the OM-anchored lipoprotein (Lpp) with the peptidoglycan; (ii) the non-covalent interaction between the outer membrane protein (Omp) A and the peptidoglycan; and (iii) the non-covalent interaction between the Tol-Pal complex (which spans from the OM across the periplasm to the cytoplasmic membrane) and the peptidoglycan (Braun and Bosch, 1972, Wang, 2002, Cascales *et al.*, 2002, Braun and Sieglin, 1970, Koebnik, 1995, Parsons *et al.*, 2006).

It is apparent that several mechanisms exist for the biogenesis of OMVs including: (i) the loss of covalent linkages between the OM and the peptidoglycan; (ii) alterations in the periplasmic space; and (iii) the supplementation of membrane curvature-inducing molecules (Schwechheimer *et al.*, 2014, Schwechheimer *et al.*, 2015, McBroom and Kuehn, 2007, Schwechheimer *et al.*, 2013, Schertzer and Whiteley, 2012).

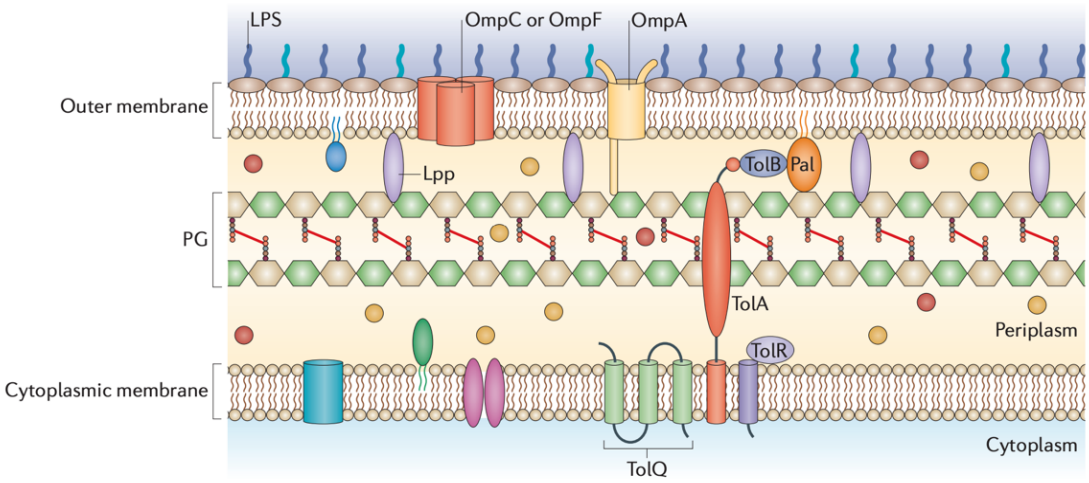

Figure 1.7: The Gram-negative cell wall. The two bilayers (i) the cytoplasmic membrane and (ii) the outer membrane (OM), form a space known as the periplasm, where the peptidoglycan (PG) is situated. The PG is made up of alternating units of N-acetylglucosamine and N-acetylmuramic acid. Attached to the N-acetylmuramic acid is a peptide chain of three to five amino acids. Cross-linking between amino acids in different linear amino sugar chains occurs. The OM is anchored by proteins which are embedded in both PG such as OmpA and Lpp and the cytoplasmic (inner) membrane by the Tol-Pal system made up of TolA, TolB, TolQ, TolR and Pal. Other proteins can also be found embedded on both cytoplasmic and outer membrane (Schwechheimer and Kuehn, 2015).

In the first proposed mechanism, the loss of the OM-anchoring proteins in the peptidoglycan leads to the formation of OMVs. The links between the OM and the peptidoglycan are dynamic, with an equilibrium of links forming and breaking (Braun and Bosch, 1972). Studies on *E. coli* and *Salmonella* Typhimurium mutants have shown that the loss of anchoring proteins such as Lpp, OmpA and the Tol-Pal system leads to increased OMV production (Bernadac *et al.*, 1998, McBroom *et al.*, 2006, Deatherage *et al.*, 2009, Turner *et al.*, 2015). Additionally, if robust crosslinks between the peptidoglycan and anchoring proteins do not form, due to altered equilibrium of peptidoglycan breakdown and synthesis, OMV production increases (Schwechheimer *et al.*, 2014, Schwechheimer *et al.*, 2015).

In the second proposed model, fragments from the peptidoglycan, LPS and misfolded proteins have been shown to accumulate in nanoterritories found within the periplasm (McBroom and Kuehn, 2007, Schwechheimer *et al.*, 2013, Schwechheimer

et al., 2014). This in turn increases periplasmic turgor pressure on the OM causing the OM to bulge and pinch off, thus forming an OMV.

The third model suggests that OMVs are induced by molecules which cause the membrane to become enriched with membrane curvature-inducing molecules such as *Pseudomonas* quinolone signal (PQS). Upon PQS association with the LPS at the lipid A region, PQS spreads within the outer leaflet of the OM. Consequently, this causes the membrane to bulge out leading to increased curvature and OMV formation (Schertzer and Whiteley, 2012). It is thought that the same mechanism is employed when bacteria are exposed to antibiotics causing membrane perturbations such as gentamicin and colistin, as studies show an increase in OMV production after antibiotic exposure (Manning and Kuehn, 2011).

Even though these are currently accepted models, other alternative mechanisms may also be possible. Promotion of OMV production by the action of flagella rotating has been suggested as a novel mechanism (Aschtgen *et al.*, 2016). Some bacteria such as *Vibrio fischeri* and *Vibrio cholerae*, have flagella which are surrounded by an OM-derived sheath (Brennan *et al.*, 2014). Blebs have frequently been observed on such flagella and studies have found that OMVs are released when flagella rotate. The molecular mechanism linking flagella rotation and OMV release remains to be elucidated, however given that other pathogens such as *Helicobacter* and *Brucella* also express such sheathed flagella, it is of interest to study whether similar mechanisms arise in different bacterial species (Fretin *et al.*, 2005, Luke and Penn, 1995).

A caveat of most of the aforementioned methods is that they have so far only been described within specific bacterial species. Indeed, it may be possible that Gram-negative bacteria may use more than one mechanism for OMV biogenesis, yet a potential conserved mechanism for OMV biogenesis has been proposed. Roier *et al.* (2016) has suggested that OMV synthesis is mediated by the maintenance of lipid asymmetry (MLA) pathway which is highly conserved among Gram-negative bacteria including *E. coli*, *V. cholerae* and *Haemophilus influenza*. This pathway has a role in

the retrograde trafficking of phospholipids from the outer leaflet of the OM to the inner membrane, thus maintaining OM asymmetry. The pathway involves an inner membrane ATP binding cassette transporter. Downregulation or mutations of genes which encode for this transporter lead to an accumulation of curvature-inducing phospholipids on the outer leaflet of the OM, ultimately leading to the bulging of the OM and its eventual budding, resulting in OMVs. Roier *et al.* (2016) has also demonstrated that genes involved in this pathway are downregulated upon low iron conditions, suggesting that the environment can influence OMV production (Roier *et al.*, 2016). Furthermore, it has been determined that the bile salt sodium taurocholate can downregulate genes which regulate this pathway in *Campylobacter jejuni*, resulting in increased OMV production. This suggests that host gut signals can influence the expression of the MLA pathway, subsequently resulting in increased OMV synthesis.

To date, it is still not clear what mechanism is utilised to ensure the packaging of proteins and genetic materials during OMV biogenesis, or whether they have been 'accidently' packaged as a result of OMV synthesis. Since OMVs have been implicated with various roles which aid the survival of parental bacteria, active packaging may indeed occur in a yet unknown process.

1.5.2 Biological functions of OMVs

The molecular content of OMVs is diverse and is either encapsulated within the OMV lumen or incorporated in the OMV membrane bilayer. OMVs permit the secretion and delivery of bacterial cargo ensuring bacterial survival and long-distance distribution of bacterial products into the environment. Generally, OMVs are known to be involved in various processes such as horizontal gene transfer, interspecies communication, interbacterial killing, nutrient acquisition, biofilm formation, protection against antimicrobial products and internal stresses, and the transportation of virulence factors into eukaryotic cells.

1.5.2.1 Internal stress protection

Bacterial treatment with denaturing agents or heat shock can lead to the accumulation of misfolded proteins in the periplasmic space. Although bacterial proteases help remove such misfolded proteins, and insoluble proteins maybe sequestered into periplasmic inclusion bodies, misfolded proteins can be exported via the vesiculation of the OM (McBroom and Kuehn, 2007). It is due to the accumulation of proteins in the periplasmic space that physical stress on the OM causes an outward force resulting in OMV release.

1.5.2.2 Interspecies communication

The ability of bacteria to sense the presence of other bacteria in the environment is mediated by quorum sensing. This allows bacterial populations to adjust their behaviour in reaction to cellular density (Papenfort and Bassler, 2016). *P. aeruginosa* has been the model organism to study quorum sensing, and studies have identified that 5% of the organism's genome is directly regulated by quorum sensing (Hentzer *et al.*, 2003, Schuster *et al.*, 2003, Wagner *et al.*, 2003, Déziel *et al.*, 2005). The Pseudomonas Quinolone Signal (PQS) is one of the main signalling molecules involved in quorum sensing and has been detected in the membrane of OMVs produced by *P. aeruginosa* (Wagner *et al.*, 2003). Since PQS molecules are hydrophobic, interaction with OMVs allows for distant transportation to other *P. aeruginosa* cells. In addition, as *P. aeruginosa* naturally exists in a polymicrobial environment, OMVs prevent the degradation of PQS by other bacteria, thus allowing for interspecies communication. Indeed, OMV formation in *P. aeruginosa* is dependent on PQS, thus demonstrating the importance of the interaction between PQS and OMVs in *P. aeruginosa* (Mashburn and Whiteley, 2005). Similar quorum sensing molecules have been identified in other bacteria such as in *Vibrio harveyi* which uses Cholera autoinducer-1, which are encapsulated in OMV, subsequently allowing communication in aqueous environments (Brameyer *et al.*, 2018).

1.5.2.3 Bacterial killing

In nature, bacterial species compete against each other for nutrients and several species have developed ways to kill competing species via the production of OMVs containing anti-microbial effectors.

A momentous study in 1998 showed that OMVs isolated from 15 different bacterial species including *E. coli*, *Pseudomonas*, *Salmonella*, *Shigella* and *Klebsiella* possessed interbacterial killing capabilities via the action of peptidoglycan hydrolases encapsulated within OMVs (Li *et al.*, 1998). Incubation of OMVs with different bacterial species displayed killing, with OMVs isolated from *P. aeruginosa* exhibiting the deadliest activity probably due to the presence of murein hydrolase and PQS which has peptidoglycan degradation abilities and bactericidal activity, respectively (Li *et al.*, 1998).

In a different study, OMVs isolated from *Lysobacter capsici* were identified to carry bacteriolytic enzymes (Afoshin *et al.*, 2020). Incubation of such OMVs with different bacterial species resulted in bacterial lysis. In order to have bacteriolytic effects, it is speculated that a fusion reaction between OMVs and the target bacterium is needed to deliver the bacteriolytic enzyme and cause lysis.

The antimicrobial abilities of OMVs are also thought to contribute to nutrient acquisition as lysed bacteria provide an extra nutritional source and decrease competition for nutrients in the environment. Such activity has been associated with OMVs released by *Myxococcus xanthus*, which contain phosphatases, proteases and secondary metabolites with antibiotic activities. These OMVs are thought to fuse with the OM of *E. coli*, which results in lysis and the release of phosphate and other nutrients, thus promoting the growth of *M. xanthus* (Evans *et al.*, 2012, Whitworth, 2011). OMVs from the myxobacteria species *Cystobacter velatus* have also exhibited antimicrobial effects on *E. coli* due to the encapsulation of cystobactamid antibiotics (Schulz *et al*., 2018). Interestingly, since such bacteria are non-pathogenic environmental isolates, they have no endotoxin activity and low inflammatory

responses arise when added to human intestinal cells (Schulz *et al.*, 2018). Therefore, the use of such OMVs provides a novel avenue for hypothetical substitute remedies for *E. coli* infections.

1.5.2.4 Nutrient acquisition

In addition to freeing nutrients via bacterial lysis, OMVs can also harbour enzymes which degrade molecular compounds in the surrounding environment for nutritional benefits. Hydrolytic and carbohydrate-binding proteins have been identified on OMVs isolated from the gut commensal bacteria *Bacteroides fragilis* and *Bacteroides thetaiotaomicron*, which mediates polysaccharide degradation. The resulting metabolites can be consumed by other bacterial species in the gut microbiota (Rakoff-Nahoum *et al.*, 2014).

A similar nutritional role has been demonstrated for OMVs produced by pathogenic *Borrelia burgdorferi*. Such OMVs carry enolase which catalyses the degradation of host matrix proteins and thereby provides a nutritional benefit for colonising *B. burgdorferi* (Toledo *et al.*, 2012).

Furthermore, OMVs from various species have been identified to be involved in iron acquisition. Iron limitation is a common external stressor for colonising pathogens, and iron depletion has been associated with increased OMV production in *Helicobacter pylori*, *E. coli* and *V. cholerae* (Roier *et al.*, 2016, Keenan and Allardyce, 2000). Indeed, siderophores, haem-scavenging proteins and haem acquisition systems have been identified in OMVs released by pathogens such as *N. meningitidis* and *Porphyromonas gingivalis* (Veith *et al.*, 2014, Lappann *et al.*, 2013). While these results suggest OMVs can capture iron, evidence on whether OMVs can be delivered back to parental cells is so far absent.

1.5.2.5 Biofilm formation

Biofilms are microbial growths which are bound by a multifaceted matrix consisting of exopolysaccharides, DNA and proteins. Biofilms can form on both biological and non-biological surfaces, allowing bacterial populations to resist and grow in stressful environments (Hall-Stoodley *et al.*, 2004). Analysis of biofilms produced by *P. aeruginosa* and *H. pylori* have identified the presence of OMVs, suggesting OMVs contribute to the development and integrity of biofilms (Beveridge, 1999).

Investigations using OMVs from *H. pylori* found that the addition of purified OMVs to growing biofilms conferred the production of thicker biofilms, thus providing resistance against external stresses (Yonezawa *et al.*, 2009, Yonezawa *et al.*, 2011). It is suggested that OMVs may act as a platform which allow exopolysaccharides, proteins and extracellular DNA to interact and adhere to surfaces thus enabling biofilms to form (Schooling and Beveridge, 2006). Indeed, studies have shown that weak biofilms are produced by bacterial strains which have a low OMV vesiculation rate (Yonezawa *et al.*, 2009).

1.5.2.6 Protection against lysis

OMVs increase the survival of bacterial populations, as OMVs can act as decoy targets against antimicrobial peptides and bacteriophages (Manning and Kuehn, 2011). OMVs isolated from *E. coli* have demonstrated the ability to sequester membrane-targeting antibiotics such as colistin and polymyxin B, resulting in OMV permeabilization and protection of growing *E. coli* populations and other bacterial species including *P. aeruginosa* (Kulkarni *et al.*, 2015, Manning and Kuehn, 2011). EHEC OMVs have also been implicated with sequestering human antibacterial peptide cathelicidin LL-37, thus protecting EHEC populations from its lethal effects (Urashima *et al.*, 2017).

OMVs can also contain antibiotic degrading enzymes which confer a further defensive strategy against antibiotics. Evidence of such enzymes first emerged from OMVs isolated from clinical isolates of *P. aeruginosa* containing β-lactamases (Ciofu *et al.*, 2000). Notably, OMVs containing β-lactamases not only provide protection to the producing organism but also to nearby bacteria from a different species (Schaar *et al.*, 2011, Schaar *et al.*, 2014). Furthermore, OMVs produced by the gut commensal *B. thetaiotaomicron*, can contain β-lactamases which confers protection against third generation cephalosporins to other commensal and pathogenic bacteria such as *Salmonella* Typhimurium (Stentz *et al.*, 2015).

In addition to antimicrobials, it has been suggested that OMVs can also sequester and inactivate bacteriophage particles, preventing bacterial cell damage. This ability has been demonstrated by OMVs isolated from *E. coli* cultures which sequester T4 bacteriophage thus inhibiting infection (Manning and Kuehn, 2011). Furthermore, OMVs isolated from *Moraxella catarrhalis*, *Neisseria gonorrhoeae*, *P. gingivalis* and *Aggregatibacter actinomycetemcomitans* have shown to aid bacterial serum resistance by sequestering components of the immune system such as antibodies and components of the complement system (Roszkowiak *et al.*, 2019, Augustyniak *et al.*, 2018, Lindholm *et al.*, 2020, Pettit and Judd, 1992, Grenier and Bélanger, 1991).

1.5.2.7 Horizontal gene transfer

The main mechanisms for horizontal gene transfer among bacteria are transformation, conjugation and transduction (Thomas and Nielsen, 2005). Yet, studies have shown that OMVs often contain DNA and provide an addition mechanism to transfer genetic material. Nucleic acid may be bound to OMVs by electrostatic interaction with LPS or encapsulated within the vesicle lumen (Dorward and Garon, 1990). However, the mechanism by which DNA becomes associated with OMVs remains to be deduced.

Previous studies have demonstrated that horizontal transfer of antibiotic resistance genes can occur via OMVs. Experiments using OMVs from *Acinetobacter baumannii* containing the $bla_{\text{OXA-24}}$ gene which encodes for β-lactamases conferred carbapenem resistance to susceptible strains of the same species (Rumbo *et al.*, 2011). In a different study, incubation of OMVs derived from EHEC O157:H7 strains harbouring chromosomal and plasmid DNA with *E. coli* K12 led to vesicle-mediated transferal of virulence genes such as *stx2* and *hlyCA* (which encodes for haemolysin), as well as antibiotic resistance (Yaron *et al.*, 2000). In addition, the multidrug resistant *E. coli* O104:H4 strain which caused the large German outbreak in 2011, has been shown to transfer genes encoding extended spectrum β-lactamases to different Enterobacteriaceae species via OMVs (Bielaszewska *et al.*, 2020). Remarkably, OMV-mediated genetic transfer was increased under simulated intestinal conditions, suggesting that resistance transfer by OMVs is likely to occur in the human intestines.

1.5.2.8 Transport of virulence factors

In addition to traditional bacterial secretion systems (such as the TTSS in EHEC), OMVs can also mediate the release of bacterial virulence factors. This pathway ensures transportation of virulence factors over long distances and simultaneous protection from the host environment and the immune response. Upon interaction with target cells, OMV entry is mediated by endocytosis, but the specific mechanism of uptake is host and species-specific (O'Donoghue and Krachler, 2016).

OMV internalisation can occur through lipid raft mediated endocytosis. Lipid rafts are eukaryotic cell membrane domains enriched with cholesterol and sphingolipids which form a compact region in the membrane and allows cell membrane invaginations to occur (Simons and Sampaio, 2011). This pathway is utilised by OMVs from *H. pylori* which contain various virulence factors such as the cytotoxin VacA (Ricci *et al*., 2005, Kaparakis *et al*., 2010). Upon OMV internalisation into host cells, VacA is released, inducing cell vacuolation and death (Parker *et al.*, 2010, Olofsson *et al.*, 2014). Similarly, OMVs from *P. gingivalis* also use lipid raft-associated endocytosis

to enter host cells and cause cell damage due to the action of released gingipains and fimbriae (Furuta *et al.*, 2009).

Lipid rafts may be associated with caveolae, which in turn allows caveolin-mediated endocytosis. Caveolae are made up of caveolin and dynamin proteins, and form 'cave-shaped' invaginations on the cell membrane (Rewatkar *et al.*, 2015). *V. cholerae* produces cholera toxin which can induce diarrhoea by activating adenylate cyclase which increases cyclic AMP (cAMP) and leads to water and chloride ion efflux into the intestinal lumen. Although cholera toxin can be secreted in its soluble form, the majority of the toxin is secreted within OMVs and enters host cells via caveolin-mediated endocytosis (Chatterjee and Chaudhuri, 2011). OMVs produced by ETEC are also internalised by host cells through this pathway. ETEC produces heat-stable and heat-labile enterotoxin (LT) which affect colonocytes by inducing electrolyte and water loss leading to diarrhoea. Interestingly, LT can be localised within and on the surface of ETEC OMVs, and in turn mediates OMV uptake by binding to the ganglioside receptor GM1 (Kesty *et al.*, 2004, Horstman and Kuehn, 2000). The pathogenic function of ETEC OMVs during infection is reinforced by their amplified production *in vivo* and their capability to induce immune responses against OMV-associated LT and other virulence factors (Roy *et al.*, 2011).

Despite the structural difference, OMVs may directly fuse with the host cell membrane and release their content. OMVs from *P. aeruginosa* and *A. actinomycetemcomitans* use this method to enter cells and release cystic fibrosis transmembrane conductance regulator inhibitory factor (Cif) toxin and cytolethal distending toxin (CDT), respectively (Bomberger *et al.*, 2009, Rompikuntal *et al.*, 2012). Cif toxin promotes the degradation of the cystic fibrosis transmembrane conductance regulator, subsequently diminishing mucociliary clearance and allowing infection establishment. Alternatively, CDT is a genotoxin which targets host DNA and induces G2 cell cycle arrest and apoptosis.

In addition to the entry routes described above, the eukaryotic membrane may also contain receptors located on clathrin-coated pits (Vercauteren *et al.*, 2010).

Internalisation is triggered by ligand binding to the cell surface receptors, leading to invaginations at these pits and the formation of clathrin-coated vesicles (Rewatkar *et al.*, 2015). Although, the receptors which trigger internalisation are not yet known, it is speculated that they differ between bacterial species. Interestingly, as well as through lipid-raft associated endocytosis, OMVs from *H. pylori* can also be internalised by clathrin-dependent endocytosis. *H. pylori* OMVs may utilise different endocytic routes due to different OMV compositions between strains and between different external pressures (Parker *et al.*, 2010), yet OMV size may also influence the method of internalisation (Turner *et al*., 2018). OMVs produced by *Brucella abortus* contain various outer membrane proteins, with immunomodulatory effects and are internalised by host cells via clathrin-dependent endocytosis. Entry into human monocytes causes the downregulation of proinflammatory cytokine production and reduced expression of MHC- class II which results in bacterial immune evasion and the attenuation of T-helper cell-mediated immune responses against *Brucella*-infected cells, therefore allowing bacterial persistence within the host (Pollak *et al.*, 2012). Notably, clathrin-dependent endocytosis is also employed for OMV-mediated transfer of EHEC virulence factors into host cells, described in more detail below (Bielaszewska *et al.*, 2013, Bielaszewska *et al.*, 2017).

1.6 OMV production by EHEC

EHEC OMV production was first demonstrated by electron microscopy in 1999 (Fig. 1.8; Kolling and Matthews, 1999). Several OMV-associated virulence factors have been identified including Stx1, Stx2, haemolysin, cytolethal distending toxin V, *Shigella* enterotoxin, flagella and LPS, as well as genetic material encoding for Stx (Bielaszewska *et al.*, 2013, Bielaszewska *et al.*, 2017, Kim *et al.*, 2010, Kolling and Matthews, 1999, Kunsmann *et al.*, 2015). Stx1 and Stx2 are exclusively localised within the OMV lumen as verified by protease K treatment and electron microscopy (Kolling and Matthews, 1999, Bielaszewska *et al.*, 2017).

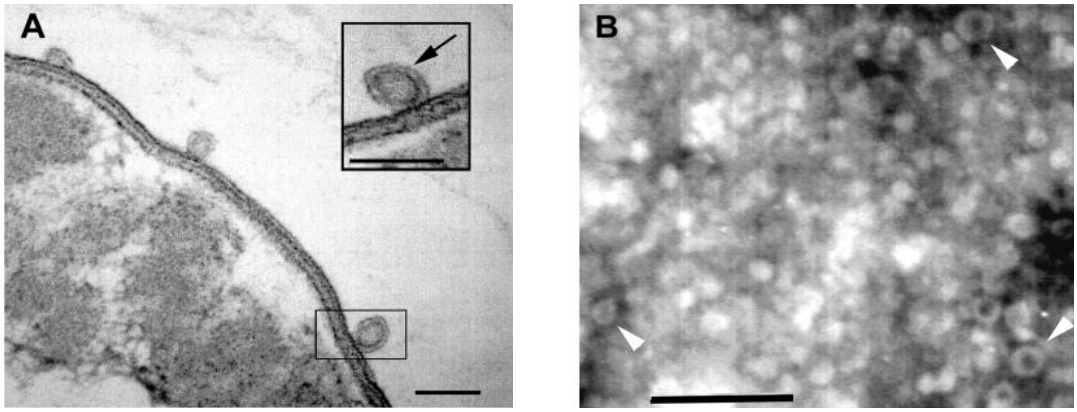

Figure 1.8: Transmission electron micrograph of OMV production by EHEC O157:H7. (A) Ultrathin sections show vesicles blebbing from the bacterial outer membrane. The inset is an enlargement of the enclosed area, bar = 50 nm. (B) Negatively stained vesicle preparations. Arrowheads indicate individual vesicles, bar = 250 nm (Kolling and Matthews, 1999).

The cytotoxic activity of OMV-associated Stxs has been confirmed using Gb3 expressing Vero cells, with loss in cytotoxicity when cells are incubated with OMVs from isogenic Δ*stx* mutants (Kim *et al.*, 2010). Furthermore, mouse model studies have demonstrated that EHEC O157:H7 OMVs can cause HUS-like disease such as renal cell damage after intraperitoneal injection, showing their possible involvement in the development of severe disease in humans (Kim *et al.*, 2011).

Previous studies have demonstrated that OMVs from EHEC O157:H7 and Stx-producing EAEC O104:H4 are internalised by clathrin-mediated endocytosis by Gb3-positive human colonic Caco-2 cells and by microvasculature endothelial cells of the brain and of the kidneys (Kunsmann *et al.*, 2015, Bielaszewska *et al.*, 2017). While OMVs are trafficked along the endosomal-lysosomal pathway, Stx2 is released from OMVs due to a change to an acidic pH level in the early endosome. Similar to soluble Stx, once freed from OMVs, Stx is retrogradely trafficked via the Golgi apparatus and ER, consequently causing cell death (Bielaszewska *et al.*, 2017).

Whether OMV internalisation and similar trafficking occurs in the colon remains to be deduced as it is generally accepted that the human intestinal epithelium lacks Gb3. Therefore, the use of Gb3-positive cells is arguably an inappropriate model to study the fate of OMVs and their associated Stx in the human colon. Further studies are

needed to truly elucidate whether EHEC OMVs are internalised by the human colonic epithelium. Moreover, the intracellular trafficking and fundamental destination of EHEC OMVs needs to be clarified as it may be possible that OMVs translocate across the intestinal barrier, consequently allowing the trafficking of virulence factors such as Stx and contribute to EHEC disease.

Various external cues can affect the vesiculation of EHEC OMVs such as exposure to antibiotics. As previously mentioned, antibiotic therapy during EHEC infection is not recommended due to the induction of Stx phage lytic cycles and enhanced HUS risk (Wong *et al.*, 2000, Smith *et al.*, 2012, Mor and Ashkenazi, 2014). Similarly, exposure to antibiotics which trigger an SOS-response (e.g., ciprofloxacin) increases OMV production and Stx2a content in EHEC O157:H7 (Bauwens *et al.*, 2017a). Moreover, environmental conditions in the gastrointestinal tract can also influence OMV production (discussed in more detail in section 1.7.8).

1.7 The effect of the intestinal environment on EHEC virulence

The human gastrointestinal tract encompasses several organs, including the oropharynx, the oesophagus, the stomach, the small intestine (duodenum, jejunum and ileum) and the large intestine (caecum, colon, rectum and anus; Gelberg, 2014). The intestinal lumen contains fluid, which is made up of various components secreted by cells which line the tract or by cells in accessory organs of the gastrointestinal system such as the gallbladder. The composition and environment of the gastric fluid varies during transit in the gastrointestinal tract. EHEC therefore needs to adapt to the various stresses (such as changes in pH, the presence of different bile salts and varying oxygen concentrations) encountered in the gastrointestinal tract in order to survive and colonise. To this aim, EHEC can sense various signals present in different regions of the gastrointestinal tract which can influence the expression of virulence genes and enable successful colonisation of EHEC.

1.7.1 Gastrointestinal pH levels

Due to gastric acid secretion, the stomach is characterised by a low pH of 1.5 to a pH 6.5 (Broesder *et al.*, 2020). *E. coli* possesses five acid resistance (AR) pathways (AR1 to AR5). The AR1 system uses the alternative σ factor and cAMP receptor protein (CRP), which provide an acid adaption and tolerance response, thus permitting the survival of EHEC in low pH (pH 2.5) that can be induced by growth in complex medium (Castanie-Cornet *et al.*, 1999, Lin *et al.*, 1995). The AR1 system is repressed by glucose due to the involvement of CRP. The mechanism by which these proteins instigate resistance is not fully known (Castanie-Cornet *et al.*, 1999). The AR2 - AR5 systems are reliant on specific extracellular amino acid (glutamate, arginine, lysine and ornithine, respectively) and consist of an antiporter and a decarboxylase enzyme (Richard and Foster, 2004, Lund *et al.*, 2014, Castanie-Cornet *et al.*, 1999, Hersh *et al.*, 1996, De Biase *et al.*, 1999). These systems confer acid resistance by consuming intracellular protons through amino acid-dependent decarboxylation reactions, therefore neutralising internal bacterial pH (House *et al.*, 2009). All systems can protect stationary phase cells from extreme acidity and prolong survival, however AR2 and AR3 have been reported to also function during the exponential phase (Castanie-Cornet *et al.*, 1999, Richard and Foster, 2004). Recently, a new acid-tolerant system has been described, known as the CpxRA acid-tolerant system. Upon the detection of acidic pH, this acid-tolerant system, activates the synthesis of unsaturated fatty acids. Augmented unsaturated fatty acid content in the cell membrane lipid, decreases membrane fluidity, therefore inhibiting the flow of protons into bacterial cells. This maintains optimum intracellular pH, thus allowing the normal growth of *E. coli* (Xu *et al*., 2020).

EHEC also possesses two periplasmic heat shock proteins, HdeA and HdeB, which are activated and become molecular chaperones under acidic conditions (Gajiwala and Burley, 2000). These activated chaperones bind to a range of polypeptides and prevent aggregation thus protecting such proteins from acidic pH levels as low as 2.5 (Benjamin and Datta, 1995, Lin *et al.*, 1996).

Studies which have evaluated the gene expression profiles of EHEC O157:H7 strains after enduring acidic stress, revealed expression changes in genes involved in motility and the TTSS (House *et al.*, 2009). In acid stressed EHEC, flagella synthesis genes are upregulated and is accompanied with increased motility levels (House *et al.*, 2009). In contrast, genes associated with the TTSS are downregulated, indicating that through a sensory mechanism, EHEC does not colonise in the stomach but rather moves onto the neutral gastrointestinal tract (House *et al.*, 2009). The downregulation of LEE genes under acidic pH is mediated by the increased expression of the regulator GadE (Kailasan Vanaja *et al.*, 2009, Laaberki *et al.*, 2006). GadE also activates the glutamate decarboxylate-dependent acid resistance system, thus it acts as link between acid resistance and virulence (Laaberki *et al.*, 2006, Kailasan Vanaja *et al.*, 2009). Regarding Stx expression, studies have shown that under acidic conditions, Stx expression is repressed (Yuk and Marshall, 2004).

1.7.2 Bile salts

After passage through the stomach, EHEC is exposed to the antimicrobial effects of bile salts in the small intestine. Bile is made in the liver, stored in the gallbladder and excreted into the intestinal lumen upon digestion (Hofmann, 1999). Bile salts are the most prevalent organic solutes in bile, with the primary bile salts cholate and chenodeoxycholate making up 80 - 90% of total bile salt content in the human small intestine (Chiang, 2013). In the gut, bile salts form micelles with fatty acids originating from dietary fats, thus allowing for their absorption (Gass *et al.*, 2007). Most bile salts are reabsorbed by active mechanisms at the terminal ileum, yet a small amount of the salts may transit to the caecum and colon. Through faecal measurements and examinations of cadavers, it is estimated that bile salt concentrations in the colon are around 500µM to 3mM (Hamilton *et al.*, 2007, Peleman *et al.*, 2017). Yet due to biotransformation by the microbiota, the majority of the colonic bile salt pool consists of the secondary bile salts deoxycholic acid and lithocholic acid (Ridlon *et al.*, 2006). Bile salts can also act as antimicrobial agents as they can damage bacterial membranes, dissipating transmembrane electrical potential. This consequently

results in a reduction in internal pH, consequently inducing DNA damage and protein denaturation (Merritt and Donaldson, 2009, Prieto *et al.*, 2004, Kurdi *et al.*, 2006, Bustos *et al.*, 2012, Rodriguez-Beltran *et al.*, 2012).

The ability for EHEC to resist the lethal activity of bile salts transpires by modifying the expression of porins and efflux pumps. Bile salts enter EHEC through the outer membrane porin F (OmpF). Yet, studies have demonstrated that upon bile salt exposure EHEC expression of OmpF is inhibited, thus reducing the outer membrane permeability to bile salts (Hamner *et al.*, 2013). In addition, EHEC exposure to bile salts results in increased expression of the AcrAB efflux pump, which actively pumps out bile salts, thus providing resistance (Thanassi *et al.*, 1997, Ma *et al.*, 1995).

Expression of EHEC virulence genes can be influenced by the concentration of bile salts. While bile salt concentrations similar to those in the small intestine reduce expression of the LEE genes (Hamner *et al.*, 2013), expression of adhesive fimbriae involved in EHEC colonisation is enhanced in bile salts levels akin to those in the colon (Arenas-Hernandez *et al.*, 2014). The concentration of bile salts in the small intestine also increases expression of genes associated with iron scavenging in EHEC O157:H7 (Hamner *et al.*, 2013), thus suggesting that bile salts may be an environmental signal which can influence EHEC to adapt to the iron-limiting conditions found in the intestine. Interestingly, small intestinal levels of bile salts do not influence the expression of Stx (Hamner *et al.*, 2013).

1.7.3 Short chained fatty acids

Short chained fatty acids (SCFAs) are a metabolic product released by commensal bacteria in the colon (Louis and Flint, 2009, Louis and Flint, 2017). The main SCFA in the gastrointestinal tract include acetate, butyrate and propionate (den Besten *et al.*, 2013). Nevertheless, the concentrations and composition of SCFAs differ throughout the colon and can be influenced by diet, with concentrations generally increase during passage through the intestinal tract.

Interestingly, unlike ileal levels of SCFA, colonic levels of SCFAs have been shown to increase the expression of adherence-conferring outer-membrane lha protein, which contributes to EHEC adhesion (Herold *et al.*, 2009b). Furthermore, murine studies have shown that when fed high fibre diets with high levels of the SCFA butyrate, EHEC colonisation increases up to 100-fold (Zumbrun *et al.*, 2013). Indeed, it has been demonstrated that butyrate alone can upregulate LEE gene expression, thereby enhancing EHEC adherence (Nakanishi *et al.*, 2009). In addition, studies have demonstrated that SCFA acetate, propionate and butyrate increases the expression of flagella-associated genes, yet butyrate can induce the expression of flagella and LEE genes (Tobe *et al.*, 2011). Therefore, it is proposed that SCFA concentrations in the small intestine only upregulate flagellar synthesis, thus enhancing EHEC motility. Yet as SCFA levels rise in the colon, sufficient butyrate is produced therefore inducing LEE expression, resulting in colonic adherence.

Currently, the effect of SCFAs on Stx expression is not known due to a lack of studies. Yet, SCFAs which are produced in the colon are absorbed and can be transported to the kidneys (Pluznick, 2016). Interestingly, butyrate increases Gb3 expression in human saphenous vein endothelial cells, consequently increasing the sensitivity and cytotoxicity of Stx (Keusch *et al.*, 1996). It may be possible that the same arises in the kidneys, therefore increasing renal damage upon EHEC infection.

1.7.4 Mucus

In order to colonise the intestinal epithelium, EHEC needs to penetrate the overlaying mucus layer composed of glycosylated mucin proteins (Johansson *et al.*, 2011). In the human intestine, MUC2 is the predominant mucin secreted by goblet cells (Hansson, 2019). While the mucus layer in the small intestine is thin and allows nutrient absorption, the colonic epithelium is covered by a dense adherent inner mucus layer overlaid by a loose penetrable outer layer which is colonised by the microbiota (Johansson *et al.*, 2011). Using human colonic biopsies and colonoids, studies have demonstrated that EHEC can reduce the inner mucus layer via the zinc

metalloprotease StcE and other mechanisms, thereby gaining access to the epithelial surface (Hews *et al.*, 2017, In *et al.*, 2016a)

In the colon, mucus provides a major carbon source as it contains many sugars such, as fucose. Sugars can be harvested by members of the microbiota, such as *B. thetaiotaomicron* and made available for consumption by other bacterial species (Hooper *et al.*, 1999). Interestingly, LEE expression can be regulated by fucose. Upon sensing fucose, the histidine sensor kinase FusK, phosphorylates FusR and binds to the Ler regulatory region, consequently inhibiting the expression of LEE genes (Pacheco *et al.*, 2012). This contributes to the relocation of EHEC from the lumen to the epithelial surface, where sugars are predominantly associated to mucin. This in turn allows the expression of LEE genes, subsequently permitting adherence. Interestingly, studies have demonstrated that when other mucus-derived sugars including galacturonic acid, gluconic acid, glucuronic acid, pyruvate, sialic acid, or mannose are the sole carbon source, there is increased expression of TTSS genes in EHEC (Carlson-Banning and Sperandio, 2016). The mechanisms of how such sugars affect the expression of LEE-associated genes and contribute to colonic adhesion has not been fully elucidated.

1.7.5 Hormones

Intestinal epithelial cells produce neurochemicals including catecholamine dopamine (Eisenhofer *et al.*, 1997). From dopamine, different hormones can be formed including epinephrine and norepinephrine. These hormones augment EHEC growth in both *in vitro* and *in vivo* models (Lyte *et al.*, 1996, Lyte *et al.*, 1997, Lyte and Bailey, 1997). The hormone signals are sensed by bacterial adrenergic receptors, quorum-sensing *E. coli* regulator (Qse) C and QseE (Hughes *et al.*, 2009, Njoroge and Sperandio, 2012, Reading *et al.*, 2009). Autophosphorylation of QseC and QseE follows upon sensing epinephrine or norepinephrine. This in turn invokes the phosphorylation of their respective response regulators. QseB, KdpE and QseF are the associated response regulators of QseC (Hughes *et al.*, 2009). Phosphorylation of

QseB invokes the expression of flagella genes which in turn provides greater motility in EHEC (Sperandio *et al.*, 2002). The quorum sensing molecule autoinducer-3 has also been implicated in activating the QseBC two-complement system (Sperandio *et al.*, 2003). Phosphorylated KdpE in conjunction with Cra induces the expression of LEE genes by directly binding to the Ler promoter. Cra is a global regulator of genes involved in carbon metabolism (gluconeogenesis), where affinity of Cra to the Ler promoter is catabolite dependent (Shimada *et al.*, 2011). Thus, LEE expression is induced by KdpE and Cra in gluconeogenic environments such as those in the mucus layer, whereas in a glycolytic environment, LEE expression is not induced (Njoroge *et al.*, 2012, Njoroge *et al.*, 2013).

Autophosphorylation of QseE invokes the phosphorylation of QseF, which in turn increases expression of Stx genes (Hughes *et al.*, 2009). QseF can also inhibit the expression of *fus* genes which are involved in the sensing of fucose, therefore relieving the Ler regulatory region from fucose mediated inhibition of the LEE (Pacheco *et al.*, 2012).

1.7.6 Oxygen

Using non-invasive methods, initial studies have detected gradual decreases in oxygen levels during transit in the gastrointestinal tract (Kalantar-Zadeh *et al.*, 2018). Oxygen levels decrease as it diffuses into mucosal tissue and is used for respiration by host cells and bacteria. Using gas sensing electronic capsules, the oxygen-equivalent gas profiles is estimated to be 65% in the stomach, lowering to 5% during transit in the small intestines, with levels decreasing to under 1% in the colon (Kalantar-Zadeh *et al.*, 2018). In addition, a radial gradient from the gut lumen to the mucosal surface exists due to oxygen diffusing from the capillary vascular supply (Albenberg *et al.*, 2014). This results in increased oxygen levels as proximity to the mucosal surface increases.

The ability to adapt to fluctuations in oxygen levels is important for *E. coli* colonisation of the intestine. This has been demonstrated in mouse models which have shown that functional aerobic and anaerobic respiration are required for successful colonisation by *E. coli* (Jones *et al.*, 2007). Jones *et al.*, (2007), demonstrated that mutant *E. coli* strains which lacked the ability to use either respiration pathways were out competed by wild type strains. To tolerate changes in oxygen levels, *E. coli* possesses two respiratory oxidases; cytochrome *bo3* oxidase and cytochrome *bd* oxidase and can utilise a range of electronic terminators such as nitrate, trimethylamine-N-oxidase for anaerobic respiration and mixed acid fermentation (Gunsalus and Park, 1994, Stolper *et al.*, 2010, Förster and Gescher, 2014, Chang *et al.*, 2004). Switching of aerobiosis to anaerobiosis or microaerobiosis is governed by the regulators Fnr (anaerobiosis) and ArcA (microaerobiosis; Dibden and Green, 2005, Alexeeva *et al.*, 2003).

In chemostatic growth conditions, oxygen limitation inhibits EHEC growth (James and Keevil, 1999), but enhances adherence to epithelial cells suggesting the induction of adhesin proteins (James and Keevil, 1999). In a different study, anaerobic growth in LB medium reduced expression of the EHEC TTSS and associated effector proteins (Ando *et al.*, 2007). Interestingly, the addition of alternative terminal electron acceptors such as nitrate in anaerobic cultures restore the expression of the TTSS and allow the formation of A/E lesions on colonic-derived Caco-2 cells (Ando *et al.*, 2007). Similarly, the same occurs when EHEC is grown in Dulbecco's Modified Eagle Medium (Carlson-Banning and Sperandio, 2016). Interestingly, under anaerobic conditions the KdpE and FusR regulators represses the expression of the TTSS. Yet in aerobic conditions and in the presence of gluconeogenic sugars - similar to microenvironment near the colonic epithelium - Cra and KdpE upregulate LEE expression, therefore coordinating intimate adherence. Furthermore, in aerobic conditions, FusR does not repress LEE unless fucose or pyruvate are present (Carlson-Banning and Sperandio, 2016).

Previous studies have demonstrated that EHEC expression of the TTSS and ability to adhere to colonic epithelium is enhanced by microaerobic conditions (Schuller and

Phillips, 2010). It has been demonstrated that the oxygen-responsive small RNA DicF is involved in the regulation of the TTSS, where under oxygen-limited conditions, DicF increases TTSS expression (Melson and Kendall, 2019). This oxygen dependent regulation allows EHEC to control the expression of the TTSS with radial oxygen gradient in the intestine, with minimal LEE gene expression (and energy expense) in the anaerobic gut lumen.

In contrast to TTSS, Stx production is enhanced in aerobic conditions versus microaerobic conditions (Tran *et al.*, 2014). This may be due to the production of reactive oxygen species during aerobic respiration which results in induction of phage lytic cycle and subsequent Stx synthesis and release (González-Flecha and Demple, 1995, Loś *et al*., 2010).

1.7.7 Ethanolamine

The gastrointestinal tract generates various membrane lipid metabolites including ethanolamine which is a breakdown product of phosphatidylethanolamine (Albright *et al.*, 1973, Zhou *et al.*, 2017). Ethanolamine can serve as a nitrogen source for EHEC in the human colon (Bertin *et al.*, 2011). In addition, ethanolamine increases the expression of virulence regulators involved in LEE transcription, resulting in increased A/E lesion formation on host cells (Kendall *et al*., 2012, Luzader *et al*., 2013). Furthermore, ethanolamine can increase Stx expression. Enhanced transcript levels of *QseA*, *QseE* and *QseC* by EHEC upon ethanolamine exposure suggests the involvement of quorum sensing proteins (Kendall *et al.*, 2012).

1.7.8 Influence of intestinal conditions on EHEC OMV production

In addition to influencing EHEC growth and virulence gene expression, environmental factors in the gastrointestinal tract can also influence OMV production and OMV-

mediated Stx release. While Stx2 was predominantly released as soluble toxin under aerobic conditions, Stx2 release within OMVs predominated under anaerobic conditions. In contrast Stx1 release was mainly associated with OMVs under both conditions (Yokoyama *et al.*, 2000).

Another study demonstrated that exposure of EHEC O157:H7 to simulated colonic (SCEM) and simulated ileal environment medium resulted in a significant increase in OMV and OMV-associated Stx2a release compared to LB medium, with further increases observed under microaerobic versus aerobic conditions (Bauwens *et al.*, 2017b). In addition, EHEC OMV production was augmented by the presence of mucin glycoproteins and human α- defensin 5, a key antimicrobial peptide released in the small intestine. Bauwens *et al.* (2017b) also demonstrated that EHEC growth in acidic conditions (pH4) strongly enhanced OMV vesiculation and OMV-associated Stx2a release.

1.8 Summary

EHEC virulence is mainly associated with the injection of effector proteins into the host cell via a TTSS, and the production of Stxs which targets and damages various renal and endothelial cells. Nevertheless, various EHEC virulence factors including Stx can be encapsulated by OMVs. Since OMVs permit the transportation of virulence factors over long distances and mediate the delivery of such virulence factors into host cells, EHEC OMVs may contribute to the development of systemic disease.

1.9 Aims and objectives

This PhD project aims to test the hypothesis that various human colonic conditions augment the production of EHEC OMVs, leading to their internalisation into the colonic epithelium and subsequent translocation across the epithelium. This

translocation consequently allows to the delivery of OMVs to the kidneys, causing cytotoxicity by OMV-associated Stx.

1.9.1 Objectives

1. To evaluate the effect the colonic environment has on EHEC growth and OMV production (Chapter 3).

A protocol was first established to allow the successful isolation of EHEC OMVs. This protocol was then applied to evaluate the effect of EHEC growth phase on OMV production. Subsequently by identifying the optimal growth phase for OMV production, the influence of various colonic cues was evaluated including the presence of colonic cells, physiologically relevant osmolarity levels and bile salts.

2. To determine the intracellular trafficking of EHEC OMVs by the human colonic epithelium and investigate the intracellular trafficking of OMV and OMV-associated Stx by kidney cells (Chapter 4).

Colonic derived Caco-2 cells and T84 cell lines, and human colonoid model were used to determine if EHEC OMVs can be internalised by the human colonic epithelium. Following this, the influence of cell polarisation on OMV intracellular trafficking and translocation was evaluated. Additionally, internalisation and intracellular trafficking of OMVs and OMV-associated Stx by renal cells was investigated.

Chapter Two: Material and Methods

2.1 Bacterial strains and growth conditions

The EHEC strains used in this study are presented in table 2.1. Work involving Stx-producing EHEC strains was carried out at containment level (CL) 3, whereas work on Stx-negative EHEC strains was conducted at CL2. To start a culture, -80^{o}C glycerol stocks of specific EHEC strains were collected and placed on dry ice. A sterile pipette tip was used to transfer the bacterial glycerol (Fisher scientific) stock onto a Luria-Bertani (LB) Lennox Agar (Formedium, prepared according to manufacturers instructions) plate and then incubated overnight (18 hours) at 37°C. Subsequently, agar plates with grown EHEC colonies were stored at 4°C for up to 1 month. Bacteria were passaged no more than 2 times before reversion to glycerol stocks to prevent the accumulation of mutations.

To begin EHEC growth for further experimentation, EHEC colonies were collected from an agar plate and grown overnight (18 hours) in 2mL of LB Lennox broth (Sigma prepared according to manufactures instructions) at 37^{o}C, standing.

For EHEC growth analysis and OMV isolation, bacterial overnight cultures were diluted at a ratio of 1:100 in either LB Lennox broth, tryptic soy broth (Sigma, prepared according to manufacturer's instructions), Dulbecco's Modified Eagle's Medium with high glucose (DMEM; Sigma D5671), Dulbecco's Modified Eagle's Medium: Nutrient Mixture F-12 medium (DMEM/F-12; Sigma D4621) or simulated colonic environmental medium (SCEM; Polzin *et al.*, 2013; composed of 6.25g/L BD Bacto tryptone (BD Biosciences), 0.88g/L NaCl (Sigma), 0.43g/L KH_2PO_4 (Fisher Scientific), 1.7 g/L $NaHCO_3$ (Sigma), 2.7 g/L $KHCO_3$ (Sigma), 2.6 g/L of D-glucose (Sigma), 4 g/L of bile salt no. 3 (Oxoid) and pH adjusted to pH 7. Upon preparation, SCEM was autoclaved and subsequently D-glucose was added after being filter sterilised). Bacterial cultures were grown in either 50mL falcon tubes shaking at 180 rpm or in T75 flasks on a rocking platform at 37^{o}C for the stated amount of time.

Strain	Serotype	Description	Reference
EDL933	O157:H7	Wild type strain isolated from the 1982 US outbreak, Stx1 and Stx2 positive	(Riley *et al.*, 1983)
86-24	O157:H7	Wild type strain isolated from the 1986 US outbreak, Stx2 positive	(Griffin *et al.*, 1988)
TUV 93-0	O157:H7	Derivative of EHEC strain EDL933, Stx1 and Stx2 negative	(Girard *et al.*, 2007)
85-170	O157:H7	Derivative of EHEC strain 84-289, Stx1 and Stx2 negative	(Tzipori *et al.*, 1987)

Table 2.1: List of EHEC strains used in this study.

2.2 Quantifying bacterial growth

To quantify bacterial density, absorbance at 600 nm (OD_{600}) was determined using a spectrophotometer. A mL of undiluted culture was used for OD_{600} measurements, however for OD_{600} readings above 0.8, a 1:5 or 1:10 dilution of culture in growth medium was prepared to accurately determine absorbance.

To determine viable bacterial counts, EHEC cultures were serially diluted in phosphate-buffered saline (PBS; Oxoid) and 10µL of each dilution were spotted onto LB agar in triplicate (Miles and Misra method). Plates were incubated overnight at 37^{o}C, and colony forming units (cfu) per mL was determined the next day by counting droplets forming 5 - 50 colonies.

2.3 Cell culture

2.3.1 Cryopreservation and resurrection of cell lines

Long-term storage of eukaryotic cell lines was achieved by cryopreservation in liquid nitrogen (vapour phase, -190°C). To produce frozen stocks, cells were suspended at a density of 2 to 4 x10^6 cells in 1mL of culture medium containing dimethyl sulfoxide (DMSO, 5% v/v for T84 cells and 10% v/v for all other cells lines used in this study, Sigma) and aliquoted into cryotubes. To avoid the formation of ice crystal within the stocks, stocks were placed in a Mr Frosty Freezing™ Container (Thermo Fisher Scientific) holding isopropanol and subsequently frozen overnight at -80°C before being transferred to liquid nitrogen storage.

To start a culture from frozen stocks, cells were thawed by part submersion of the cryotube in water (37°C). The suspension was transferred into 5mL of pre-warmed cell culture medium and centrifuged at 180 x *g* for 6 minutes. The supernatant was removed, and the cell pellet was resuspended in 7mL of warm cell culture medium. The whole suspension was then transferred into a 25cm^2 (T25) culture flask (Sarstedt) and grown until confluent.

2.3.2 Cell culture conditions and passaging

Cell lines were cultured in T25 flasks at 37°C in a 5% CO_2 atmosphere. The human colonic carcinoma Caco-2 cell line (ATCC HTB-37), the human cervix carcinoma HeLa cell line (ATCC CCL-23) and the African green monkey kidney Vero cell line (ATCC CCL-81) were grown in DMEM containing high glucose levels, supplemented with 1x non-essential amino acids (Sigma), 10% foetal bovine serum (FBS; Sigma) and 4mM L-glutamine (Sigma). The human colonic carcinoma T84 cell line (ATCC CCL-248) was cultured in DMEM/F-12 medium (Sigma), supplemented with 10% FBS (Sigma) and

2.5mM L-glutamine (Sigma). Cells grown in T25 flasks were provided with 7mL culture medium.

Cells were allowed to grow to full confluence prior to passage and/or seeding into wells for experimentation. Upon reaching confluence in T25 flasks, cell medium was removed, and the cells were washed with sterile PBS. For T84 cells, prior to trypsinisation, cells were briefly rinsed with 500µL of 0.25% trypsin-0.02% ethylenediaminetetraacetic acid (EDTA) solution (Sigma). Following this, 500µL of 0.25% trypsin-EDTA solution was added to the monolayer and incubated at 37°C until cell detachment from the culture flask base. Cell aggregates were homogenised by repeated pipette aspiration in 4.5mL of cell culture medium. Once fully mixed, cell suspension was transferred into new culture flasks at a dilution ratio of 1:5 (T84 cells), 1:10 (Caco-2, Hep-2 cells) or 1:20 (Vero cells).

2.3.3 Seeding adhesion plates for OMV internalisation assay

After trypsinisation and resuspension of cells, in order to distinguish dead cells, 50µL of the cell suspension was diluted with 50µL of 0.4% (v/v) trypan blue solution (Sigma) which would stain dead cells blue. The cell suspension was loaded into a Neubauer counting chamber (Hawksley; depth 0.1mm) and inspected using an inverted light microscope (Zeiss, Invertoscope ID03). To achieve the number of cells per mL, the average sum of the number of viable cells visible in two haemocytometer fields multiplied by 10^4 was calculated.

Succeeding this, the following equation was used to calculate the volume of the cell suspension needed for seeding into cell culture wells:

Total volume of the cell suspension needed for seeding = total number of cells required/cell concentration of cell suspension (cells per mL)

This volume was then diluted into the required volume of culture medium needed for seeding.

Cells were seeded into 24-well plates (Sarstedt), containing sterile circular coverslips (13mm diameter, Academy Science Products) which allow for subsequent staining and microscopy analysis. A mL of cell suspension and medium was added per well, with seeding cell densities of 1.5 x 10^5/well for T84 and Vero cells, 1.2 x 10^5 cells/well for Caco-2 cells, and 1.0 x 10^5 cells/well for HEp-2 cells being added. Seeded plates were incubated at 37°C in a 5% CO_2 atmosphere, with the culture medium being exchanged the day before use.

2.3.4 Seeding cells on Transwell inserts

Transwells were used in order to grow polarised epithelial cells thereby mimicking the intestinal epithelial layer. Caco-2 cells were grown on polyester Transwells with an insert membrane growth area of 1.12cm^2 and pore sizes of 0.4µm (Corning Costar). Cells were seeded in the apical compartment at a seeding density of 5 x 10^4 cells per well, with a total volume of 500µL of supplemented DMEM and cells in the inner chamber and 1500µL of DMEM in the outer chamber. One well per plate was not seeded with cells allowing a baseline control when measuring the transepithelial electrical resistance (TEER).

After seeding, the medium was exchanged after four days of growth to prevent acidification by replacing 300µL in the inner chamber and 800µL in the outer chamber. Medium was then changed every other day using the same volumes. From day 10, TEER was measured by using an EVOM voltohmmeter with an STX2 chopstick electrode (WPI) to assess polarisation and barrier formation of Caco-2 cells. A steady TEER of 1500 $\Omega \times cm^2$ for Caco-2 cells indicated full differentiation which was typically reached after 14 days of growth.

To avoid contamination, culture medium was supplemented with 1% (v/v) penicillin-streptomycin (10,000 U/ml and 10mg/ml stock, respectively; Sigma). Antibiotics were removed the day before infection by replacing the medium with supplemented DMEM without antibiotics.

2.4 Colonoid culture

2.4.1 Dissociation of intestinal organoids and seeding on Transwell inserts

Colonoid lines derived from histologically normal endoscopic biopsies of the transverse colon of a male patient (60-year-old) were established by S. Schüller. Colonoid cell lines at passage 5 were used to examine the interaction between EHEC OMVs and two-dimensional colonoid cultures.

To establish two-dimensional colonoid cultures, polyester 6.5mm Transwell® (Corning) with an insert membrane growth area of 0.33cm^2 and pore sizes of 0.4µm were first coated with 100µL of human collagen IV (at a final concentration of 35µg/mL from a 1mg/mL stock; Sigma) and incubated for two days at 4^{o}C. After removing the collagen solution, the filters were washed twice with complete medium without growth factor (CMGF-; DMEM/F-12 medium (Sigma) supplemented with 5mL 1M HEPES at pH 8.0 (Sigma) and 5 mL GlutaMAX-I (Thermo Fisher Scientific) per 500 mL bottle).

Culture of two-dimensional colonoids was performed as described by In *et al.* (2016b). Briefly, colonoids grown on Matrigel were suspended in 600µL of Gentle Cell Dissociation Reagent (Stemcell Technologies) and the plate was placed on an orbital shaker at 200 rpm for 10 minutes at room temperature. Subsequently, the sample was mixed and collected into a tube after which two volumes of CMGF- was added. This was centrifuged at 240 x *g* for 10 minutes at 4^{o}C.

With enough volume to add 100µL per filter insert, the cell pellet was resuspended in warm CMGF+ (made up of 11.2mL of CMGF-, 25mL of Wnt-3A-conditioned medium (made internally), 7.5mL of R-spondin 1-conditioned medium (made internally), 5mL of noggin-conditioned medium (made internally), 1mL B27 (100µL of N-Acetyl-L-cysteine (500 mM stock solution in dd$H_2$0m; Sigma)), 50µL of human epidermal growth factor (50µg/mL stock solution in PBS/0.1% bovine serum albumin (BSA; Sigma), Sigma), 5µL of [Leu15]-gastrin (100µM stock solution in PBS/0.1% BSA; Sigma), 50µL of A 83-01 (500µM stock solution in DMSO; Sigma), 5µL of SB 202190 (100 mM stock solution in DMSO; Sigma), 100µL of primocin (at 50 mg/mL; Fisher Scientific), supplemented with 10µM CHIR 99021 (Sigma) and 10µM Y-27632 (Sigma).

Organoids from one Matrigel droplet allows for the seeding of two 6.5mm Transwell®. Prior to adding cell suspension into wells, 600µL of CMGF+ was added into the outer chamber and then 100µL of cell suspension was added per filter insert. The plates were then incubated at 37°C in air supplemented with 5% CO_2. Two days after seeding, CMGF+ was replaced. Medium was then exchanged every 2 - 3 days until confluence was reached. TEER was measured (as described in section 2.3.3) to assess polarisation and barrier formation, with a steady TEER of 300 $\Omega \times cm^2$ indicating growth and polarisation. After two weeks, to differentiate organoid monolayers, CMGF+ lacking Wnt-3A-conditioned medium, R-spondin 1 conditioned medium, SB 202190 and primocin was used, with medium replaced every 2 days for 5 days.

2.5 Outer membrane vesicle isolation

EHEC overnight cultures (prepared as indicated in section 2.1) were inoculated at a 1:100 dilution into media in either Falcon tubes or T75 flasks. Once grown in the desired conditions, a total of 1.1mL of the bacterial culture samples per flask/Falcon tube was collected for OD_{600} absorbance measurements and viable cell count determination by using the Miles and Misra technique (as indicated in section 2.2).

To purify OMVs, bacterial cultures were spun at 4000 x *g* for 15 minutes at 4°C in 25mL aliquots in 50mL Falcon tubes. The obtained supernatant containing OMVs was then filter-sterilised using polypropylene filters with pore sizes of 0.45µm (Fisher Scientific). The sterile supernatant was then concentrated using cellulose membranes centrifugal units, with a molecular weight cut-off (MWCO) of 100 kDa (Merck Millipore) by spinning the samples at 6000 x *g* at 4°C. Once the whole supernatant was concentrated to 1mL, 15mL of PBS was added to the concentrated sample and spun at 6000 x *g* at 4°C until the sample was concentrated to a final volume of 1mL. OMVs were subsequently pelleted by ultracentrifugation (Beckman Coulter sealing tubes, Beckman LE-80 Ultracentrifuge) at 130,000 x *g* for 2 hours at 4°C, with the pellet being re-suspended in 500µL PBS. To confirm sterility, 10µL of OMV preparation samples were spotted onto LB agar plates and incubated overnight at 37°C.

To quantify OMV yields by Bradford protein assay and Sodium dodecyl sulphate polyacrylamide gel electrophoresis (SDS-PAGE), Amicon Ultra 0.5 centrifugal devices with cellulose membrane filter with a 100 kDa MWCO (Merck Millipore) were used to concentrate samples. In order to activate the filter devices, 500µL of d.H_2O was added into the filter device and spun in a microcentrifuge at 14,000 x *g* until a volume of 20µL was reached. OMV samples were then loaded and spun at the same speed until concentrated to a final volume of 30µL.

2.6 Bradford protein assay

Protein content of OMV samples was determined using the Bio-Rad protein assay which is based on the Bradford dye-binding method. Briefly, 10µL of bovine serum albumin (BSA; Sigma) protein standards (0µg/mL to 500µg/mL) and OMV diluted samples (1:5) were prepared and aliquoted into microtiter plate wells. Samples and standards were mixed with 190µL of Bio-Rad protein assay dye reagent solution (prepared by a 1:4 dilution in dH_2O) and incubated for 5 minutes at room

temperature. Absorbance at 595nm was measured using a benchmark plus plate reader (Bio-Rad).

2.7 Sodium dodecyl sulphate polyacrylamide gel electrophoresis

OMV-associated proteins were separated by Sodium dodecyl sulphate polyacrylamide gel electrophoresis (SDS-PAGE) using a Mini-PROTEAN Tetra System device (Bio-rad). The running gel (12.5%) was made of 2.5mL of 4x running gel buffer (1.5M Tris (Fisher Scientific), 0.4% (w/v) SDS (Fisher Scientific) adjusted to pH 8.8 with concentrated hydrochloric acid (HCl)), 4mL of Acrylamide/Bis-acrylamide (30% solution; Sigma), 3.5mL of d.H_2O, 50µL of 10% Ammonium persulfate (APS; Sigma) and 10µL of Tetramethylethylenediamine (TEMED; Sigma). This was overlaid by a 3% stacking gel prepared from 1.25mL of 4x stacking gel buffer (0.5M Tris, 0.4% (w/v) SDS adjusted to pH 6.8 with concentrated HCl), 500µL of Acrylamide/Bis-acrylamide (30% solution), 3.2mL of d.H_20, 50µL of 10% APS and 5µL of TEMED. Well combs were inserted before polymerisation of the stacking gel. Once polymerised, gels were stored at 4^oC for up to a month.

To separate proteins, polyacrylamide gels were first inserted into the running tank filled with 1x Running buffer (diluted from a 10x Running Buffer (0.25M Tris, 2M Glycine at 144.0 g/L and 1% (w/v) SDS, at pH 8.3)). The combs were then removed, and the wells rinsed with 1x Running buffer. A total of 10µL of sample was mixed with 2.5µL of 5x Reducing sample buffer (RSB; 2.5mL Glycerol (Sigma), 0.5g SDS (Fisher Scientific), 625µL of Tris (Fisher Scientific), 0.39g of Dithiothreitol (ForMedium Ltd.), 5mL Bromophenol blue (Sigma) and 1.9mL of d.H_20) and denatured by boiling the sample on a heating block for 5 minutes. When OMVs were isolated from EHEC cultures grown with human cells, DMEM, DMEM/F-12 medium and SCEM, OMV samples were diluted 1:10 in PBS prior to boiling. Boiled samples were loaded into each well, along with 5µL of pre-stained protein marker (Blue Prestained Protein

Standard, Broad Range 11-190 kDa, NEB). Gels were run at 200V, 20W, 100 mA for 50 minutes using a Mini-PROTEAN Tetra Cell device (Bio-Rad).

At the end of the run, gels were removed from the glass plates and stained with GelCode TM Blue Safe Protein Stain (Thermo Fisher Scientific) according to the manufacturer's instructions. Gels were imaged using a FluorChemE system (proteinsimple).

For OmpA and OmpF/C densitometric quantification, ImageJ software was used (https://imagej.nih.gov/ij/; Java-based image processing program developed at the National Institutes of Health).

2.8 Western blot

In order to transfer separated proteins from a polyacrylamide gel onto Polyvinylidene difluoride membranes (VWR; GE Healthcare), membranes were first submerged in 100% methanol for 10 seconds and then submerged in blotting buffer (200mM Glycine, 25mM Tris at pH 8.8) for 15 minutes on a rocking platform. After protein separation, polyacrylamide gels were washed in d.H_20 for 5 minutes and then submerged in blotting buffer for 15 minutes on a rocking platform. Proteins were subsequently transferred onto the methanol treated membrane by wet blotting at 100V constant for 60 minutes in blotting buffer.

After protein transfer, membranes were blocked in 5% (w/v) skimmed milk powder in Tris buffered saline containing 0.05% (v/v) Tween-20 (TBST; 5M NaCl (Thermo Fisher Scientific), 1M Tris (Thermo Fisher Scientific), pH adjusted at 8.0 with HCl and 0.5 mL/L Tween-20 (Thermo Fisher Scientific)), at room temperature for 60 minutes on a rocking platform. After washing in TBST for 10 minutes, membranes were incubated with primary antibody which were diluted in TBST overnight at 4°C (Table 2.2).

After washing in TBST, blots were incubated with species specific horseradish peroxidase-conjugated anti-IgG (1:200,000 dilution in TBST, Sigma) for 60 minutes. This was followed by a 30-minute wash in TBST to remove non-bound antibodies. The membranes were developed using peroxide solution (Thermo Fisher Scientific) and Luminol enhancer solution (Thermo Fisher Scientific), prepared at a 1:1 ratio and imaged with a FluorChem E Imager (ProteinSimple).

Antibody	Species	Dilution	Source
Anti-OmpA	Rabbit	1:2000	Antibody Research Corporation
Anti-Stx2 204	Rabbit	1:1000	A. Kane, Tufts Medical Centre

Table 2.2: Primary antibodies used for Western blotting in this study.

2.9 Dynamic Light Scattering analysis

OMV size distribution was determined by using a Zatasizer Nano-ZS (Malvern Instruments, UK). After resuspending OMV pellets post-ultracentrifugation, to avoid artefacts due to multi-scattering, OMV samples were diluted 1:500 in 1mL of PBS. To measure samples, a standard operating procedure was set to using a laser wavelength of 659nm so to measure samples with a refractive index of 1.450 and an absorption of 0.001. Attained results were the sum of three measurements of eleven reads.

2.10 NanoParticle Tracking Analysis

OMV size and particle concentration were acquired by using a LM 12 viewing unit of a NanoSight LM10 instrument and its corresponding NanoParticle Tracking and Analysis (NTA) software system. This system provides a way to measure particle size in liquids by relating such particles to their Brownian motion. To analyse OMV sizes and concentrations, OMV suspensions were diluted in PBS to a concentration which

would allow optimum analysis by the software. Optical camera level and gain settings were manually set and were maintained for all analyses.

Each sample was evaluated three times for 60 seconds at room temperature. Frame sequences were evaluated using consistent manual particle detection and tracking boundaries.

2.11 EHEC growth analysis

EHEC growth was assessed in LB medium and SCEM with and without bile salts over a 24-hour period. Overnight EHEC cultures (prepared as indicated in section 2.1) were inoculated at 1:100 into LB medium or SCEM with or without bile salts and grown at 37^{o}C, shaking at 180 rpm. OD_{600} was measured hourly for the first 6 hours in LB and SCEM cultures and then at 24 hours (as indicated in section 2.1.1). Furthermore, at every second hour, viable bacteria counts were made for SCEM cultures containing and lacking bile salts for the first 6 hours and then at 24 hours (as indicated in section 2.1.1).

2.12 Examining the effect of carbon dioxide on OMV production and composition

To study the effect of CO_2 on EHEC OMV production and composition, overnight EHEC cultures (prepared as indicated in section 2.1) were inoculated at 1:100 into LB medium. EHEC cultures were grown in T75 flasks on a rocking platform, max speed at 37^{o}C for 24 hours in normal atmospheric conditions (air) or 5% CO_2/air (cell culture incubator).

At the end of the incubation, the media was collected and then treated for OMV isolation (as indicated in section 2.5). OMV yields were quantified by Bradford assay

and SDS-PAGE (as indicated in section 2.6 and 2.7, respectively). Furthermore, EHEC growth was assessed by viable bacterial counts and OD_{600} measurements (as indicated in section 2.2).

2.13 Examining the effect of the presence of human cells on OMV production and composition

To study the effect of human host cells on EHEC OMV production and composition, monolayers of cervical-derived HeLa cells or colonic-derived T84 cells were grown in T75 flasks and then infected with EHEC strains.

Four T75 flasks were seeded with cells and grown until confluence was reached. Growth medium was exchanged when required. Bacterial overnight cultures were prepared as indicated in section 2.1. On the day of infection, cell culture media was exchanged with 25mL of non-supplemented media (DMEM for HeLa cells and DMEM/F-12 medium for T84 cells) and two flasks were inoculated with 250µL of bacterial overnight culture (prepared as indicated in section 2.1). To examine whether human host cell derived contaminants would be present using the OMV purification protocol, the remaining two flasks were not infected and only incubated with non-supplemented medium. Furthermore, to examine the effect of the cell media on OMV production, overnight EHEC cultures (prepared as indicated in section 2.1) were inoculated at 1:100 into two T75 flasks containing non-supplemented medium. All six flasks were then incubated in 5% CO_2 atmosphere at 37^{o}C for 24 hours on a rocking platform at maximum speed. At the end of the incubation, the media was collected and then treated for OMV isolation (as indicated in section 2.5). OMV yields were quantified by Bradford assay and SDS-PAGE (as indicated in section 2.6 and 2.7, respectively). Furthermore, EHEC growth was assessed by viable bacterial counts and OD_{600} measurements (as indicated in section 2.2).

2.14 Examining the effect of bile salts on OMV integrity

To examine the effect of bile salts on OMV integrity, OMVs from bacterial cultures grown in SCEM lacking bile salts were incubated in SCEM media with and without bile salts for 18 hours in a shaking incubator at 180rpm. OMVs were separated from free proteins by using cellulose membrane centrifugal filter devices (100 kDa MWCO, Merck Millipore), spun at 14,000 x *g* in a microcentrifuge. Both the concentrated sample and flow through were collected.

To determine if proteins were present in the flow through, trichloroacetic acid (TCA, Sigma) precipitation was carried out. Flow-through samples and 100% TCA (w/v) in d.H_2O were cooled on ice for 15 minutes. Subsequently, both the sample and 100% TCA were mixed to make up a final concentration of 10% TCA. Samples were incubated for 30 minutes on ice, then spun at 21,000 *x g* in a microcentrifuge for 15 minutes at 4^oC. The supernatant was discarded carefully without disturbing the pellet and the pellet was re-suspended in 18µL of 1x RSB (from 5x RSB diluted in d.H_2O). If samples appeared yellow, 2µL of 2M of Tris was added to the sample in order to neutralise pH. Both the concentrate and flow through samples were separated by SDS-PAGE and analysed by Western blot (as indicated in section 2.7 and 2.8).

2.15 Lipophilic tracer staining of OMV

To stain OMVs with the lipophilic tracer Dil or DiO (Molecular probes), lipophilic tracer was added to the desired OMV aliquot at a 1:100 dilution and incubated for 30 minutes at 37^oC in the dark. To remove unbound dye, cellulose membrane centrifugal filter devices with 30 kDa MWCO (Merck Millipore) were used. In order to activate the filter devices, 500µL of d.H_2O was added into the filter device and spun in a microcentrifuge at 14,000 *x g* until a volume of 20µL was reached. The stained OMV sample was then added to the filter device and spun at the same speed until concentrated to a volume of 20µL. To wash the sample, 500µL of PBS was added to

the filter, and the sample was concentrated to a final volume 20µL. This was repeated three times. The sample was then collected by inverting the filter device into a clean sterile Eppendorf microcentrifuge tube and spinning at 1000 *x g* for 2 minutes.

2.16 Stx2 and OMV internalisation assays in eukaryotic cells

To examine the internalisation of Stx2, eukaryotic cells were grown in 24 well plates. Confluent cell monolayers replenished with supplemented cell medium eighteen hours prior to Stx2 incubation. On the day of Stx2 incubation, medium was removed and replenished with a total of 250µL of non-supplemented medium containing 1.25µg of pure Stx2 was added to cells grown in 24-well plates. After six hours, a further 250µL of non-supplemented medium was added per well for incubations lasting 24 hours. Incubations were made in 5% CO_2 atmosphere at 37^{o}C.

To examine the internalisation of OMVs in non-polarised cells, eukaryotic cells were grown in 24 well plates, yet cells were grown in transwell plate inserts to study OMV internalisation in polarised cells. Confluent cell monolayers were replenished with supplemented cell culture medium eighteen hours before OMV incubation with eukaryotic cell monolayers. On the day of OMV inoculation, cell culture medium was removed and replaced with non-supplemented cell culture medium.

In order to examine whether OMVs could be internalised by host eukaryotic cells, OMVs were isolated from EHEC LB cultures grown at 37^{o}C with 5% CO_2 supplementation in normal atmospheric conditions. To examine internalisation, initial experiments utilised lipophilic dyed (DiO- or DiI-) OMVs. Following this, non-dyed OMVs were used to investigate OMV intracellular trafficking and OMV translocation across eukaryotic cells.

A total of 250µL of non-supplemented medium containing 10µg of OMVs (as determined by protein content) was added to cells grown in 24-well plates or 1.12cm^2

transwell plates inserts. After six hours, a further 250µL of non-supplemented medium was added per well for incubations lasting 24 hours. Incubations were made in 5% CO_2 atmosphere at 37°C.

To examine whether OMVs would affect the barrier integrity of the polarised cell monolayers, TEER readings were measured prior to OMV incubation to confirm membrane integrity. Medium from both the apical and basolateral side of the polarised monolayer was replaced with fresh non-supplemented medium with the apical medium containing OMVs isolated from EHEC strain 85-170. Immediately after OMV addition, TEER readings were measured, corresponding to the first time point (t = 0). TEER measurements were made hourly for the first 5 hours and then at 24 hours, with measurements being converted to a percentage change in TEER values compared to the TEER value measured at t = 0. Furthermore, TEER values were normalised by subtracting the value of empty wells only containing cell medium from the TEER values gained at each time point. After five hours, a further 250µL of non-supplemented cell culture medium was added to wells which would be incubated with OMVs for 24 hours.

When examining the interaction between OMVs and colonoid two-dimensional monolayers grown on 0.33cm^2 transwell plate inserts, eighteen hours before OMV inoculation, medium was replaced with fresh CMGF+ lacking Wnt-3A-conditioned medium, R-spondin 1 conditioned medium, SB 202190 and primocin. On the day of the inoculation, medium from Transwells was removed and replaced with 50µL of non-supplemented DMEM/F-12 medium containing 2.5µg of OMVs (as determined by protein content). Incubations were made in 5% CO_2 atmosphere at 37°C. TEER measurements were made at the beginning of the experiment (t = 0) and then at 5 and 24 hours post-OMV inoculation. TEER measurements were converted to a percentage change in TEER values compared to the TEER value measured at t = 0. Furthermore, TEER values were normalised by subtracting the value of empty wells only containing cell medium from the TEER values gained at each time point. After five hours, a further 50µL of non-supplemented DMEM/F-12 medium was added to wells.

2.17 Immunofluorescence staining and image analysis

After completing an experiment, monolayers were washed in PBS and fixed with either 3.7% formaldehyde (FA) in PBS for 15 minutes, ice-cold methanol for 10 minutes on ice or ice-cold acetone-methanol (1:1) for 10 minutes on ice. After washing, fixed samples were permeabilised and non-specific binding sites were blocked with 0.1% Triton-X-100 (Sigma) and 0.5% BSA (Sigma) in PBS for 20 minutes at room temperature.

Samples were incubated with primary antibodies diluted in PBS containing 0.5% BSA for 1 hour at room temperature (table 2.3). The samples were then washed in PBS for 10 minutes on a rocking platform, and subsequently incubated with species specific antibodies labelled with either Alexa Fluor 488, 568 or 647 (Life Technologies, 1:400) diluted in PBS containing 0.5% BSA for 30 minutes at room temperature in the dark. When desired, 4',6-diamidino-2-phenylindole (DAPI; 1:5000; Roche) and fluorescein isothiocyanate (FITC)-conjugated phalloidin (1:200; Sigma) were added during the final antibody incubation to detect for DNA and filamentous actin, respectively. Following the final antibody incubation, samples were washed in PBS for 30 minutes on a rocking platform and mounted on glass microscopy slides (R & L Slaughter) in Vectashield mountant (Vector Laboratories) to reduce photo-bleaching. Slides were stored at 4°C in the dark.

Samples were imaged using either a standard widefield fluorescence microscope (Zeiss Axio imager M2 or Leica DM6000 B microscope) or confocal microscope (Zeiss LSM800), using fixed exposure settings. Images were performed with up to four excitation wavelengths including 405nm (blue, DAPI), 488nm (green, FITC and Alexa-488 immunostaining), 561nm (red, Alexa-568 immunostaining) and 650nm (far red, Alexa-647 immunostaining). Imaging parameters are summarised in table 2.4 and 2.5. Furthermore, optimal pixel sizes were utilised when confocal microscopy was used.

Primary antibody	Host species	Dilution factor	Source	Fixation
Anti-P4HB antibody (ER)	Mouse	1:150	Abcam	3.7 % FA
Anti-58K Golgi protein antibody (Golgi apparatus)	Mouse	1:100	Abcam	100% methanol
Anti-LAMP1 antibody (Late endosomes/ lysosomes)	Mouse	1:500	Abcam	Acetone and methanol mixture (1:1)
Anti-*Escherichia coli* specific LPS antibody (OMVs)	Rabbit	1:1000	US Biological	3.7% FA, 100% methanol or acetone and methanol mixture (1:1)
Anti-Stx2 204	Rabbit	1:1000	A. Kane, Tufts Medical Centre	3.7% FA or 100% methanol

Table 2.3: Primary antibodies used for immunofluorescence staining in this study.

To quantify colocalization between signals of interest, images were assessed using the JaCoP plugin (Bolte and Cordelières, 2006) in ImageJ (National Institute of Health). Single cells were selected and analysed to determine the Manders colocalization coefficients. Prior to measurements, threshold values for M1 and M2 were set manually.

Microscope	Magnification	NA	Immersion	Actual pixel size, x/y (nm)
Zeiss Axio Imager M2	10x	0.3	Air	645
	20x	0.5	Air	323
	40x	0.75	Water	161
	63x	1.4	Oil	102
	100x	1.3	Oil	110
Leica Ariol 6000B	40x	0.75	Air	185
	63x	1.3	Oil	118

Table 2.4: Widefield microscope specifications and the pixel sizes of images taken for this study.

Microscope	Magnification	NA	Immersion	Actual pixel size, x/y (nm)
Zeiss LSM 800	40x	1.1	Water	106
	63x	1.2	Water	76

Table 2.5: Confocal microscope specifications and the pixel sizes of images taken for this study.

2.18 Transmission electron microscopy

After ultracentrifugation, OMV pellets were resuspended in 250µL of PBS. Following this, 5µL was applied onto carbon coated Formvar copper grids (Agar Scientific) for 2 minutes. The samples were negatively stained by washed the grid six times with 2% (w/v) uranyle acetate (BDH) solution in water for 2 minutes. Excess stain was removed, and the grid were air-dried. The samples were examined and imaged by Kathyrn Cross (Electron Microscopy Facility, Institute of Food Research) using a Tecnai G2 20 Twin transmission electron microscope (FEI) at 200 kV.

2.19 Statistical analysis

GraphPad Prism Version 6 software was used for statistical analysis for this project. For the comparison of two groups, results were analysed using parametric student *T*-test. For the comparison of three or more groups, parametric analysis of variance (ANOVA) with Tukey's post-hoc multiple comparison test was used. Results are expressed as means +/- standard deviation (SD). A *P* value of < 0.05 was considered significant, with degrees of statistical significance presented as: * = $P < 0.05$; ** = $P < 0.01$; *** = $P < 0.001$, **** = $P < 0.0001$.

Chapter Three: The influence of the colonic milieu on EHEC OMV production

3.1 Introduction

Prior to colonic colonisation, EHEC is exposed to various environmental stressors in the gastrointestinal tract. Examples of abiotic stresses include changes in pH, limited iron levels and the presence of bile salts (Fallingborg, 1999, Hofmann, 2009, Lacy *et al.*, 2011). Biotic stressors are instigated by cells which line the gastrointestinal tract, releasing neurochemicals and various antimicrobial compounds such as nitric oxide, defensins and antimicrobial peptides (Sharma *et al.*, 2007, Muniz *et al.*, 2012). Furthermore, EHEC competes for essential compounds as nutritional molecules are consumed by the microbiota (Blachier *et al.*, 2009, Rowland *et al.*, 2018). These different stressors can influence the expression of different virulence genes, consequently coordinating the successive colonisation of EHEC in the host. Furthermore, EHEC has adapted various methods to resist against such host stressors such as altering outer membrane lipid composition to resist changes in pH, and increased expression of efflux pumps to dispose of intracellular bile salts (Thanassi *et al.*, 1997, Yuk and Marshall, 2004).

Conversely, OMVs have also been shown to perform various roles which can aid bacterial survival and contribute to bacterial pathogenesis. A role OMVs have been implicated with, includes the transferral of virulence factors such as toxins to target host cells (Ricci *et al.*, 2005, Parker *et al.*, 2010, Chatterjee and Chaudhuri, 2011, Horstman and Kuehn, 2000, Kesty *et al.*, 2004, Bomberger *et al.*, 2009, Bielaszewska *et al.*, 2013, Bielaszewska *et al.*, 2017). The secretion of such virulence factors in OMVs ensures their transportation over long distances whilst they are protected from external environments to host cells. Another role which OMVs are involve in includes the clearing of misfolded and denatured proteins from the periplasmic space when bacteria are exposed to high temperatures (McBroom and Kuehn, 2007). OMVs can also defend bacteria from antimicrobial compounds through sequestration and degradation of such components as enzymes such as cephalosporinases can be encapsulated in OMVs (McBroom and Kuehn, 2007, Ciofu *et al.*, 2000, Kim *et al.*, 2018, Liao *et al.*, 2015, Stentz *et al.*, 2015, Kim *et al.*, 2020, Kulkarni *et al.*, 2015). Accordingly, increased OMV production has been observed in bacteria when exposed

to stressful conditions, including high temperatures, acidic pH, exposure to antimicrobial agents, reduced iron levels, and oxidative stress (Manning and Kuehn, 2011, McBroom and Kuehn, 2007, Roier *et al.*, 2016, Bauwens *et al.*, 2017b, Lekmeechai *et al.*, 2018).

To evaluate OMV production in response to different environmental conditions, previous studies have isolated OMVs from bacterial cultures grown under respective conditions by removing intact bacteria from the culture through centrifugation and sterile filtration (Bauwens *et al.*, 2017b, Bauwens *et al.*, 2017a, Manning and Kuehn, 2011, MacDonald and Kuehn, 2013, Horstman and Kuehn, 2000). Following this, the sterile supernatant undergoes ultrafiltration, typically using a membrane with a 100 kDa molecular weight cut-off (MWCO; Chutkan *et al.*, 2013). To achieve this, studies have utilised different ultrafiltration arrangements such as: (i) ultrafiltration driven by pumping the solution through a membrane, (ii) tangential flow (crossflow) filtration concentrator, and (iii) centrifugal ultrafiltration units (Klimentová and Stulík, 2015, Stentz *et al.*, 2015, Bauwens *et al.*, 2017b, Jones *et al.*, 2020).

Subsequent quantification of OMVs can be performed through different methods. Since proteins are one of the major constituents of OMVs, protein-based techniques such as Bradford protein assays have been used to quantify OMV yield (Bradford, 1976, Klimentová and Stulík, 2015). Alternatively, previous studies have quantified *E. coli* OMV yields by densitometric measurements of the ubiquitously located outer membrane proteins (Omp) F/C and A, after proteins separation by SDS-PAGE (McBroom and Kuehn, 2007, Manning and Kuehn, 2011, Horstman and Kuehn, 2000, Lee *et al.*, 2007, Schwechheimer *et al.*, 2014, Bonnington and Kuehn, 2016).

OMVs can also be enumerated by nanoparticle tracking analysis (NTA), with the size and concentration of OMVs being determined (Saveyn *et al.*, 2010, Hong *et al.*, 2019, Gerritzen *et al.*, 2017, Vestad *et al.*, 2017). NTA determines the Brownian motion of particles in a solution by a camera which records the scattered light produced by the particles when a laser bean illuminates the sample. Dynamic light scattering (DLS) may also be used to determine the size distribution of OMVs (Stetefeld *et al.*, 2016).

To achieve measurements by DLS, the Brownian motion of particles in the suspension is measured by quantifying the rate at which the intensity of scattered light fluctuates due to diffusing particles. DLS software determines the diffusion coefficient of OMVs resulting in the particle sizes being determined (Hallett *et al.*, 1991, Kim *et al.*, 2018, Kulkarni *et al.*, 2015). Electron microscopy is another technique which has been used to visualise and determine OMV sizes (Kolling and Matthews, 1999, Parker *et al.*, 2010, Bielaszewska *et al.*, 2013).

When quantifying OMV yield, it is vital to normalise results due to differences in bacterial growth under different conditions. Previous studies have used various methods to normalise data such as OD_{600}, total cfu, cfu/mL or bacterial pellet weight (Bauwens *et al.*, 2017b, Deatherage *et al.*, 2009, McBroom *et al.*, 2006, Wessel *et al.*, 2013, Schwechheimer *et al.*, 2015, Schwechheimer *et al.*, 2014). In this investigation, OMV production was normalised by OD_{600} rather than viable bacterial counts (cfu) to account for OMVs produced by bacteria which have died prior to OMV isolation.

As OMVs are known to protect bacteria from external stresses, this study aimed to assess the influence of the colonic milieu on EHEC OMV production. Since the colonic milieu has various components which can stress EHEC, it is hypothesised that colonic conditions investigated in this study increase OMV production. This was elucidated by addressing the following objectives:

1. Establishing a protocol for EHEC OMV isolation and subsequent analysis of quantity, size and protein composition.
2. Characterising the effect of growth phase and different media composition on OMV production.
3. Determining the influence of 5% carbon dioxide, colonic host cells, simulated colonic environment medium (SCEM) and bile salts on EHEC OMV production.

3.2 Results

3.2.1 Establishing a protocol for OMV isolation from EHEC cultures

To develop a standard protocol for EHEC OMV isolation, Stx-negative EHEC strains TUV 93-0 and 85-170 were grown in LB medium shaking at 37^{o}C for 24 hours. After centrifugation, the supernatant was sterilised by using filter units with 0.45µm pore sizes to ensure the collection of larger OMVs. The filtered supernatant was then concentrated by ultrafiltration using centrifugal units made up of cellulose membranes with a 100 kDa MWCO.

Since previous studies have isolated OMVs through crossflow tangential filtration without an ultracentrifugation (UC) step, it was examined whether UC was necessary for this study after samples undergo ultrafiltration using centrifugal units (Stentz *et al.*, 2015, Jones *et al.*, 2020). To elucidate this, half of the sample was subjected to UC and the protein profiles were examined by SDS-PAGE. As shown in Fig. 3.1, UC samples showed two protein bands with a molecular size of approximately 32 kDa, which correspond to the *E. coli* outer membrane proteins (Omp) F/C and A, generally used for *E. coli* OMV quantification (McBroom and Kuehn, 2007, Manning and Kuehn, 2011, Horstman and Kuehn, 2000, Lee *et al.*, 2007, Schwechheimer *et al.*, 2014, Bonnington and Kuehn, 2016). However, these bands were obscured by contaminating protein bands in samples not subjected to UC, hence indicating the requirement of an UC step. To verify the absence of viable EHEC, OMV samples were plated onto LB agar plates, which resulted in no growth.

OMV samples were subsequently labelled with lipophilic dyes DiO and DiI, which integrate into the phospholipid membrane of OMVs. As shown in Fig. 3.2, the images produced by florescence microscopy revealed florescent spherical entities, suggesting the presence of small phospholipid bodies. OMV samples were also subjected to transmission electron microscopy which demonstrated the presence of spherical bodies with diameters of 20nm to 120nm (Fig. 3.3, arrows).

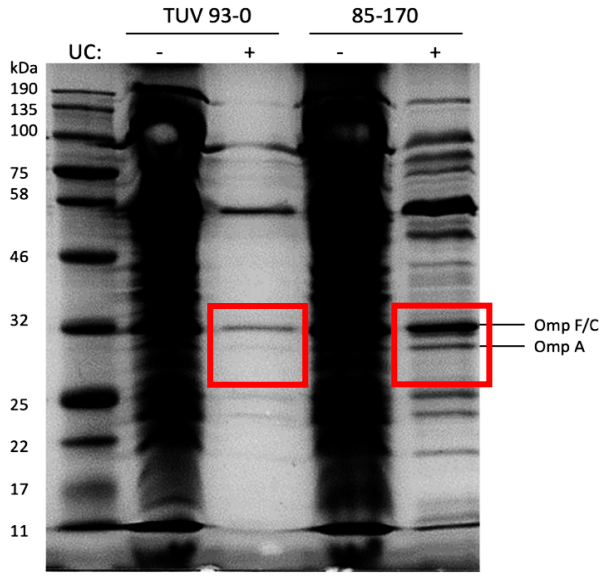

Figure 3.1: Ultracentrifugation is required for EHEC OMV isolation. Overnight cultures of EHEC strain TUV 93-0 and 85-170 were inoculated in LB medium (1:100) and grown shaking at 37°C for 24 hours. OMVs were subsequently concentrated from supernatants and subjected to UC (+) or left untreated (-). Proteins were separated by SDS-PAGE. OmpF/C and OmpA are highlighted. Gel image is representative of two independent experiments.

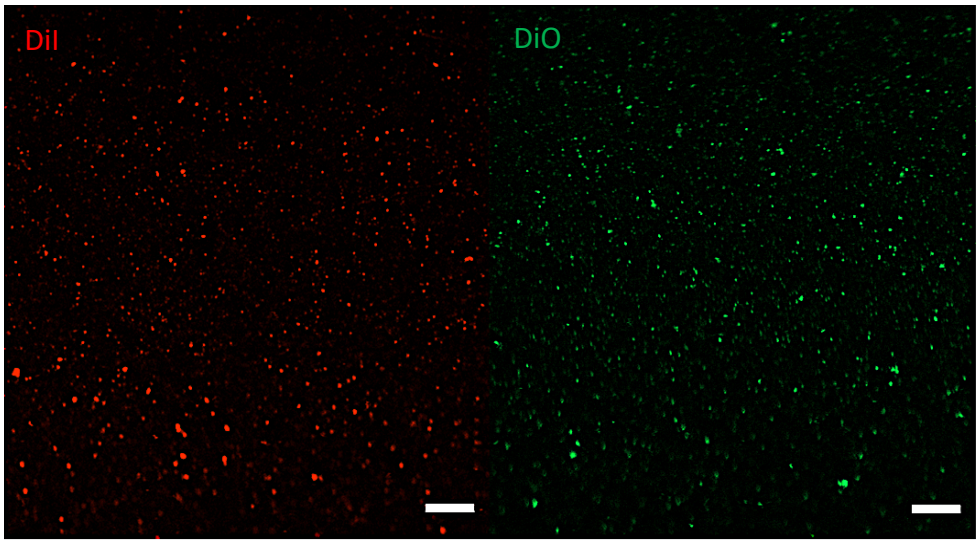

Figure 3.2: Fluorescence micrograph of OMVs isolated from EHEC 85-170 grown in LB medium for 24 hours labelled with DiI or DiO lipophilic dye. Isolated OMVs were labelled with dye DiI (red) or DiO (green). Shown are representative images from three independent experiments. Images were produced at a resolution as close to the optimal resolution permitted by the system. Images were attained by using a Zeiss Axio imager M2 widefield microscopy fitted with a 40x water emersion objective (EC Plan-Neofluar 40x, NA = 0.75, Zeiss). Scale bars = 10µm.

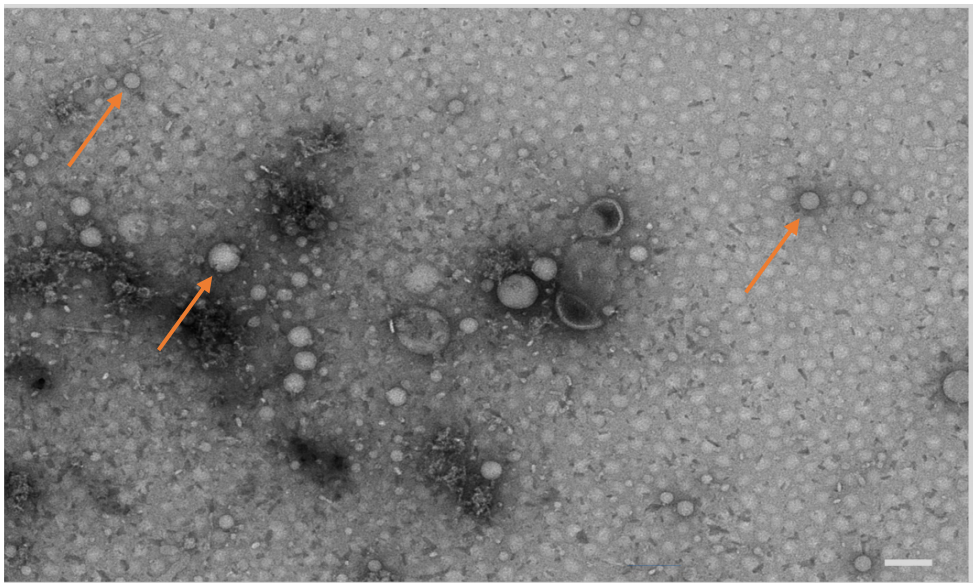

Figure 3.3: Transmission electron micrograph of OMVs isolated from EHEC 85-170 grown in LB medium for 24 hours. Shown are representative images of two independent experiments. Arrows indicate OMVs. Scale bar = 100nm.

Previous studies have demonstrated that medium components can be detected in OMV sample preparations, which can affect subsequent analysis (Cecil *et al.*, 2016). To exclude the presence of LB medium contaminants in OMV preparations, cultures of EHEC strain 85-170 grown in LB and sterile LB medium were treated for OMV purification using the established protocol. Samples were subsequently examined using SDS-PAGE and assessed by dynamic light scattering (DLS) which would detect nanoparticle contaminants.

The resulting polyacrylamide gel revealed that the OMV preparation from cultured EHEC 85-170 demonstrated a similar protein profile to that shown in Fig. 3.4A. In contrast, no proteins were present in the samples obtained from sterile LB medium (Fig. 3.4A). In addition, DLS analysis did not detect any nanoparticles in the OMV preparation from the sterile medium sample, whereas nanoparticles (OMVs) with a size range of above 43.82nm and under 825nm were identified in samples from EHEC cultures (Fig. 3.4B). In conclusion, both these techniques confirm that LB medium contaminants are not present in EHEC OMV preparations. Therefore, it was decided that the optimised protocol will be used to isolate OMVs for this investigation (Fig. 3.5).

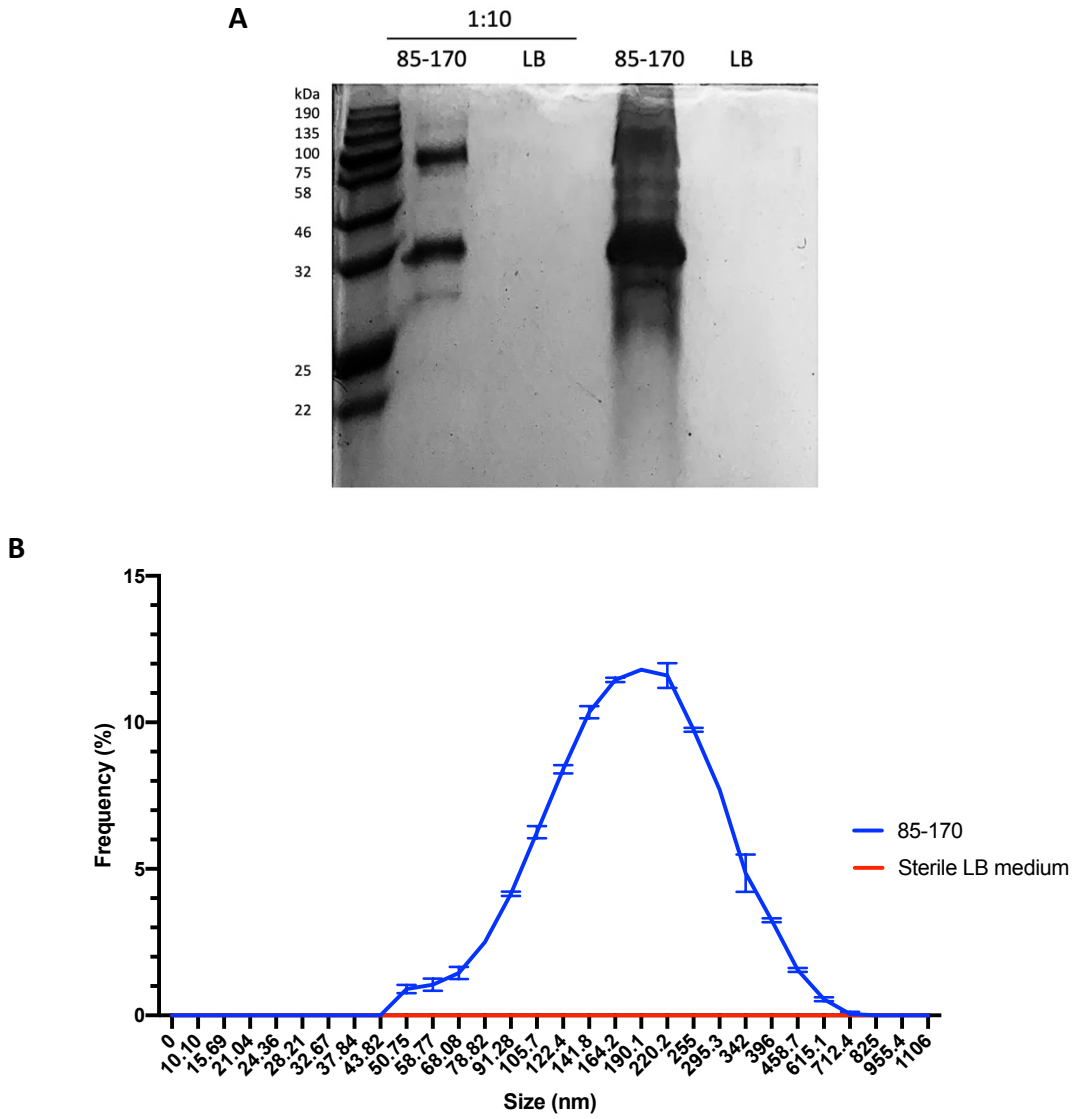

Figure 3.4: EHEC OMV preparations do not contain contaminants from LB medium. Overnight cultures of EHEC strain 85-170 were inoculated in LB medium (1:100) and grown shaking at 37°C for 24 hours. EHEC culture and the same volume of sterile LB medium were treated for OMV isolation. (A) Neat and diluted (1:10) samples were separated by SDS-PAGE. Gel image is representative of two independent experiments. (B) Dynamic light scattering confirms the absence of nanoparticles in LB samples. The size distribution of EHEC 85-170 as means ± SD of two independent experiments performed in duplicate.

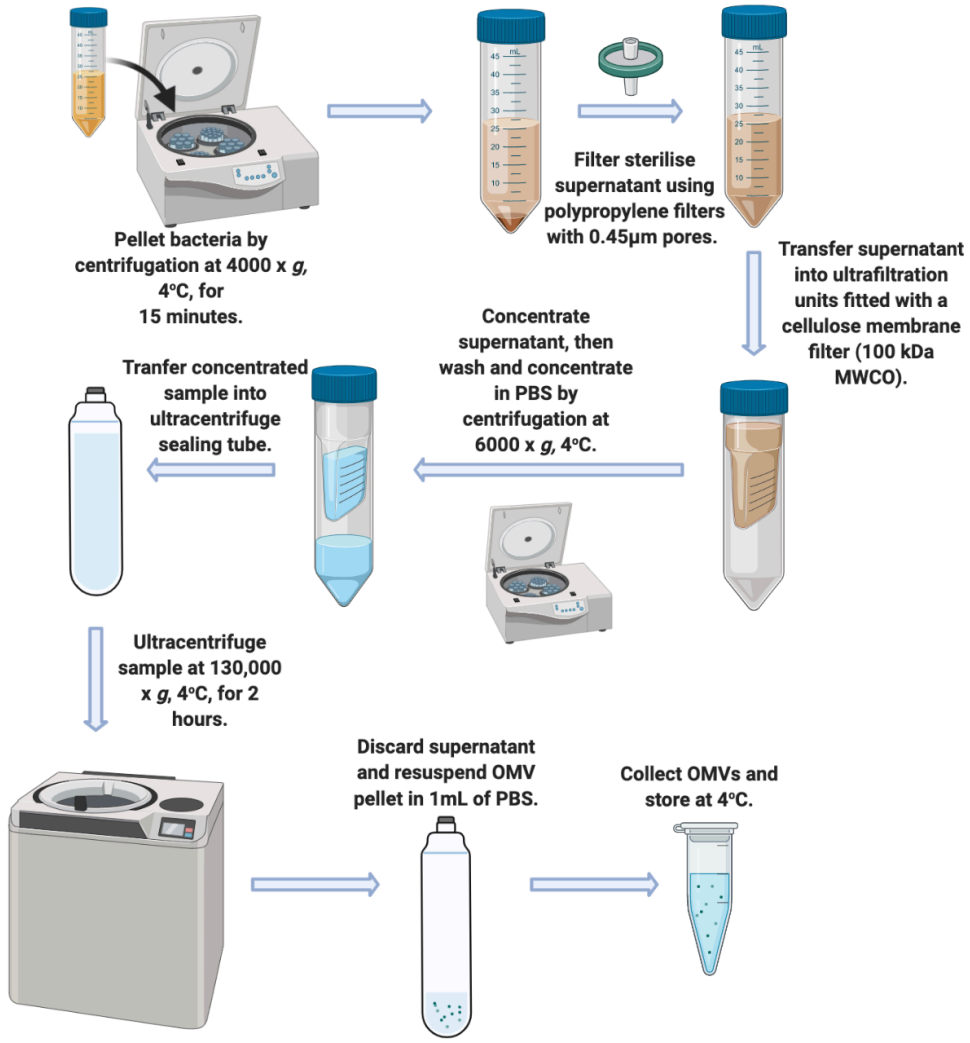

Figure 3.5: Flow chart of the protocol used to isolate EHEC OMVs in this investigation. MWCO = molecular weight cut-off. Created by BioRender.com

3.2.2 OMV yield increases during EHEC growth

Previous studies have demonstrated that OMV production is dependent on bacterial growth phase, with the highest OMV yield being attained from stationary phase cultures in various bacterial species including non-pathogenic *E. coli* (Gerritzen *et al.*, 2017, Bauman and Kuehn, 2006, Manabe *et al.*, 2013, McCaig *et al.*, 2013, Tashiro *et al.*, 2010). To determine the growth kinetics of EHEC strains TUV 93-0 and 85-170 in LB medium, overnight cultures of bacteria were inoculated at a 1:100 dilution in LB medium and grown shaking at 37°C. Growth was then evaluated by measuring the optical density at 600nm (OD_{600}) over 24-hour growth periods.

As shown in Fig. 3.6, both EHEC strains exhibit similar growth curves. After a 1-hour lag phase, both strains entered the exponential (log) growth phase. After 4 hours, bacterial growth slowed and the curve plateaued after 8 hours, indicating the approach of the stationary phase. Only a slight increase in OD_{600} was observed after 8 hours, indicating that stationary phase was reached.

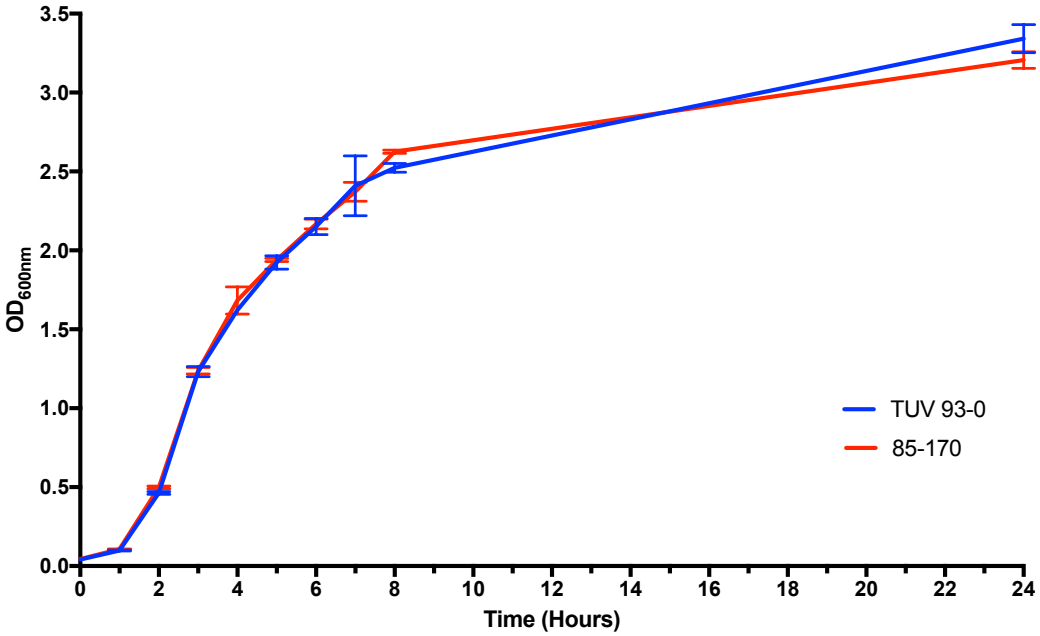

Figure 3.6: Growth curve of EHEC TUV 93-0 and 85-170 over a 24-hour growth period in LB medium. Overnight EHEC cultures were inoculated in LB medium (1:100) and grown shaking at 37°C. Data is shown as means ± SD of three independent experiments performed in duplicate.

To determine the effect of growth phase on OMV production, 4-, 7- and 24-hour time points were selected to represent the log, late log and stationary phase of EHEC growth, respectively. EHEC LB cultures were incubated for the respective time periods and OMVs were isolated according to the established protocol. OMV yields were quantified by Bradford protein assay and densitometric measurements of OmpA and OmpF/C after SDS-PAGE, hereafter termed as the Omp density area. All data was normalised to the OD_{600} of the harvested cultures to account for differences in bacterial numbers at different growth phases (Fig. 3.7). For both strains the lowest OD_{600} were attained from 4-hour cultures, with significantly higher OD_{600} being attained with longer incubation periods (Fig. 3.7; $P < 0.001$). However, the OD_{600} measurement of harvested cultures were significantly lower compared to those shown in Fig. 3.6 (Fig S1A, $P < 0.001$ and $P < 0.0001$ after 7- and 24-hour culture

periods for EHEC strain TUV 93-0, and $P < 0.01$ at 4 hours and $P < 0.001$ at longer incubation periods for EHEC strain 85-170).

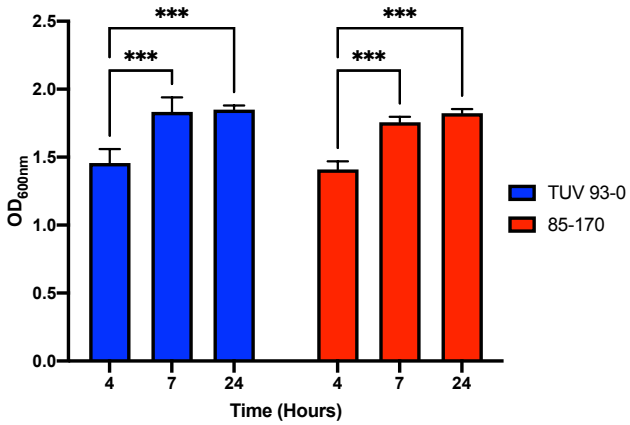

Figure 3.7: Higher OD_{600} values are obtained from EHEC cultures when grown for longer time periods. Overnight cultures of EHEC strains TUV 93-0 and 85-170 were inoculated in LB medium (1:100) and grown shaking at 37°C for 4, 7 and 24 hours. Data is shown as means ± SD of three independent experiments, performed in duplicates. *** = $P < 0.001$.

Data attained from Bradford protein assay showed that relative OMV protein content of both strains increased over time, with the highest yield being obtained from both strains after a 24-hour growth period (Fig. 3.8A), yet differences were only significant for EHEC strain 85-170 between 4-hour and 24-hour cultures ($P < 0.05$). On average, according to Bradford protein assay, OMV yields exhibited an 8-fold and 2.8-fold increase between 4- and 24-hour cultures for EHEC strains TUV 93-0 and 85-170, respectively. In addition, yields obtained from 24-hour cultures of EHEC strain 85-170 were significantly higher than those attained from 24-hour cultures of EHEC TUV 93-0 ($P < 0.05$).

SDS-PAGE indicated similar protein profiles of the isolated OMVs at the different time points (Fig. 3.8B). Additionally, increases in Omp band intensities for both EHEC strains were noted over time. This was confirmed by densitometric analysis of Omp proteins, with maximal OMV production at stationary phase (Fig. 3.8C). Using densitometric values, OMV yields exhibited a 4-fold and 6.5-fold increase between 4- and 24-hour cultures for EHEC strains TUV 93-0 and 85-170, respectively.

Furthermore, for both EHEC strains statistical tests confirmed significant differences between yields obtained between 4- and 24- hour cultures ($P < 0.001$ for EHEC strain TUV 93-0, $P < 0.0001$ for EHEC strain 85-170), and 7- and 24-hour cultures of the same strain ($P < 0.01$ for EHEC strain TUV 93-0, $P < 0.0001$ for EHEC strain 86-170). In addition, significantly higher OMVs yields were attained from EHEC 85-170 cultures compared to TUV 93-0 cultures after 7- ($P < 0.01$) and 24-hour ($P < 0.0001$) incubation periods.

Overall, both quantitative methods indicated that 24-hour stationary EHEC cultures produced the highest OMV yield, thus 24-hour growth cultures will be used for future experiments.

Having established optimal parameters for OMV isolation from Stx-negative EHEC strains, OMVs were subsequently isolated from the Stx-producing EHEC strain EDL933. Due to safety regulations in the containment level (CL) 3 laboratory, EHEC growth through of shaking cultures in Falcon tubes was not permitted. Instead, bacteria were grown in T75 cell culture flasks on a rocking platform at 37^{o}C. As well as measuring OD_{600} measurements, viable cell counts were quantified using the Miles and Misra method i.e., a 100µL aliquot of the culture was serially diluted and three 10µL spots per dilution were plated out on LB agar.

After 24 hours growth periods, EDL933 cultures reached an OD of 3.16 ± 0.18 and a viable cell count of 5.68×10^8 cfu/mL ± 2.37×10^8 was attained. OMVs were quantified by using Bradford protein assay and Omp densitometric analysis (table 3.1). Overall, both quantitative methods detected significantly higher OMV values than that of EHEC strain TUV 93-0 and 85-170 grown in shaking Falcon tubes, yet this could be due to cultures being grown in T75 flasks rather than in Falcon tubes. Furthermore, the OMV protein pattern (Fig. 3.9) was similar to those of strains TUV 93-0 and 85-170 with prominent Omp F/C and OmpA bands at approximately 32 kDa.

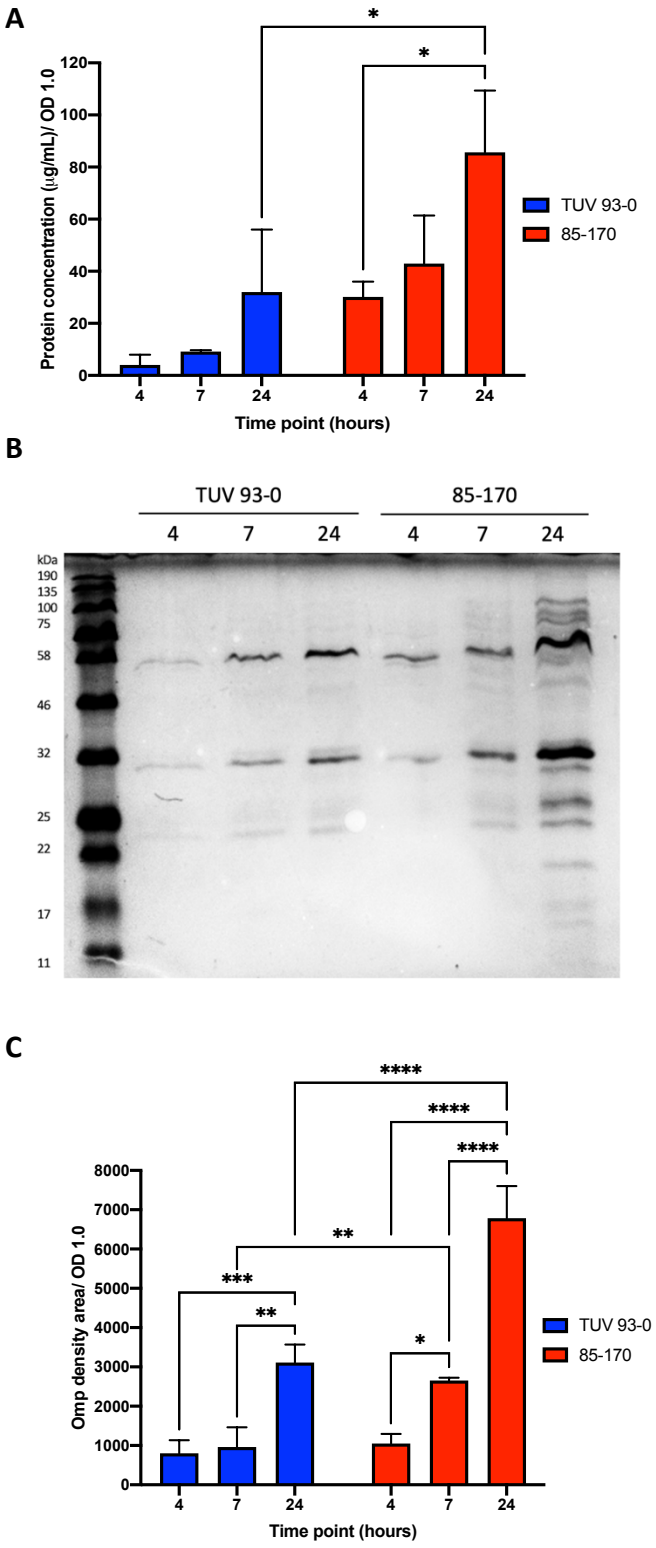

Figure 3.8: EHEC OMV production is dependent on growth phase. OMVs were isolated from 4-, 7- and 24- hour cultures of Stx-negative EHEC strains TUV 93-0 and 85-170. A) OMV quantification by Bradford protein assay. B) SDS-PAGE of OMV samples. C) Densitometric analysis of Omp proteins. Data was normalised to the OD_{600} of processed bacterial cultures. Data is shown as means ± SD of three independent experiments, performed in duplicates. * = $P < 0.05$, ** = $P < 0.01$, *** = $P < 0.001$, **** = $P < 0.0001$.

Mode of quantification	Values
Bradford protein assay (µg/mL)	365.9 ± 211
Omp density area	40564 ± 2427

Table 3.1: OMV production by stationary phase cultures of Stx-positive EHEC strain EDL933 grown in LB medium. OMVs were isolated from 24-hour EHEC cultures and quantified by Bradford protein assay and Omp densitometry. Data was normalised using OD_{600} of processed bacterial cultures. Data is shown as means ± SD of two independent experiments performed in triplicate.

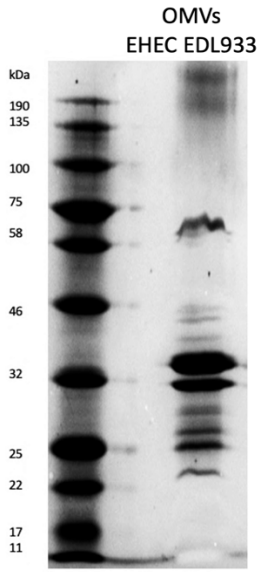

Figure 3.9: Protein composition of OMVs isolated from stationary phase LB cultures of EHEC EDL933. OMVs were isolated from 24-hour EHEC cultures and OMV proteins were separated by SDS-PAGE.

3.2.3 EHEC OMV production can be affected by different culture media

Previous studies have shown that bacterial growth in different media can affect OMV yield and composition (Choi *et al.*, 2014, Brameyer *et al.*, 2018, Vasilyeva *et al.*, 2009). Here, the effect of a different media (Tryptic soy broth (TSB) and DMEM/F-12 medium) on OMV production was assessed. In addition, EHEC growth was quantified by OD_{600} and viable cell counts (cfu/mL).

After a 24-hour growth period, similar viable cell counts were attained when EHEC strains were grown in TSB versus LB medium (Fig 3.10A). Additionally, similar OD_{600} values were obtained from EHEC strains grown in TSB compared to LB medium (Fig 3.10B).

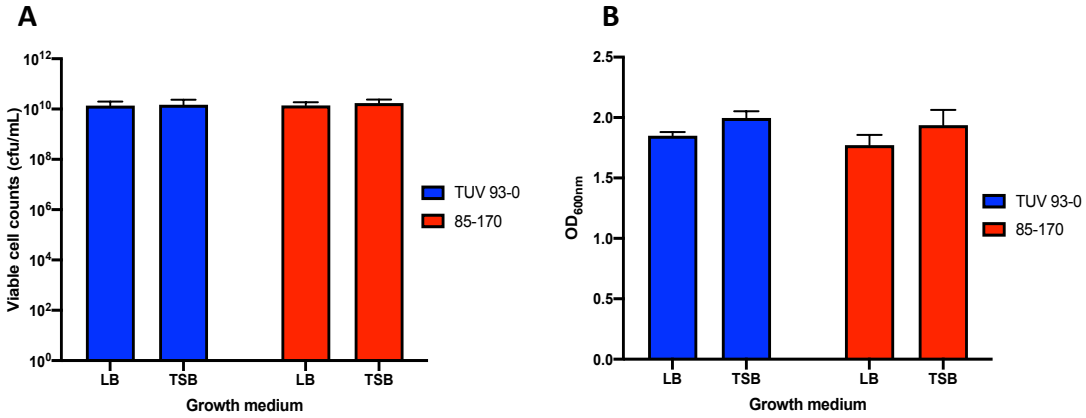

Figure 3.10: No significant difference in EHEC growth arises between TSB and LB cultures. Overnight cultures of EHEC strains TUV 93-0 and 85-170 were inoculated in either LB or TSB media (1:100) and grown shaking at 37°C for 24 hours. Growth was assessed by (A) viable cell counts and (B) OD_{600} measurements. Data is shown as means ± SD of at least two independent experiments performed in triplicates.

For both EHEC strains, Bradford protein assay demonstrated a significantly higher yield when OMVs were isolated from EHEC TSB cultures than in EHEC LB cultures (Fig. 3.11A, $P < 0.0001$). No significant differences were detected between EHEC strains when grown in the same medium. As shown on Fig. 3.11B, dissimilar OMV protein patterns were displayed when EHEC was cultured in different media. Omp densitometric analysis indicated that compared to LB, OMV production in TSB medium increased by 1.6 and 3 times for EHEC strains 85-170 and TUV 93-0, respectively, yet the increase was only significant for EHEC TUV 93-0 (Fig. 3.11C, $P < 0.05$).

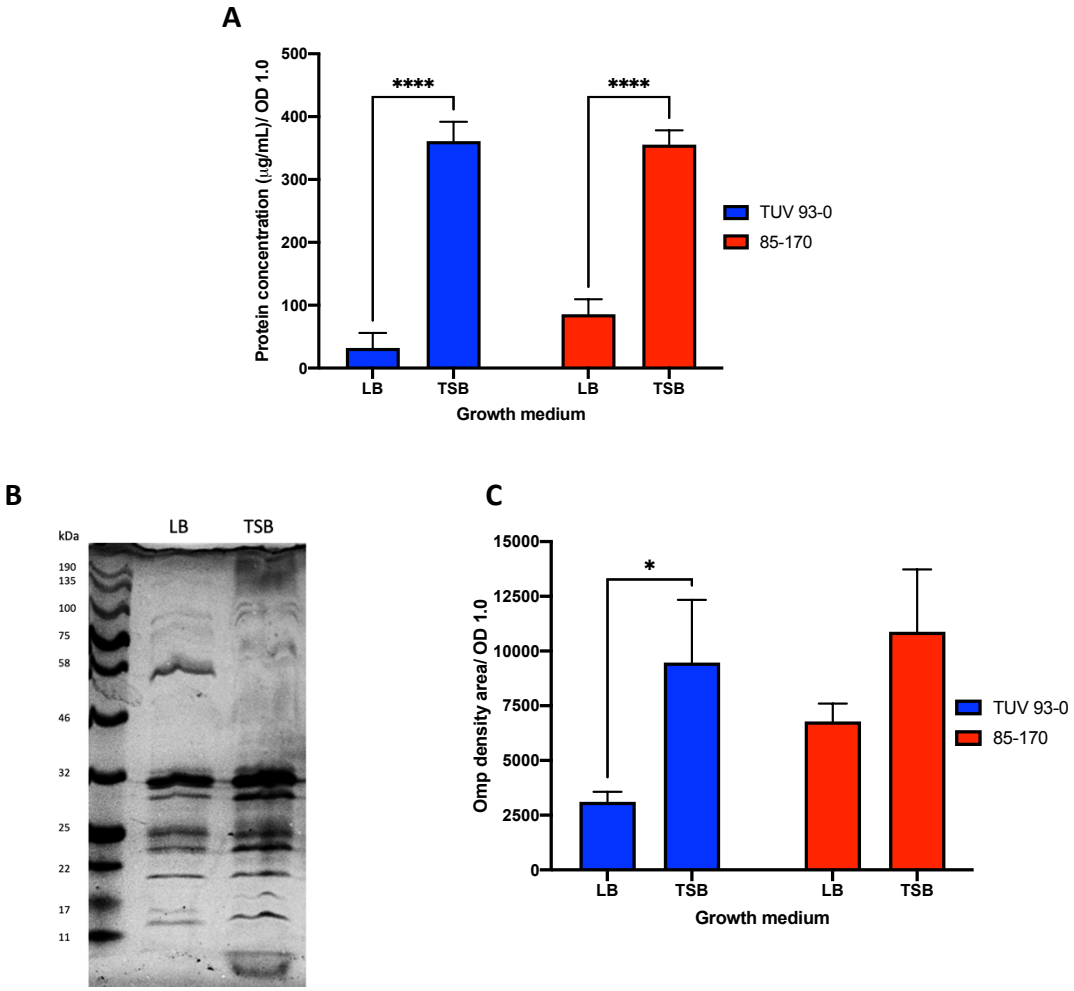

Figure 3.11: Compared to LB cultures, OMV production is higher when EHEC is cultured in TSB. OMVs were isolated from cultures of TUV 93-0 and 85-170 grown in either LB or TSB media for 24 hours. A) OMV quantification by Bradford protein assay. B) SDS-PAGE of OMV samples isolated EHEC 85-170. C) Densitometric analysis of Omp proteins. Data was normalised to the OD_{600} of processed bacterial cultures. Data is shown as means ± SD of at least three independent experiments, performed in duplicates. * = $P < 0.05$, **** = $P < 0.0001$.

To determine the effect of DMEM/F-12 medium on EHEC OMV production, Stx-positive EHEC strains EDL933 and 86-24 were used. For both strains, OMVs were isolated from LB or DMEM/F-12 cultures which were grown in T75 flasks at 37°C for 24 hours. Bacterial growth was also assessed by determining cell density and measuring OD_{600}. As shown in Fig. 3.12, similar viable cell counts (A) and OD_{600} values (B) were obtained for both EHEC strains between the two conditions examined. In addition, no significant difference in growth was detected between the two strains.

Isolated OMVs were separated on a polyacrylamide gel and protein profiles showed differences between strains and between conditions (Fig. 3.13A). Omp densitometric analysis indicated that both EHEC strains produced similar OMV yields as statistical tests failed to detect significant differences, even though strain 86-24 produced a 2.2- and 1.6-fold higher OMV yield than EHEC EDL933 when grown in LB and DMEM/F-12 media, respectively (Fig. 3.13B). Furthermore, even though the data suggests DMEM/F-12 cultures produced higher OMV yields than LB cultures, the differences did not reach statistical significance.

Previous studies have shown that EHEC OMVs isolated from Stx-producing strains contain Stx2 (Kolling and Matthews, 1999). To confirm the presence of Stx2 in OMVs isolated from EHEC strains EDL933 and 86-24, Western blots using a polyclonal Stx2-specific antiserum were performed. While the antibody detected purified Stx, a weak signal was detected in OMV samples, with the signal migrating at a slightly higher molecular weight compared to purified Stx2 (Fig. 3.14B). Equal loading of OMV samples was confirmed by probing the blot with anti-OmpA (Fig. 3.14A).

To determine if the faint signal was specific for Stx2, OMVs were purified from wild-type EDL933 and an isogenic Stx2 mutant. OMV protein profiles from both strains were similar (Fig. 3.15A) and equal loading was confirmed by probing for OmpA (Fig. 3.15B). However, blotting the membrane with anti-Stx2 produced signals for both the wild type and Stx-negative strain, indicating that the detected signals were not specific for Stx2 (Fig 3.15C).

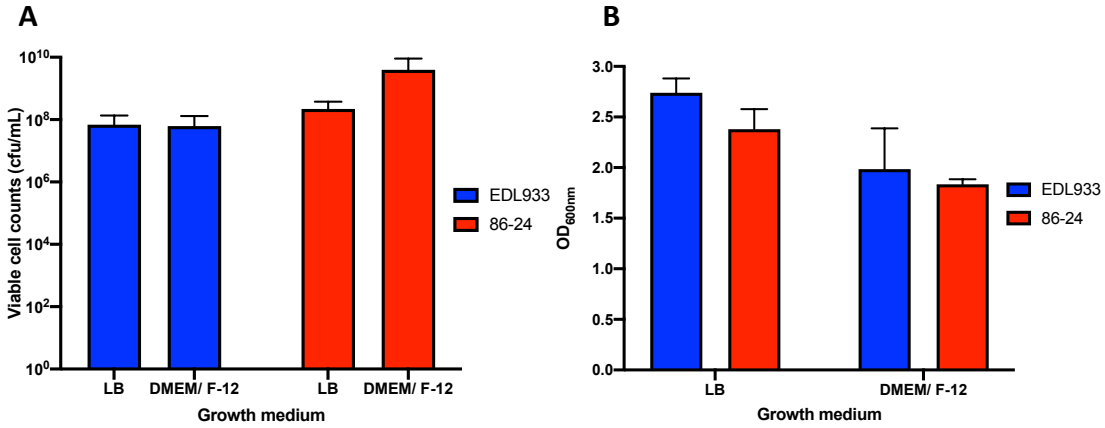

Figure 3.12: Between DMEM/F-12 and LB cultures, EHEC growth is not significantly different. Overnight cultures of EHEC strains EDL933 and 86-24 were inoculated in LB or DMEM/F-12 media (1:100) and grown shaking at 37°C for 24 hours. Growth was assessed by (A) viable cell counts and (B) OD_{600} measurements. Data is shown as means ± SD of at least two independent experiments performed in triplicates.

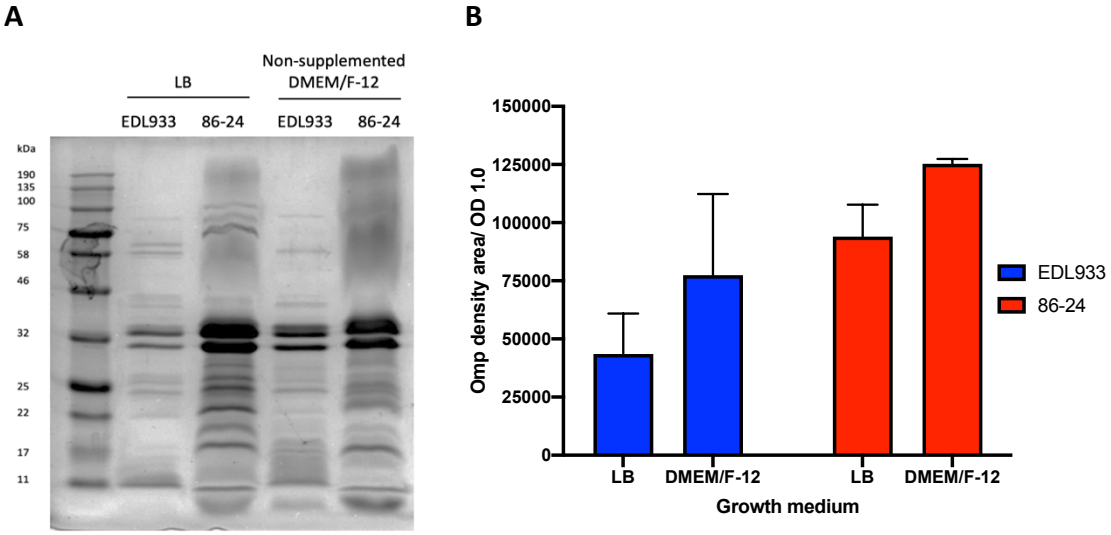

Figure 3.13: EHEC OMV production is not significantly different between LB and DMEM/F-12 cultures. OMVs were isolated from EHEC cultures of strains EDL933 and 86-24 grown in LB or DMEM/F-12 media. A) SDS-PAGE of EHEC OMV samples. B) Densitometric measurements of Omps. Data was normalised using OD_{600} of processed bacterial cultures. Data is shown as means ± SD of at least two independent experiments.

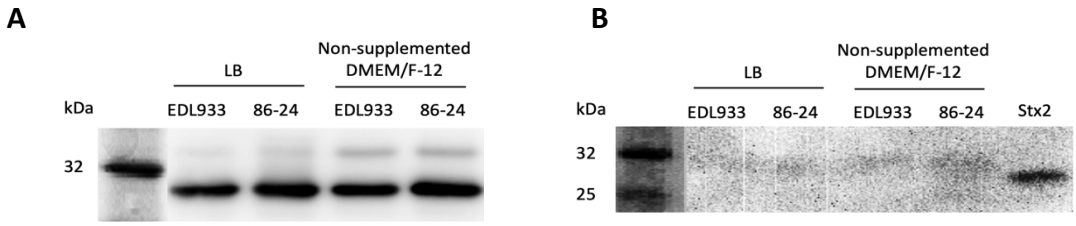

Figure 3.14: Western blot of OMVs isolated from strains EDL933 and 86-24 grown in either LB or DMEM/F-12 media. OMV isolated proteins were separated by SDS-PAGE, blotted onto Polyvinylidene difluoride membranes and subsequently probed with (A) anti-OmpA or (B) anti-Stx2A. Purified Stx2 was included as a positive control.

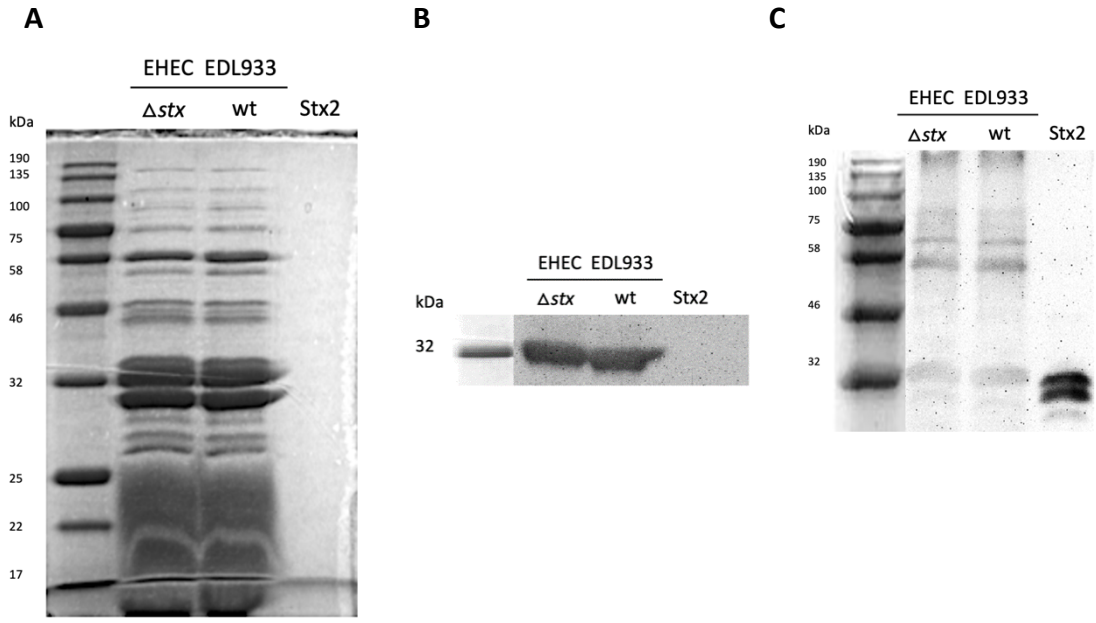

Figure 3.15: Cross reaction of anti-Stx2 with non-specific proteins occurs. OMVs isolated from LB cultures of wild-type (wt) EDL933 and an isogenic Stx mutant (Δ*stx*) were separated by SDS-PAGE (A) and probed with (B) anti-OmpA or (C) anti-Stx2. Purified Stx2 was included as a positive control.

3.2.4 Carbon dioxide does not significantly affect EHEC OMV production

Various gases are present in the human gastrointestinal lumen including carbon dioxide (CO_2; Lacy *et al.*, 2011, Levitt and Bond, 1970). CO_2 enters the gastrointestinal tract due to swallowing of atmospheric gas, bacterial fermentation of carbohydrates and colonocyte release of bicarbonate so to neutralise hydrochloric acid (Lacy *et al.*,

2011). Using electronic gas sensing capsules, colonic CO_2 levels have been estimated to be 5-30% (Kalantar-Zadeh *et al.*, 2018). Therefore, the effect of 5% CO_2 on EHEC OMV production was evaluated. In these experiments, EHEC cultures were grown rocking in T75 flasks in a 37°C incubator gassed with 5% CO_2 (5% CO_2/air; cell culture incubator), or under normal atmospheric conditions (air).

As shown in Fig. 3.16A, EHEC growth in 5% CO_2/ air versus air resulted in a significantly higher viable cell count in EHEC strains TUV 93-0 and 85-170 with a 10.4- and 13.7-fold increase, respectively ($P < 0.05$). This was reflected in significantly higher OD_{600} values attained from both EHEC strains when grown in 5% CO_2/ air than growth in air (Fig. 3.16B, $P < 0.05$).

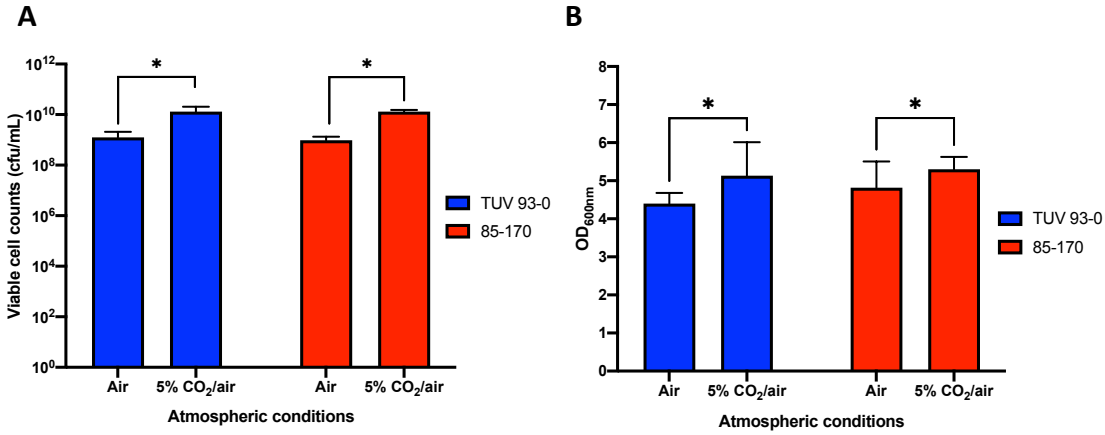

Figure 3.16: EHEC growth significantly increases when supplemented with 5% CO_2/air. Overnight cultures of EHEC strains TUV 93-0 and 85-170 were inoculated in LB (1:100) and grown rocking at 37°C for 24 hours in 5% CO_2/air or air atmosphere. Growth was assessed by (A) viable cell counts and (B) OD_{600} measurements. Data is shown as means ± SD of three independent experiments performed in triplicates. * = $P < 0.05$.

OMV protein profiles were similar when cultures were grown under both conditions (Fig. 3.17B). Bradford protein assay and Omp densitometric analysis indicated that no significant difference in OMV yields is obtained from cultures grown in 5% CO_2/air versus air (Fig. 3.17A and Fig 3.17C, respectively). Furthermore, even though results indicated that under both atmospheric conditions EHEC 85-170 produced higher OMV yields than EHEC strain TUV 93-0, statistical tests failed to detect any significant differences.

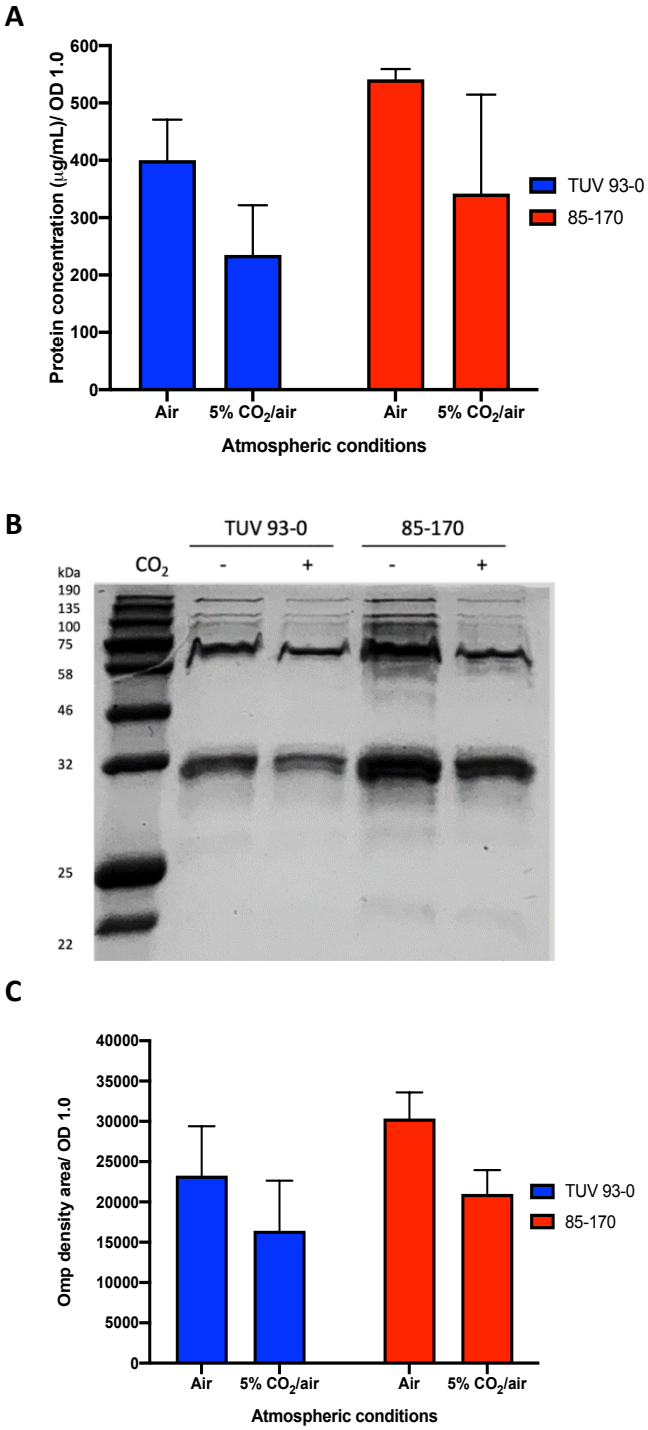

Figure 3.17: EHEC OMV production is not significantly affected when cultures are supplemented with 5% CO_2/air. OMVs were isolated from cultures of TUV 93-0 and 85-170 grown in LB for 24 hours in air atmosphere or 5% CO_2/air. A) OMV quantification by Bradford protein assay. B) SDS-PAGE of EHEC OMV samples. C) Densitometric analysis of Omp proteins. Data was normalised using OD_{600} of processed bacterial cultures. Data is shown as means ± SD of three independent experiments, performed in triplicates.

Using dynamic light scattering (DLS) technology, the size distribution of OMVs was determined (Fig. 3.18A). By averaging the most common OMV size, it was elucidated that the size of OMVs produced by EHEC 85-170 cultures in air were significantly larger than OMVs isolated from EHEC TUV 93-0 cultures in air (Fig. 3.18B, $P < 0.05$). Statistical tests did not detect significant differences between OMVs isolated from similar cultures when grown in 5% CO_2/air. Furthermore, similar sizes were attained from cultures of the same strains when grown in different atmospheric conditions.

Taken together, these results suggests that 5% CO_2/air enhanced EHEC growth but does not increase OMV yields.

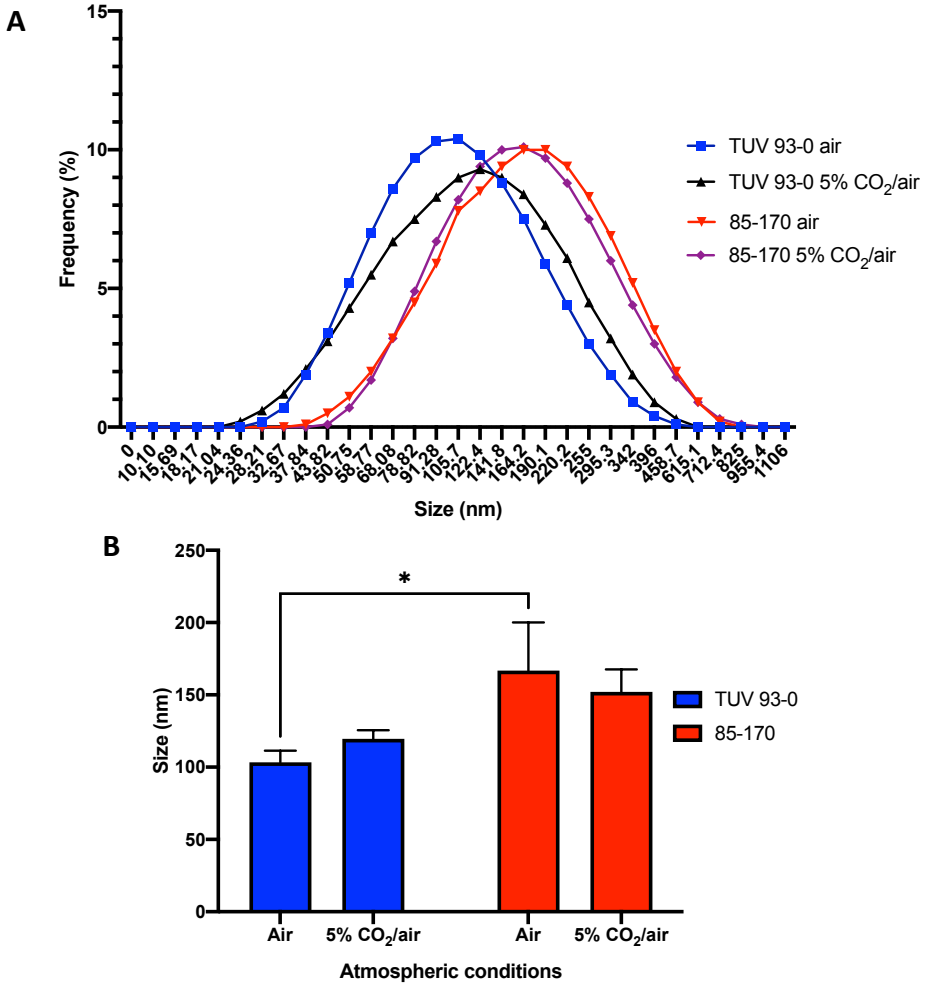

Figure 3.18: Dynamic light scattering data from EHEC OMVs isolated from stationary phase LB cultures grown in air atmosphere or 5% CO_2/air. A) Representative size distribution of EHEC OMVs. Data is the result from one independent experiment. B) Mean of the most frequent EHEC OMV size during stationary phase in LB grown in air or 5% CO_2/air. Data is shown as means ± SD of three independent experiments. * = $P < 0.05$.

3.2.5 The presence of human cells does not significantly affect OMV yield

During passage and colonisation in the gastrointestinal tract, EHEC is exposed to colonic host cells and their secreted products such as antimicrobial peptides. Thus, it was of interest to evaluate the effect the presence of human cells on EHEC OMV production.

To achieve eukaryotic cell growth, cell culture media is usually supplemented with foetal bovine serum (FBS), which provides various growth factors and nutrients. To evaluate whether the addition of FBS would affect OMV preparations, EHEC strain 85-170 was cultured in T75 culture flasks containing either LB medium, non-supplemented or supplemented DMEM. In addition, since this investigation will assess the effect human cell lines have on OMV production, these tests were undertaken in 5% CO_2/air which is needed to maintain eukaryotic cells.

As shown by SDS-PAGE (Fig. 3.19), the Omp bands were obscured by contaminating protein bands in samples isolated from supplemented DMEM cultures. In addition, a major band around 58 kDa in size showed up in OMV preparations from supplemented DMEM, which probably represents contaminating bovine serum albumin. Consequently, the contaminants obscured Omp densitometric analysis thus preventing accurate OMV quantification. Nevertheless, clear Omp bands were attained from cultures grown in non-supplemented DMEM. Furthermore, the presence of protein contaminants affected OMV quantification by Bradford protein assay as significantly higher protein yields were gained from OMV samples from supplemented medium (Fig. 3.20, $P < 0.0001$). Therefore, to evaluate the effect of human cells on EHEC OMV production, incubations were performed in non-supplemented cell culture medium.

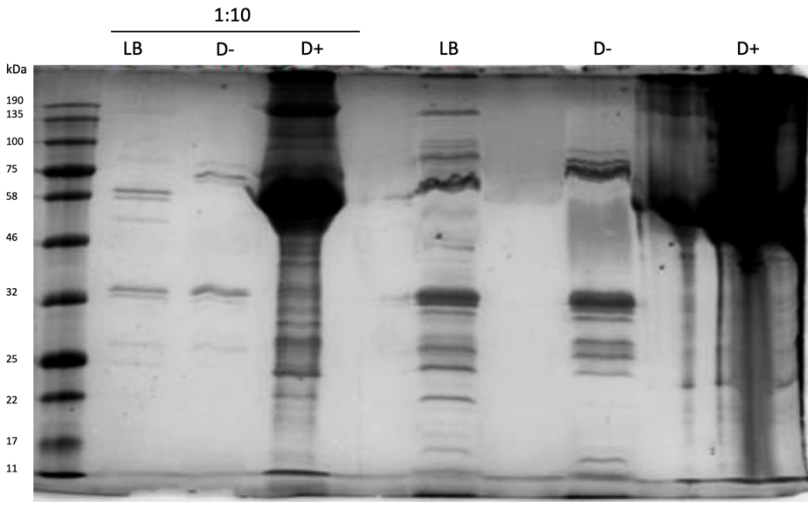

Figure 3.19: Protein composition of OMVs isolated from EHEC cultures grown in LB, non-supplemented DMEM or supplemented DMEM. OMVs were isolated from overnight cultures of EHEC strain 85-170 which were inoculated in either LB, non-supplemented (D -) or supplemented (D +) DMEM (1:100) and grown at 37°C rocking for 24-hours in 5% CO_2/air. Diluted samples (1:10) were also examined by SDS-PAGE. Gel image is representative of two independent experiments.

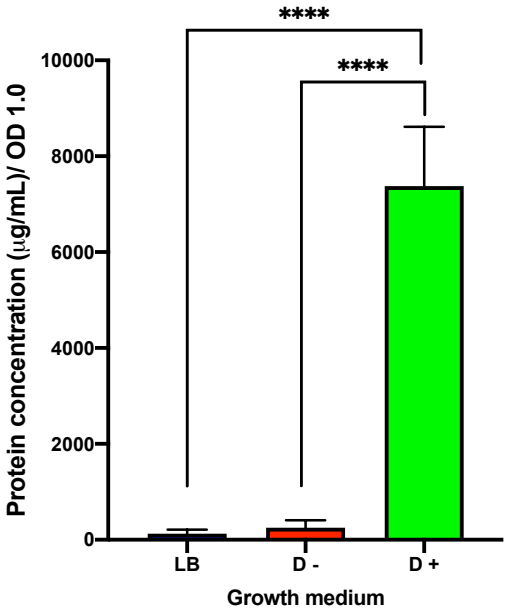

Figure 3.20: Protein concentration of OMV yields isolated from EHEC grown in LB, non-supplemented DMEM (D -) or supplemented DMEM (D +). Data is shown as means ± SD of two independent experiments. **** = $P < 0.0001$.

To optimise the assay, the effect of fast-growing cervical cancer cell line HeLa was used. EHEC 85-170 was grown in T75 flasks containing non-supplemented DMEM with or without confluent HeLa cell monolayers for 24 hours at 37°C in 5% CO_2/air. Quantification of viable cell counts showed no significant differences between cultures grown with and without the presence of HeLa cells (Fig. 3.21A). This was also reflected by the OD_{600} measurements between both cultures (Fig. 3.21B).

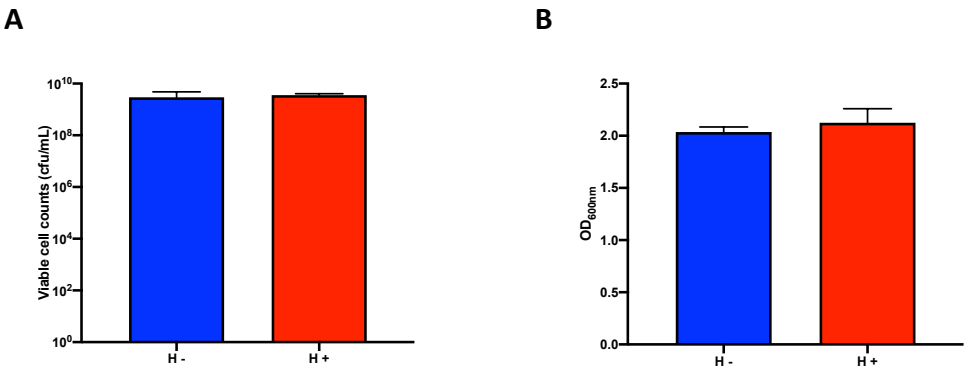

Figure 3.21: EHEC growth is not significantly affected by the presence of HeLa cell monolayers. Overnight cultures of EHEC strain 85-170 were inoculated in non-supplemented DMEM (1:100) with (H +) or without (H -) HeLa cell monolayers and grown rocking at 37°C for 24 hours in 5% CO_2/ air. Growth was assessed by (A) viable cell counts and (B) OD_{600} measurements. Data is shown as means ± SD of two independent experiments performed in triplicates.

EHEC cultures and medium from non-infected HeLa cells (control) were subjected to OMV isolation. As proteins were also present in control medium from HeLa cells (Fig. 3.22A), Bradford protein assay could not be used for OMV quantification in these experiments. Comparative analysis of the polyacrylamide gel showed distinct protein profiles of vesicles isolated from EHEC and HeLa cells monocultures and a combination of the two in EHEC-HeLa cell co-cultures (Fig. 3.22B). Notably, most proteins of HeLa cell origin exhibited a molecular weight above 58 kDa, thus did not affect OMV quantification by Omp densitometric analysis. As shown in Fig. 3.22C, no significant differences were detected between OMV yield between EHEC cultures with and without the presence of HeLa cells when Omp densitometric analysis was used.

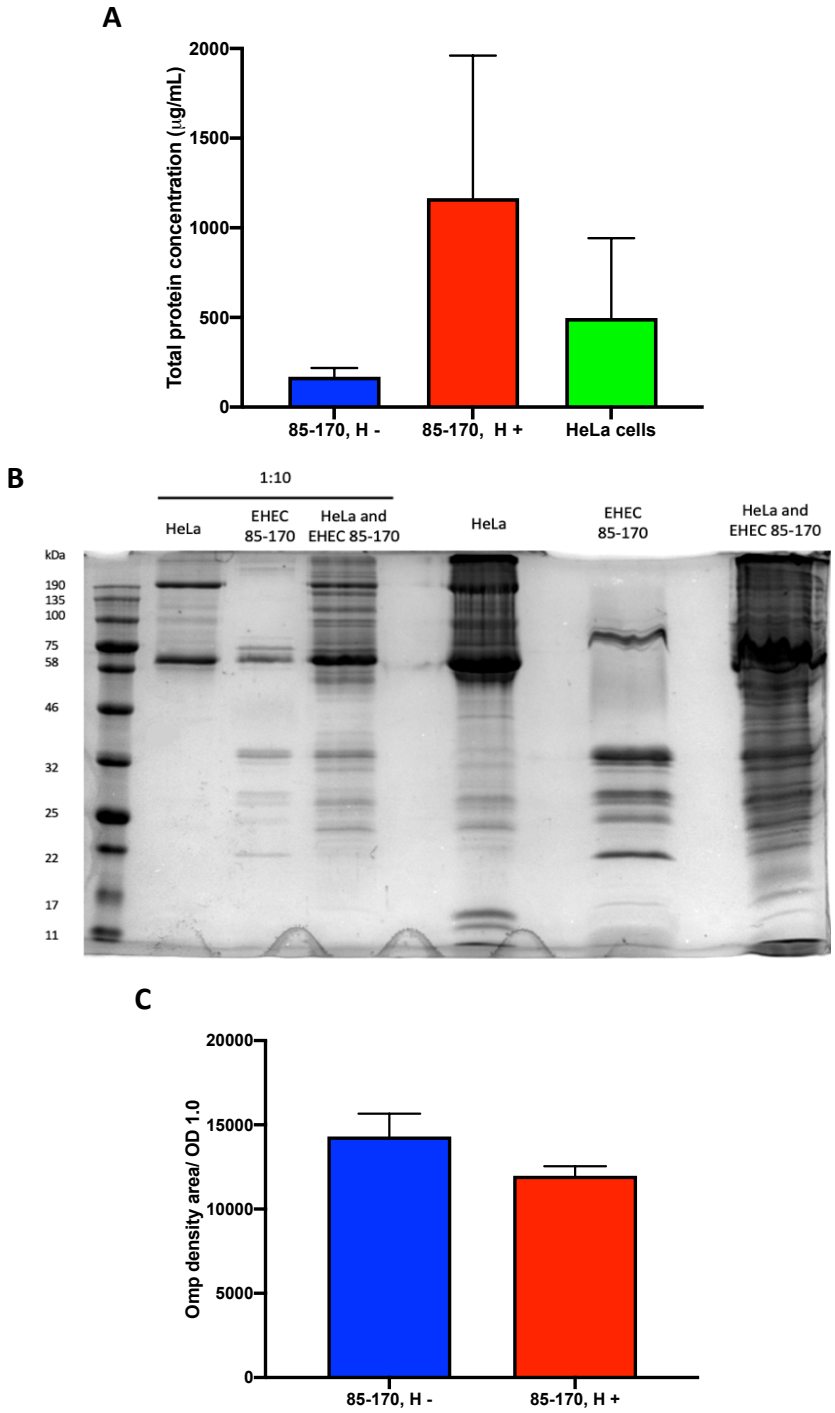

Figure 3.22: No significant difference in OMV yield is attained between EHEC 85-170 cultures with and without HeLa cell monolayers. OMVs were isolated from cultures of EHEC 85-170 grown in non-supplemented DMEM with (H +) or without (H -) HeLa cell monolayers in 5% CO_2/ air for 24 hours. HeLa cells were also cultured on their own and treated for OMV isolation to serve as controls. A) Protein content of samples were quantified by Bradford protein assay and is shown as total protein content. B) Protein composition of vesicles released by EHEC and HeLa cells. Samples were also diluted 1:10. C) Densitometric analysis of Omp proteins. Data was normalised using OD_{600} of processed bacterial cultures. Data is shown as means ± SD of three independent experiments.

Following this, the effect of colonic T84 cells on OMV production by EHEC strains TUV 93-0 and 85-170 was examined. Human T84 colonic carcinoma cells were chosen as they resemble colonic crypt cells and like the human colonic epithelium, do not express the Stx receptor known as Gb3 (Devriese *et al*., 2017, Schuller *et al.*, 2004). Incubations were performed as described above (EHEC and T84 cells alone and in co-culture).

After a 24-hour growth period, no significant differences were detected between viable bacterial counts for both EHEC strains 85-170 and TUV 93-0, when grown in the presence of T84 cells versus the absence of T84 cells (Fig. 3.23A). Similarly, this was reflected with the measured OD_{600} values for both EHEC strains (Fig. 3.23B) grown in the two conditions.

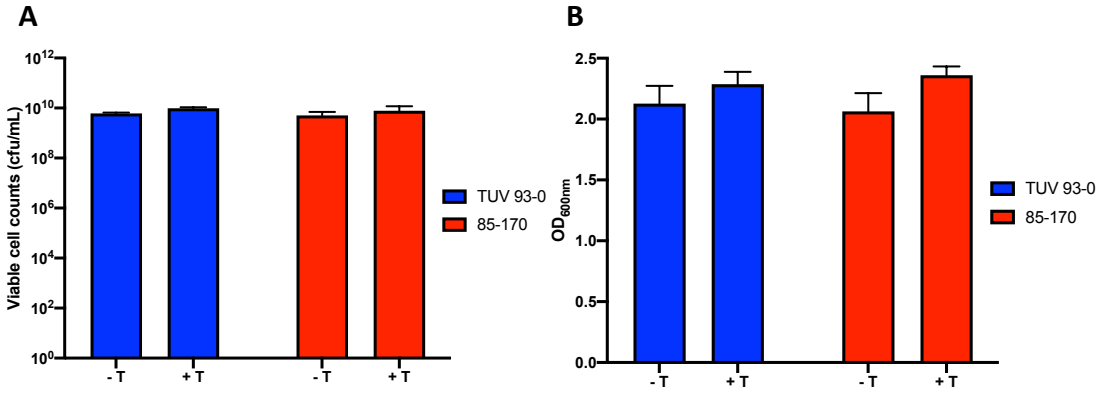

Figure 3.23: EHEC growth is not significantly affected by the presence of T84 cell monolayers. Overnight cultures of EHEC strains TUV 93-0 and 85-170 were inoculated in non-supplemented DMEM/F-12 medium (1:100) with (+ T) or without (- T) T84 cell monolayers and grown rocking at 37°C for 24 hours in 5% CO_2/ air. Growth was assessed by (A) viable cell counts and (B) OD_{600} measurements. Data is shown as means ± SD of three independent experiments performed in duplicate.

EHEC cultures and medium from non-infected T84 cells (control) were subjected to OMV isolation. As proteins were also present in control medium from T84 cells (Fig. 3.24A), Bradford protein assay could not be used for OMV quantification. Similar to the results described for HeLa cells, protein separation by SDS-PAGE showed specific protein patterns for vesicles isolated from T84 cells and EHEC, with a combination of the two observed in preparations from the co-cultures (Fig. 3.24B and C,

respectively). Notably, very little T84 cell-derived protein were present at the molecular weight range of OmpA and Omp F/A (circa 32 kDa), therefore Omp densitometry could be used to quantify EHEC OMV production in the presence and absence of T84 cells.

Generally, densitometric quantification showed a 28% reduction for both strains when grown in the presence of T84 cells but this did not reach statistical significance (Fig 3.24D). Furthermore, no significant differences were detected between EHEC strains grown under similar conditions.

In summary, these results indicate no significant difference in EHEC growth or OMV production in the presence of colonic T84 cells.

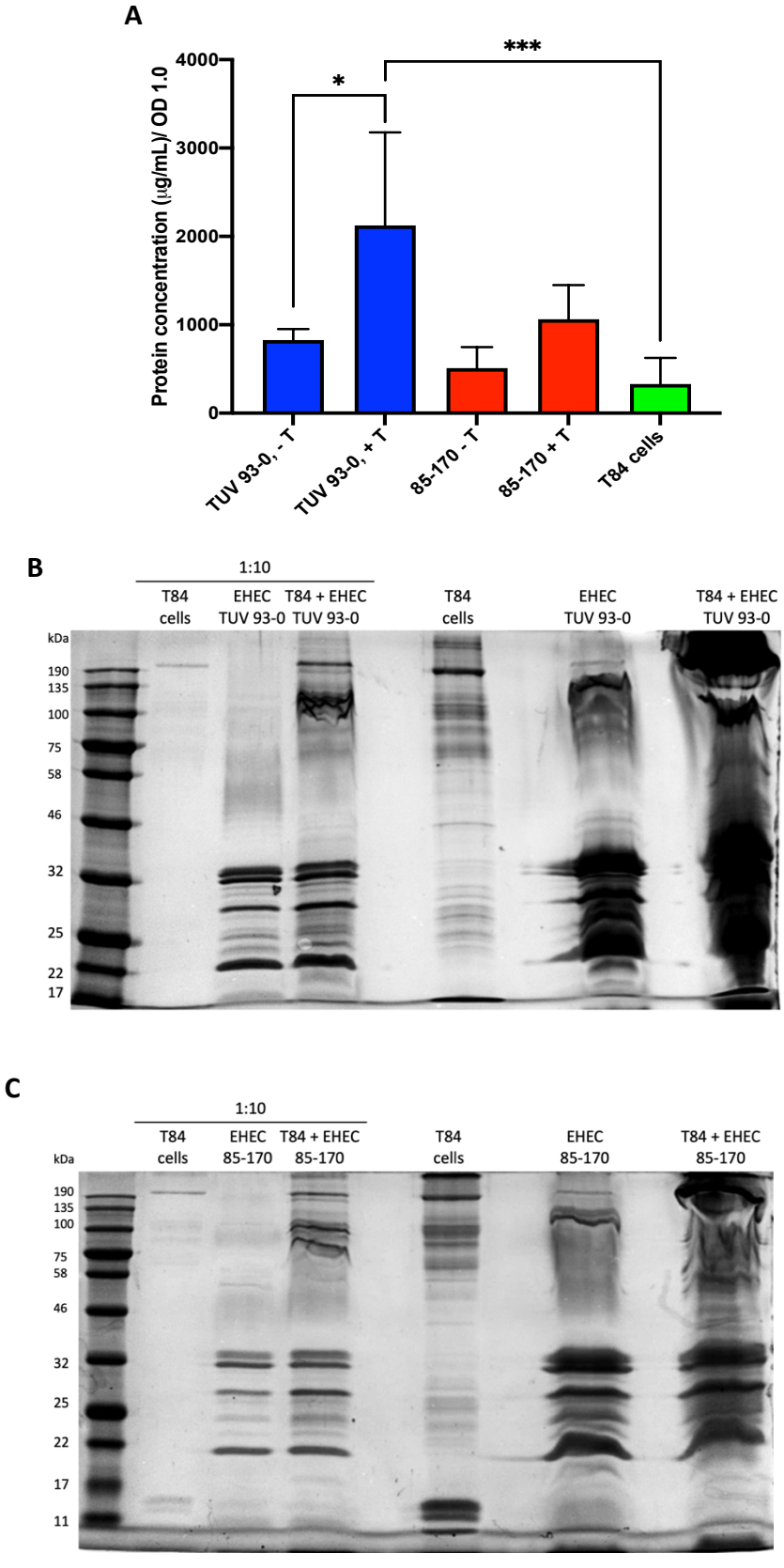
A
Protein concentration (µg/mL)/ OD 1.0
4000
3000
2000
1000
0
*
***
TUV 93-0, - T
TUV 93-0, + T
85-170 - T
85-170 + T
T84 cells
B
1:10
T84 cells
EHEC TUV 93-0
T84 + EHEC TUV 93-0
T84 cells
EHEC TUV 93-0
T84 + EHEC TUV 93-0
kDa
190
135
100
75
58
46
32
25
22
17
C
1:10
T84 cells
EHEC 85-170
T84 + EHEC 85-170
T84 cells
EHEC 85-170
T84 + EHEC 85-170
kDa
190
135
100
75
58
46
32
25
22
17
11

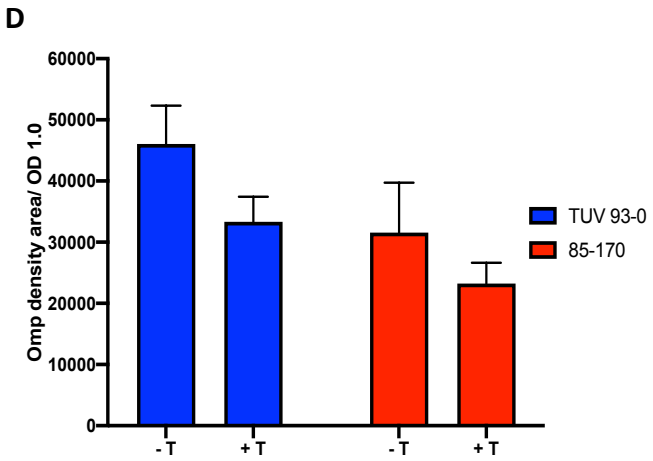

Figure 3.24: No significant differences in OMV yield is attained between EHEC cultures with or without T84 cells monolayers. OMVs were isolated from EHEC cultures of TUV 93-0 and 85-170 grown in non-supplemented DMEM/F-12 medium with (+ T) or without (- T) T84 cell monolayers in 5% CO_2/air for 24 hours, rocking at 37°C. T84 cells were cultured on their own and treated for OMV isolation to serve as controls. A) Protein content of samples were quantified by Bradford protein assay and is shown as total protein content. Protein composition from isolated T84 cell derived vesicles and OMV samples from EHEC strains (B) TUV 93-0 and (C) 85-170. Samples were also diluted 1:10. D) Densitometric analysis of Omp proteins. Data was normalised using OD_{600} of processed bacterial cultures. Data is shown as means ± SD of three independent experiments, performed in duplicates. * = $P < 0.05$, *** = $P < 0.001$.

3.2.6 Bile salts significantly increase OMV production

Simulated colonic environmental medium (SCEM) reproduces several parameters within the human colon including neutral pH, osmolarity and the presence of secondary bile salts, and thus represents an optimal medium to investigate the effects of the colonic milieu on EHEC OMV production (Beumer *et al.*, 1992). However, previous studies have reported that bile salts have outer membrane-damaging effects on bacteria, thus causing bacterial cell lysis and the release of cytoplasmic proteins (Merritt and Donaldson, 2009). Consequently, EHEC lysis by SCEM could lead to artificial vesicle formation from fragmented membranes and cause OMV sample contamination (Turnbull *et al.*, 2016, Devos *et al.*, 2017). To determine whether the concentration of bile salts in SCEM (4.73mM) leads to bacterial lysis, EHEC strains TUV 93-0 and 85-170 were grown shaking at 37°C in SCEM

with or without bile salts for 24 hours. Growth was determined by OD_{600} and viable cell counts. As shown in Fig. 3.25A and B, both EHEC strains demonstrated similar OD_{600} measurements and viable cell counts throughout the growth period in both media, thus indicating that bile salt concentrations used in SCEM does not induce bacterial lysis.

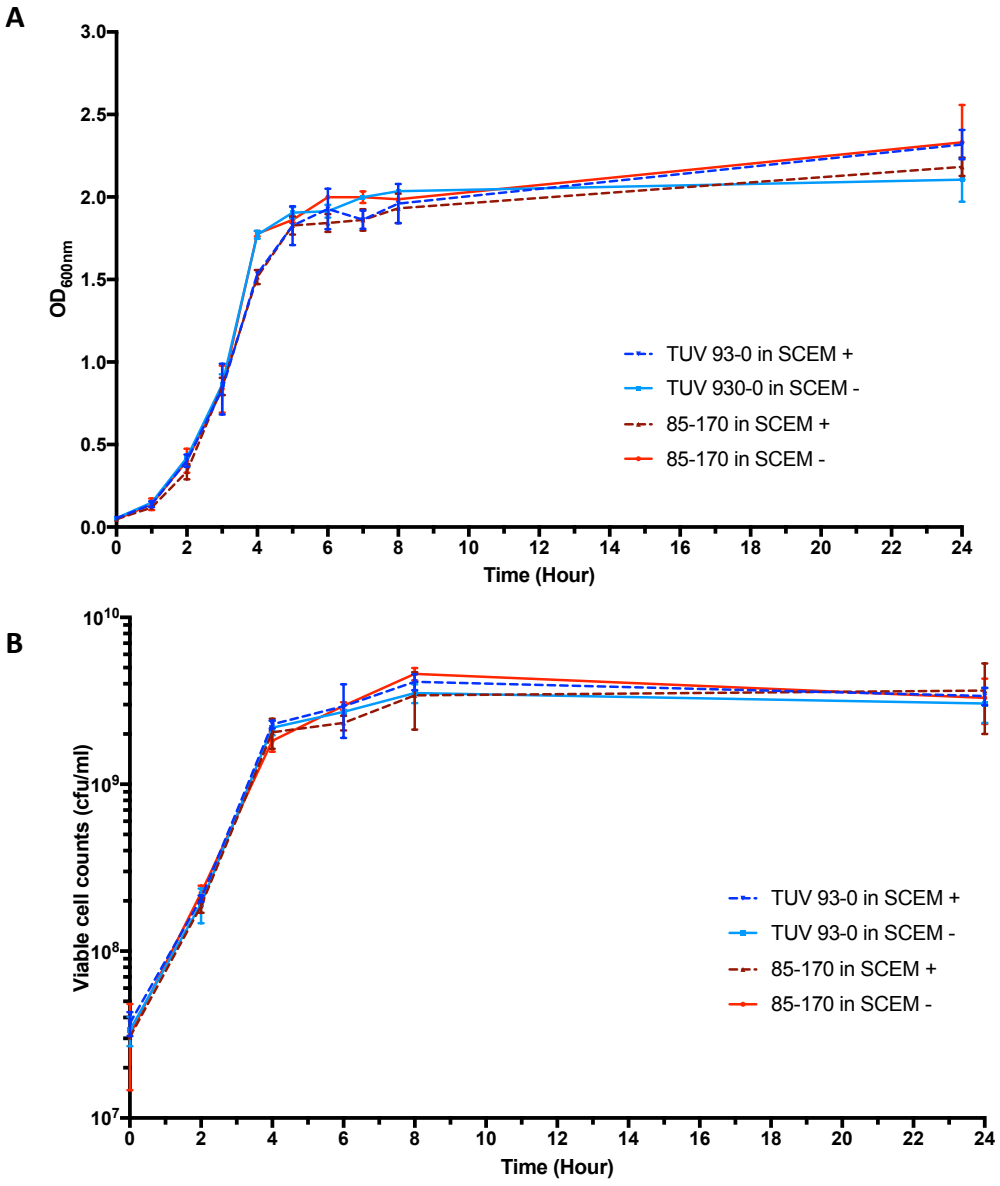

Figure 3.25: Growth curves of EHEC TUV 93-0 and 85-170 over a 24-hour growth period in SCEM with or without bile salts. Overnight cultures of bacteria were inoculated in SCEM (1:100) with (+) or without (-) bile salts and grown shaking at 37°C for 24 hours. Bacterial growth was determined by (A) OD_{600} and (B) colony forming units per mL (cfu/mL). Data is shown as means ± SD of three independent experiments performed in duplicates.

To exclude the presence of SCEM-derived contaminants in OMV preparations, 24-hour EHEC cultures in SCEM and sterile SCEM were subjected to OMV purification. Sample were subsequently examined for contaminants by SDS-PAGE and DLS. As shown in Fig. 3.26A, no proteins were present in OMV preparations from sterile SCEM, yet a protein pattern was produced from the treated SCEM culture. Similarly, DLS analysis did not detect any nanoparticles in SCEM-derived samples (Fig. 3.26B). This indicates that no medium contaminants are isolated along with OMVs.

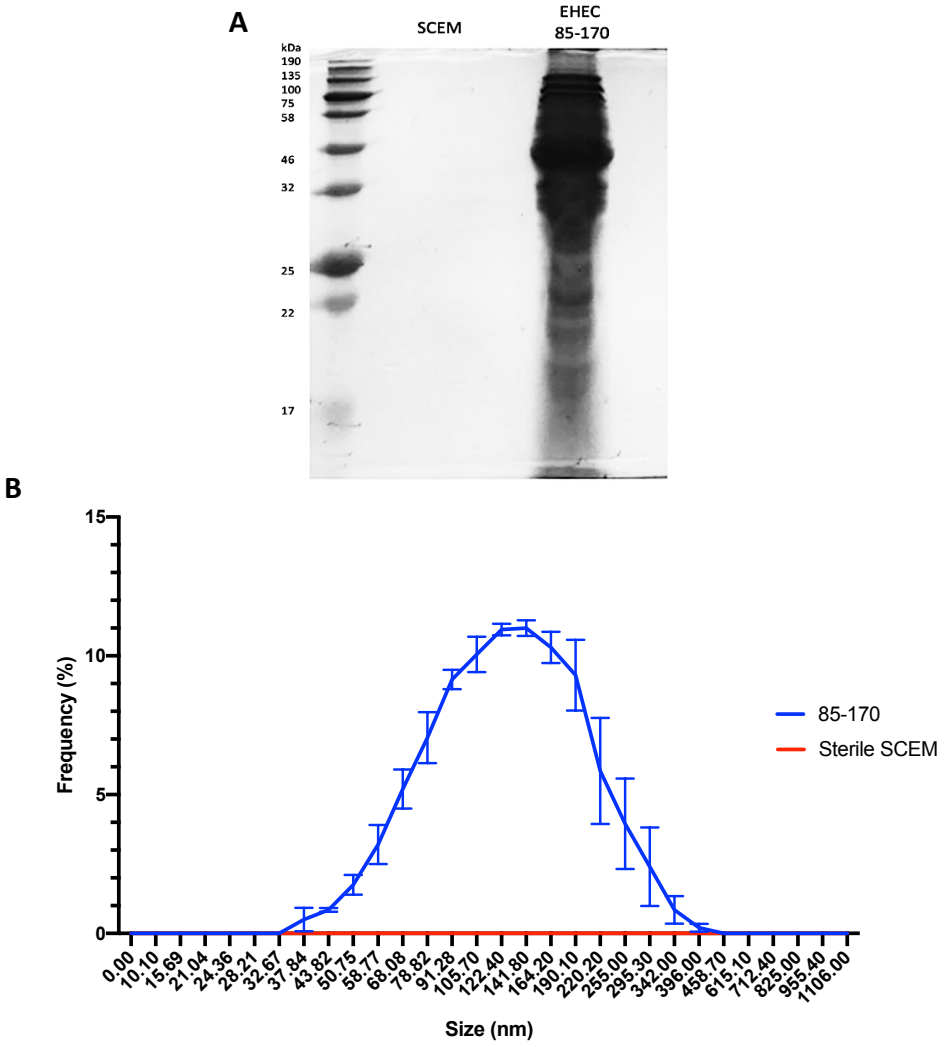

Figure 3.26: EHEC OMV preparations do not contain contaminants from SCEM. Overnight cultures of EHEC strain 85-170 were inoculated in SCEM (1:100) and grown shaking at 37°C for 24 hours. EHEC culture and the same volume of sterile SCEM were treated for OMV isolation. A) Neat samples were separated by SDS-PAGE. Gel image is representative of two independent experiments. B) Dynamic light scattering confirms the absence of particles in sterile SCEM samples. Furthermore, the size distribution of EHEC 85-170 is shown as means ± SD of two independent experiments performed in duplicate.

To assess the impact of SCEM and bile salts on EHEC OMV production, EHEC strains 85-170 and TUV 93-0 were grown for 18 hours in LB and SCEM with and without bile salts, and cultures were subsequently treated for OMV isolation. Furthermore, bacterial growth was monitored by OD_{600} measurements and viable cell counts. A shorter incubation period was chosen as the high viscosity of OMV samples isolated from 24-hour SCEM cultures was observed in initial experiments.

Interestingly, for both EHEC strains, viable cell counts significantly decreased when grown in SCEM containing bile salts compared to LB medium (Fig. 3.27A, $P < 0.001$ for EHEC strain TUV 93-0 and $P < 0.01$ for EHEC strain 85-170). A reduction in viable cell counts also occurred between SCEM cultures without bile and LB, yet this was only significant for EHEC strain TUV 93-0 ($P < 0.05$). While the reduction in bacterial numbers in SCEM without bile salts versus LB was also reflected by decreased OD_{600} values, bacterial densities of SCEM cultures with bile salts were not significantly different from those of LB cultures (Fig 3.27B). Curiously, OD_{600} measurements and viable cell counts were lower than those obtained for previous growth curves in SCEM (Fig. 3.25A and B, respectively). However, due to no 18-hour data points in the growth curve analysis, direct statistical comparisons could not be made.

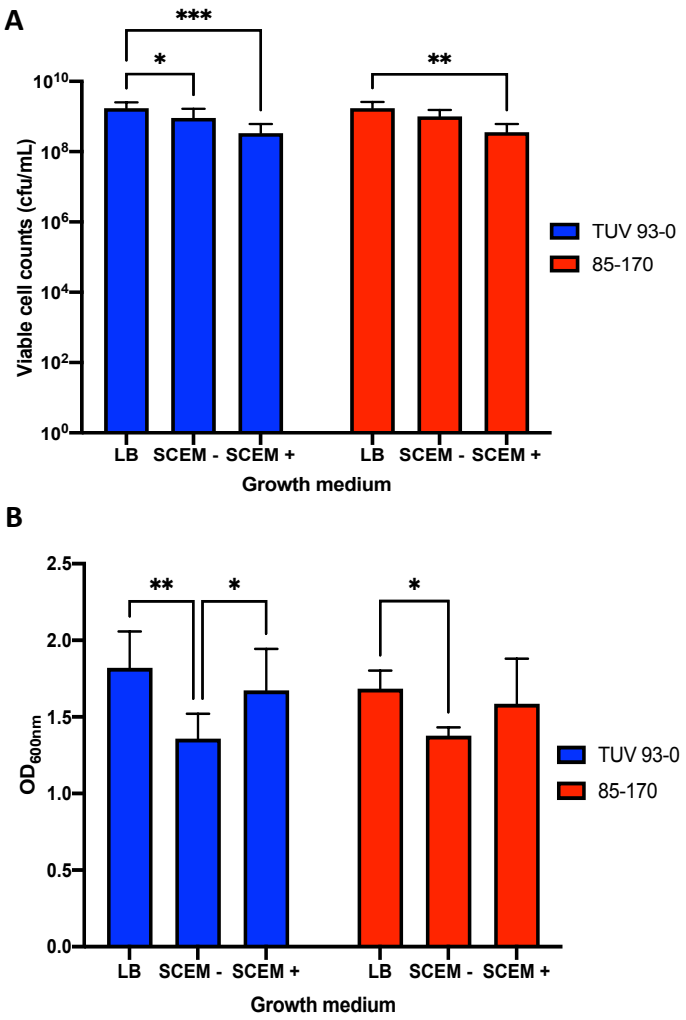

Figure 3.27: Viable cell counts decrease when EHEC is grown in the presence of bile salts in EHEC cultures used for OMV isolation, yet OD_{600} is not significantly affected. Overnight cultures of EHEC strains TUV 93-0 and 85-170 were inoculated in LB or SCEM with (+) or without (-) bile salts (1:100) and grown shaking at 37°C for 18 hours. Growth was assessed by (A) viable cell counts and (B) OD_{600} measurements. Data is shown as means ± SD of six independent experiments performed in triplicates. * = $P < 0.05$, ** = $P < 0.01$, *** = $P < 0.001$.

Analysis of OMV samples by Bradford protein assay demonstrated that similar values were attained from EHEC strains TUV 93-0 and 85-170 under all culture media (Fig. 3.28A).

The protein profiles of OMVs isolated from EHEC strain TUV 93-0 grown in LB and all SCEM cultures were similar except for the diffuse smear in the higher molecular weight region present in OMVs isolated for EHEC strain TUV 93-0. For EHEC 85-170, OMV protein profiles appeared similar between LB and SCEM without bile salt

culture, with additional band appearing in cultures grown in SCEM with bile salts (Fig. 3.28B and C, respectively). Furthermore, a 1 in 10 dilution of the OMV samples from SCEM cultures for both EHEC strains was needed in order to clearly visualise protein profile, suggesting a higher OMV yield in SCEM cultures versus to LB cultures.

Omp densitometry indicated that both EHEC strains produced the lowest OMV yield when cultured in LB medium, with a 6-fold increase in OMV yield in SCEM cultures without bile salts and a further 2.8-fold increase being produced in SCEM cultures containing bile salts (Fig. 3.28D). Significant differences were detected between SCEM cultures containing bile salts and both SCEM cultures lacking bile salts ($P < 0.01$) and LB cultures ($P < 0.001$) for both EHEC strains. No significant differences were detected between EHEC strains grown under the same conditions.

A

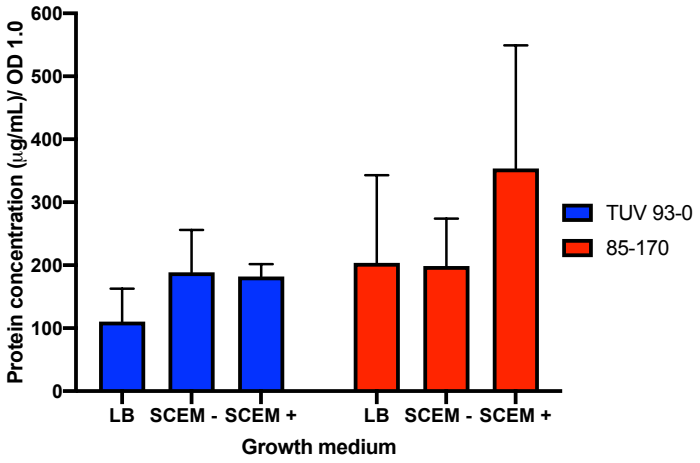
Protein concentration (µg/mL)/ OD 1.0
600
500
400
300
200
100
0
LB
SCEM -
SCEM +
LB
SCEM -
SCEM +
Growth medium
TUV 93-0
85-170

B

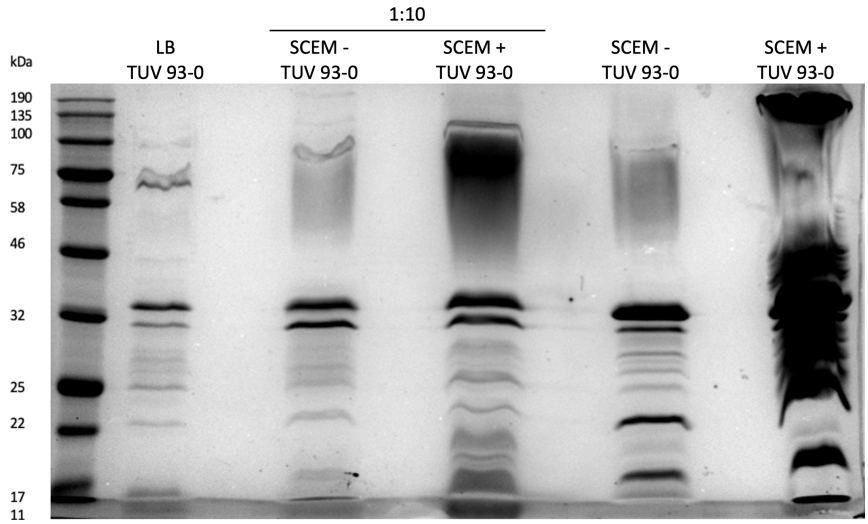
1:10
kDa
LB
TUV 93-0
SCEM -
TUV 93-0
SCEM +
TUV 93-0
SCEM -
TUV 93-0
SCEM +
TUV 93-0
190
135
100
75
58
46
32
25
22
17
11

C

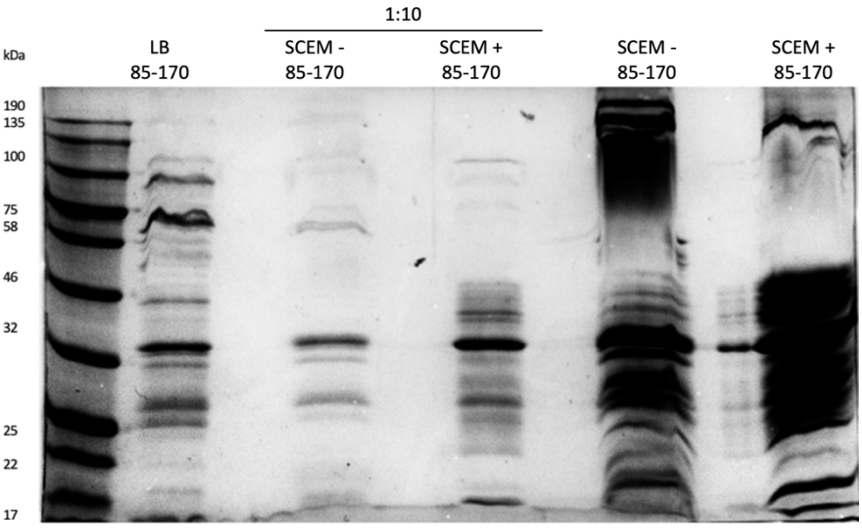
1:10
kDa
LB
85-170
SCEM -
85-170
SCEM +
85-170
SCEM -
85-170
SCEM +
85-170
190
135
100
75
58
46
32
25
22
17

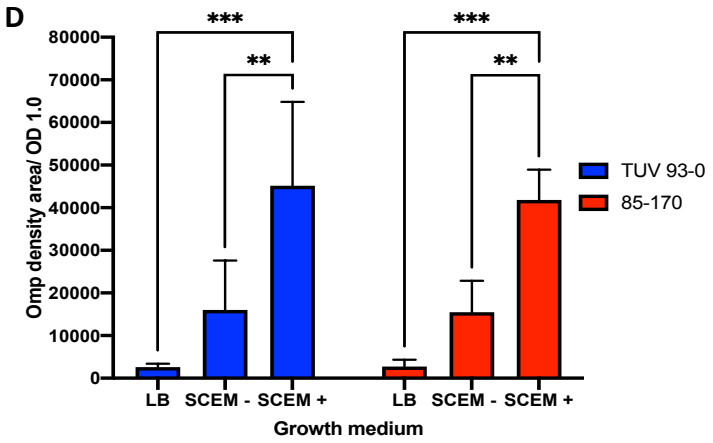

Figure 3.28: EHEC OMV production increases when cultured in the presence of bile salts. Overnight cultures of EHEC strain TUV 93-0 and 85-170 were inoculated in LB medium or SCEM with (+) or without (-) bile salts (1:100) and grown shaking at 37°C for 18 hours. The cultures were then treated for OMV purification. A) Isolated OMVs were quantified by Bradford protein assay. Protein composition of isolated EHEC OMVs from (B) TUV 93-0 or (C) 85-170 cultures. D) Densitometric Omp analysis. Data was normalised using OD_{600} of processed bacterial cultures. Data is shown as means ± SD of five independent experiments. ** = $P < 0.01$, *** = $P < 0.001$.

OMV sizes were also analysed using the Nanoparticle tracking analysis (NTA) system, which produced OMV size distribution curves (representative curves shown in Fig. 3.29). By analysing the mean of the most common OMV size (Fig. 3.30), both strains produced significantly smaller OMVs when cultured in SCEM lacking bile salts compared to culture in LB ($P < 0.01$ for EHEC strain TUV 93-0 and $P < 0.001$ and EHEC 85-170) or SCEM with bile salts ($P < 0.01$ for EHEC strain TUV 93-0 and $P < 0.05$ for EHEC strain 85-170). Furthermore, results suggested OMV sizes were larger in LB cultures of EHEC TUV 93-0 and 85-170 ($P < 0.01$).

The NTA system also allowed for the quantification of OMV particles. Generally, higher OMV yields were obtained from EHEC strains grown in SCEM with bile salts compared to when EHEC was grown in the other two media (Fig. 3.31), however this did not reach significance.

Overall, this data suggests that growth in SCEM containing bile salts EHEC viability significantly reduces but OMV production is significantly enhanced.

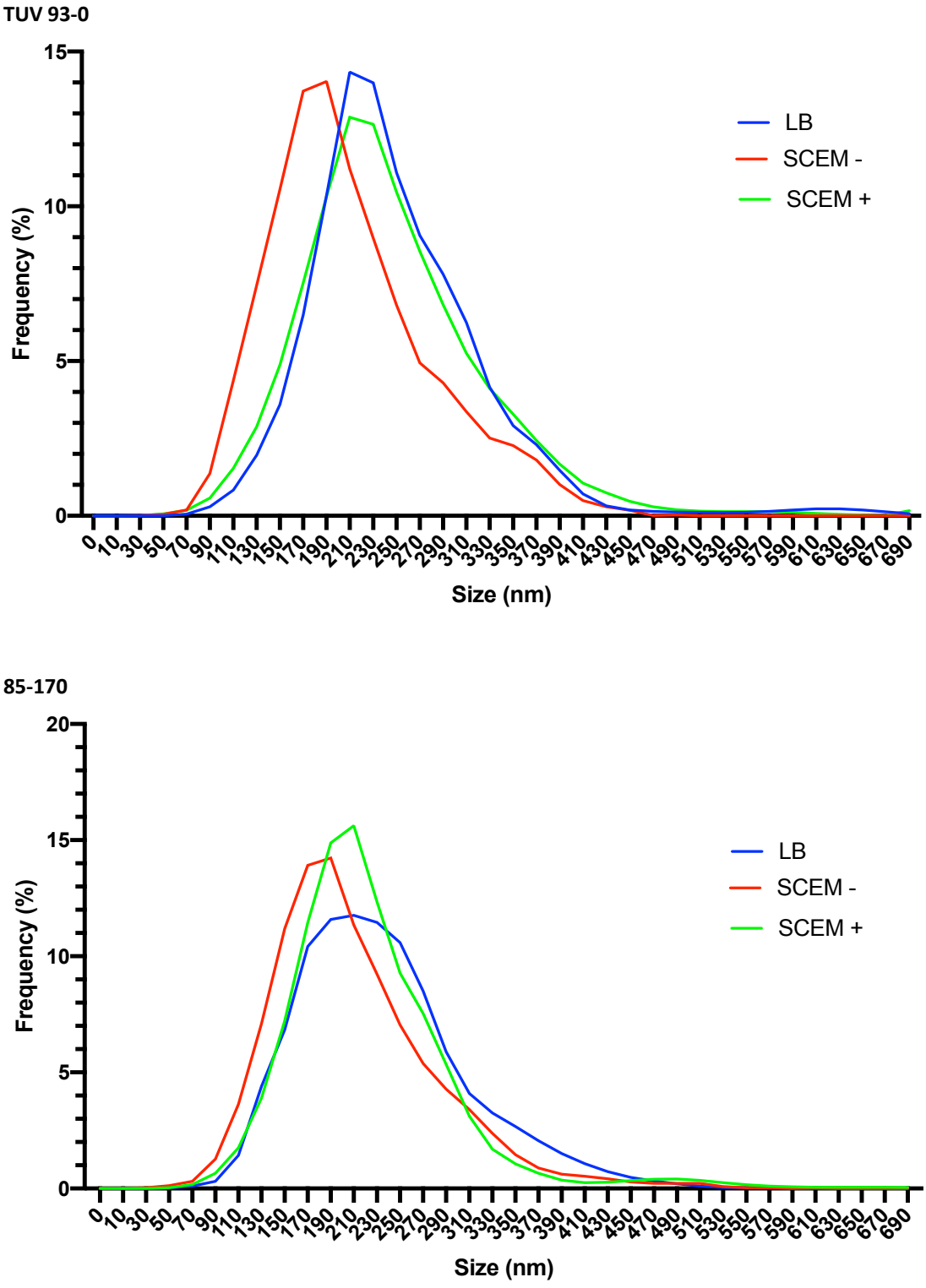

Figure 3.29: Size distribution of EHEC OMVs isolated during stationary phase in LB and SCEM with (+) and without (-) bile salts. OMVs from EHEC TUV 93-0 and 85-170 cultures were examined by Nanoparticle tracking analysis using the Nanosight LM10 instrument. Data is shown as a result from an independent experiment.

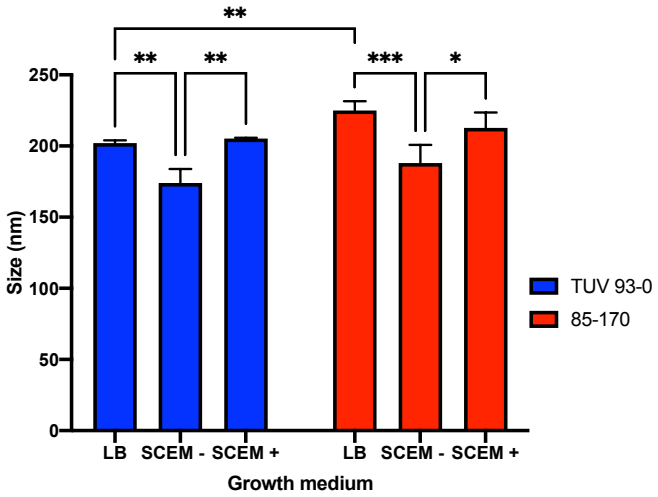

Figure 3.30: EHEC OMV sizes during stationary phase cultures in LB and SCEM with (+) and without (-) bile salts. OMVs from EHEC TUV 93-0 and 85-170 cultures were examined by Nanoparticle tracking analysis using the Nanosight LM10 instrument. Data is shown as the mean of the most frequent OMV size ± SD of at three independent experiments. * = $P < 0.05$, ** = $P < 0.01$, *** = $P < 0.001$.

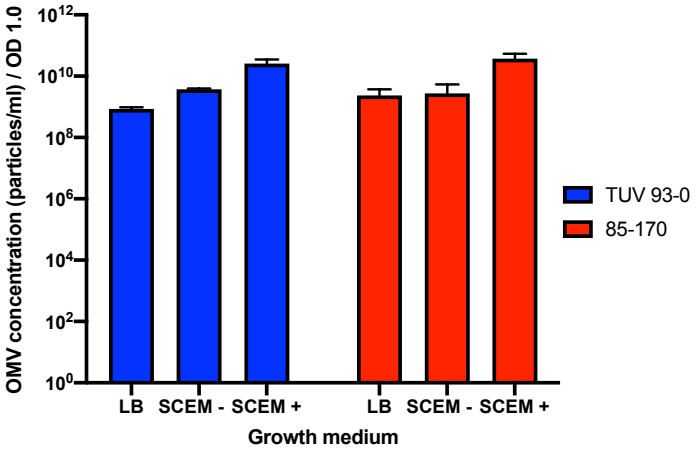

Figure 3.31: EHEC OMV concentrations obtained from LB cultures and SCEM cultures with (+) and without (-) bile salts. OMVs from EHEC TUV 93-0 and 85-170 cultures were examined by Nanoparticle tracking analysis using the Nanosight LM10 instrument. Data was normalised using OD_{600} of processed bacterial cultures. Data is shown as means ± SD of at least two independent experiments.

3.2.7 Bile salts do not affect OMV integrity

Bile salts can dissolve membrane lipids and cause integral membranes to disassociate (Merritt and Donaldson, 2009). To investigate whether bile salt concentrations in SCEM could dissolve OMVs, OMVs isolated from EHEC strains 85-170 and TUV 93-0 cultures in SCEM without bile salts were incubated in SCEM with or without bile salts, shaking at 180 rpm for 18 hours at 37^{o}C. OMVs were then recovered by ultrafiltration using spin columns with a 100 kDa MWCO. Non-OMV-associated proteins in the flow-through were precipitated with trichloroacetic acid. Both ultrafiltrate and flow-through were analysed by SDS-PAGE. As shown in Fig 3.32, bile salts do not cause protein release from OMVs, since the protein profiles between OMV samples incubated with or without bile salts were similar. Moreover, minimal protein content was present in the flow-through. Probing of Western blots with anti-OmpA only detected the protein in the ultrafiltrates containing OMVs and not in the flow throughs (Fig. 3.32).

TUV 93-0

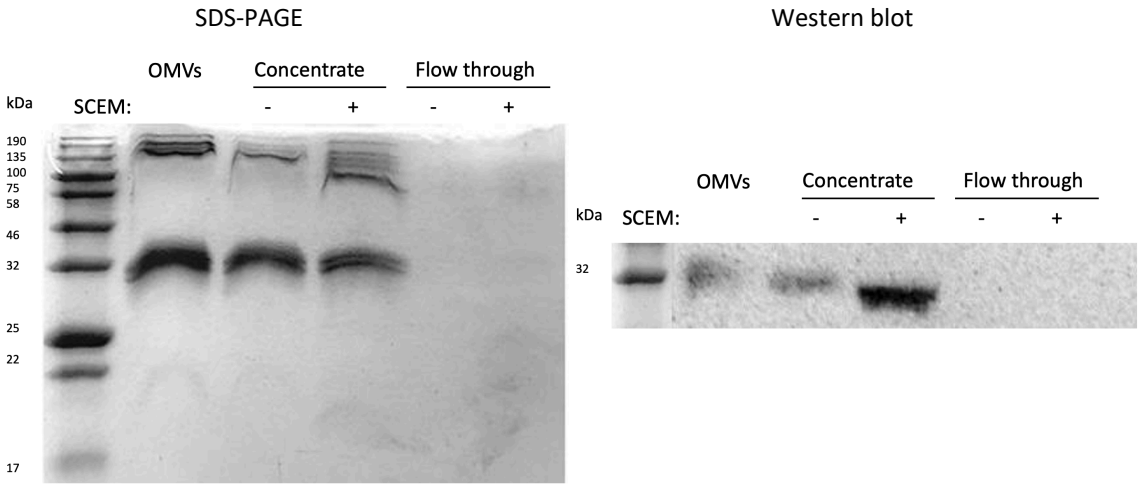

85-170

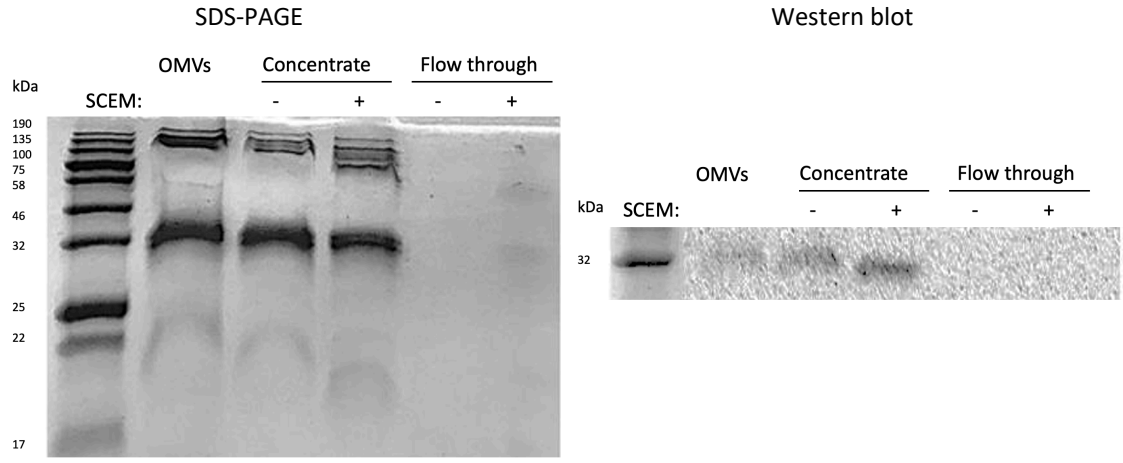

Figure 3.32: Bile salts do not affect OMV integrity. OMVs isolated from EHEC TUV 93-0 and 85-170 grown in SCEM for 18-hours without bile salts were incubated for 18 hours in SCEM with (+) or without (-) bile salts, shaking at 37°C. Subsequently, OMVs were isolated by ultrafiltration (100K MWCO) and proteins in the flow through were concentrated by trichloroacetic acid precipitation. Original OMV samples without treatment were included as positive controls (OMVs). The concentrated sample and flow throughs were analysed by SDS-PAGE and Western blot with anti-OmpA.

3.3 Discussion

OMVs are constitutively shed by Gram-negative bacteria and production is considered to be essential for bacterial survival. The coordinated modulation of OMV synthesis enables bacteria to counter the lethal effects of harsh environments. Therefore, the impact on EHEC OMV production by different physiologically relevant conditions encountered in the gastrointestinal tract was investigated such as 5% CO_2 levels, human colonic cells and bile salts.

3.3.1 OMV purification and quantification

In order to study how different colonic settings affect EHEC OMV production, a workflow to isolate OMVs was optimised. After cultures were grown in the desired conditions, low speed centrifugation and supernatant filtration using filter units with pore sizes of 0.45µm was applied to separate bacteria from the supernatant. In this study, cellulose membrane filters were used for ultrafiltration as it is suggested that polyethersulphone filters have a high adsorption of proteins and macromolecules (Klimentová and Stulík, 2015). Previous OMV studies have isolated OMVs through tangential flow filtration without the need of ultracentrifugation (Stentz *et al.*, 2015, Jones *et al.*, 2020). In this study, it was established that ultracentrifugation was needed to isolate OMVs and accurately quantify OMV yield when ultrafiltration columns were used as the Omp bands needed to carry out densitometry were obscured in samples which lacked ultracentrifugation. OMV isolation was verified through (i) the presence of Omps which produced distinctive bands at the 32 kDa region when OMV proteins were separated via SDS-PAGE; (ii) fluorescence labelling of OMVs and visualisation through fluorescence microscopy; and (iii) transmission election microscopy (TEM). Using TEM, OMVs isolated from LB cultures ranged from 20nm to 120nm in diameter. The size of OMVs isolated from similar growth phase LB cultures ranged from 43nm to 615nm when DLS was applied; and 70nm to 510nm when NTA was utilised. Indeed, these sizes fall into published OMV sizes which range from 20nm to 300nm in diameter (Schwechheimer and Kuehn, 2015).

Previous studies have used different techniques to quantify *E. coli* OMV yields, including Bradford protein assay and densitometric analysis of Omps (Klimentová and Stulík, 2015, Manning and Kuehn, 2011, Schwechheimer *et al.*, 2014). In this investigation both aforementioned quantification methods were used, yet in this study Omp densitometry is considered to be more accurate over Bradford protein assay, as contaminating proteins such as flagella, fimbria, pili and large protein complexes can also be isolated along with OMVs after ultracentrifugation, as shown in Bauman and Kuehn (2006). In order to avoid such contaminants, additional purification steps have been used by other studies such as density gradient centrifugation (DGC) and size exclusion chromatography (Bauman and Kuehn, 2006, Bitar *et al.*, 2019, Cecil *et al.*, 2016). DGC is based on the lipid content of particles, and due to the lipid content of OMVs differing to that of contaminating proteins, OMVs will separate from contaminants (Horstman and Kuehn, 2000, Bauman and Kuehn, 2006). Another caveat of using Bradford protein assay to quantify OMV yield is that an increase in total protein content cannot always be interpreted as the isolation of more OMVs, as OMV protein content may differ between different growth conditions. In contrast, OMV quantification through densitometric analysis of Omps is not affected by larger-sized contaminating protein aggregates and is only dependent on ubiquitously present Omps (McBroom and Kuehn, 2007, Manning and Kuehn, 2011), therefore it is likely to provide a more accurate methods of measuring EHEC OMV yield.

Other studies have quantified OMVs using lipid-based techniques. This includes using the lipophilic dye FM4-64, which fluoresces upon integration with the phospholipid membrane of OMVs (Manning and Kuehn, 2011, MacDonald and Kuehn, 2013, Schwechheimer *et al.*, 2014). The fluorescence intensities which are produced correlate to the number of OMVs, thus producing a quantifiable measurement. Another way to measure OMV yield is by recording the absorbance of phospholipids from OMV samples which have been processed with chloroform extraction (Stewart, 1980, Schertzer *et al.*, 2010, Wessel *et al.*, 2013). This method relies on the formation of complexes between OMV phospholipids and ammonium ferrothiocyanate which produces a colorimetric readout.

Flow-cytometry is an alternative way to measure OMV yield and gain particle sizes, yet conventional machines can only measure particles larger than standard light wavelengths such as eukaryotic cells and bacterial cells. Previous studies have used highly sensitive nanoparticle flow cytometers to measure OMVs which have been dyed with a florescent dye such as FM-1 43, FITC and FM 4-64 in order to amply OMV signal (Cecil *et al.*, 2016, van der Vlist *et al.*, 2012). Yet standardisation with flow beads which are within OMV size distribution is essential as inappropriate sized beads can result in misrepresentative quantitative values (Cecil *et al.*, 2016). Furthermore, florescent dyes can affect OMV stability, with protein and DNA staining dyes resulting in increased OMV breakdown. Nevertheless, some lipid-based dyes do not affect OMV stability, therefore, the dye which is used to label OMVs needs to be considered prior to measuring OMVs via flow cytometry.

Previously, studies have suggested that protein contaminants from rich bacterial growth medium may be purified along with OMVs (Cecil *et al.*, 2016). In this study, through SDS-PAGE analysis and DLS examination it was verified that medium-derived contaminants were not present when sterile LB medium and SCEM were treated with the established OMV isolation procedure. Nevertheless, in this study it was concluded that supplemented cell culture medium (DMEM, high glucose) could not be used as protein contaminants are also purified, consequently obscuring Omp densitometry. BSA may be one of the main protein contaminants as it is one of the major components of FBS with a molecular weight of 66 kDa. In contrast, no contaminants were present when non-supplemented EHEC cultures were treated for OMV isolation. Likewise, Bradford protein assay detected a significantly higher protein content in OMV samples from supplemented DMEM EHEC cultures compared to non-supplemented DMEM EHEC cultures. Thus, to examine the effect of human cells on OMV production, subsequent cultures were made in non-supplemented cell medium once confluent monolayers were attained.

3.3.2 OMV production is dependent on bacterial growth phase

After the establishment of an OMV isolation protocol, the growth phase to achieve optimal OMV yield was determined. Here, EHEC OMV yield was highest after a 24-hour growth period i.e., stationary phase, as determined by both Bradford protein assay and densitometric quantification of Omp proteins. While late growth phases might provide higher OMV yields, after a long growth period bacterial lysis may result in membrane fragmentation and self-assembly into microvesicles known as outer-inner membrane vesicles and explosive outer-membrane vesicles (Pérez-Cruz *et al.*, 2013, Devos *et al.*, 2017, Turnbull *et al.*, 2016). Such vesicles may carry cytoplasmic contents and lead to potential protein contaminations when analysing OMV protein patterns. Here it is assumed that OMVs isolated from 24-hour cultures do not contain the aforementioned vesicles formed from membrane fragments, as the protein patterns between OMVs isolated after 24-hour cultures were similar to those of cultures grown for a shorter period.

These results are in agreement with a study undertaken with non-pathogenic *E. coli*, which also demonstrated that it is during the stationary growth phase that OMV production and release is at its optimum level, with similar protein composition between OMVs isolated at different growth phases (Manabe *et al.*, 2013). Similarly, the highest OMV yields are produced from stationary growth phase cultures of *Pseudomonas aeruginosa* and *Francisella novicida*, yet OMV protein contents differed between different growth phases (Tashiro *et al.*, 2010, McCaig *et al.*, 2013, Bauman and Kuehn, 2006). Using NTA, it has also been determined that the highest OMVs yields produced by *Neisseria meningitidis* occurs during stationary phase (Gerritzen *et al.*, 2017).

Strikingly, the OD_{600} values attained from EHEC cultures harvested for OMV isolation were significantly lower compared to those previously recorded for the construction of EHEC growth curves (Fig S1). This may be due to frequent opening of Falcon tubes during growth curve analysis which might have provided the growing culture with more oxygen compared to end-point cultures for OMV isolation. In the presence of

oxygen, *E. coli* can carry out aerobic respiration which generates more energy and allows faster growth compared to anaerobic respiration or mixed-acid fermentation which is used at low oxygen concentrations (Yasid *et al.*, 2016, Zhu *et al.*, 2011).

For safety reasons, Stx-positive EHEC cultures were grown in T75 flasks which allowed better aeration of cultures than Falcon tubes. This was reflected in higher optical densities of LB cultures achieved by EDL933 compared to the EDL933 derivative TUV 93-0 strain (OD_{600} 1.85 vs 3.16). As EDL933 cultures were grown differently than those of TUV 93-0 (rocking flasks vs. shaking tubes), OMV production could not be directly compared. No studies have been undertaken to determine whether there is a difference in OMV vesiculation between wild type EHEC strains and mutant Δ*stx* strains. Whether Stx or other virulence factors affect EHEC OMV vesiculation remains to be deduced.

3.3.3 Medium composition can affect EHEC OMV yield and composition

To determine whether EHEC growth in different medium affected OMV yield and composition, LB and Tryptic Soy broth (TSB) cultures of EHEC strains 85-170 and TUV 93-0 were compared. Unlike LB, TSB contains a ready to use carbon source, in the form of dextrose. In LB, catabolic amino acids are the main carbon sources, which first needs to be converted to usable carbon sources by EHEC enzymes. Consequently, this means that more energy is used in order for EHEC to grow in LB compared to media which has readily available carbon sources (Sezonov *et al.*, 2007). Final bacterial cell counts and OD_{600} values were similar between both media, however both Bradford protein assay and densitometric measurements of Omps indicated that OMV yields were higher when EHEC strains were grown in TSB. OMV protein profiles between isolated samples did not show major differences, suggesting that the different composition of LB and TSB does not affect OMV composition.

Differences in OMV yields have been observed in different bacterial species when grown in different media. When OMV yield was compared between *Pseudomonas*

putida cultures in LB and minimal medium, the highest yield was been attained from LB cultures grown (Choi *et al.*, 2014). Increased OMV production has also been detected by *Vibrio harveyi* cultures when grown in nutritional rich Luria marine medium compared to minimal autoinducer bioassay medium (Brameyer *et al.*, 2018). Nevertheless, bacterial growth in rich medium does not always increase OMV yield, as studies have shown that growth of *Lysobacter* sp. in limited nutritional broth produced higher OMV yields than cultures in nutritionally rich medium (Vasilyeva *et al.*, 2009).

The effect of DMEM/F-12 medium on two clinically relevant Stx-producing EHEC strains; EDL933 and 86-24 was examined. DMEM/F-12 medium contains glucose, amino acids, vitamins and inorganic salts and has been shown to support the growth of other *E. coli* pathotypes such as EAEC (Ellis *et al.*, 2020). Indeed, this medium is mainly used to grow mammalian cells, yet supplementation with FBS is needed as the medium does not contain growth hormones. In this study, the growth between the two EHEC strains in DMEM/F-12 medium was similar to that of LB cultures. Regarding OMV production, no statistical differences were attained between yields for both EHEC strains when cultured in DMEM/F-12 medium, however it may be possible that more replicates would make differences significant. The different protein pattern produced between OMVs isolated from cultures grown in different medium, implied that in different media, different proteins were expressed.

A weak Stx2 signal was detected by Western blots which is in contrast to other studies which have demonstrated Stx release within OMVs (Kolling and Matthews, 1999). It is speculated that this is due to the insufficient sensitivity of the antibody, as the presence of Stx was confirmed by immunofluorescence imaging when studying OMV trafficking in host cells (chapter 4, Fig. 4.7).

3.3.4 EHEC OMV production is not significantly affected by the presence of 5% carbon dioxide

Using an electronic gas sensing capsule, CO_2 levels in colonic liquid has been measured to be from 5% to 30% of the total gas profile in the colon (Kalantar-Zadeh *et al.*, 2018). Therefore, in this investigation the effect of 5% CO_2 on EHEC OMV production was evaluated. CO_2 becomes present in the gastrointestinal tract through various ways including (i) the swallowing of air, (ii) as a result of hydrogen ions present in gastric acid reacting with bicarbonate produced by cells, and (iii) as a by-product following bacterial fermentation.

In this study, supplementation of EHEC cultures with 5% CO_2 significantly increased viable cell counts and OD_{600} measurements for both EHEC TUV 93-0 and 85-170. This is comparable to findings from earlier studies which showed that the growth rate of *E. coli* increases with a 0.3% CO_2 supplementation, compared to normal atmospheric CO_2 concentrations of 0.03% (Repaske and Clayton, 1978). Furthermore, a previous study has demonstrated that optimal growth rate is obtained by *E. coli* in anaerobic conditions when supplemented with 5% CO_2, therefore emphasising the growth benefits of CO_2 for *E. coli* (Lacoursiere *et al.*, 1986). In contrast, another study suggests that in 5% CO_2, *E. coli* growth is inhibited yet this study only evaluated growth after 4- and 8-hour incubation periods (Eklund, 1984).

E. coli can utilize CO_2 in order to produce bicarbonate molecules which are needed for nucleotide base synthesis, fatty acid synthesis and carboxylation reactions (Holms, 1996, Merlin *et al.*, 2003). Due to the relatively low levels of CO_2 in normal atmospheric conditions and rapid diffusion of CO_2 from cells, *E. coli* possesses carbonic anhydrases to converts CO_2 to bicarbonate and maintain intracellular levels of bicarbonate (Merlin *et al*., 2003, Capasso and Supuran, 2015). In solution, CO_2 and bicarbonate spontaneously equilibrate, and it may be due to the higher levels of bicarbonate in CO_2 supplemented cultures that significantly higher growth levels arise in this investigation. Indeed, studies have shown that CO_2 supplementation permits the growth of mutant *E. coli* strains deficient of functional carbonic

anhydrases (Merlin *et al.*, 2003). For EHEC, bicarbonate levels can also influence the expression of virulence genes through RscB and GrvA proteins (Morgan *et al.*, 2013, Morgan *et al.*, 2016). In acidic environments, RscB can form a heterodimer with GadE and activate the glutamate-dependent acid resistance pathway, which represses the expression of LEE. However, when sensing bicarbonate through GrvA, the glutamate-dependent acid resistance pathway is repressed and expression of the TTSS is induced (Morgan *et al.*, 2016, Abe *et al.*, 2002).

In contrast to enhanced EHEC growth, the presence of 5% CO_2 did not result in significant increases in OMV yields. To the best of my knowledge, no studies have been performed to evaluate the effect of CO_2 on OMV production in other bacterial species. Speculatively, since EHEC growth is augmented in 5% CO_2, it is unlikely that EHEC undergoes major external stresses. This would correlate with the reduced OMV yields, since increased vesiculation has been associated with increased bacterial stresses (Maredia *et al.*, 2012, MacDonald and Kuehn, 2013, McBroom and Kuehn, 2007, Schwechheimer *et al.*, 2013, Baumgarten *et al.*, 2012, McBroom *et al.*, 2006, Orench-Rivera and Kuehn, 2016, Bauwens *et al.*, 2017a, Bauwens *et al.*, 2017b).

3.3.5 The presence of human cell lines does not significantly affect OMV yields

To determine the effect of host cells on EHEC OMV production, EHEC was cultured in the presence of cervical HeLa cells generally used to investigate EHEC A/E lesion formation (Knutton *et al.*, 1989) and the more biologically relevant Gb3-negative colon carcinoma cell line T84 (Schuller *et al.*, 2004). Here, bacteria and cells were also cultured alone in non-supplemented cell culture medium to serve as controls. Like the intestinal epithelium, T84 cells can synthesise antimicrobial peptides such as lysozyme and cationic human beta-defensins (hBD; O'Neil *et al.*, 1999, Ou *et al.*, 2009, Bernet-Camard *et al.*, 1996). Studies have also demonstrated that upon EHEC infection the expression of hBD2 by T84 cells is induced (Lewis *et al.*, 2016). Thus, it was anticipated that EHEC growth would be affected when grown in the presence of T84 cells due to the antimicrobial abilities of hBD2 produced by T84 cells (Mathew

and Nagaraj, 2017). Here there was no significant difference in bacterial growth in the presence of cell monolayers compared to the absence of host cells.

Interestingly, distinct protein bands were produced on polyacrylamide gels when non-infected medium samples from both HeLa and T84 cells were treated for OMV isolation and then evaluated. The presence of proteins in cell-derived samples, was also supported by Bradford protein assay. It is likely that these proteins are derived from extracellular vesicles such as exosomes. Like OMVs, exosomes can be purified by ultrafiltration and ultracentrifugation as they are similar in size (30 to 150nm; Doyle and Wang, 2019, Nath Neerukonda *et al.*, 2019). Furthermore, exosomes contain cell-derived proteins and genetic material (Kowal *et al.*, 2016). Notably, it has been shown that T84 cells can secrete exosomes which can interact with dendritic cells and instigate and immune response (Mallegol *et al.*, 2007).

Due to the presence of proteins in host cell-derived OMV preparations, Bradford protein assay was unsuitable for OMV quantification as it does not distinguish between EHEC- and host cell-derived proteins. In contrast, densitometric analysis of Omps was not affected by the presence of exosomes as these contained negligible amounts of proteins in the 32 kDa range. Densitometry results indicated similar EHEC OMV yields between the presence and absence of cell monolayers. It was predicted that lower OMV yields would be attained in the presence of host cells as it may have been possible that OMV internalisation by host cells occurs. To prevent OMV internalisation, uptake inhibitors such as dynasore and nystatin, could have been used. However, these drugs have an effect on cellular lipid rafts, cholesterol and actin which can impede the host response of T84 cells to EHEC and thereby artificially affect EHEC OMV production (Preta *et al.*, 2015). Nevertheless, subsequent experiments in this thesis concluded that such internalisation is unlikely for T84 cells as results from internalisation experiments demonstrate that EHEC OMV uptake by this cell line was negligible (Chapter 4, Fig. 4. 29, Fig. 4. 30 and Fig. 4. 31).

Another approach used to examine the influence of host cells on OMV production without the possibility of OMV internalisation by host cells has been used by Bauwens

et al. (2017), where EHEC was cultured in medium supplemented with lysates from Caco-2 cells. In contrast to results presented here, the presence of cell lysates augments EHEC OMV production (Bauwens *et al.*, 2017b). However, these results should be interpreted with caution as cell lysates contain intracellular proteins to which EHEC is not normally exposed to during infection. Different investigations have demonstrated that in the presence of membrane damaging AMPs such as polymyxin and human α-defensin 5, *E. coli* OMV yields increase which correlates with enhanced bacterial survival (Manning and Kuehn, 2011, Bauwens *et al.*, 2017a, Kulkarni *et al.*, 2015, Urashima *et al.*, 2017). Since OMV yields did not increase in this study, it is speculated that the level of AMPs produced by T84 cells in this investigation does not affect EHEC growth of OMV vesiculation.

3.3.6 Simulated colonic environment medium and bile salts stimulate the production of EHEC OMVs

In this study, simulated colonic environment medium (SCEM) was used to examine the effect of the abiotic parameters of the colon on EHEC OMV production as it exhibits physiologically relevant pH, osmotic concentrations and the presence of bile salts (Beumer *et al.*, 1992). Previous studies have confirmed that EHEC growth in SCEM induces the expression of proteins involved in nucleotide and amino acid synthesis, virulence and stress response (Polzin *et al.*, 2013, Müsken *et al.*, 2008). Another important requirement for intestinal colonisation is the adaption of bacterial cells to bile salts as such molecules can damage the bacterial outer membrane and DNA (Begley *et al.*, 2005). Previous investigations have verified that incubation of EHEC in medium containing bile salts decreases the expression of OmpF resulting in reduced outer membrane permeability (Hamner *et al.*, 2013). In addition, the expression of the AcrAB efflux pump is upregulated at 100µM of bile salts which actively exports bile salts from the bacterium and renders them resistant to bile salt exposure (Rosenberg *et al.*, 2003). This resistance is reflected in the growth curve

produced in this study which revealed that EHEC strains 85-170 and TUV 93-0 have similar growth kinetics in SCEM with or without bile salts.

Curiously, when OMVs were harvested from 18-hour SCEM EHEC cultures, a 3-fold decrease in viable cell counts was detected for both strains in the presence of bile salts compared to SCEM without bile salts. In addition, EHEC viable cell counts were lower in SCEM cultures lacking bile salts than in LB cultures. This is in agreement with data presented in Bauwens *et al.* (2017) which revealed that EHEC viable cell counts in SCEM with bile salts were lower than that of LB cultures. Likewise, OD_{600} measurements in this study differed for both strains between constructed growth curves and endpoint cultures grown for OMV isolation. As initial growth curves did not detect a difference between EHEC growth in SCEM with or without bile salts, it is speculated that oxygen availability may explain these contradictory results. While growth curve analysis was carried out by frequently opening flasks, cultures for OMV isolation were not provided with hourly doses of air. Bile salts are known to function as oxygen carriers and antioxidants, and thus may lead to restriction of oxygen levels and aerobic respiration during EHEC growth in closed containers, therefore inhibiting the rate of EHEC growth (Feroci *et al.*, 2007).

In addition to attenuating EHEC growth, culture in SCEM also affected OMV production for both strains, compared to LB cultures. Higher yields were attained from SCEM cultures versus LB cultures, with a further increase in yield from cultures grown in the presence of bile salts. This is consistent with results from Bauwens *et al.* (2017), which demonstrated enhanced EHEC OMV production in SCEM with bile salts versus LB medium. Nevertheless, while densitometric measurements in Bauwens *et al.* (2017), detected a 39-fold increase in OMV yield in SCEM cultures with bile salts compared to LB cultures, densitometric measurements in this study suggest an 18- and 15-fold increase in OMV yield for EHEC strains TUV 93-0 and 85-170, respectively. In contrast to this investigation which used OD_{600} for OMV yield normalisation, Bauwens *et al.* (2017) normalised OMV yields by using viable bacterial counts. While bile salts reduced EHEC viable cell counts to a bigger extent than OD_{600} measurements, this would consequently lead to higher adjusted OMV yields which

would explain the observed discrepancy. Interestingly, data attained through NTA did not suggest a significant increase in OMV particles, nevertheless with more replicates it may be possible that results are significant as data in this investigation shows increased trends when EHEC is grown in SCEM, with higher yields in medium supplemented with bile salts.

The protein patterns differed between OMV samples isolated from cultures grown in different media. Notably, the densitometric analysis of Omps is likely to be affected due to downregulated expression of OmpF by bile salt exposure as described above. Therefore, the protein-independent nanoparticle analysis performed is likely to be more accurate in this case. Other studies have shown that the bile salt taurocholate (approximately 1.86mM) increases OMV production in *Campylobacter jejuni* and leads to changes in OMV protein composition resulting in increased proteolytic activity, cytotoxicity and immunogenicity to T84 cells (Elmi *et al.*, 2018). NTA determined that EHEC cultures in SCEM without bile salts produced significantly smaller OMVs compared to EHEC cultures grown in LB and SCEM with bile salts. While Bauwens *et al.* (2017) did not analyse EHEC OMV production in SCEM without bile salts, OMV sizes gained in Bauwens *et al.* (2017) for EHEC LB and SCEM cultures were smaller compared to OMV sizes obtained in this investigation (LB: 115nm versus 202nm and 225nm for EHEC TUV 93-0 and 85-170, respectively; SCEM containing bile salts: 115nm versus 205nm and 213nm for EHEC TUV 93-0 and 85-170, respectively).

Antibiotics which activate the SOS response in EHEC have been associated with increased OMV production (Bauwens *et al.*, 2017a). Similarly, when *P. aeruginosa* is exposed to DNA-damaging antibiotics, OMV vesiculation increases due to the activation of the SOS response which leads to antibiotic sequestration and bacterial protection (Maredia *et al.*, 2012). As bile salts also induce an SOS response in *E. coli*, this might constitute a mechanism for enhanced OMV production under these conditions (Kandell and Bernstein, 1991, Begley *et al.*, 2005). Yet, a recent study has revealed that the bile salt sodium taurocholate reduces the expression of genes which regulate the lipid asymmetry pathway in *C. jejuni*, resulting in increased OMV vesiculation (Davies *et al.*, 2019). The lipid asymmetry pathway is highly conserved in

Gram-negatives and has been implicated as a general pathway that is involved in OMV biogenesis (Roier *et al.*, 2016). Downregulation of the lipid asymmetry pathway leads to phospholipid accumulation on the outer leaflet of the bacterial outer membrane, consequently leading to asymmetric expansion and OMV formation. Mutants deficient of components involved in this pathway have demonstrated increased OMV productions. As *E. coli* OMV production can be regulated through the lipid asymmetry pathway, it is speculated that bile salts used in this study may increase OMV biogenesis this same pathway (Roier *et al.*, 2016). Whether EHEC OMVs sequester bile salts and thereby provide protection remains to be deduced.

SCEM contains 4.73 mM of bile salts composed of a 50:50 ratio of cholic and deoxycholic acid. Not only does this bile salt concentration exceeds physiological colonic levels but the concentration of the primary bile salt cholic acid far exceeds what is physiologically found in the colon. Due to the chemical diversity of bile salts and molecular complexity of biological matter such as bile and stool, the development of sensitive and accurate analytical methods to quantify bile salt concentrations *in vivo* is challenging (Sarafian *et al.*, 2015). In the duodenum, it is estimated that bile salt concentrations can range from 4mM (starved state) to 10mM (fed state; Riethorst *et al.*, 2016). Levels start to decrease in the small intestines, due to active absorption in the terminal ileum, with an estimated 5% of bile salts passing into the colon. Primary bile salts which enter the colon are subsequently transformed (through dihydroxylation and deconjugation reactions) into secondary bile salts such as deoxycholic acid and lithocholic acid (Ridlon *et al.*, 2006). Autopsy studies conducted on 24 hours post-mortem cadavers have detected approximately 600 µM of bile salts in the cecum, with deoxycholic acid and lithocholic acid making up 34% (204 µM) and 26% (156 µM) of the total bile salt pool, respectively (Hamilton *et al.*, 2007). Nevertheless, these estimates may not be accurate due to the influence of post-mortem changes and patient antibiotic intake prior to death. Recent studies have measured bile salt concentration in healthy faecal samples to be 500 µM to 3mM, with deoxycholic acid and lithocholic acid making up 60% and 38% of the total bile salt pool, respectively (Peleman *et al.*, 2017). Since the bile salt concentrations used for SCEM far exceeds physiological levels, the fold increase in OMV production

suggested in this study may be overestimated to what occurs *in vivo*. Nevertheless, as OMV integrity was not affected by the augmented bile salt levels used in SCEM this study suggests that colonic levels of bile salts do not destroy EHEC OMVs.

3.3.7 Summary

Here, it has been demonstrated that the rate of EHEC vesiculation can be affected by different colonic conditions in distinctive ways. Firstly, this study determined that OMV production is growth phase-dependent, with stationary phase EHEC bacteria producing the highest OMV yield. Likewise, it has been demonstrated that different medium compositions can affect OMV vesiculation as significantly higher OMV yields were attained when EHEC was grown in TSB medium compared to LB medium, but similar yields were attained between LB and DMEM/F-12 EHEC cultures. This study also demonstrated that EHEC cultures in SCEM, which emulates various colonic abiotic factors, produced higher OMVs yields compared to LB cultures. Moreover, the addition of bile salts in SCEM further augmented OMV yield. In contrast, the supplementation of 5% CO_2 to EHEC cultures and the presence of human colonic cells did not affect EHEC OMV production, suggesting not all colonic cues affect OMV production.

Due to the loss of containment level 3 laboratory access, further work on Stx-producing EHEC strains could not continue. However, due to the use of derivate Stx-producing EHEC, it is anticipated that the effect different conditions have on such strains will be similar to Stx-producing EHEC. Coupled with the data presented here, it can be speculated that upon the ingestion, EHEC OMV vesiculation initially increases during EHEC passage in the gut lumen, aiding nutrient acquisition and providing protection against harsh conditions such as bile salts. Yet, once EHEC interacts with colonic cells, OMV vesiculation decreases with some OMVs possibly being internalised by colonic cells.

Chapter Four: The interaction between EHEC OMVs and physiologically relevant host cells

4.1 Introduction

EHEC infections can progress into haemorrhagic colitis and haemolytic uraemic syndrome (HUS; Karmali *et al.*, 1983a, Riley *et al.*, 1983, Tarr *et al.*, 2005). Upon colonisation of the colonic epithelium, two virulence strategies are implemented by EHEC: (i) the formation of A/E lesions, and (ii) the production of Stx (Kaper *et al.*, 2004). The development of HUS is associated with the release of Stx which targets Gb3-expressing cells located throughout the vasculature, the central nervous system and the kidneys (Obata *et al.*, 2008, Obrig, 2010). Soluble Stx is released by EHEC through the activation of the phage lytic cycle resulting in bacterial cell lysis (Neely and Friedman, 1998). Given that cells in the human intestinal epithelium do not express Gb3 receptors, it is not fully understood how the translocation of soluble Stx across the colonic epithelia into the vascular system occurs (Schuller *et al.*, 2004, Kovbasnjuk *et al.*, 2005).

Various trafficking pathways have been proposed to explain how soluble Stx crosses the epithelia, including a macropinocytosis-mediated internalisation and subsequent translocation by colonocytes, and neutrophil-mediated disruption of the intestinal barrier which consequently allows paracellular trafficking of soluble Stx into the vascular system (Hurley *et al.*, 2001, Malyukova *et al.*, 2009, Lukyanenko *et al.*, 2011, In *et al.*, 2013). Yet, Stx has also been detected within EHEC OMVs, hence providing an alternative pathway for Stx release and interaction with host cells (Kolling and Matthews, 1999). Moreover, Yokoyoma *et al.* (2000), elucidated that under low oxygen conditions, akin to those found in the colon, Stx is mainly released via OMVs.

Previous studies have demonstrated that OMVs contribute to bacterial pathogenesis by delivering virulence factors into host cells. OMVs produced by *V. cholerae* carry virulence factors including cholera toxin and PrtV metalloprotease, which are involved in inducing diarrhoea and degrading substrate proteins such as fibronectin in tissues, respectively (Chatterjee and Chaudhuri, 2011, Elluri *et al.*, 2014, Rompikuntal *et al.*, 2015). Similarly, LT can be encapsulated by OMVs produced by ETEC, which can cause increased cAMP production in target cells, leading to

diarrhoea in the host during ETEC infections (Horstman and Kuehn, 2000, Kesty *et al.*, 2004). Typhoid toxin can also be encapsulated by OMVs produced by *Salmonella enterica*, which can result in DNA damage and the activation of the host DNA damage response in target cells (Guidi *et al.*, 2013).

The biological relevance of EHEC OMVs was confirmed in murine investigation, where intraperitoneal injections of EHEC OMVs resulted in the development of disease and renal cell damage (Kim *et al.*, 2011). Along with Stx, other virulence factors which can be released via EHEC OMVs include haemolysin (Hly), flagellin, cytolethal distending toxin V (CdtV) and Shigella enterotoxin 1 (Kolling and Matthews, 1999, Yokoyama *et al.*, 2000, Bielaszewska *et al.*, 2013, Kunsmann *et al.*, 2015). Using colonic-derived non-polarised Caco-2 cells and human microvascular endothelial cells, EHEC OMV internalisation has been demonstrated to be mediated by dynamin-dependent (and partially clathrin-mediated) endocytosis (Bielaszewska *et al.*, 2017). It has also been demonstrated that upon OMV transportation to late endosomes, Stx2, CdtV and Hly are separated from OMVs and are trafficked to ribosomes, nucleus and mitochondria, respectively, consequently leading to cell apoptosis (Bielaszewska *et al.*, 2017).

To determine OMV trafficking and the trafficking of OMV-associated virulence factors, non-polarised Caco-2 cells were used. Yet, the use of non-polarised Caco-2 cells to study what arises *in vivo* may not be appropriate. Physiologically, the intestinal epithelium is arranged in a polarised manner and expresses intercellular junctions such as tight junctions, which prevent paracellular trafficking of luminal contents and separating the apical and basolateral cell surfaces (Zihni *et al.*, 2016, Schneeberger *et al.*, 2018, Furness *et al.*, 1999). Accordingly, the distribution of surface proteins and cytoskeletal components differs between the basal and apical cell membranes (van der Wouden *et al.*, 2003, Weisz and Rodriguez-Boulan, 2009). The use of Caco-2 cells may also be questioned as mature Caco-2 cells are akin to small intestinal enterocytes due to their comparatively long microvilli and expression of brush boarder hydrolases unique to the small intestine (Devriese *et al.*, 2017). Furthermore, due to the expression of the Gb3 receptor by Caco-2 cells, the use of

this cell line may not be truly reflective of what occurs *in vivo*, therefore questioning the reliability of these results (Schuller *et al.*, 2004, Kovbasnjuk *et al.*, 2005).

In order to address these limitations, physiologically relevant colonic and renal cell lines were utilised in this investigation so to study the interaction between OMVs and the host, at both the site of bacterial infection (colon) and the main Stx target site (kidneys). In this investigation, to mimic the colon, the interaction between OMVs and polarised colonic cells was examined. Furthermore, the interaction between colonic T84 cells and OMVs was investigated as these crypt-like cells do not express Gb3 in the fully differentiated state (Schuller *et al.*, 2004). To evaluate whether the results achieved by using cell monocultures fully represents what occurs *in vivo*, the interaction between EHEC OMVs and two-dimensional human-derived colonoid was also studied, as differentiated colonoids contain similar cell compositions as that of the colonic epithelium.

By elucidating whether EHEC OMVs are internalised by polarised cells and determining the subsequent trafficking, this study will address whether OMVs provide a potential mechanism for Stx translocation across the colonic epithelium. As previous investigations have demonstrated the internalisation of EHEC OMV by non-polarised Caco-2 cells and microvasculature cells, it is hypothesised that EHEC OMV internalisation can occur in the colon, with subsequent translocation in polarised cells.

The objectives of this study were to:

1. Determine whether OMVs can be internalised by the colon by using various models such as Caco-2 cells, T84 cells and human colonoid models.
2. Investigate the intracellular trafficking of OMVs in non-polarised and polarised colonic models.
3. Elucidate whether EHEC OMVs can translocate across polarised colonic monolayers.
4. Evaluate if renal cells can internalise EHEC OMVs and elucidate the intracellular trafficking of OMVs and OMV-associated Stx.

4.2 Results

4.2.1 Optimisation of EHEC O157 OMV internalisation and detection assay

EHEC infections can lead to the development of HUS, which entails kidney damage due to the action of Stx (Karmali *et al.*, 1983a, Obrig, 2010). As previous studies have demonstrated the encapsulation of Stx within EHEC OMVs, Stx transportation from the colonic lumen to the kidneys may involve OMVs during infection (Kolling and Matthews, 1999, Bielaszewska *et al.*, 2017). To evaluate the interaction between OMVs and OMV-associated Stx2 with the kidneys, African green monkey renal Vero cells were used as such cells readily internalise soluble Stx due to the expression of Gb3. They have also been used in previous studies to determine the intracellular trafficking of soluble Stx (Konowalchuk *et al.*, 1977, Lingwood *et al.*, 1987).

To study OMV internalisation, previous studies have utilised lipophilic dyes to label OMV membranes, thus allowing OMV uptake and trafficking to be studied by fluorescence microscopy (Parker *et al.*, 2010, Bielaszewska *et al.*, 2013, Kunsmann *et al.*, 2015, Jones *et al.*, 2020). Therefore, in the first part of this investigation OMVs isolated from EHEC strains were labelled with lipophilic DiO dye (DiO-OMVs).

To deduce whether renal Vero cells can internalise EHEC OMVs, cells were seeded onto coverslip and cultured for 5 days until full confluency was reached. To determine whether starvation was required for OMV internalisation, Vero cells were incubated in supplemented DMEM or in non-supplemented DMEM 24 hours prior to OMV inoculation. Pathophysiological EHEC OMV concentrations in the colon and kidneys during infection is unknown, thus the use of arbitrary OMV concentrations may lead to artificial results. Nevertheless, it was decided that the amount of OMVs used in this investigation would be similar to those used by previous studies so that some comparisons can be achieved (Bielaszewska *et al.*, 2013, Bielaszewska *et al.*, 2017). After quantifying OMV protein content through Bradford protein assay, Vero cell monolayers were incubated for 5 and 24 hours with 10μg of DiO-dyed OMVs (DiO-

OMVs) protein isolated from LB cultures of EHEC 85-170, and monolayers were subsequently visualised by fluorescence microscopy.

As shown in Fig. 4.1, confluent Vero cell monolayers interacted with DiO-OMVs isolated from EHEC strain 85-170 after 5-hours of incubation. Furthermore, examination of monolayers incubated with DiO-OMVs for 24 hours showed a similar staining pattern. Starved Vero cell monolayers exhibited fragmentation; however, this was probably due to the lack of nutrients in the non-supplemented DMEM as non-treated control monolayers showed a similar phenotype. Therefore, to study OMV internalisation and trafficking, subsequent experiments were performed using 10μg of EHEC OMVs in non-supplemented cell medium without prior starvation.

The use of lipophilic dyes may produce misleading results as the possibility of free dye interacting with host cells may arise due to insufficient washing of the lipophilic dyed OMV sample (Mulcahy *et al.*, 2014, O'Donoghue and Krachler, 2016). In addition, previous studies have demonstrated that dye molecules can alter OMV membranes and may affect OMV function and intracellular trafficking (Lulevich *et al.*, 2009). Another possible drawback of the use of lipophilic dyes is the leaching of fluorescent molecules onto cellular membranes, resulting in a fluorescence pattern which arises due to dyed membranes rather than OMV trafficking. To confirm that the stained pattern produced by intracellular DiO label was not a result of internalisation of free dye molecules or leached dye molecules staining organelle membranes, an *E. coli* specific anti-LPS antibody was used to detect OMVs. This antibody was chosen as it has been shown to label EHEC OMVs in previous studies (Bielaszewska *et al.*, 2017).

Confluent Vero cell monolayers were incubated with DiO-OMVs or DiI-dyed OMVs (DiI-OMVs) for 5 hours and then immunostained. As shown in Fig. 4.2 little colocalised staining was exhibited. Colocalisation was quantified by Manders colocalisation coefficients (Fig 4.3), with a M1 value (% of red fluorophore colocalising with green fluorophore) and a M2 value (% of green fluorophore colocalising with red fluorophore) of 36.5% and 11.68% being detected, respectively, between DiO-OMV

signal and LPS signal. Similar colocalisation values were attained between LPS signal and DiI-OMVs with a M1 value of 7.4% and M2 value of 40.54%. Interestingly, a higher proportion of LPS signal overlaps with the lipophilic dye signal for both dyes than lipophilic dye with LPS signal, suggesting that some intracellular OMVs retain the dye molecules, yet some dye molecules may also leach onto intracellular membranes. To verify that free dye molecules are not present in dyed OMV samples, Vero cell monolayers were incubated with the flow-through attained from the last wash step after the OMV staining procedure with lipophilic dyes. As shown in Fig. 4.2, Vero cells lack staining, therefore confirming the absence of soluble dye molecules in lipophilic stained OMVs and suggesting the leaching of dye molecules onto organelle membranes upon the internalisation of lipophilic dyed OMVs.

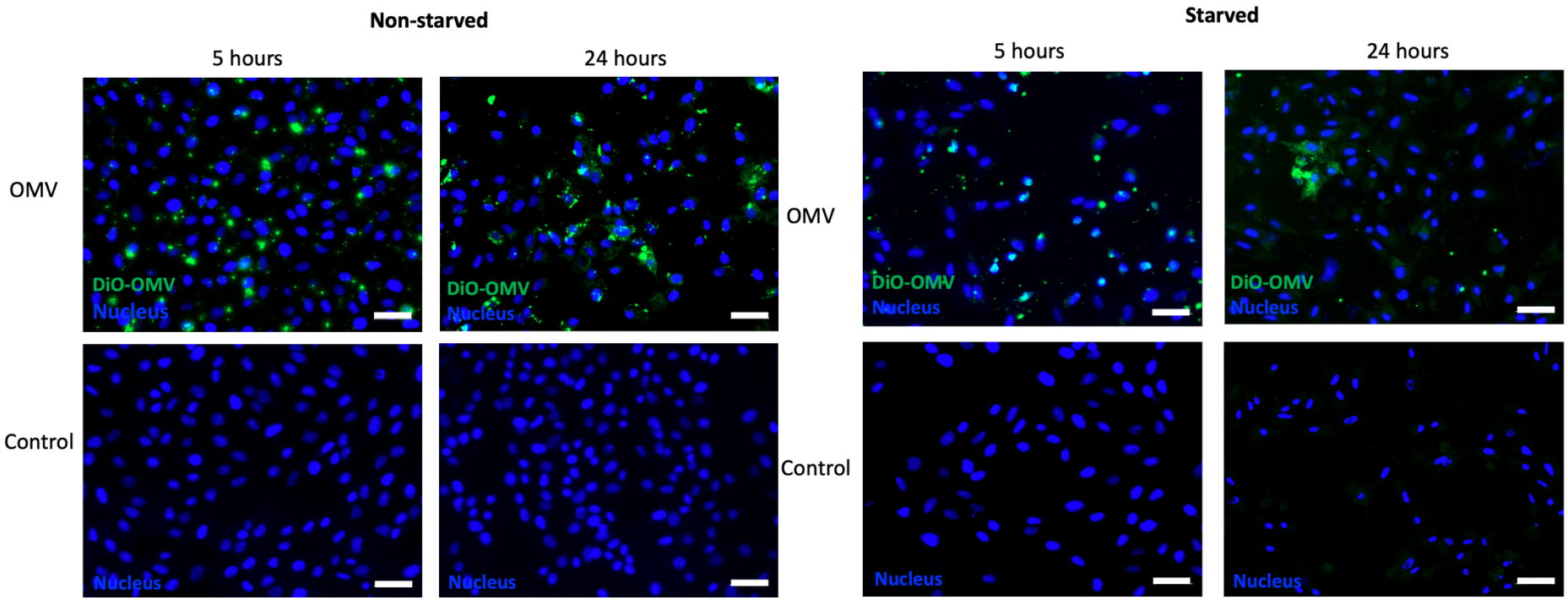

Figure 4.1: Starvation is not needed for DiO-OMVs isolated from LB cultures of EHEC 85-170 to interact with Vero cells. Vero cells were incubated with supplemented (non-starved) or non-supplemented (starved) DMEM, 24 hours prior to OMV incubation. Monolayers were subsequently incubated for 5 and 24 hours with 10μg of DiO-OMVs (green). Cell nuclei were labelled with DAPI (blue). Images are representative of three independent experiments, performed in duplicate. Images were produced at a resolution as close to the optimal resolution permitted by the system. Images were attained by using a Zeiss Axio imager M2 widefield microscope fitted with a 10x objective (EC Plan-Neofluar, NA = 0.30, Zeiss). Scale bars = 50μm.

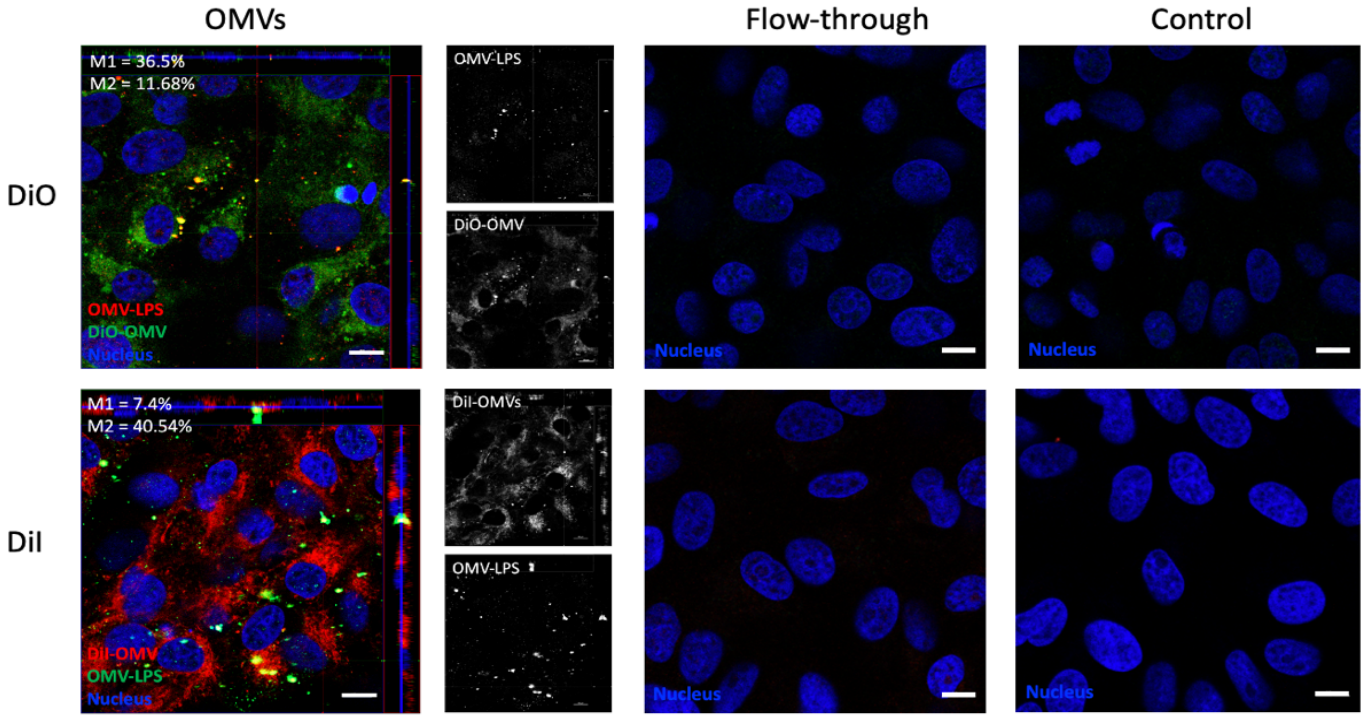

Figure 4.2: DiO and DiI molecules leach onto intracellular membranes in Vero cells. Confluent Vero cell monolayers were incubated for 5 hours with 10μg of DiO-OMVs (green) or DiI-OMVs (red) isolated from LB cultures of EHEC 85-170. Cells were also incubated with flow-through from the final wash step after staining OMVs with the lipophilic dyes. OMVs were detected with *E. coli* specific anti-LPS (red in cells incubated with DiO-OMVs and green in cells incubated with DiI-OMVs) and cell nuclei were labelled with DAPI (blue). Images are representative of more than three independent experiments, performed in duplicate. The main image represents merged images from three separate channels, with channels representing the red and green channels shown individually in the side panels. The percentage of colocalisation (M1, % of red fluorophore overlapping with green fluorophore; and M2, % of green fluorophore overlapping with red fluorophore) are indicated by the white numbers. Images were produced at a resolution as close to the optimal resolution permitted by the system. Images were attained by using a Zeiss LSM800 confocal microscope fitted with a 63x water immersion objective (C-apochromat, NA = 1.2, Zeiss). Scale bars = 10μm.

.

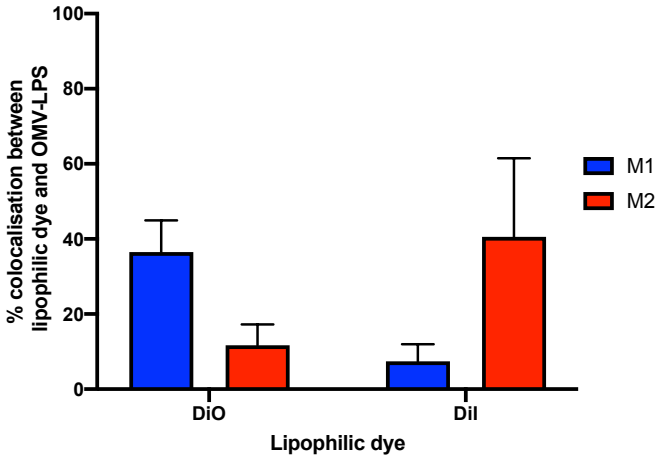

Figure 4.3: Quantification of signal colocalisation between DiO or DiI molecules and OMV-LPS signals in Fig. 4.2. M1 = % of red fluorophores which colocalised with green fluorophores, M2 = % of green fluorophores which colocalised with red fluorophores. Data is shown as the means of colocalisation ± SD of five different cells.

4.2.2 Upon the internalisation of OMVs isolated from EHEC by renal Vero cells, OMV-associated Stx splits and follows a different trafficking pathway

Having established that EHEC OMVs can interact with Vero cells, the interaction between Vero cells and OMV-associated Stx2 isolated from LB cultures of EHEC strain EDL933 was examined. Even though both Stx1 and Stx2 are encapsulated within OMVs produced by EHEC (Kolling and Matthews, 1999), the intracellular trafficking of Stx2 was chosen as Stx2 is associated with the development of severe disease (Werber *et al.*, 2003, Orth *et al.*, 2007, Kawano *et al.*, 2008, Byrne *et al.*, 2015).

To establish a protocol for immunofluorescence detection of Stx2, confluent Vero cell monolayers were incubated with 1.25μg of purified Stx2 for 5 hours and immunostained using a polyclonal anti-Stx2 antibody. As shown in Fig. 4.4, Stx2 labelling was localised to the perinuclear region. To confirm that this staining was specific for internalised Stx2, cells were subsequently immunostained for the endoplasmic reticulum (ER), since soluble Stx is known to be retrogradely trafficked to the ER (Sandvig *et al.*, 1992). Colocalisation of the two markers was observed (Fig. 4.5) and quantified (Fig 4.6 A and B). Quantification of the signals produced a M1 rate of 76.02%, suggesting that 76.02%

of the total Stx2 signal colocalised with the ER (Fig. 4.6A), and a M2 rate of 34.72% suggesting that only 34.72% of the ER compartment contained Stx2 (Fig 4.6B). Overall, these results suggest Stx2 is being trafficked to the ER which is consistent with previous results (Sandvig *et al*., 1992).

Following these results, DiO-OMVs isolated from LB cultures of Stx-producing EHEC strain EDL933 were incubated with confluent Vero cell monolayers for 3 and 5 hours and were subsequently stained for Stx2. As shown in Fig. 4.7, Vero cells internalised DiO-OMVs after a 3-hour incubation period, with DiO fluorescence being retained after 5 hours. Stx2 was also detected within cells after being incubated with the same DiO-OMVs for 3- and 5-hours, yet the intracellular localisation of DiO dye and Stx2 differed. This difference in location, suggests that upon OMV internalisation, OMV-associated Stx2 is freed and follows a different intracellular trafficking pathway to that of OMVs or DiO molecules. Colocalisation rate were quantified and confirmed the different intracellular locations, as low M1 and M2 values were obtained after both 3- and 5-hour incubation periods (Fig. 4.8A and B, respectively). Interestingly, not all cells which internalised DiO-OMVs exhibited intracellular Stx2, suggesting not all OMVs produced by EHEC EDL933 contains Stx2.

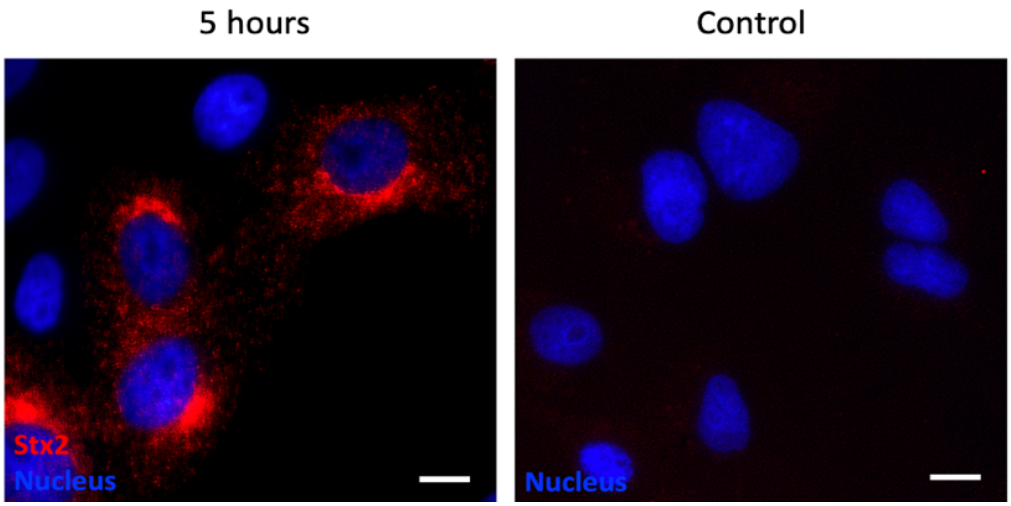

Figure 4.4: Soluble Stx2 are internalised by Vero cells after a 5-hour incubation period. Cells were immunostained for Stx2 (red), and cell nuclei were labelled with DAPI (blue). Images are representative of more than three independent experiments performed in duplicate. Images were produced at a resolution as close to the optimal resolution permitted by the system. Images were attained by using a Zeiss Axio imager M2 widefield microscope fitted with a 63x oil immersion objective (Plan-Apochromat, NA = 1.4, Zeiss). Scale bars = 10μm.

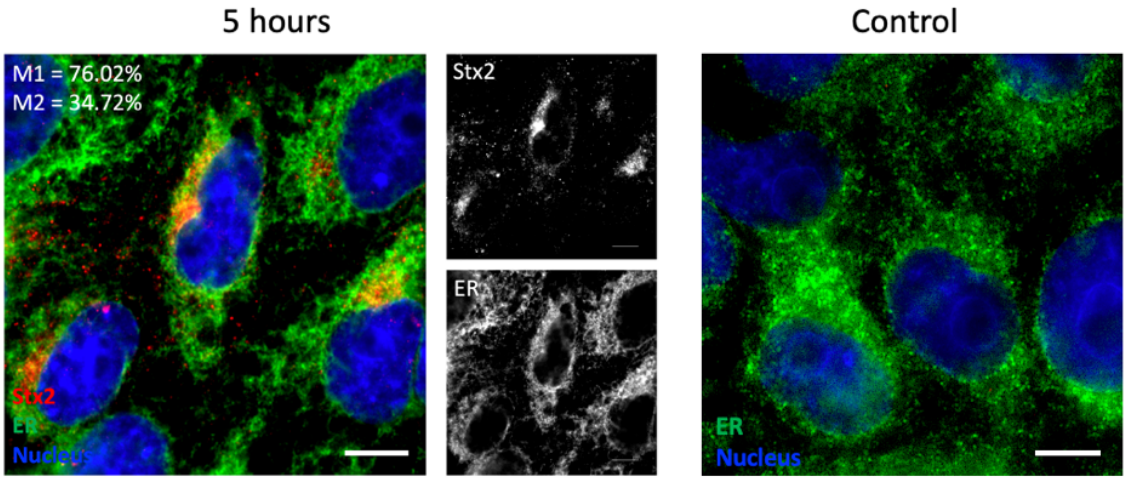

Figure 4.5: Some colocalisation occurs between internalised soluble Stx2 and the ER in Vero cells after a 5-hour incubation period. Cells were immunostained for the ER (green) and Stx2 (red), and cell nuclei were labelled with DAPI (blue). Images are representative of two independent experiments performed in duplicate. The main image represents merged images from three separate channels, with the red and green channels shown individually in the side panels. The percentage of colocalisation (M1 = % of Stx2 signal colocalising with the ER, M2 = % of ER compartment containing Stx2 signal) are indicated by the white numbers. Images were produced at a resolution as close to the optimal resolution permitted by the system. Images were attained by using a Zeiss Axio imager M2 widefield microscope fitted with a 100x oil immersion objective (EC Plan-Neofluar, NA = 1.3, Zeiss). Scale bars = 10μm.

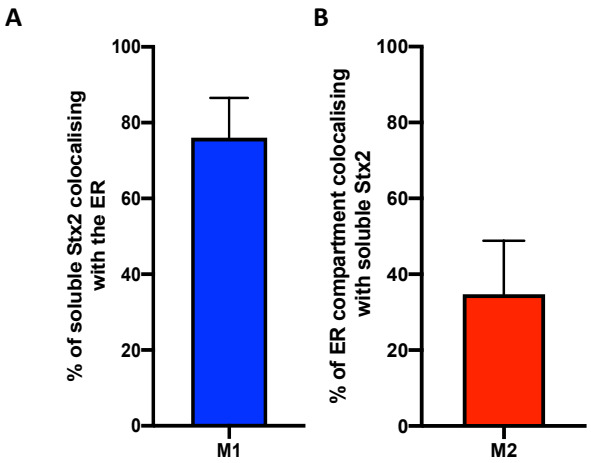

Figure 4.6: Quantification of signal colocalisation between internalised soluble Stx2 and the ER in Fig. 4.5. A) Graphical presentation of the mean percentage of Stx2 signal colocalising with ER signal ± SD of five representative cells (M1). B) Graphical presentation of the mean percentage of the ER signal containing Stx2 signal ± SD of five representative cells (M2).

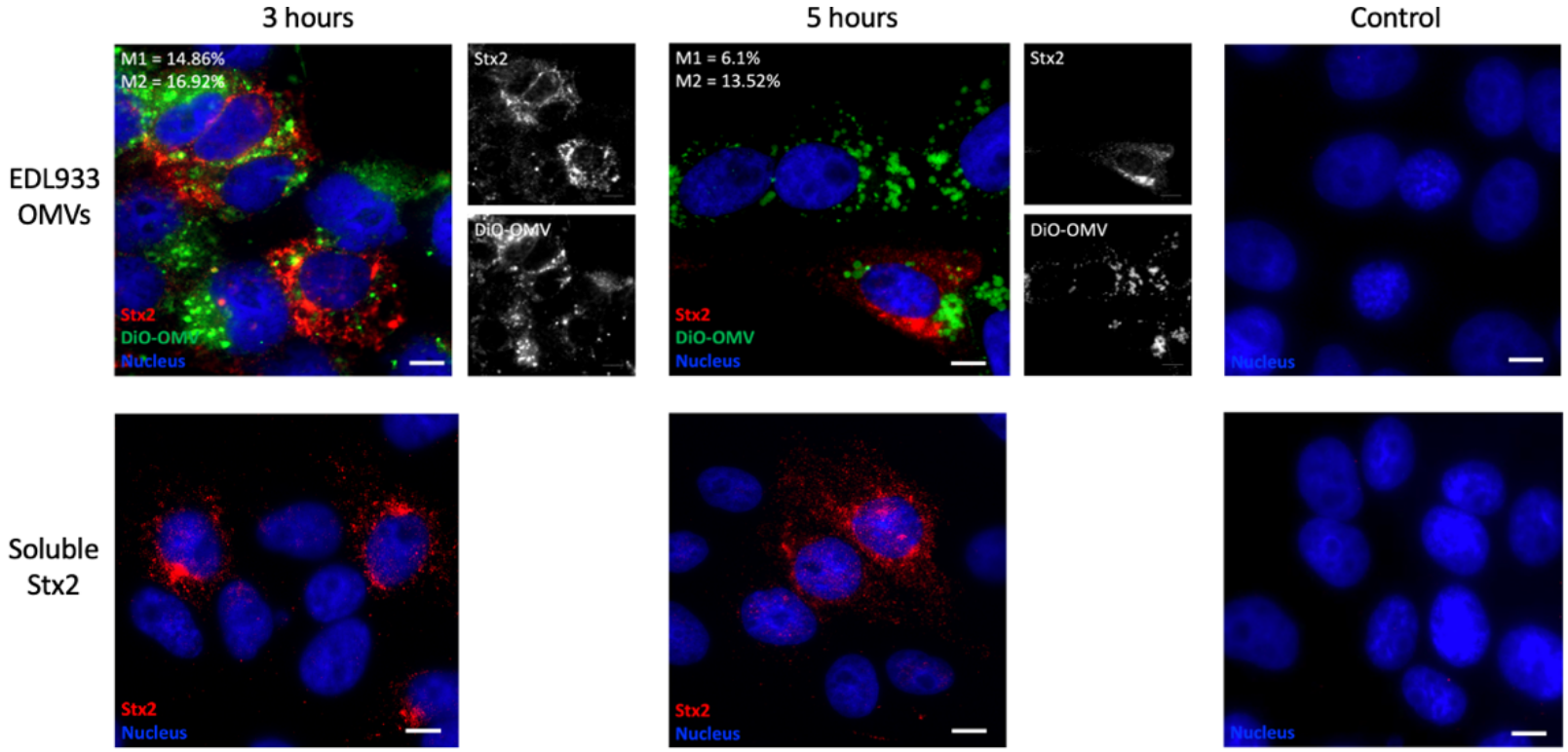

Figure 4.7: Internalised EHEC OMVs and OMV-associated Stx2 follow different intracellular trafficking pathways in Vero cells. After 3- and 5-hour incubation periods with 10μg of DiO-OMVs (green) isolated from LB cultures of EHEC EDL933, Vero cells were immunostained for Stx2 (red), and cell nuclei were labelled with DAPI (blue). Images are representative of three independent experiments, performed in duplicate. The main image represents merged images from three separate channels, with the red and green channels shown individually in the side panels. The percentage of colocalisation (M1 = % of Stx2 signal colocalising with DiO, M2 = % of DiO containing Stx2 signal) are indicated by the white numbers. Images were produced at a resolution as close to the optimal resolution permitted by the system. Images were attained by using a Zeiss Axio imager M2 widefield microscope fitted with a 63x oil immersion objective (Plan-Apochromat, NA = 1.4, Zeiss). Scale bars = 10μm.

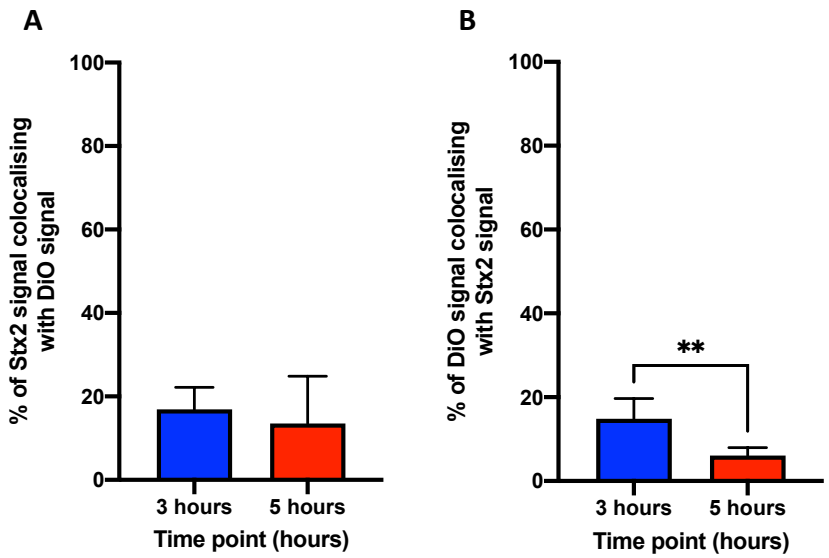

Figure 4.8: Quantification and statistical analysis of signal colocalisation between DiO-OMVs and Stx2 in Fig. 4.7. A) Graphical presentation of the mean percentage of Stx2 signal colocalising with DiO signal ± SD of five representative cells (M1). B) Graphical presentation of the mean percentage of DiO signal colocalising with Stx2 signal ± SD of five representative cells (M2). ** = $P < 0.01$.

4.2.3 OMV-associated Stx2 from EHEC O157 is trafficked to the Golgi apparatus and subsequently the ER in renal Vero cells

To elucidate the intracellular trafficking of OMV-associated Stx2 in Vero cells, confluent Vero cell monolayers were incubated with OMVs isolated from EHEC strain EDL933 for 1, 3 and 5 hours and subsequently immunostained for Stx2 and either the Golgi apparatus or the ER as these are the main organelles involved in the intracellular trafficking of soluble Stx (Sandvig *et al*., 1992, Falguieres *et al*., 2001).

As shown in Fig. 4.9, Stx2 colocalisation with the Golgi apparatus and the ER was time dependent. After an hour of incubation, OMV-derived Stx2 was internalised and colocalised with the Golgi apparatus, with longer incubation times reducing colocalisation. The colocalisation rates of Stx2 signal with that of the Golgi apparatus (M1) were measured to be 62.92%, 9.66% and 10.86% after 1-, 3- and 5-hour incubations, respectively (Fig 4.10A), with the initial decrease being significant ($P < 0.01$). Furthermore, after 1-, 3- and 5-hour incubations, 89.76%, 90.12% and 90.86% of the Golgi apparatus compartment was detected to have Stx2 signal (Fig 4.10B). These

results suggest that after initial transportation to the Golgi apparatus, Stx2 is subsequently transported to another organelle. Stx2 colocalisation with the ER significantly increased over time ($P < 0.05$), with colocalisation rates of 21.22%, 61.28% and 82% after 1-, 3- and 5-hour incubations, respectively (Fig. 4.10A). Similarly, the level of the ER compartment containing Stx2 signal significantly increased overtime ($P < 0.01$), with colocalisation rates of 10.72%, 45.54% and 80.3% after 1-, 3- and 5-hour incubations, respectively (Fig 4.10B). These results indicate that after OMV internalisation, OMV-associated Stx2 follows a retrograde transport via the Golgi apparatus to the ER.

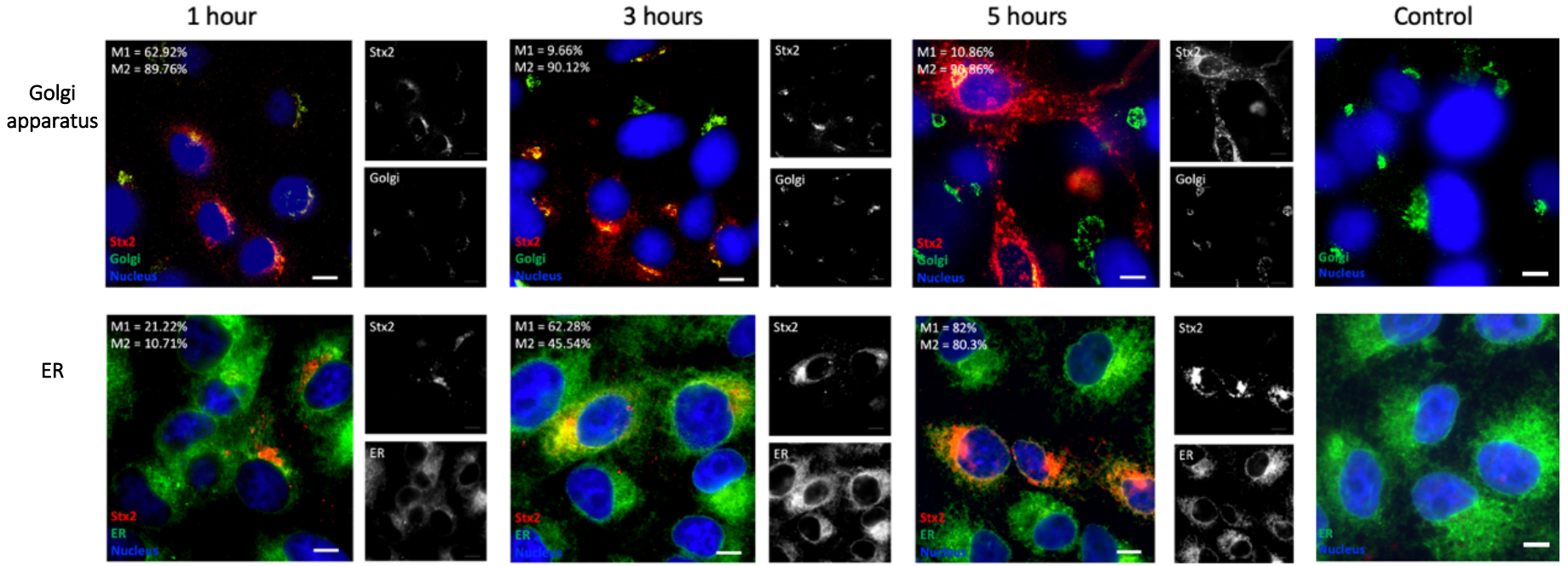

Figure 4.9: Upon the internalisation of EHEC OMVs, OMV-associated Stx2 follows retrograde trafficking to the ER via the Golgi apparatus in Vero cells. Confluent Vero cell monolayers were incubated for 1, 3 and 5 hours with 10μg of OMVs isolated from LB cultures of EHEC EDL933. Cells were immunostained for Stx2 (red) and either the Golgi apparatus (green) or ER (green) and cell nuclei were labelled with DAPI (blue). Images are representative of more than three independent experiments, performed in duplicate. The main image represents merged images from three separate channels, with the red and green channels shown individually in the side panels. The percentage of colocalisation (M1, % of Stx2 overlapping with organelle compartments; and M2, % of organelle compartment containing Stx2 signal) are indicated by the white numbers. Images were produced at a resolution as close to the optimal resolution permitted by the system. Images were attained by using a Leica DM6000 B widefield microscope fitted with a 63x oil immersion objective (HCX PL S – APO, NA = 1.30, Leica). Scale bars = 10μm.

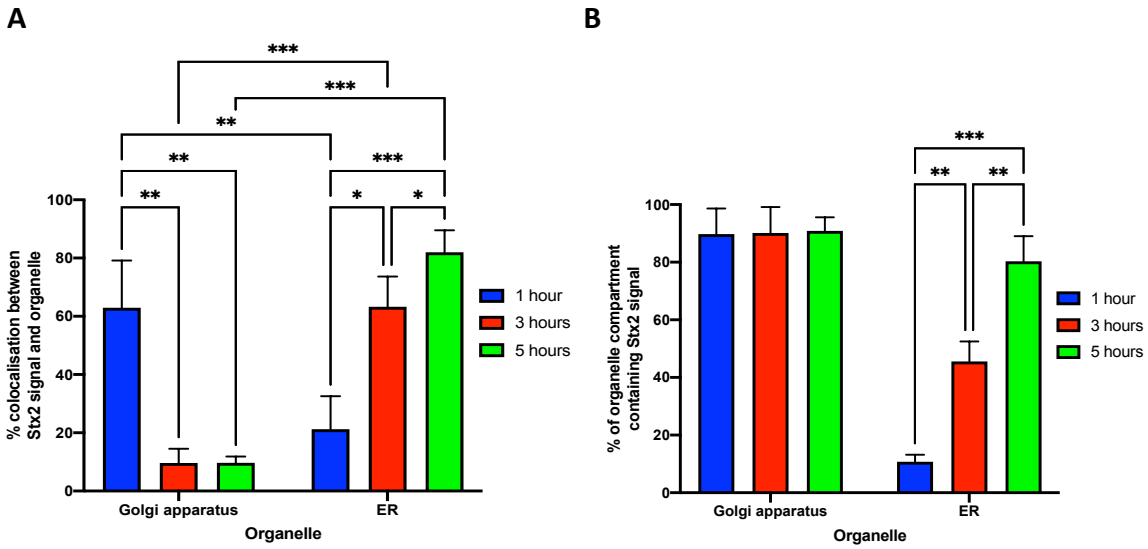

Figure 4.10: Quantification and statistical analysis of colocalisation between Stx2 and the Golgi apparatus or ER shown in Fig. 4.9. A) Graphical presentation of the mean percentage of Stx2 signal colocalising with organelle compartment signal ± SD of five representative cells (M1). B) Graphical presentation of the mean percentage of organelle compartment signal containing Stx2 signal ± SD of five representative cells (M2). * = $P < 0.05$, ** = $P < 0.01$, *** = $P < 0.001$.

4.2.4 EHEC O157 OMVs are trafficked to the late endosomes/lysosomal compartments upon internalisation into Vero cells.

Having demonstrated intracellular transportation of OMV-associated Stx to the Golgi apparatus and the ER, the intracellular destination of the respective OMVs was determined. To deduce this, confluent Vero cell monolayers were incubated with OMVs isolated from EHEC strain EDL933 for 1, 3 and 5 hours and subsequently stained for OMVs using the *E. coli* specific LPS targeting antibody (hereafter termed OMV-LPS) and either the Golgi apparatus or the ER (Fig. 4.11). Weak colocalisation was detected as low M1 and M2 colocalisation values were attained at all time points (Fig. 4.12A and B, respectively), suggesting OMVs are not trafficked to neither the Golgi apparatus nor the ER.

Since previous studies have demonstrated that EHEC OMVs are transported to the lysosomes in human brain endothelial cells, the trafficking of OMVs to late endosomal/ lysosomal compartments in Vero cells was investigated (Bielaszewska *et al.*, 2017).

Unfortunately, due to the move of the Schüller group to the UEA in 2019, access to containment level 3 laboratories at the Quadram Institute was no longer available. Therefore, studies were continued using OMVs from the Stx-negative EHEC strain 85-170 and TUV 93-0 (derivate of Stx producing 84-289 and EDL933 EHEC strains). Confluent Vero cell monolayers were inoculated with OMVs isolated from both EHEC strains for 3 and 5 hours. As demonstrated in Fig. 4.13, OMV-LPS staining colocalised with late endosomal/lysosomal compartment signal after 3-hour incubation periods for both EHEC strains. Colocalisation rates between signals were quantified and suggested that 48.84% and 63.5% of all OMV-LPS staining colocalising with late endosomal/lysosomal compartments for OMVs isolated from EHEC strains 85-170 and TUV 9-30, respectively (Fig 4.14A). Statistical testing also detected a significant difference ($P < 0.05$) between the two strains, implying more OMVs from EHEC TUV 93-0 are trafficked to the late endosomal/lysosomal compartment after 3-hour incubation periods than OMVs from EHEC 85-170. Colocalisation rates for both strains significantly increased after a 5-hour incubation ($P < 0.01$), to 79.48% and 86.18% for strains 85-170 and TUV 9-30, respectively. The different values between the OMVs from both EHEC strains were not statistically significantly. It was also determined that 58.88% and 61.5% of total lysosomal compartments contained OMV-LPS signal when incubated with OMVs isolated from EHEC stains 85-170 and TUV 9-30 after 3-hour incubation periods, respectively (Fig. 4.14B). Furthermore after 5-hour incubation periods, 70.34% and 75.46% of total late endosomal/lysosomal compartments contained OMV-LPS signal for OMVs isolated from EHEC stains 85-170 and TUV 9-30, respectively.

Overall, these results indicate that unlike internalised OMV-associated Stx2, EHEC OMVs are trafficked to the late endosomal/lysosomal compartments in Vero cells after 3-hour incubation period.

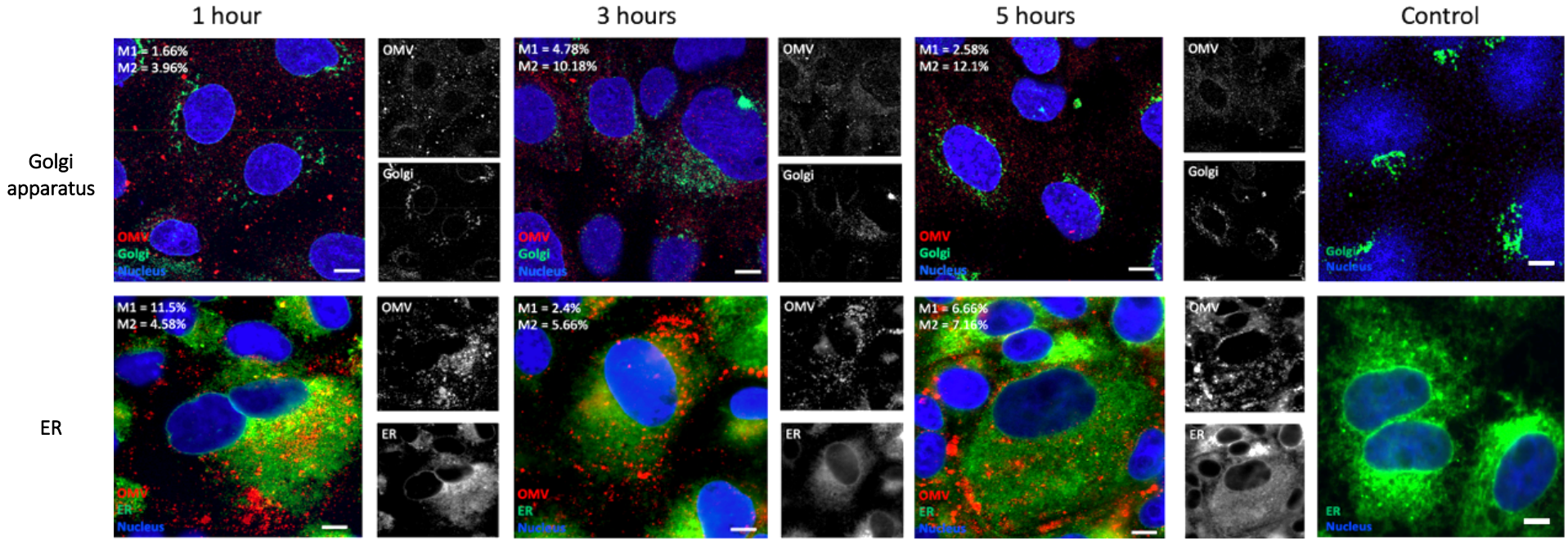

Figure 4.11: Internalised EHEC OMVs are not trafficked to the Golgi apparatus nor the ER in Vero cells. Confluent Vero cell monolayers were incubated for 1, 3 and 5 hours with 10μg of OMVs isolated from LB cultures of EDL933. Cells were immunostained for OMVs using *E. coli* specific anti-LPS (red) and either the Golgi apparatus (green) of the ER (green), and cell nuclei were labelled with DAPI (blue). Images are representative of more than three independent experiments, performed in duplicates. The main image represents merged images from three separate channels, with channels representing the red and green channels shown individually in the side panels. The percentage of colocalisation (M1 = % of OMV-LPS signal colocalising with organelle compartment signal, M2 = % of organelle compartment signal containing OMV-LPS signal) are indicated by the white numbers. Images were produced at a resolution as close to the optimal resolution permitted by the system. Images were attained by using a Zeiss Axio imager M2 widefield microscope fitted with a 63x oil objective (Plan-Apochromat, NA = 1.4, Zeiss) to assess OMV trafficking to the Golgi apparatus, or using a Leica DM6000 B widefield microscope fitted with a 63x oil objective (HCX PL S - APO, NA = 1.30, Leica) to assess OMV trafficking to the ER. Scale bars = 10μm.

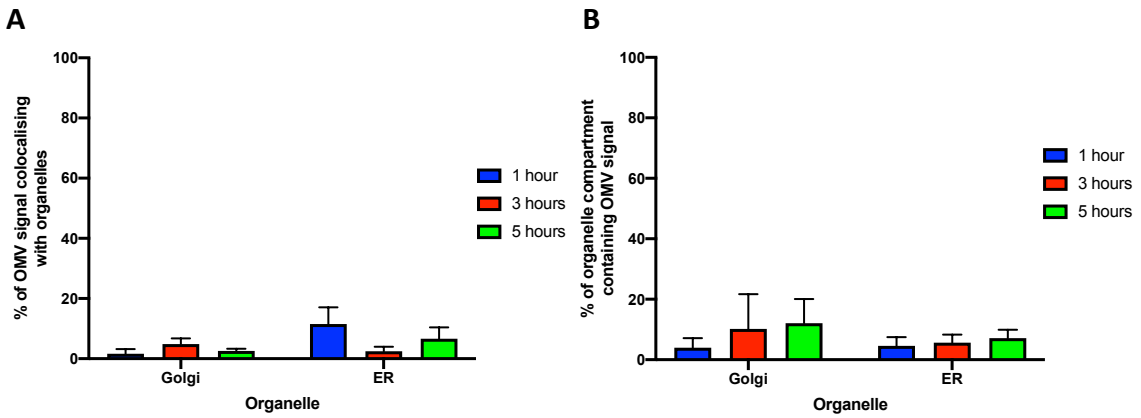

Figure 4.12: Quantification and statistical analysis of signal colocalisation between OMVs and the Golgi apparatus or ER shown in Fig. 4.11. A) Graphical presentation of the mean percentage of OMV signal colocalising with organelle signal ± SD of five representative cells (M1). B) Graphical presentation of the mean percentage of organelle compartment signal containing OMV signal ± SD of five representative cells (M2).

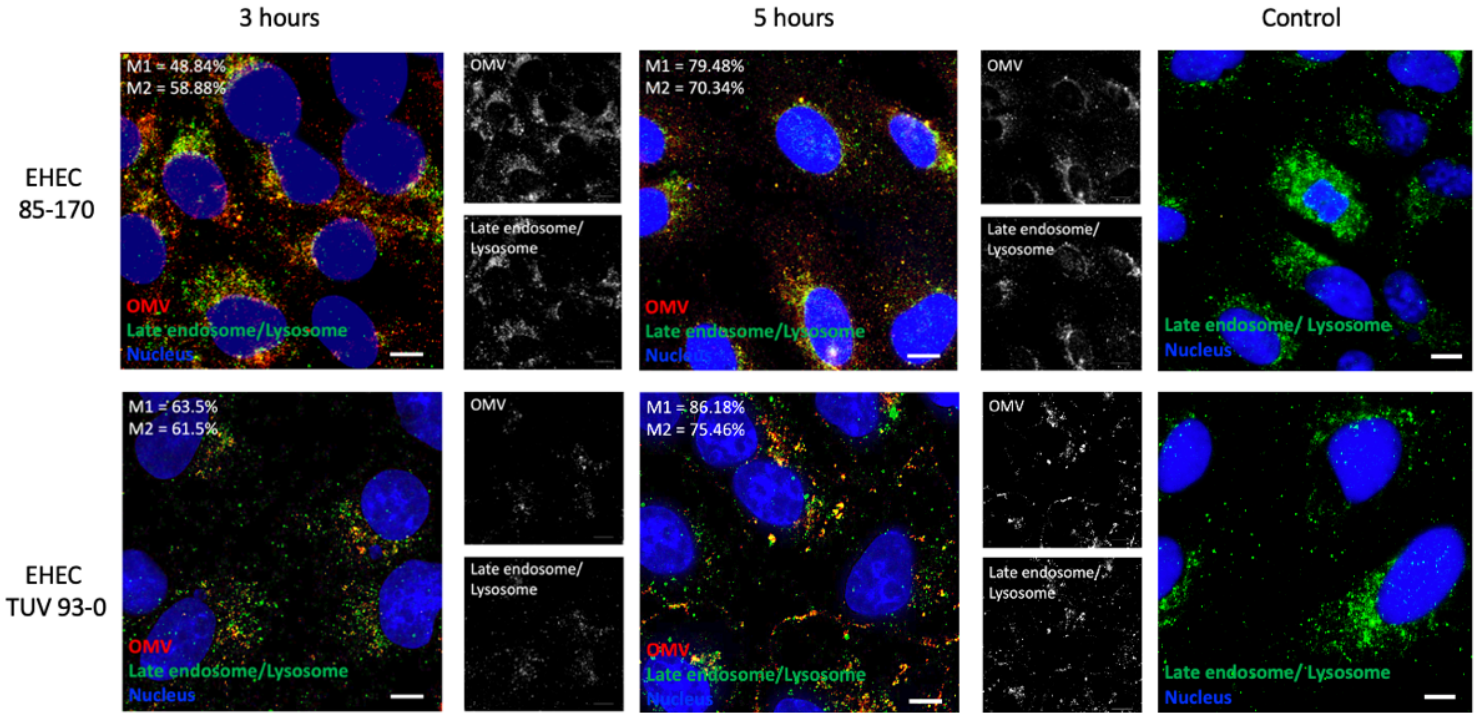

Figure 4.13: EHEC OMVs are trafficked to late endosomal/lysosomal compartments in Vero cells. Confluent Vero cell monolayers were incubated for 3 and 5 hours with 10μg of OMVs isolated from LB cultures EHEC 85-170 and TUV 93-0. Cells were immunostained for OMVs using *E. coli* specific anti-LPS (red) and late endosomal/lysosomal compartments (green), and cell nuclei were labelled with DAPI (blue). Images are representative of more than three independent experiments, performed in duplicates. The main image represents merged images from three separate channels, with channels representing the red and green channels shown individually in the side panels. The percentage of colocalisation (M1 = % of OMV-LPS signal colocalising with late endosomal/lysosomal signal, M2 = % of late endosomal/ lysosomal signal containing OMV-LPS signal) are indicated by the numbers in white. Images were produced at a resolution as close to the optimal resolution permitted by the system. Images were attained by using a Zeiss Axio imager M2 widefield microscope fitted with a 63x oil objective (Plan-Apochromat, NA = 1.4, Zeiss). Scale bars = 10μm.

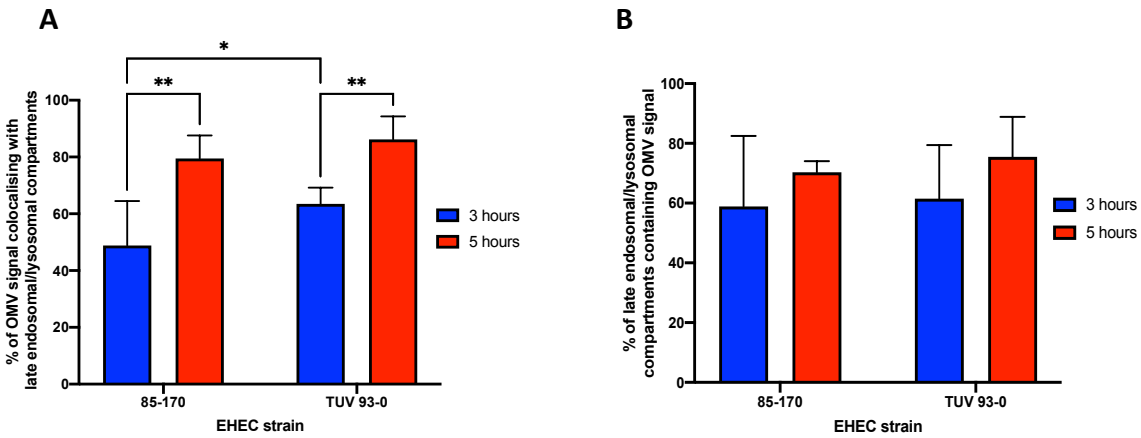

Figure 4.14: Quantification and statistical analysis of signal colocalisation between OMVs isolated from EHEC strains 85-170 or TUV 93-0 and late endosomal/lysosomal compartments in Fig. 4.13. A) Graphical presentation of the mean percentage of OMV signal colocalising with late endosomal/lysosomal compartment signal ± SD of five representative cells (M1). B) Graphical presentation of the mean percentage of late endosomal/lysosomal compartment signal colocalising with OMV signal ± SD of five representative cells (M2). * = $P < 0.05$, ** = $P < 0.01$.

4.2.5 OMVs from EHEC O157 are internalised and trafficked to late endosomal/lysosomal compartments in non-polarised colonic-derived Caco-2 cells.

Upon ingestion, EHEC colonises the colonic epithelium (Lewis *et al.*, 2015). To determine EHEC OMV internalisation and trafficking in the colonic epithelium, the colonic-derived Caco-2 cell line was used. OMVs isolated from EHEC strain 85-170 were used for subsequent work as OMV yield from EHEC cultures of strain 85-170 was slightly higher compared to strain TUV 93-0 when grown in CO_2 supplement (Chapter 3, Fig 3.17).

To determine whether EHEC OMVs are internalised, once confluent monolayers of Caco-2 cells were grown on coverslips, monolayers were incubated with DiO-OMVs or DiI-OMVs for 3 and 5 hours. Cells were subsequently immunostained for OMVs using *E. coli* specific anti-LPS to determine if the dye would remain associated with OMVs within Caco-2 cells. Confocal laser microscopy showed that OMVs interacted with Caco-2 cells as both lipophilic dyes signals were detected (Fig. 4.15). Little colocalisation was

detected between the dyes and anti-LPS signals after 3-hour incubations, with colocalisation reducing after 5 hours (table 4.1). Some 5-hour colocalisation values were lower than the colocalisation values attained using Vero cells (Fig. S2A and B; DiO M1 $P < 0.0001$, DiI M2 $P < 0.01$).

	Colocalisation between DiO (green) and OMV-LPS signal (red)		**Colocalisation between DiI (red) and OMV-LPS signal (green)**	
	M1, % of LPS signal colocalising with DiO signal	**M2, % of DiO signal colocalising with LPS signal**	**M1, % of DiI signal colocalising with LPS signal**	**M2, % of LPS signal colocalising with DiI signal**
3 hours	20.98% ± 12.66	20.42% ± 8.6	21.5% ± 10.6	17.06% ± 5.74
5 hours	10.58% ± 2.98	20.15% ± 19.23	11.14% ± 8.25	15.42% ± 7.39

Table 4.1: Manders coefficient values measuring colocalisation between DiO or DiI molecules and OMV-LPS signals in Caco-2 cells. M1 = % of red fluorophores which colocalised with green fluorophores, M2 = % of green fluorophores which colocalised with red fluorophores. Data is shown as the means of colocalisation ± SD of ten different cells.

Since both dyes produced a staining pattern similar to that of the ER, Caco-2 cells were incubated with EHEC DiI-OMVs or DiO-OMVs for 5-hours and immunostained for the ER. As shown in Fig. 4.16, little colocalisation between the dye molecules and ER signal was detected. Colocalisation was quantified, with Manders values of 11.59% (M1) and 23.34% (M2) being attained between DiO signal and the ER, and 31.87% (M1) and 8.18% (M2) being attained between DiI and the ER (Fig. 4.17), suggesting that some dye molecules may be leaching onto the ER.

Since these experiments indicate that lipophilic dye potentially leaches and integrate onto membrane bound organelles, the *E. coli* specific anti-LPS antibody was used to verify EHEC OMV internalisation into Caco-2 cells and to examine sequential intercellular trafficking of EHEC OMVs. To verify EHEC OMV internalisation by Caco-2 cells, monolayers were immunostained for EHEC OMVs and actin. As shown in Fig. 4.18,

internalised EHEC OMVs were detected within Caco-2 cells after 3 hours, with a similar staining pattern being produced after 5 hours.

Having demonstrated EHEC OMV transportation to late endosomal/lysosomal compartments in Vero cells, it was determined whether EHEC OMVs would also be trafficked to the same compartments in Caco-2 cells. Representative images shown on Fig. 4.19, indicate that OMVs colocalised with late endosomal/lysosomal compartments after 3- and 5-hour incubation periods. Colocalisation between signals was quantified and it was determined that 13.76% and 40.12% of the total OMV-LPS signal colocalised with late endosomal/lysosomal compartments after 3- and 5- hours, respectively (Fig. 4.20A). Low colocalisation rates were attained between OMV-LPS signal and both the Golgi apparatus and the ER after both incubation periods. These were significantly lower to rates attained with late endosomal/lysosomal compartments (Fig. 4.20A, $P < 0.01$ and $P < 0.05$ after 3 hours for the Golgi apparatus and ER, respectively, and $P < 0.0001$ after 5 hours), suggesting OMVs are not trafficked to the Golgi apparatus nor the ER. In addition, after 3-hour incubation periods, 24.42% of late endosomal/lysosomal compartments colocalised with OMV-LPS signal and increased to 40.7% after 5-hour, however this increase was not statistically significant (Fig 4.20B). Significantly lower values were attained when examining the percentage of organelles compartments containing OMV-LPS signal for both the Golgi and ER ($P < 0.001$ for Golgi and ER vs. late endosomal/lysosomal compartments after 3 hours and 5 hours).

Compared to Vero cells, significantly lower levels of OMVs colocalised with late endosomal/lysosomal compartments for both time points in Caco-2 cells ($P < 0.0001$, Fig. S3A) suggesting OMV trafficking to these compartments is slower in Caco-2 cells than in Vero cells. In addition, a significantly higher proportion of late endosomal/ lysosomal compartments contained OMV signals in Vero cells, compared to Caco-2 cells ($P < 0.0001$, Fig S3B).

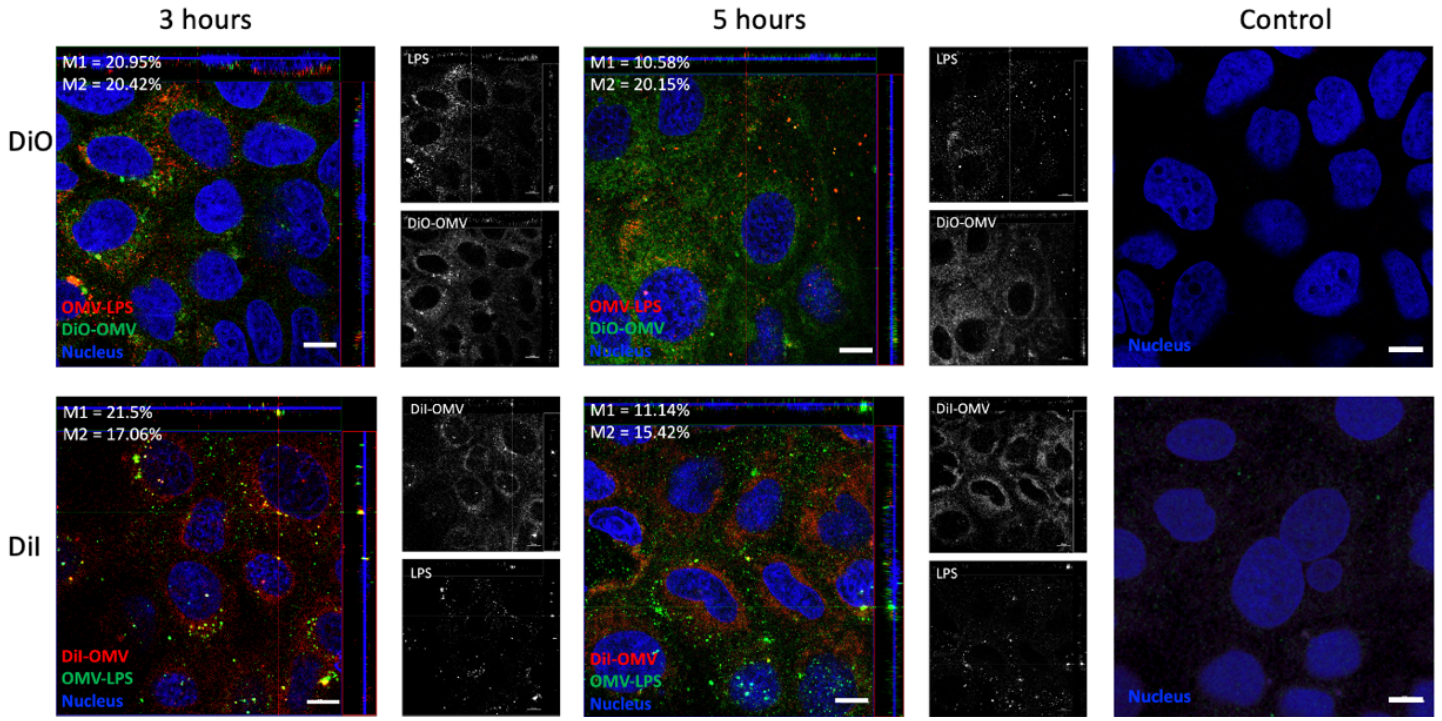

Figure 4.15: Little colocalisation is exhibited between internalised DiO or DiI molecules and OMV-LPS in Caco-2 cells. Confluent Caco-2 cell monolayers were incubated for 3- and 5-hours with 10μg of DiO-OMVs (green) and DiI-OMVs (red) isolated from LB cultures of EHEC 85-170. Cells were immunostained for OMVs using *E. coli* specific anti-LPS (red in cells incubated with DiO-OMVs and green in cells incubated with DiI-OMVs) and cell nuclei were labelled with DAPI (blue). Images are representative of more than two independent experiments performed in duplicate. The main image represents merged images from three separate channels, with channels representing the red and green channels shown individually in the side panels. The percentage of colocalisation (M1 = % of red fluorophore overlapping with green fluorophore; M2 = % of green fluorophore overlapping with red fluorophore) are indicated by the white numbers. Images were produced at a resolution as close to the optimal resolution permitted by the system. Images were attained by using a Zeiss LSM800 confocal microscope fitted with a 63x water immersion objective (C-apochromat, NA = 1.2, Zeiss). Scale bars = 10μm.

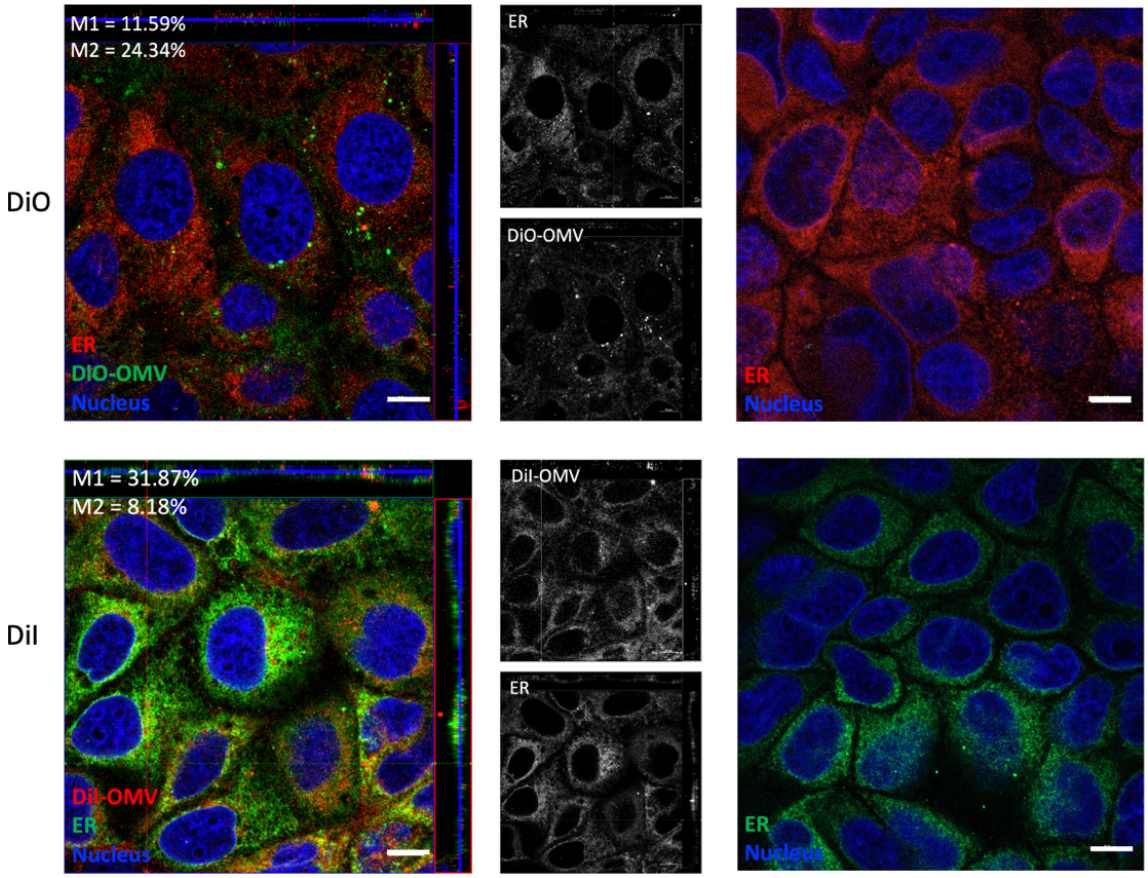

Figure 4.16: Similar colocalisation rates are attained in Caco-2 cells between internalised DiO or DiI molecules and the ER, compared to internalised dye molecules and OMV-LPS signals. Confluent Caco-2 cell monolayers were incubated for 5 hours with 10μg of DiO-OMVs (green) and DiI-OMVs (red) isolated from LB cultures EHEC 85-170. Cells were immunostained for the ER (red in cells incubated with DiO-OMVs and green in cells incubated with DiI-OMVs) and cell nuclei were labelled with DAPI (blue). Images are representative of two independent experiments, performed in duplicate. The main image represents merged images from separate channels, with channels representing the red and green channels shown individually in the side panels. The percentage of colocalisation (M1 = % of red fluorophore overlapping with green fluorophore; and M2 = % of green fluorophore overlapping with red fluorophore) are indicated by the white numbers. Images were produced at a resolution as close to the optimal resolution permitted by the system. Images were attained by using a Zeiss LSM800 confocal microscope fitted with a 63x water immersion objective (C-apochromat, NA = 1.2, Zeiss). Scale bars = 10μm.

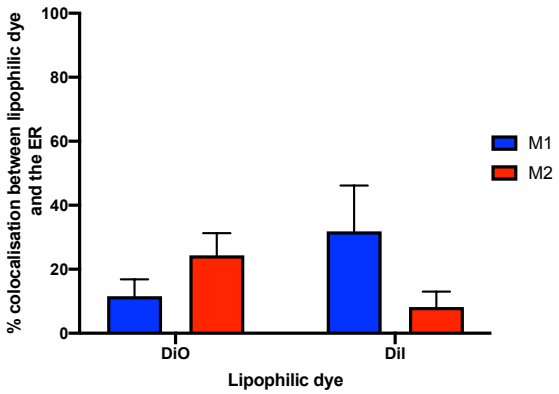

Figure 4.17: Quantification of signal colocalisation between DiO or DiI molecules and the ER in Fig. 4.16. M1= % of red fluorophores which colocalised with green fluorophores, M2 = % of green fluorophores which colocalised with red fluorophores. Data is shown as the means of colocalisation ± SD of at least five different cells.

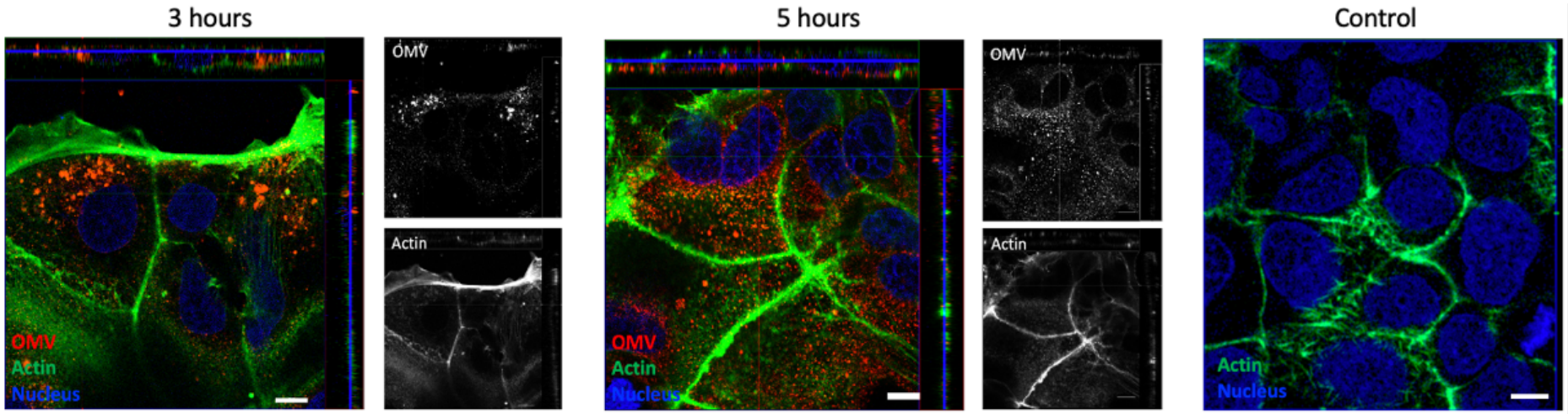

Figure 4.18: EHEC OMVs are internalised by non-polarised Caco-2 cells. Confluent Caco-2 cell monolayers were incubated for 3 and 5 hours with 10μg of OMVs isolated from LB cultures of EHEC 85-170. Cells were immunostained for OMVs using *E. coli* specific anti-LPS (red), actin (green, FITC-phalloidin) and cell nuclei were labelled with DAPI (blue). Images are representative of three independent experiments, performed in duplicate. The main image represents merged images from three separate channels, with the red and green channels shown individually in the side panels. Images were produced at a resolution as close to the optimal resolution permitted by the system. Images were attained by using a Zeiss LSM800 confocal microscope fitted with a 63x water immersion objective (C-apochromat, NA = 1.2, Zeiss). Scale bars = 10μm.

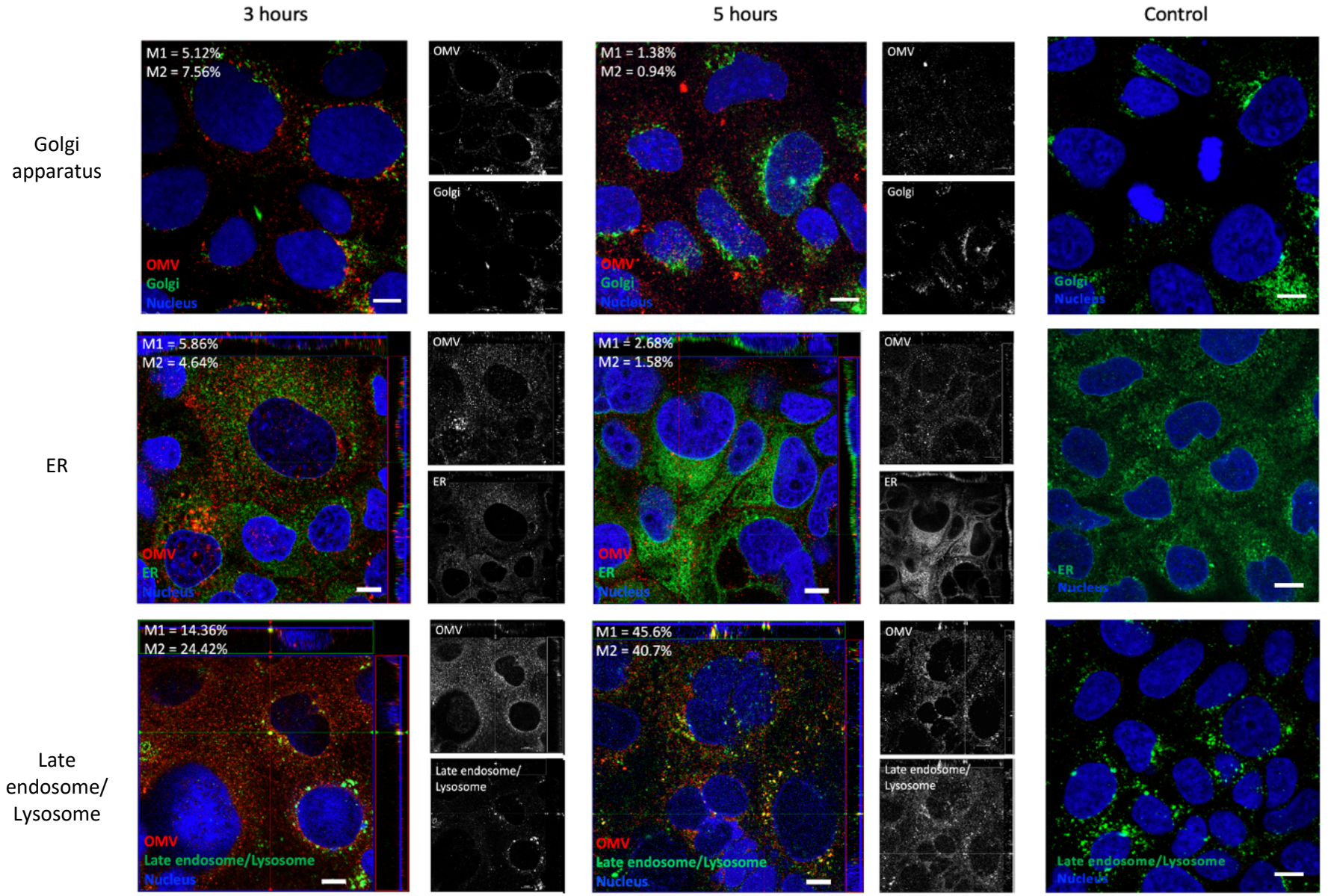
3 hours
5 hours
Control
Golgi apparatus
ER
Late endosome/ Lysosome
M1 = 5.12%
M2 = 7.56%
OMV
Golgi
Nucleus
M1 = 1.38%
M2 = 0.94%
M1 = 5.86%
M2 = 4.64%
ER
M1 = 2.68%
M2 = 1.58%
M1 = 14.36%
M2 = 24.42%
Late endosome/Lysosome
M1 = 45.6%
M2 = 40.7%

Figure 4.19: Internalised EHEC OMVs are trafficked to late endosomal/lysosomal compartments in non-polarised Caco-2 cells. Confluent Caco-2 cell monolayers were incubated for 3 and 5 hours with 10μg of OMVs isolated from LB cultures of EHEC 85-170. Cells were immunostained for OMVs using *E. coli* specific anti-LPS (red) and either the Golgi apparatus (green), ER (green), or late endosomal/lysosomal compartments (green), and cell nuclei were labelled with DAPI (blue). Images are representative of three independent experiments, performed in duplicate. The main image represents merged images from three separate channels, with the red and green channels shown individually in the side panels. The percentage of colocalisation (M1 = % of OMV-LPS signal colocalising with organelle compartment signal, M2 = % of organelle compartment signal containing OMV-LPS signal) are indicated by the white numbers. Images were produced at a resolution as close to the optimal resolution permitted by the system. Images were attained by using a Zeiss LSM800 confocal microscope fitted with a 63x water immersion objective (C-apochromat, NA = 1.2, Zeiss). Scale bars = 10μm.

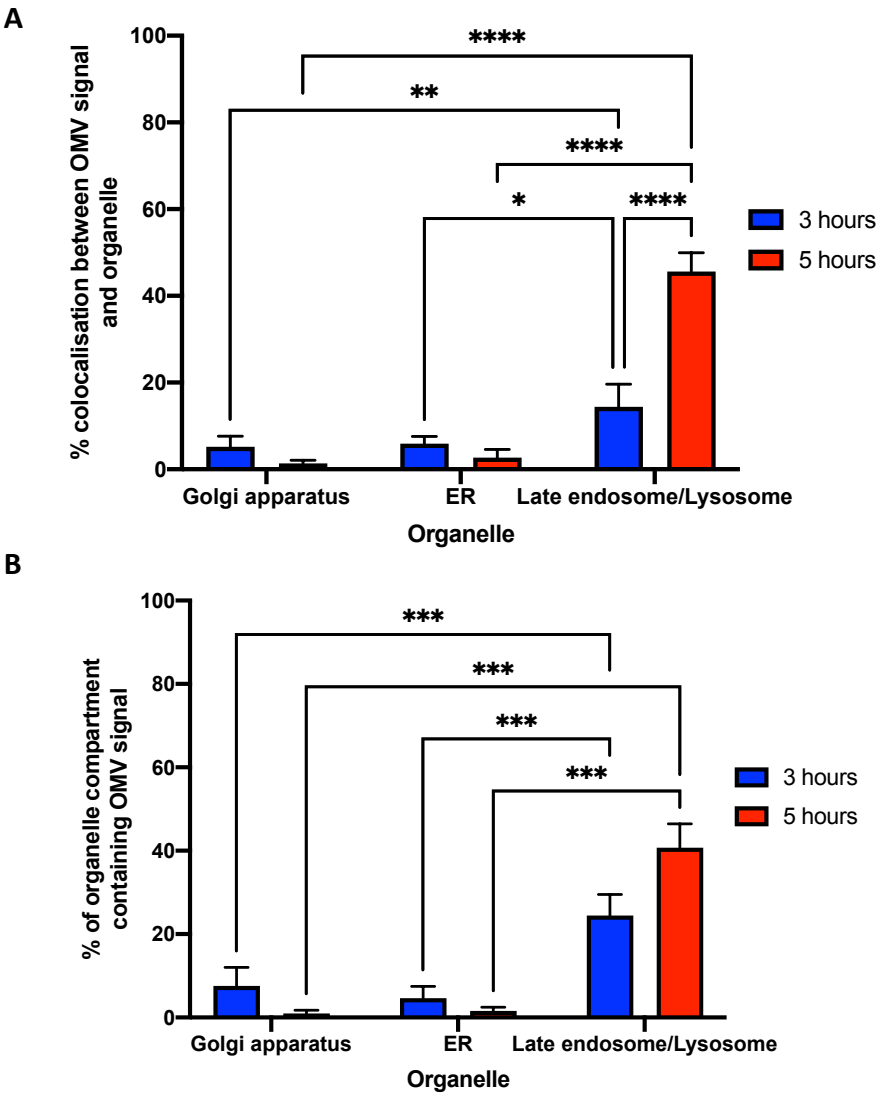

Figure 4.20: Quantification and statistical analysis of signal colocalisation between EHEC OMVs and either the Golgi apparatus, ER or late endosomal/lysosomal compartments in Fig. 4.19. A) Graphical presentation of the mean percentage of OMV signal colocalising with organelle signal ± SD of five representative cells (M1). B) Graphical presentation of the mean percentage of organelle compartment signal containing OMV signal ± SD of five representative cells (M2). * = $P < 0.05$, ** = $P < 0.01$, *** = $P < 0.001$, **** = $P < 0.0001$.

To confirm OMV trafficking to late endosomal/lysosomal compartments within confluent Caco-2 cells, these experiments were repeated with OMVs isolated from Stx-producing strain EDL933. As shown in Fig. 4.21, OMV-LPS staining colocalised with late endosomal/lysosomal compartments both after 3- and 5-hours incubation periods, with colocalisation rates of 21.1% after 3-hour incubations and significantly increasing to 38.4% after 5-hours (Fig 4. 22A, $P < 0.01$). Likewise, after 3-hour incubation periods 18.86% of late endosomal/lysosomal compartments contained OMV-LPS signal, with a

significantly higher rate of 40.92% of late endosomal/lysosomal compartments containing OMV-LPS signal after 5-hour incubation periods (Fig 4.22B, $P < 0.01$). Comparatively, these values are similar to those attained from Caco-2 cells incubated with OMVs isolated from EHEC 85-170 (Fig S4A and B).

Since OMV-associated Stx2 was trafficked to the ER in Vero cells by 5 hours, it was anticipated that OMV-associated Stx2 would also colocalise with the ER by 5 hours. Subsequent immunostaining of Stx2 and the ER showed little signal overlap, with Manders colocalisation quantifying 12.86% of the total Stx2 signal colocalising with ER staining, which was statically lower between the signals Vero cells at the same time point (Fig S5A; 82%, $P < 0.0001$). Likewise, 11.62% of the total ER staining contained Stx2 signal, which was statically lower than that in Vero cells (Fig S5B, 80.3%, $P < 0.0001$). Such results suggest that there may be a slower trafficking system for Stx2 as well.

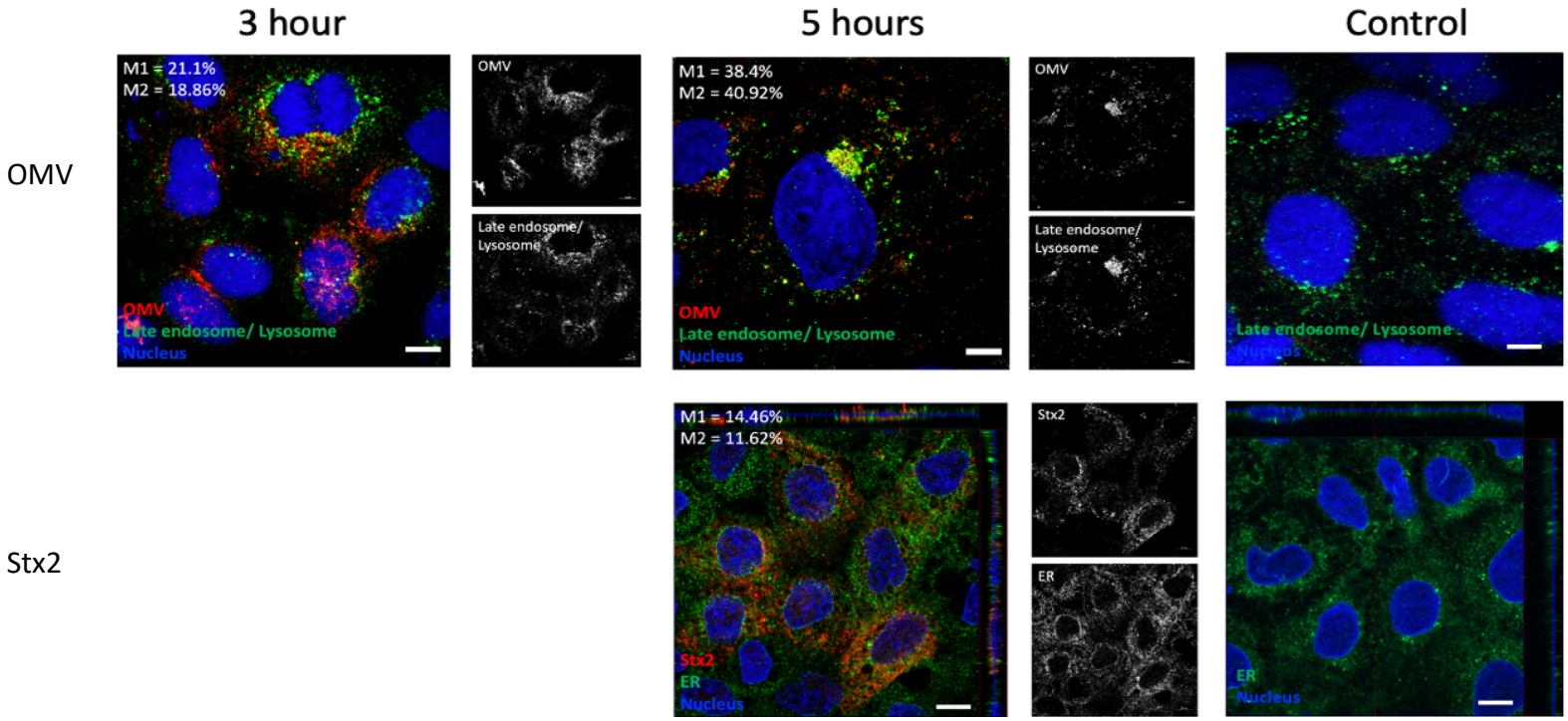

Figure 4.21: Fluorescence microscopy images of Caco-2 cells incubated with OMVs isolated from LB cultures of EHEC EDL933. Confluent Caco-2 cell monolayers were incubated for 3 and 5 hours with 10μg of OMVs isolated from LB cultures of EHEC EDL933. Cells were immunostained for either OMVs using *E. coli* specific anti-LPS (red) or Stx2 (red) and either late endosomal/lysosomal compartments (green) or the ER (green) and cell nuclei were labelled with DAPI (blue). Images are representative of two independent experiments, performed in duplicate. The main image represents merged images from three separate channels, with channels representing the red and green channels shown individually in the side panels. The percentage of colocalisation (M1 = % of red fluorophore overlapping with green fluorophore; and M2 = % of green fluorophore overlapping with red fluorophore) are indicated by the white numbers. Images were produced at a resolution as close to the optimal resolution permitted by the system. Images were attained by using a Zeiss LSM800 confocal microscope fitted with a 63x water immersion objective (C-apochromat, NA = 1.2, Zeiss). Scale bars = 10μm.

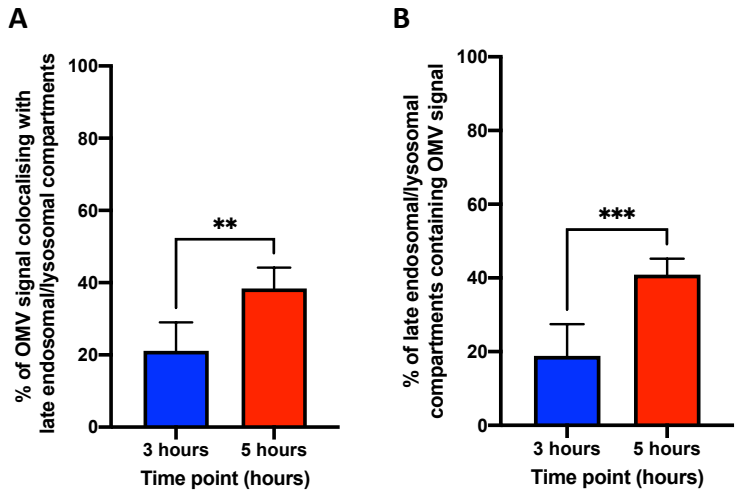

Figure 4.22: Quantification and statistical analysis of signal colocalisation between EHEC OMVs and late endosomal/lysosomal compartments in Fig. 4.21. A) Graphical presentation of the mean percentage of OMV colocalising with late endosome/lysosome signal ± SD of five representative cells (M1). B) Graphical presentation of the mean percentage of late endosome/lysosome compartment containing OMV signal ± SD of five representative cells (M2). ** = $P < 0.01$, *** = $P < 0.001$.

4.2.6 EHEC OMVs trafficking in polarised colonic-derived Caco-2 cells

Cells which make up the intestinal epithelium are arranged in a polarised manner and express intercellular junctions such as tight junctions, which prevent paracellular trafficking of luminal contents, and separate apical and basolateral cell surfaces (Zihni *et al.*, 2016, Schneeberger *et al.*, 2018). Cell polarisation also instigates the distribution and expression of surface proteins, and cytoskeletal components to differs between the basal and apical cell membranes (van der Wouden *et al.*, 2003, Weisz and Rodriguez-Boulan, 2009). Therefore, it was determined whether Caco-2 cells in this physiologically relevant arrangement could also internalise EHEC OMVs, and whether the intracellular trafficking pathways of OMVs would be the same.

To support polarisation, Caco-2 cells were grown on collagen-coated Transwell membrane inserts and polarisation was monitored by measuring the transepithelial electrical resistance (TEER; Fig. 4.23A; Madara *et al.*, 1987). Monolayers were used after TEER readings reached 1500 Ω x cm^2, which is regarded as an indicator of polarisation

(Lu *et al.*, 1996). This was confirmed by confocal microscopy which demonstrated the formation of columnar-shaped cells with an apical actin-rich brush border (Fig. 4.23B and C).

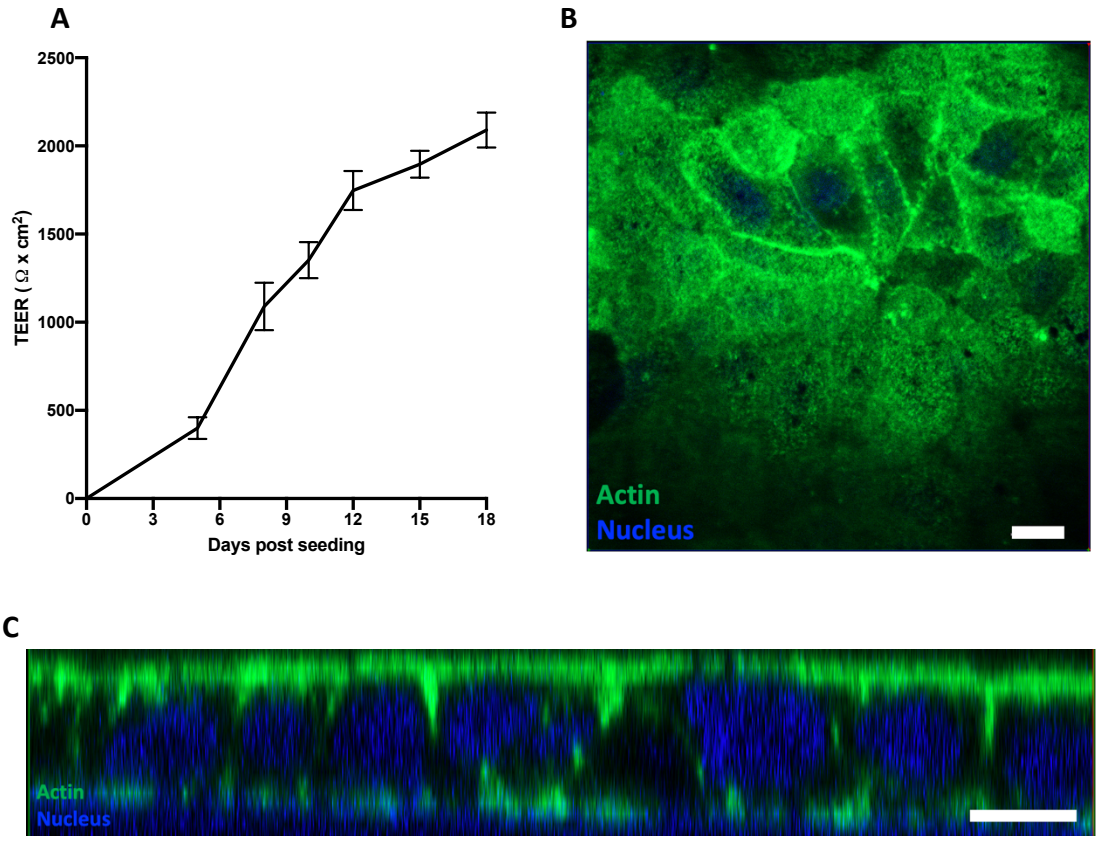

Figure 4.23: Characteristics of polarised Caco-2 cells. Cells were grown on Transwell inserts for 18 days. (A) Transepithelial electrical resistance (TEER) was monitored from 5 days post-seeding. Data is shown as means ± SD of three independent experiments performed in triplicates. (B) Confluent cells were stained with FITC-phalloidin (actin) and DAPI (nucleus). Immunofluorescence image shows the formation of a confluent polarised monolayer and the apical brush border. (C) The confocal XZ scan image of actin-stained cells (FITC-phalloidin, green) shows the column-shaped morphology of the cells. Images are representative of five independent experiments. Images were produced at a resolution as close to the optimal resolution permitted by the system. Images were attained by using a Zeiss LSM800 confocal microscope fitted with a 63x water immersion objective (C-apochromat, NA = 1.2, Zeiss). Scale bars = 10μm (B) and 20μm (C).

To determine whether EHEC OMVs disrupt the epithelial barrier, polarised Caco-2 epithelia were incubated with OMVs from LB cultures of EHEC 85-170 for 24 hours. TEER readings were recorded hourly for the first 5 hours and at the end of 24-hour incubation

periods. As shown in Fig. 4.24, compared to control samples, incubations with EHEC OMVs did not affect epithelial barrier function.

To deduce whether OMVs could be internalised by polarised Caco-2 cells, after an incubation period of 3, 5 and 24 hours with OMVs, monolayers were stained for OMVs and actin using the anti-LPS antibody and FITC-phalloidin, respectively. As shown in Fig 4.25, intracellular OMVs were detected within Caco-2 cells after 3 hours, with increased OMV signal observed after longer incubations periods.

Since EHEC OMVs were trafficked to late endosomes/lysosomes in non-polarised Caco-2 cells, it was determined whether EHEC OMVs were also trafficked to the same organelles. As shown in Fig 4.26, some colocalisation between EHEC OMVs and late endosomes/lysosomes was detected. Quantification of colocalisation indicated that 11.96%, 15.72% and 28.04% of the total OMV-LPS signal colocalised with the late endosomal/lysosomal compartments after 3-, 5- and 24-hour incubation periods, respectively (Fig. 4.27A). In addition, little colocalisation between OMV-LPS signal with the Golgi apparatus and the ER was detected at the different time points. Statistical analysis detected a significantly lower colocalisation rate between OMV-LPS signal and both the ER and the Golgi apparatus compared to OMV-LPS and late endosomal/lysosomal compartments after 24-hour incubation periods (Fig 4.27A, $P < 0.01$ and $P < 0.001$, respectively). Likewise, it was measured that 10.38%, 25.26% and 27.08% of late endosomal/lysosomal compartments contained OMV-LPS signal, with other organelle compartments containing significantly lower colocalisation rates for each time point (Fig 4.27B, $P < 0.0001$).

Comparatively, colocalisation rates between OMV-LPS and late endosomal/lysosomal compartments in non-polarised and polarised Caco-2 cells were similar after 3-hour incubations, however total OMV-LPS signal colocalisation with the late endosomal/lysosomal compartments after 5-hour incubation periods were significant lower in polarised Caco-2 cells than in non-polarised cells ($P < 0.0001$, Fig. S6A).

Given the low colocalisation of OMVs in late endosomes/lysosomes, the possibility of OMV translocation across the epithelium was examined. To this aim, the basolateral medium was collected from the Caco-2 Transwells, concentrated and added to confluent Vero cell monolayers for 24 hours. Subsequent immunostaining with anti-LPS and microscopy examination confirmed the presence of OMVs in the basolateral medium as early as 3 hours, indicating OMV translocation across polarised Caco-2 cells (Fig. 4.28). Since EHEC OMVs did not affect epithelial barrier function, this would indicate that OMV translocation via the transcellular route occurred.

Taken together, these results indicate that polarised Caco-2 cells internalise EHEC OMVs without any consequential disruption of the epithelial barrier. Furthermore, OMVs may have two distinct intracellular trafficking pathways including transport to late endosomal/lysosomal compartments and translocation to the basolateral side of the epithelium.

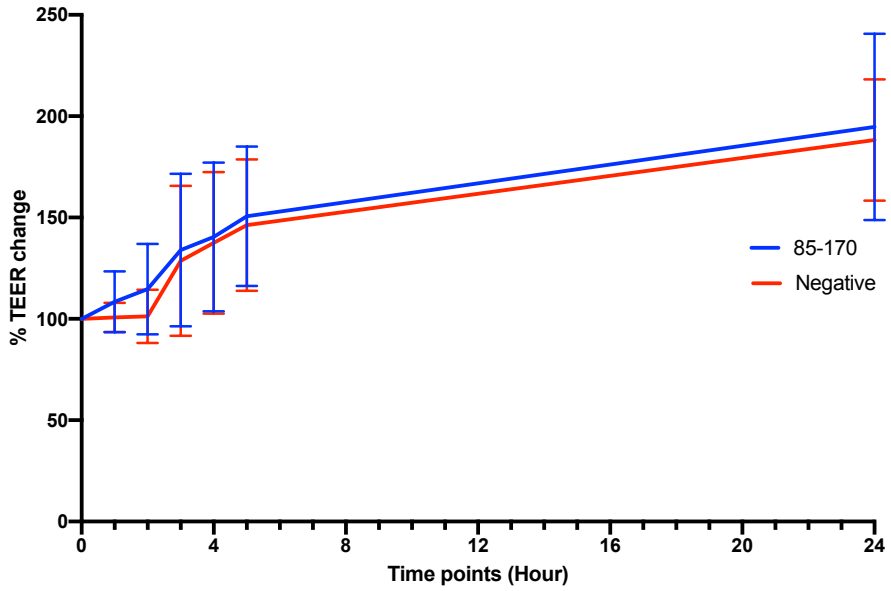

Figure 4.24: EHEC OMVs do not affect the epithelial barrier function of polarised Caco-2 cell monolayers. Caco-2 transwell inserts were incubated with EHEC OMV isolated from LB cultures of EHEC 85-170 for 24 hours. Data is shown as a mean percentage of the TEER compared to TEER measured at time '0' ± SD four independent experiments performed in triplicate

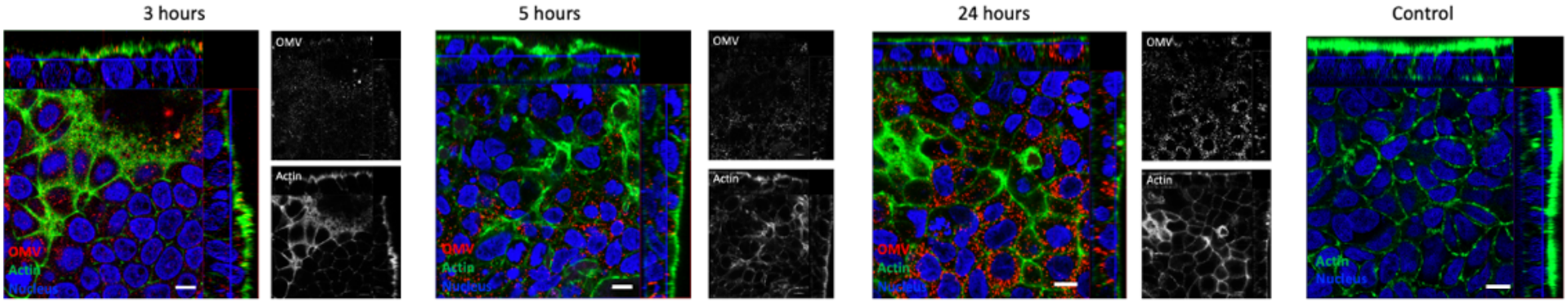

Figure 4.25: EHEC OMVs are internalised by polarised Caco-2 cells. Confluent Caco-2 cell monolayers were incubated for 3, 5 and 24 hours with 10μg of OMVs isolated from LB cultures of EHEC 85-170. Cells were immunostained for OMVs using *E. coli* specific anti-LPS (red), actin (green, FITC-phalloidin) and cell nuclei were labelled with DAPI (blue). Images are representative of three independent experiments, performed in duplicate. The main image represents merged images from three separate channels, with the red and green channels shown individually in the side panels. Images were produced at a resolution as close to the optimal resolution permitted by the system. Images were attained by using a Zeiss LSM800 confocal microscope fitted with a 63x water immersion objective (C-apochromat, NA = 1.2, Zeiss). Scale bars = 10μm.

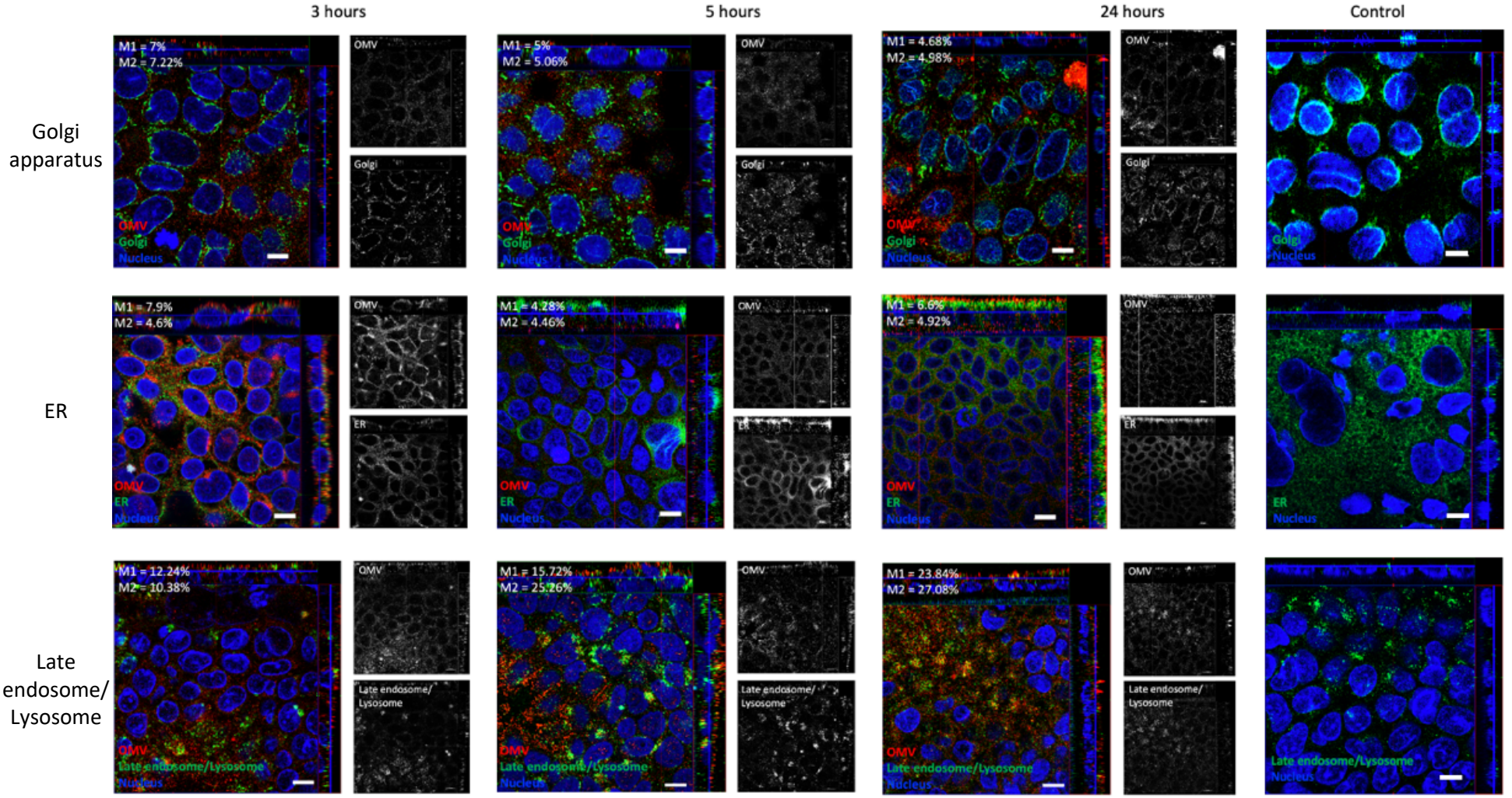
3 hours
5 hours
24 hours
Control
Golgi apparatus
ER
Late endosome/ Lysosome
M1 = 7%
M2 = 7.22%
M1 = 5%
M2 = 5.06%
M1 = 4.68%
M2 = 4.98%
M1 = 7.9%
M2 = 4.6%
M1 = 4.28%
M2 = 4.46%
M1 = 6.6%
M2 = 4.92%
M1 = 12.24%
M2 = 10.38%
M1 = 15.72%
M2 = 25.26%
M1 = 23.84%
M2 = 27.08%
OMV
Golgi
ER
Late endosome/ Lysosome
Nucleus

Figure 4.26: Fluorescence micrographs depicting intracellular trafficking of EHEC OMVs in polarised Caco-2 cell monolayers. Confluent polarised Caco-2 cell monolayers were incubated for 3, 5 and 24 hours with 10μg of OMVs isolated from LB cultures of EHEC 85-170. Cells were immunostained for OMVs using *E. coli* specific anti-LPS (red) and either late endosomal/lysosomal compartments (green), the Golgi apparatus (green) or the ER (green), and cell nuclei were labelled with DAPI (blue). Images are representative of three independent experiments, performed in duplicate. The main image represents merged images from three separate channels, with the red and green channels shown individually in the side panels. The percentage of colocalisation (M1 = % of OMV-LPS signal colocalising with organelle compartment signal, M2 = % of organelle compartment signal containing OMV-LPS signal) are indicated by the white numbers. Images were produced at a resolution as close to the optimal resolution permitted by the system. Images were attained by using a Zeiss LSM800 confocal microscope fitted with a 63x water immersion objective (C-apochromat, NA = 1.2, Zeiss). Scale bars = 10μm.

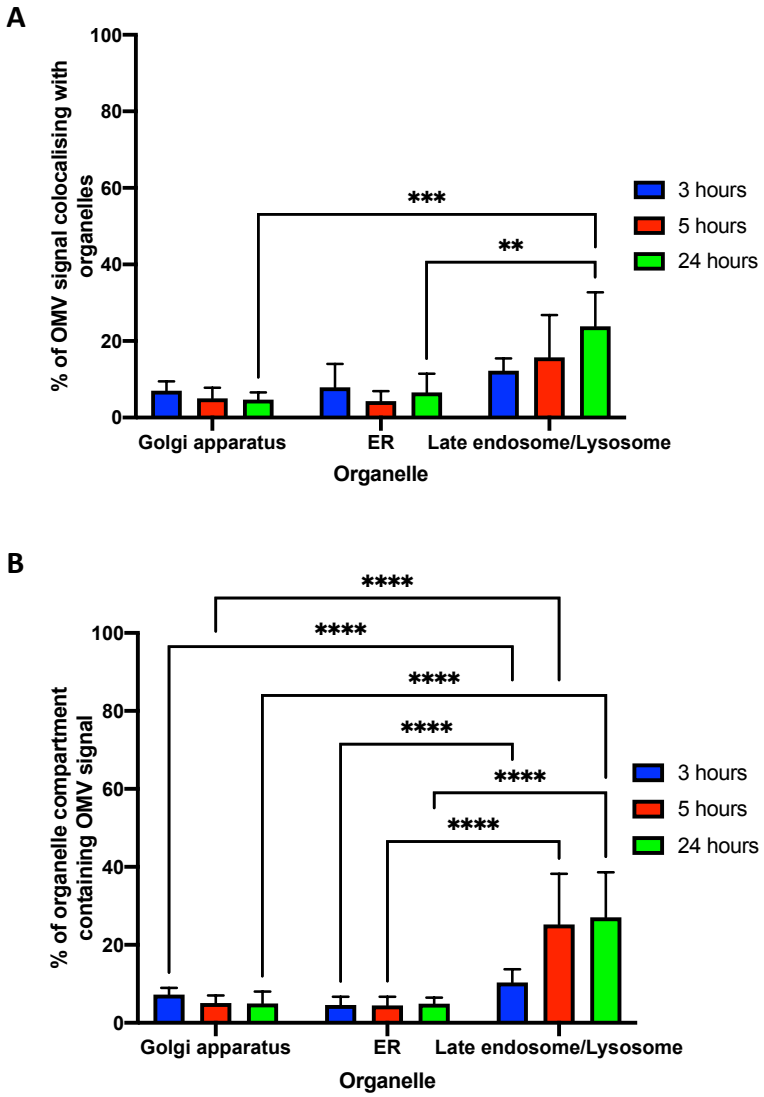

Figure 4.27: Quantification and statistical analysis of signal colocalisation between OMVs isolated from EHEC 85-170 and either the Golgi apparatus, ER or late endosomal/lysosomal compartments in Fig. 4.26. A) Graphical presentation of the mean percentage of OMV signal colocalising with organelle signal ± SD of five representative cells (M1). B) Graphical presentation of the mean percentage of organelle compartment signal containing OMV signal ± SD of five representative cells (M2). ** = $P < 0.01$, *** = $P < 0.001$, **** = $P < 0.0001$.

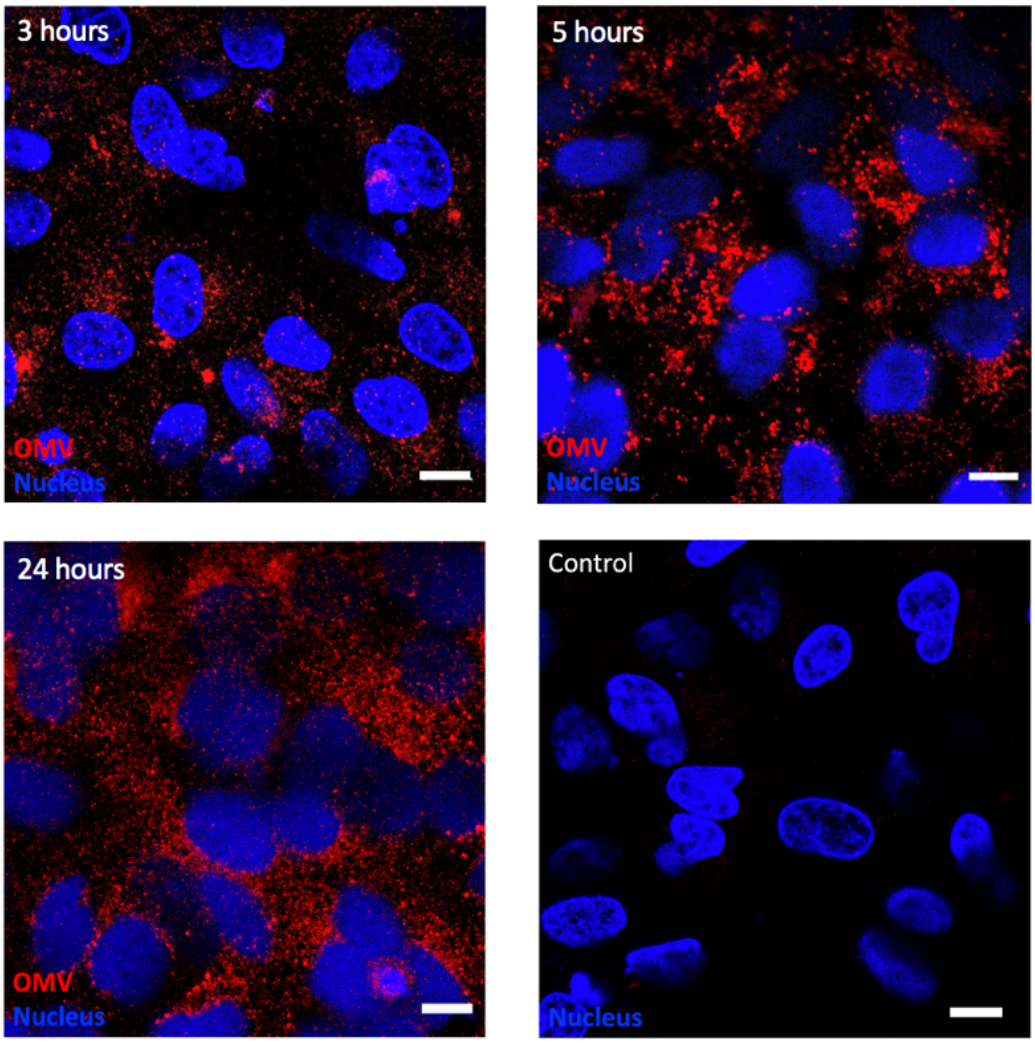

Figure 4.28: Basolateral medium collected from polarised Caco-2 grown on Transwells contain OMVs, indicating OMV translocation. Basolateral medium was collected from Transwells after 3-, 5- and 24-hour apical incubation periods with OMVs. Medium was concentrated and subsequently incubated with confluent Vero cell monolayers for 24 hours. Vero cells were immunostained for OMVs using *E. coli* specific anti-LPS (red) and cell nuclei were labelled with DAPI (blue). Images are representative of more than three independent experiments. Images were produced at a resolution as close to the optimal resolution permitted by the system. Images were attained by using a Zeiss LSM800 confocal microscope fitted with a 63x water immersion objective (C-apochromat, NA = 1.2, Zeiss). Scale bars = 10μm.

4.2.7 Colonic T84 cells exhibits minimal uptake of EHEC OMVs

Although Caco-2 cells originate from the colon, they morphologically resemble enterocytes from the small intestine as they have comparatively long microvilli when

polarised and express brush boarder hydrolases (Devriese *et al.*, 2017). Furthermore, Caco-2 cells express the Stx receptor Gb3, which is not usually present in the colon (Jacewicz *et al.*, 1995, Schuller *et al.*, 2004). In contrast, T84 cell more closely resembles the morphology of colonocytes and do not express Gb3, therefore making this cell line a more physiologically relevant model to study EHEC infections in the colon than Caco-2 cells (Schuller *et al.*, 2004, Kovbasnjuk *et al.*, 2005, Devriese *et al.*, 2017).

To examine whether EHEC OMVs can interact with T84 cells, semi-confluent cell monolayers were incubated with DiO-OMVs isolated from EHEC 85-170 for 5 and 24 hours. As shown in Fig. 4.29, EHEC OMVs only associated with T84 cells located on the edges of cell islands after 5 hours. Unlike previous results achieved with Vero and Caco-2 cells, an increase in OMV uptake was not observed with longer incubation periods. To validate that the DiO signals were OMVs, monolayers were immunostained with *E. coli* specific anti-LPS. The attained images showed colocalisation between the dye and the anti-LPS signal (Fig 4.29), with Manders colocalisation analysis confirming colocalisation between the different signals (table 4.2).

	DiO-OMV	
	M1	**M2**
5 hours	62.49% ± 26.85	61.4% ± 18.04
24 hours	60.57% ± 15.92	45.72% ± 14.66

Table 4.2: Manders coefficient values measuring colocalisation between DiO signals and OMV-LPS signals in T84 cells. M1= % of LPS signal colocalising with DiO signal, M2 = % of DiO signal colocalising with LPS signal. Data is shown as the means of colocalisation ± SD of eight representative cells.

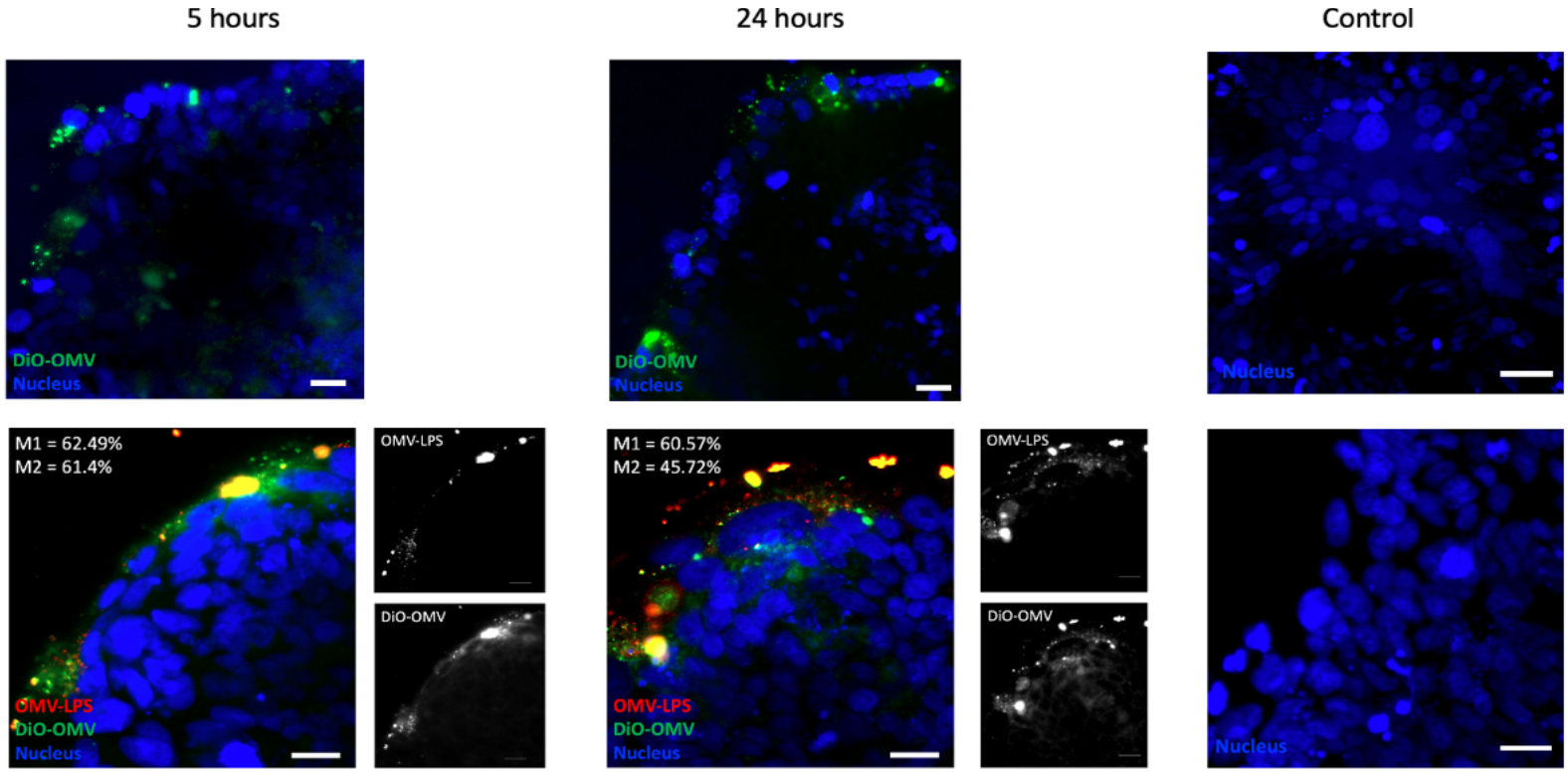

Figure 4.29: Colocalisation of DiO molecules and OMV-LPS signal arises in T84 cells. Semi-confluent T84 cells were incubated for 5 and 24 hours with 10µg of DiO-OMVs (green) isolated from LB cultures of EHEC 85-170. OMVs were detected using *E. coli* specific anti-LPS (red) and cell nuclei were labelled with DAPI (blue). Images are representative of three independent experiments, performed in duplicate. The main image represents merged images from three separate channels, with channels representing the red and green channels shown individually in the side panels. The percentage of colocalisation (M1= % of OMV-LPS signal colocalising with DiO signal, M2 = % DiO signal colocalising with OMV-LPS signal) are indicated by the numbers in white. Images were produced at a resolution as close to the optimal resolution permitted by the system. Images were attained by using a Zeiss Axio imager M2 widefield microscope fitted with a 40x water immersion objective (EC Plan-Neofluar, NA = 0.75, Zeiss). Scale bars = 20µm.

As cells only located in the peripheries of growing cell islands exhibited interaction DiO-OMVs, it was subsequently tested whether confluent T84 cell monolayers needed to be starved for OMV internalisation. This was carried out by incubating confluent monolayers in supplemented or non-supplemented DMEM/F-12 medium 24 hours prior to EHEC OMV inoculation. Following this, DiO-OMVs were added to confluent monolayers and incubated for 5 hours. As shown in Fig 4.30, the interaction between DiO-OMVs isolated from EHEC strain 85-170 and T84 cells was similar under both conditions, suggesting that little OMV interaction occurs irrespective of nutrient starvation in T84 cells.

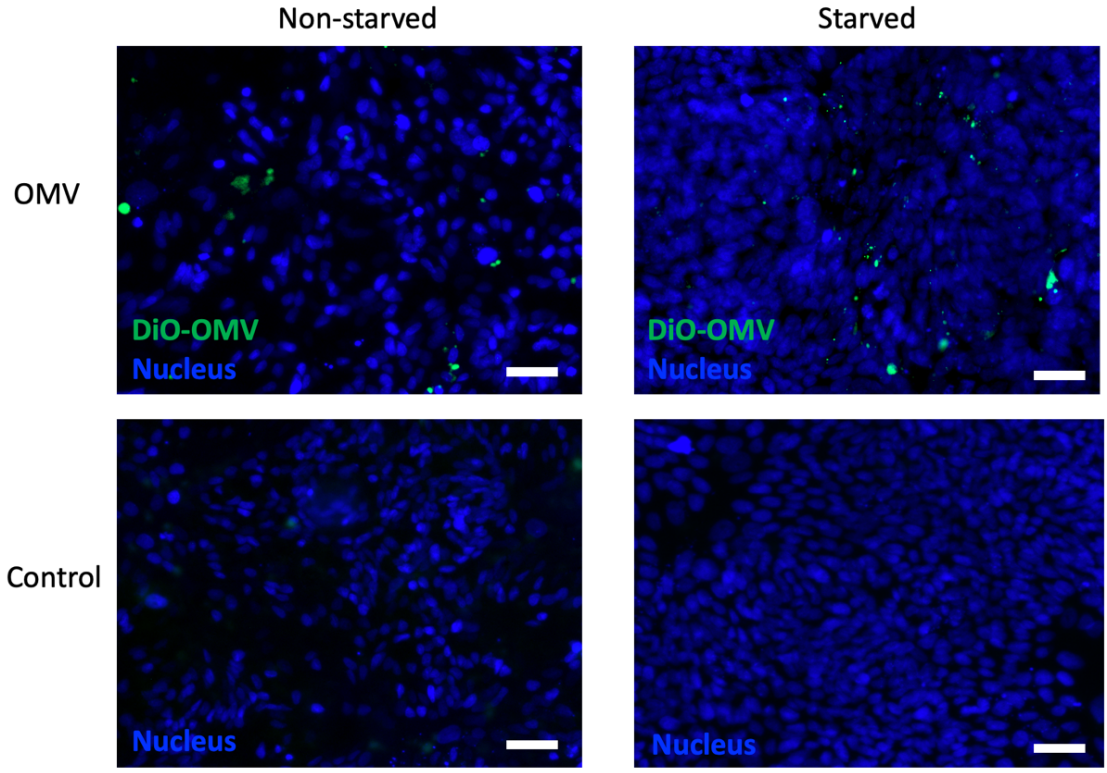

Figure 4.30: Little OMV interaction occurs with T84 cells. T84 cells were incubated with supplemented (non-starved) or non-supplemented (starved) DMEM/F-12 medium for 24 hours prior to OMV inoculation. After a 5-hour incubation period with DiO-OMVs (green) isolated from LB cultures of EHEC 85-170, cell nuclei were labelled with DAPI (blue). Images were produced at a resolution as close to the optimal resolution permitted by the system. Images are representative of three independent experiments performed in duplicate. Images were attained by using a Zeiss Axio M2 widefield microscopy fitted with a 20x objective (EC Plan-Neofluar, NA = 0.50, Zeiss). Scale bars = 50μm.

To determine whether a higher OMV amount would increase OMV interaction with T84 cells, increasing amounts of DiO-OMVs isolated from EHEC strain 85-170 were added to confluent T84 cell monolayers and incubated for 24 hours. As shown in Fig. 4.31, very little uptake was observed and higher doses of DiO-OMVs (12μg - 48μg of OMV protein) did not result in an increased level of association with EHEC OMV.

To evaluate whether T84 cells could internalise OMV-associated Stx without OMV internalisation, DiI-OMVs from Stx-producing EHEC strain EDL933 and soluble Stx2 (control) were incubated with T84 and Vero cells (positive control) for 5 and 24 hours. As shown in Fig. 4.32, only a few T84 cells located at the margins of cell islands exhibited any association with OMVs, whereas all Vero cells exhibited OMV uptake after 5-hour incubation periods with OMVs. Internalised Stx2 derived from EHEC OMVs was rarely detected in T84 cell monolayers, yet cells which contained Stx2 showed colocalisation with internalised DiI. This was confirmed using Manders colocalisation analysis (M1), which detected a colocalisation rate of 71.89% (Fig 4.33A). Unlike T84 cells, many Vero cells contained internalised Stx2 with comparatively significantly lower colocalisation rates with the dye (Fig. 4.33A, 7.24%, $P < 0.0001$). Limited OMV internalisation was also exhibited in confluent T84 cell monolayers after 24 hours, with a colocalisation rate (M1) of 91.48% between Stx2 and dye, suggesting Stx2 retention within OMVs. However, after incubation for the same time period, the integrity of the Vero cell monolayer was disrupted due to cell death, with the remaining cells containing OMVs and Stx2, with an 8.54% colocalisation rate (M1) between the two signals (Fig. 4.33A). Similar colocalisation rates were also attained when the level of Stx2 colocalisation with DiI signal was examined (M2) for both T84 cells and Vero cells, with significantly lower colocalisation rates being attained with Vero cells (Fig. 4.33B, $P < 0.001$).

Overall, the results obtained from semi-confluent and confluent T84 cell monolayers showed that T84 cell association with OMVs was limited to peripheral cells. Furthermore, intracellular Stx2 did not dissociate from OMVs when interacting with T84 cells.

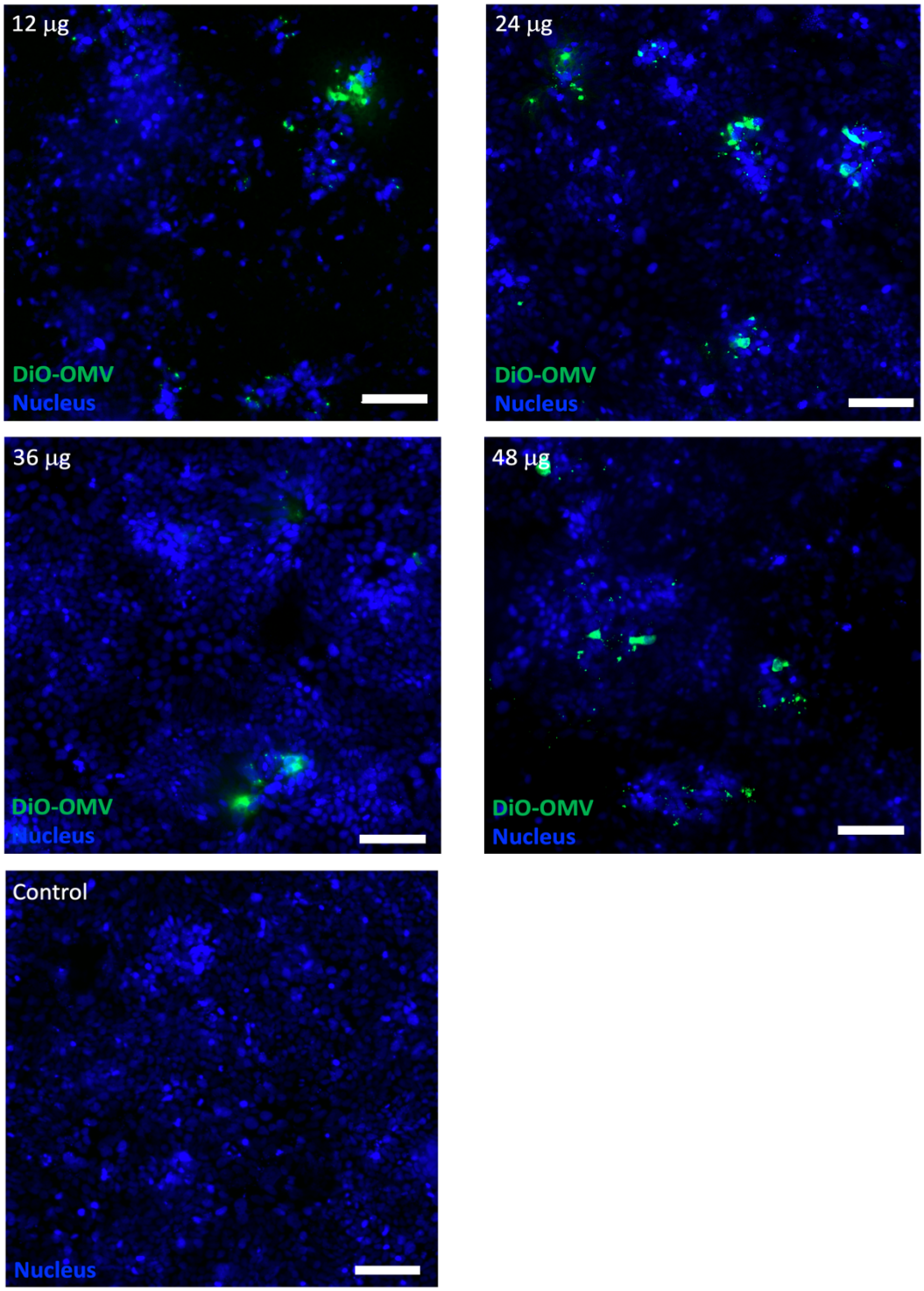

Figure 4.31: Higher OMV doses do not exhibit increased OMV association with confluent T84 monolayers. DiO-OMVs (green) isolated from LB cultures of EHEC 85-170 for were administered at different doses (12µg - 48µg OMV protein) and incubated for 24 hours. Cell nuclei were labelled with DAPI (blue). Images were produced at a resolution as close to the optimal resolution permitted by the system. Images are representative of more than two independent experiments performed in duplicate. Images were attained by using a Zeiss Axio imager M2 widefield microscope fitted with a 10x objective (EC Plan-Neofluar, NA = 0.30, Zeiss). Scale bars = 100µm.

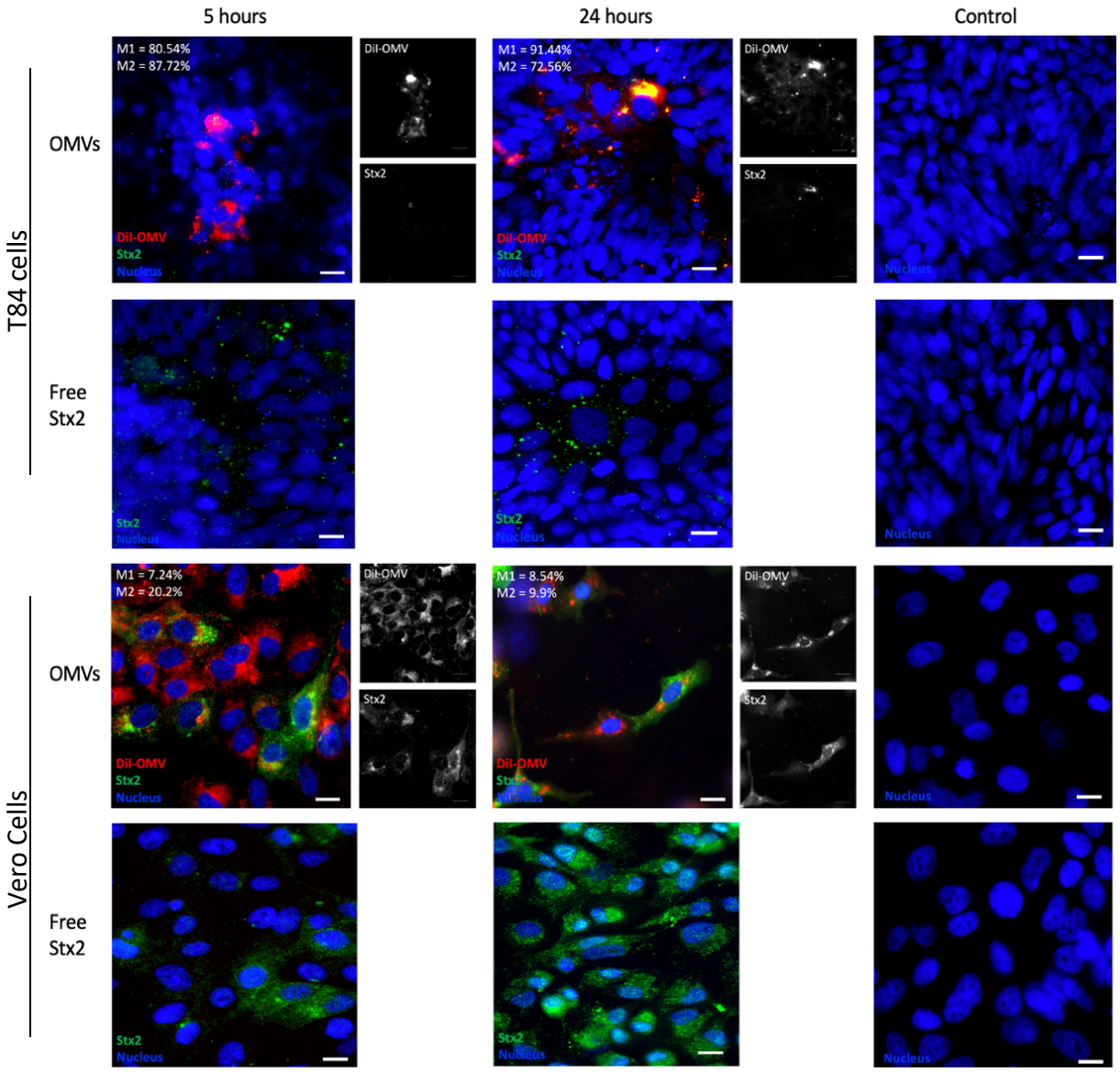

Figure 4.32: Fluorescence microscopy images of T84 and Vero cells incubated with DiI-OMVs isolated from LB cultures of EHEC EDL933 or with soluble Stx2, for 5 and 24 hours. Cell monolayers were incubated with DiI-OMVs (red), immunostained for Stx2 (green) and cell nuclei were labelled with DAPI (blue). Images are representative of more than three independent experiments, performed in duplicate. The main image represents merged images from three separate channels, with the red and green channels shown individually in the side panels. The percentage of colocalisation (M1 = % of DiI signal colocalising with Stx2 signal, M2 = % of Stx2 signal containing DiI signal) are indicated by the white numbers. Images were produced at a resolution as close to the optimal resolution permitted by the system. Images were attained by using a Leica DM6000 B widefield microscope fitted with a 40x objective (HCX PL Fluotar, NA = 0.75, Leica). Scale bars = 20μm.

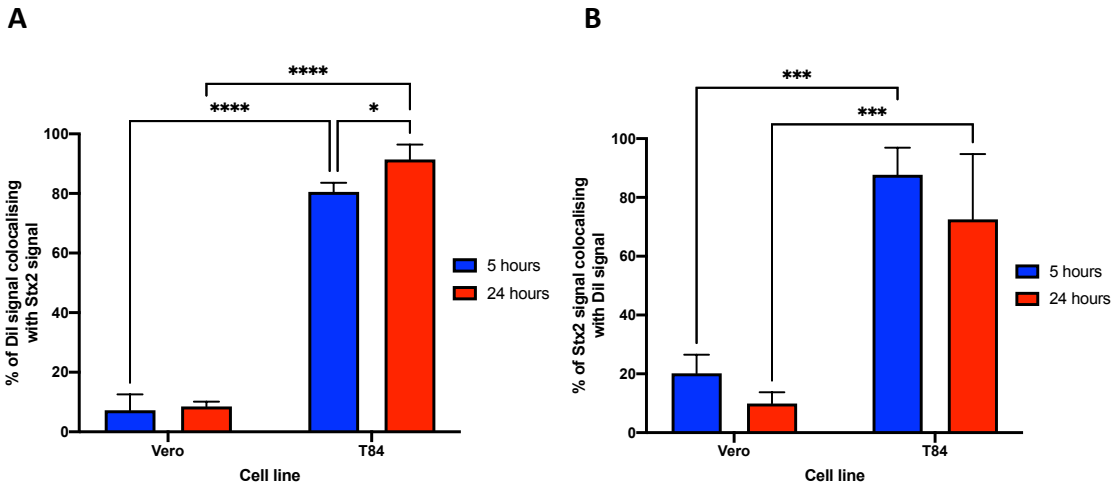

Figure 4.33: Quantification and statistical analysis of signal colocalisation between DiI signal and Stx2 signal in Fig. 4.32. A) Graphical presentation of the mean percentage of DiI signal colocalising with Stx2 signal ± SD of five representative cells (M1). B) Graphical presentation of the mean percentage of Stx2 signal colocalising with DiI signal ± SD of five representative cells (M2). * = $P < 0.05$, *** = $P < 0.001$, **** = $P < 0.0001$.

4.2.8 Differentiated human colonoids internalise EHEC OMVs

In this study, the interaction of OMVs with colonic derived Caco-2 and T84 cell lines differed. While results obtained with Caco-2 cells showed OMV internalisation by non-polarised and polarised cells, and subsequent transcellular translocation to the basolateral membrane, T84 cells exhibited limited interaction with OMVs. Due to the discrepant results, the interaction between OMVs and human-derived two-dimensional colonoid models was investigated.

This two-dimensional model was used so as to reproduce the heterogenous absorptive and secretory cell types found in the colon, thus providing results which more accurately reflect the *in vivo* interactions with OMVs compared to immortalised colonic cell lines (Furness *et al.*, 1999, In *et al.*, 2016b). To elucidate whether OMV internalisation occurs in native human colonic epithelium, colonoids derived from healthy endoscopic biopsy tissue were seeded out on Transwell inserts and differentiated into two-dimensional monolayers (In *et al.*, 2019).

Epithelial barrier function was monitored by TEER, with differentiated two-dimensional colonoids exhibiting TEER values of >300 Ω x cm^2. Resulting two-dimensional colonoids would be made up of columnar intestinal mucin-producing goblet cells, enteroendocrine cells and epithelial cells with an actin-rich brush border on the apical cell surface.

To determine whether OMV internalisation would occur, differentiated two-dimensional colonoid monolayers were incubated with OMVs isolated from EHEC 85-170 for 5 and 24 hours. As shown in Fig. 4.34, EHEC OMVs did not affect TEER values, suggesting that the barrier remained intact throughout the 24-hour incubation period. Subsequent immunostaining of two-dimensional colonoids for OMVs, actin and the mucin glycoprotein MUC2 (to label goblet cells), showed that only colonocytes exhibited the ability to internalise OMVs after 5- and 24-hour incubation periods (Fig. 4.35).

Furthermore, OMV translocation was examined by collecting the basolateral medium from confluent differentiated colonoids grown on Transwells inserts incubated with apically applied OMVs for 24 hours and incubating the concentrated basolateral medium with Vero cells for 24 hours. Immunofluorescence examination of Vero cells confirmed the presence of OMVs, indicating the translocation of OMVs across two-dimensional colonoids (Fig. 3.36).

Taken together, these results indicate that two-dimensional colonoids can internalise and allow OMV translocation via a transcellular pathway.

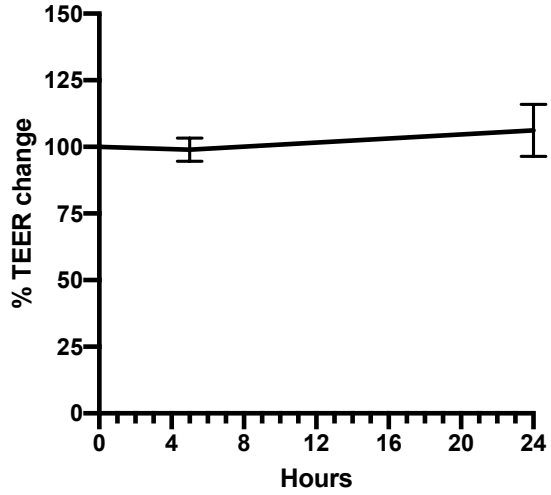

Figure 4.34: EHEC OMVs do not affect the barrier function of polarised two-dimensional colonoids. Colonoid transwell inserts were incubated for 24 hours with OMVs isolated from LB cultures of EHEC 85-170. Data is shown as a percentage of the TEER compared to TEER taken at time '0' ± SD of triplicate technical replicates.

5 hours

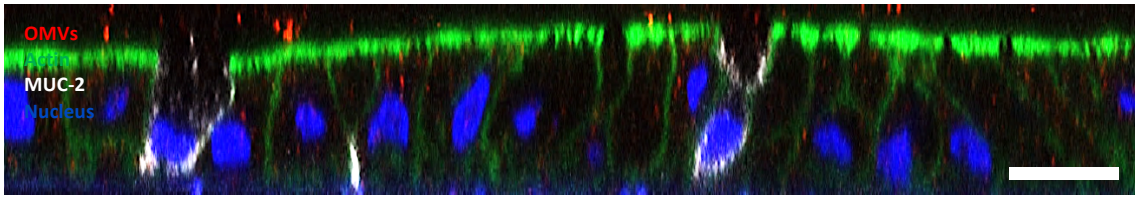

24 hours

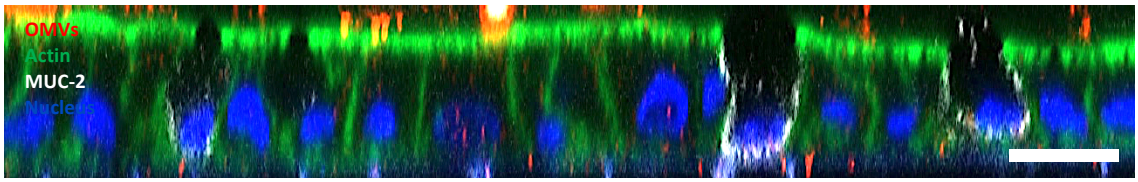

Figure 4.35: OMVs are internalised by polarised two-dimensional colonoids. Differentiated colonoids were incubated for 5 and 24 hours with OMVs isolated from LB cultures of EHEC 85-170. Cells were immunostained for OMVs using *E. coli* specific anti-LPS (red), actin (green) and mucin glycoprotein MUC2 (white), and cell nuclei were labelled with DAPI (blue). Images are representative of an independent experiment performed in duplicates. Images were produced at a resolution as close to the optimal resolution permitted by the system. Images were attained by using a Zeiss LSM800 confocal microscope fitted with a 40x water objective (LD C-apochromat, NA = 1.1, Zeiss). Scale bars = 20μm.

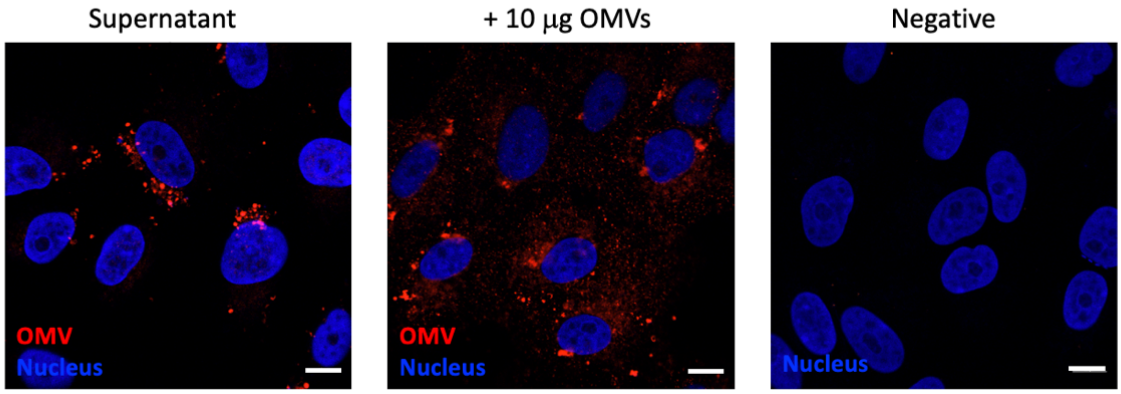

Figure 4.36: Fluorescence micrographs of Vero cells incubated with basal medium collected from polarised two-dimensional colonoids after 24-hour incubation periods with OMVs. Basolateral medium was collected from Transwells incubating with apically applied OMVs and incubated for 24 hours. Medium was concentrated and incubated with Vero cells for 24 hours. Cells were immunostained for OMVs using *E. coli* specific anti-LPS (red) and cell nuclei were stained with DAPI (blue). Images are representative of more than two independent experiments. Images were produced at a resolution as close to the optimal resolution permitted by the system. Images were attained by using a Zeiss LSM800 confocal microscope fitted with a 63x water objective (Objective C-apochromat, NA = 1.2, Zeiss). Scale bars = 10μm.

4.3 Discussion

The development of HUS occurs due to the action of Stx released by infecting EHEC. Soluble Stx is not actively secreted by a bacterial secretion system but is released after bacterial lysis following the activation of the phage lytic cycle. Stx has cytotoxic effects on Gb3-expressing endothelial cells, neurons and various renal cells such as podocytes and mesangial cells (Obata *et al.*, 2008, Obrig, 2010). To reach these cells Stx needs to cross the human colonic epithelium, yet due to the absence of Gb3 receptors in the colon, the mechanism of how this process occurs remains unclear (Schuller *et al.*, 2004, Kovbasnjuk *et al.*, 2005, Schüller, 2011).

It has been proposed that soluble Stx can cross the colonic barrier through a paracellular pathway which arises due to the disruption of tight junctions (Philpott *et al.*, 1998, Hurley *et al.*, 2001). Previous studies have demonstrated that through the TTSS which EHEC possesses, effector proteins such as EspFu, EspF, EspG and Map enter host cells and reorganise the distribution of tight junction proteins N-WASP, ZO-1, ZO-2, occludin and claudin, thereby causing a leaky barrier (Philpott *et al.*, 1998, Viswanathan *et al.*, 2004). This process can be further enhanced by paracellular transmigration of neutrophils into the gut lumen, which is a key feature during EHEC infections, as evidenced by elevated neutrophil levels in stool samples (Klein *et al.*, 2002, Bielaszewska and Karch, 2005). Interestingly, neutrophils can induce Stx2 synthesis, therefore contributing to the development of disease *in vivo* (Wagner *et al.*, 2001). Macropinocytosis has also been proposed as another route for Stx2 transmigration across the human colonic epithelium. Investigations have demonstrated that EHEC infection can stimulate macropinocytosis in colonic cells including Gb3 deficient cells which can cause the translocation of Stxs (Lukyanenko *et al*., 2011).

OMVs secreted by EHEC can encapsulate Stx (Kolling and Matthews, 1999, Bielaszewska *et al.*, 2017) and thus may provide a means of toxin transport across the intestinal epithelial barrier. Previous studies have demonstrated that EHEC OMV

can interact and be internalised by human cells including the colonic derived Caco-2 cell line (Bielaszewska *et al.*, 2013, Bielaszewska *et al.*, 2017). However, the physiological relevance of this cell line is debatable since it is physiologically similar to cells which line the small intestine rather than the colon (Devriese *et al*., 2017). In addition, the aforementioned trafficking studies have only been made using non-polarised cells, which contrasts with the morphology of cells which line the intestinal epithelium as such cells are polarised and have distinct apical and basolateral surface membranes separated by tight junctions.

Thus, in this study to deduce whether the colonic epithelium can internalise EHEC OMVs, colonic derived Caco-2 and T84 cell lines were used, as well as human derived two-dimensional colonoid monolayers. To further mimic the colonic epithelium, the ability of EHEC OMVs to translocate across polarised cell monolayers was examined in colonic cells which exhibited EHEC OMV internalisation. Furthermore, the trafficking of EHEC OMVs and OMV-associated Stx was investigated in renal Vero cells.

4.3.1 OMV labelling

Previous investigations have used various methods to label OMVs. In this investigation, to study OMV internalisation, OMVs were labelled using the lipophilic dyes DiO and DiI as previous studies have used such dyes to examine OMV internalisation and trafficking (Parker *et al.*, 2010, Bielaszewska *et al.*, 2013, Kunsmann *et al.*, 2015, Jones *et al.*, 2020). This relatively easy method allows the user to label the entire OMV population and examine OMV internalisation by eukaryotic cells using florescence microscopy.

In this study, EHEC DiO- and DiI-OMVs were internalised by renal Vero cells after 5-hour incubation periods with similar staining after 24-hours incubation periods. Similar results were also attained with lipophilic dyed OMVs were incubated with Caco-2 cells after 3-hour incubation periods. Confirmation of OMV internalisation

was demonstrated by both Vero and Caco-2 cells by examination of XZ-stacking achieved in confocal imaging which showed lipophilic dye within cells. These results are in agreement with previous studies which utilised lipophilic dye DiO and rhodamine B isothiocyanate labelled OMVs isolated from EHEC O103:H2 strain 8033 or EHEC O157:H7 strain 5791/99 and demonstrated internalisation by non-polarised Caco-2 cells and by human brain microvasculature endothelial cells (HBMEC) within 4 hours (Bielaszewska *et al.*, 2013, Bielaszewska *et al.*, 2017).

A disadvantage of using lipophilic dyes is the possibility that due to insufficient washing, excess dye will lead to labelling of host membranes (Mulcahy *et al.*, 2014). Moreover, it may be possible that internalised dye molecules can leach from OMVs and onto various membrane bound organelles, subsequently spreading dye molecules within cells and leading to artificial trafficking results. It may also be possible that dye molecules can form aggregates and enriched domains, consequently altering the mobility and rigidity of the OMV lipid bilayer (Lulevich *et al.*, 2009). Such membrane alterations may also affect the function and intracellular trafficking of OMVs. To confirm the specificity of lipophilic OMV staining, co-staining was performed using an antibody specific for *E. coli* LPS (US Biological, Polyclonal) which has been confirmed to specifically label EHEC OMVs (Bielaszewska *et al.*, 2017).

In Vero cells, low colocalisation values were attained between lipophilic dye and OMV-LPS signal when both DiO- and DiI-OMVs were utilised for 5-hour incubation periods. Similarly, low rates were attained between DiO or DiI signal and OMV-LPS signal in Caco-2 cells after 3- and 5-hours incubation periods. In contrast, high colocalisation rates between lipophilic DiO dye and OMV-LPS signal was achieved when colocalisation was examined in T84 cells with M1 values (% of red signal overlapping green signal) of 62.49% and 60.57%, and M2 values (% of green signal overlapping red signal) of 61.4% and 45.72% after 5- and 24-hour incubation periods, respectively. Low colocalisation values achieved in Vero and Caco-2 cells suggest the dissociation of dye molecules from OMVs and labelling of host cell membranes. Interestingly, examination of fluorescence images from other studies which use DiO-OMVs from other *E. coli* strains and other bacterial species demonstrate similar

labelling patterns of host membranes and a lack of vesicular patterns which would be expected for vesicles (Tyrer *et al.*, 2014, Svennerholm *et al.*, 2017, Ling *et al.*, 2019, Jones *et al.*, 2020).

In non-polarised Caco-2 cells, similar colocalisation values were achieved between the ER and internalised lipophilic dye (via labelled OMVs) to that between dye and LPS signals. This suggests that dye molecules may leach and spread to membrane-bound organelles. Due to the suspected leaching of the dye onto host membrane, antibody-mediated detection of OMVs was used to investigate the intracellular trafficking of OMVs.

4.3.2 EHEC OMV internalisation and intracellular transport

Previous studies have demonstrated EHEC OMV internalisation by Gb3-positive human colonic-derived Caco-2 cells, and human renal and brain endothelial microvasculature cells (HRMEC and HBMEC, respectively), through clathrin-mediated endocytosis (Bielaszewska *et al.*, 2013, Bielaszewska *et al.*, 2017).

In this study, OMV uptake by non-polarised Caco-2 cells was confirmed by XZ confocal scans of actin and OMV-LPS stained cells. However, unpolarised Caco-2 cells differ from native intestinal epithelium which is composed of columnar-shaped differentiated epithelial cells with distinct apical and basolateral surface membranes separated by tight junctions (Furness *et al.*, 1999, Giepmans and van Ijzendoorn, 2009, Marchiando *et al.*, 2010). Therefore, Caco-2 cells were grown on Transwell inserts which results in the formation of differentiated columnar shaped enterocyte-like cells (Lu et al., 1996, Madara et al., 1987, Devriese et al., 2017). XZ confocal scans confirmed the internalisation of EHEC OMVs into polarised Caco-2 cell monolayers after 3-hour incubation periods. The OMV staining patterns at different time points were similar to that of non-polarised Caco-2 cells.

The fate of internalised cargo via endocytic vesicles is decided in common endosomal compartments (Brown *et al.*, 2000, Garcia-Castillo *et al.*, 2017). It is known that upon internalisation, cargoes can be trafficked (i) back to the plasma membrane via recycling endosomes, (ii) sorted to the lysosomes, or (iii) sent to the trans-Golgi network (Saimani and Kim, 2017). Previous studies have demonstrated the intracellular trafficking of bacterial OMVs to lysosomes. OMVs from *P. gingivalis* which are internalised by human gingival epithelial cells first localise in endosomes and are subsequently trafficked to lysosomes (Furuta *et al.*, 2009). In addition, OMVs from commensal *E. coli* strains have been demonstrated to be trafficked along the endosomal-lysosomal pathway in polarised colonic-derived HT29 cells (Cañas *et al.*, 2016). A similar pathway has also been confirmed for (i) OMVs from EHEC O157:H7 strain 5791/99 in HBMEC, (ii) OMVs from EHEC O103:H2 strain 8033 in non-polarised Caco-2 cells and (iii) EHEC O157:H7 strain EDL933 in non-polarised DLD-1 intestinal cells (Bielaszewska *et al.*, 2013, Bielaszewska *et al.*, 2017). In agreement with this, the work presented in this study confirmed intracellular trafficking of OMVs isolated from EHEC O157 to late endosomal/lysosomal compartments in non-polarised and polarised Caco-2 cells. OMV trafficking to late endosomes/lysosomes was observed for OMVs from both Stx-positive and negative EHEC strains, suggesting that intracellular trafficking of OMVs does not rely on the encapsulation of Stx. Similarly, using non-polarised colonic DLD-1 cells, Bielaszewska *et al.* (2017) demonstrated that OMVs are transported to the lysosomes irrespective of the encapsulation of both Stx2a and Stx1a. Nevertheless, different colocalisation rates were quantified between OMVs and late endosomal/lysosomal compartments between polarised and non-polarised monolayers, with significantly lower colocalisation values in non-polarised cells after 5 hours ($P < 0.0001$) suggesting that polarised Caco-2 cells have a slower trafficking system and/or have an additional intracellular route for internalised EHEC OMVs.

In addition to Caco-2 cells, EHEC OMV transport was examined in Vero cells which are of renal origin and therefore reflect the ultimate target of systemically released Stx (Konowalchuk *et al.*, 1977, Lingwood *et al.*, 1987). The colocalisation rate between OMVs for EHEC 85-170 and TUV 93-0 and late endosomal/lysosomal

compartments reached 49% and 64% in Vero cells after 3 hours, which is comparable to the colocalisation rate of 60% after 90 minutes between EHEC OMVs and lysosomal compartments in HBMEC presented in Bielaszewska *et al.* (2017). Comparatively, colocalisation rates between OMVs from 85-170 and late endosomal/lysosomal compartments were lower in non-polarised Caco-2 cells than Vero cells after 3- and 5-hour incubation periods ($P < 0.0001$), suggesting Caco-2 cells have a slower intracellular trafficking kinetics than Vero cells. Since widefield microscopy was used to image the intracellular trafficking of OMVs in Vero cells, it may be argued that colocalisation values are overestimated due to out-of-focus and background fluorescence associated with this microscopy technique. However, due to the flatness of Vero cells this may not be a huge issue. In this study, confocal microscopy was used to examine colocalisation of OMVs and late endosomes/lysosomes in Caco-2 cells, suggesting that OMVs accumulate in late endosomal/lysosomal compartments, which can range from 100nm to 1500nm (Xu and Ren, 2015). It is likely that the colocalisation manifestations are true due to the confocal microscope being fitted with appropriate objectives being used.

T84 cells are considered to be more physiologically relevant than Caco-2 cells to simulate colonocytes, as polarized T84 cells are phenotypically similar to colonic crypt cells due to their short microvilli, whereas polarized Caco-2 cells express brush border hydrolases and long microvilli similar to a mid-villous small intestinal epithelial cell (Devriese *et al*., 2017). Furthermore, similarly to the colonic epithelium, T84 cells lack Gb3 expression whereas Caco-2 cells express Gb3 (Schuller *et al*., 2004, Kovbasnjuk *et al*., 2005). Thus, the ability of T84 cells to internalise EHEC OMVs was examined. Unlike Caco-2 cells, confluent T84 cell monolayers exhibited little internalisation of EHEC OMVs. Moreover, EHEC OMV internalisation was observed in semi-confluent monolayers by T84 cells located on the edge of cell islands. As little internalisation of EHEC OMVs was exhibited in confluent non-polarised T84 cell monolayers, the interaction between EHEC OMVs and polarised T84 cells was not examined. To date, very little work has been made to study the interaction of T84 cells with OMVs derived from other enteric pathogens. Despite extensive literature review, no

microscopic studies have reported OMV internalisation from any bacterial species by T84 cells.

The discrepant results achieved between Caco-2 cells and T84 cells did not clarify whether OMV internalisation by the colonic epithelium occurred. Due to the physiological relevance of T84 cells, results attained with this cell line may appear more reliable, and the immediate conclusion might be that very little EHEC OMV internalisation occurs in the colon. However, a weakness of using cell culture models is that immortalised cell lines derive from cancer cells have accumulated various mutations and therefore are different from normal cells. Furthermore, cell culture models lack the presence of a mucus layer and the cell mixture present in the normal intestinal epithelia such as goblet cells and neuroendocrine cells (Furness *et al.*, 1999, In *et al.*, 2016b).

To overcome these shortcomings, experiments were performed in this study using human colonic organoids, known as colonoids (In *et al.*, 2016a, In *et al.*, 2019, Clevers, 2013, Sato *et al.*, 2009, Sato and Clevers, 2013). Colonoids are derived from human adult intestinal stem cells located in the crypts of endoscopic biopsy samples and cells can differentiate into one of the three major colonic cell types including colonocytes, goblet and neuroendocrine cells (In *et al.*, 2016b, Grün *et al.*, 2015, Sato *et al.*, 2009). During growth in Matrigel, colonoids form three-dimensional closed spheres, with the apical surface facing inwards (Sato *et al.*, 2009, Foulke-Abel *et al.*, 2016). Thus, to enable EHEC OMV internalisation and translocation studies, colonoids were grown on collagen-coated Transwell filters resulting in the formation of two-dimension polarised monolayers (In *et al.*, 2016a).

Unlike T84 cells, EHEC OMVs were readily internalised into colonoid monolayers with predominant uptake by colonocytes but not by goblet cells. However, compared to polarised Caco-2 cells, polarised colonoid monolayers exhibited lower internalisation of EHEC OMVs. This in turn would suggest that EHEC OMVs are internalised in the intestinal epithelium, however the rate of internalisation is slower *in vivo* than that exhibited by polarised Caco-2 cells. So far, only one study has shown OMV

internalisation by intestinal organoids using murine caecal organoids to evaluate interaction with OMVs from *B. thetaiotaomicron* (Jones *et al.*, 2020). Therefore, this investigation is the first study to show that human intestinal organoids can be employed as a model system to study OMV uptake in the gut.

4.3.3 EHEC OMV-associated Stx2 trafficking in cell models

While EHEC OMVs undergo lysosomal degradation, several associated virulence factors are freed during OMV trafficking in the endosomal network and consequently follows different intracellular trafficking routes to their respective targets. Bielaszewska *et al.* (2017) has shown that OMVs from EHEC O157:H7 strain 5791/99 contain Stx2a, haemolysin (Hly) and cytolethal distending toxin V (cdtV). Using HBMEC, it has been demonstrated that Stx2a separates from OMVs in endosomes due to a drop in pH and follows retrograde transport via the Golgi apparatus to the ER, from where the A1 fragment is translocated to the cytosol. Interestingly, the expression of Gb3 is a prerequisite for sequential retrograde transport of Stx2 as investigations showed that OMV-associated Stx2 trafficked to the lysosome rather than the ER in intestinal epithelial DLD-1 cells which are Gb3-negative. Similarly, the B-subunit of cdtV, the DNase-like component of CdtV, follows retrograde transport to the Golgi apparatus and the ER but is ultimately trafficked to the nucleus. Furthermore, using the HBMEC it has been demonstrated that Hly separates from OMVs in the lysosomes, and is transported to mitochondria.

This study confirmed that OMV-associated Stx2 produced by EHEC strain EDL933 are transported to the Golgi apparatus and the ER in Gb3 positive Vero cells. Interestingly, not all cells which internalised DiO-OMVs exhibited Stx2 staining, suggesting that not all OMVs produced by EDL933 contain Stx2. Fluorescence microscopy demonstrated Stx2 separation from OMVs and trafficking to the Golgi apparatus after an hour of incubation with subsequent transport to the ER after 3 hours; with cell death by a 24-hour period. This is similar to studies made by Bielaszewska *et al*. (2017), which incubated HBMEC with OMV-associated Stx2a from

EHEC O157:H7 strain 5791/99 and demonstrated trafficking of Stx2a to the Golgi apparatus within 30 minutes and to the ER by 4 hours.

In this study, to deduce the intracellular trafficking of OMV-associated Stx, widefield microscopy was utilised. Even though such microscopic techniques provide a fast means to attain results, colocalisation values attained here may be overemphasised due to background noise. This study did not examine the overlap between the Golgi apparatus and the ER. As it may be possible that the two compartments overlap, it may be possible that colocalisation values may be overemphasised.

Different results were obtained for non-polarised Caco-2 cells, where confocal microscopy was utilised. Very little colocalisation values were attained between Stx2 with the ER after 5 hours of incubation. This is in contrast to Vero cells, suggesting slower kinetics and/or a different intracellular trafficking route, yet due to the use of widefield microscopy to analyse Stx2 trafficking in Vero cells, this cannot be concluded.

In contrast to Caco-2 and Vero cells, little OMV and Stx2 internalisation was detected in Gb3 negative T84 monolayers. However, co-localization of DiO-OMVs with Stx2 signal was high, suggesting a lack of Stx2 dissociation from OMV upon interaction by T84 cells. This is in agreement with previous investigations which concluded that retrograde transport of OMV-associated Stx2 is Gb3-dependent as OMVs incubation with colonic Gb3-negative DLD-1 cells resulted in OMVs and Stx2 being trafficked to the lysosomes, and a lack of cytotoxicity (Bielaszewska *et al*., 2017). Results obtained in this study suggest that OMVs and Stx are trafficked to similar intracellular destinations in T84 cells. Speculatively, it is suspected that both entities are trafficked to the late endosome/lysosome, but this will need to be confirmed. T84 cells were also inoculated with soluble Stx2 to serve as a control. Microscopy demonstrated the internalisation of soluble Stx2 by T84 cells but a lack of cytotoxic effects. This is coherent with results from another study which used the same amount of free Stx2 and demonstrated transportation to the ER after 6 hours, without any cytotoxic consequences in T84 cells (Schuller *et al.*, 2004).

In conclusion, the findings presented in this study suggest that intracellular trafficking of OMV-associated Stx2 in Vero cells is similar to that of soluble Stx2 resulting in retrograde transport in the ER with subsequent cell death. This process seems to be dependent on the expression of Gb3, as T84 cells did not support retrograde toxin trafficking and cytotoxicity. Nevertheless, it may be possible that Gb3-negative intestinal epithelium allows transcytosis of OMV-associated Stx which could subsequently damage Gb3-expressing microvascular cells in the lamina propria.

4.3.4 OMV translocation

Translocation of OMVs across the intestinal epithelium may occur via a transcellular or paracellular routes. The latter mechanism is supported by work on OMVs from *C. jejuni* which has demonstrated a reduction of the T84 cell barrier function due to degradation of tight junction proteins such as occludin and E-cadherin by the action of OMV-associated high temperature requirement A protease and Cj1365c proteases (Elmi *et al.*, 2016). Interestingly, protease activity was enhanced when OMVs were isolated from *C. jejuni* cultures grown in the presence of bile salts (Elmi *et al.*, 2018). OMVs isolated from *P. gingivalis* have also demonstrated the ability to compromise tight junctions between lung epithelial cells (He *et al.*, 2020). It is speculated that this degradation is mediated by the protease gingipain, which would allow paracellular OMV transport into deeper tissue. In contrast, the opposite effect has been observed for OMVs from probiotic and commensal *E. coli* strains, where such OMVs strengthen the epithelial barrier of Caco-2 and T84 cells by promoting expression of tight junction proteins (Alvarez *et al.*, 2016, Cañas *et al.*, 2016, Alvarez *et al.*, 2019). Furthermore, the integrity of the epithelial barrier was maintained when monolayers were infected with barrier disrupting EPEC and OMVs isolated from probiotic and commensal *E. coli* (Alvarez *et al*., 2019).

In this study, the application of EHEC OMVs for 24 hours did not affect the epithelial barrier function of polarised Caco-2 cells nor of colonoid monolayers suggesting a lack of cytotoxic effect or tight junction degradation. Nevertheless, results attained

in this investigation suggest that EHEC OMVs are trafficked across polarised Caco-2 and colonoid monolayers as evidenced by the application of sampled basal medium to Vero cells for 24 hours and subsequent imaging of internalised EHEC OMVs. EHEC OMV translocation across Caco-2 and colonoid monolayers was detected after 3 and 24 hours of incubation, respectively. Given the maintenance of epithelial resistance, these results suggest that EHEC OMVs can penetrate the colonic epithelium via a transcellular pathway, which does not involve the Golgi apparatus or the ER. Here, it is speculated that EHEC OMV translocation across polarised epithelial may involve recycling endosomes. Recycling endosomes are involved in recycling internalised proteins and lipids back to the plasma membrane (Stoops and Caplan, 2014, He and Guo, 2009, Cramm-Behrens *et al.*, 2008, Garcia-Castillo *et al.*, 2017). Examples of compounds which are known to be trafficked across polarised cell via recycling endosomes include antibodies and cholera toxin (Saslowsky *et al.*, 2013, Brown *et al.*, 2000). Furthermore, intracellular pathogens such as *P. gingivalis* exploit such intracellular vesicles to exit from host cells (Takeuchi *et al.*, 2011).

In conclusion, these findings suggest that EHEC OMVs are endocytosed by colonic epithelia cells and translocate across the epithelium, with little intracellular trafficking to host cell late endosome/lysosomes. When considering the *in vivo* situation, the evidence gathered implies that OMVs allow Stx2 to cross the colonic epithelium and subsequently enter the vascular system.

4.3.5 Summary

In this investigation, it has been demonstrated that EHEC OMVs can cross the colonic epithelium. First, it was confirmed that non-polarised and polarised Caco-2 monolayers internalised EHEC OMVs. Nevertheless, very little OMV internalisation was detected in confluent non-polarised T84 monolayers. This questioned the reliability of the results attained by the Caco-2 cell line as T84 cells are regarded as a more physiological relevant cell line than Caco-2 cell. In order to determine whether OMVs are internalised by the colonic epithelium, a two-dimensional colonoid models

were used. In this model, OMV internalisation was achieved without comprise of the barrier integrity.

EHEC OMV internalisation was also achieved in renal Vero cells, and it was demonstrated that upon OMV internalisation, Stx2 is freed and follows retrograde transportation to the Golgi apparatus and then the ER. Similarly, Stx2 disassociation from OMVs was demonstrated in non-polarised Caco-2 cells. In both Vero and Caco-2 cells, OMVs are transported to the late endosomal/lysosomal compartments, yet there was a lower colocalisation rate in polarised Caco-2 cell monolayers.

Following this, it was elucidated by using polarised Caco-2 cells and colonoid monolayers that OMVs can cross the epithelial barrier without compromising the epithelial barrier, therefore suggesting a transcellular trafficking pathway.

In summary, the results achieved in this investigation suggest that EHEC OMVs can cross the intestinal epithelium. Furthermore, the trafficking of OMV-associated Stx in renal cells is similar to soluble Stx, which ultimately results in cell lysis. Additionally, due to the discrepancies gained in OMV trafficking using different cell lines, the importance of using appropriate physiological cell models to study *in vivo* interactions has been highlighted.

Chapter Five: Conclusions and future work

The aim of this PhD project was to elucidate how EHEC OMVs may contribute to the development of diseases upon EHEC infection in the intestines. The first part of the study evaluated how the colonic milieu influences EHEC OMV production. This was achieved by examining the effects of different settings mimicking the colonic environment on EHEC OMV yields. The secondary part of this project examined how EHEC OMVs interact with host cells including colonic epithelial cells, and to deduce whether OMV translocation across the colonic epithelium could arise. In this section, the main outcomes from this investigation are summarised and the potential future work which can arise from this study will be proposed.

5.1 Summary of key findings

The gastrointestinal tract is a hostile milieu for colonising EHEC. In order to successfully establish in the colon, infecting EHEC has a variety of mechanisms to overcome these stresses, including the release of OMVs. OMVs have been identified as a bacterial stress response, enabling survival in harsh environments (McBroom and Kuehn, 2007, Sampath *et al.*, 2018, Bauwens *et al.*, 2017a, Bauwens *et al.*, 2017b, Urashima *et al.*, 2017). Therefore, in the first part of this investigation the effect different colonic cues have on EHEC OMV vesiculation was examined.

This investigation builds on studies which have demonstrated that different intestinal conditions such as gastric pH and microaerobic conditions, increase EHEC vesiculation (Bauwens *et al.*, 2017b). In this investigation, it was first deduced that the highest OMV yields were attained by stationary phase cultures. By comparing EHEC OMV yields attained from LB cultures to TSB or DMEM/F-12 cultures, it was confirmed that different conditions can influence OMV vesiculation. In agreement with Bauwens *et al.* (2017b), this study confirms that simulated colonic environmental medium (SCEM) increases the rate of OMV vesiculation. In context to bacterial pathogenesis, this suggests that EHEC upregulates OMV vesiculation in the colonic lumen due to the presence of stressors such as bile salts. In addition, this

study confirmed that bile salts do not disrupt the integrity of OMVs, suggesting their ability to remain viable in the host intestine. This investigation also concluded that the presence of colonic CO_2 levels and the presence of colonic epithelial T84 cells do not significantly affect EHEC OMV vesiculation, indicating not all factors in the colon augment EHEC OMV production.

Previous work has demonstrated that EHEC OMVs can be internalised by human epithelial and endothelial cells and thereby act as a vehicle for the delivery of virulence factors (Bielaszewska *et al.*, 2017). In this study, OMV uptake and trafficking in human colonic cells was investigated. Although absolute quantification is lacking, results in this study show that OMV internalisation into Gb3-positive Caco-2 cells was higher compared to Gb3-negative T84 cells. Moreover, internalisation into colonocytes in two-dimensional colonoid monolayers was achieved, suggesting internalisation occurs *in vivo*. In addition, OMVs translocation across polarised Caco-2 cells and colonoids without compromise of epithelial barrier function was achieved.

This work provides evidence that OMV translocation across the intestinal epithelium occurs via a transcellular route. Speculatively, OMVs may play a relevant role in the delivery of virulence proteins including Stx across the colonic epithelium. This investigation provides evidence that EHEC OMVs may contribute to HUS development as OMV-associated Stx follows the same retrograde pathway in Gb3 expressing cells and causes cell death. Lastly, this work highlights the effectiveness of organoids to study OMV uptake in the gut due to discrepancies between different colonic cells.

5.2 Future experiments

The increase in OMV vesiculation in the presence of bile salts suggests that OMVs may have a defensive role, protecting EHEC from the lethal effects of bile salts. To deduce whether this occurs, growth of *E. coli* mutants lacking bile salt resistance

genes (e.g., efflux pump *acrA* and *acrB*) in lethal bile salt levels can be carried out with and without the addition of OMVs isolated from wild type EHEC strains grown in SCEM containing bile salts. If growth is not affected with the addition of OMVs, this would indicate that OMVs sequester bile salts and protect growing bacterial cells.

Throughout this study, it was noted that different OMV protein profiles were attained when EHEC cultures were grown in different conditions. It would be of interest to elucidate the proteins which are expressed under different conditions through mass spectrometry. Furthermore, it would be of interest to elucidate whether different virulence factors are encapsulated by OMVs in certain conditions. Indeed, previous studies have shown that in the presence of bile salts, OMVs produced by *C. jejuni* increase protease ability which degrade tight junction proteins and corrupt the integrity of the epithelial barrier (Elmi *et al.*, 2018). Subsequently, it would be beneficial to deduce whether OMVs isolated from EHEC SCEM cultures compromise the epithelial barrier through a similar mechanism.

Furthermore, the internalisation capabilities of OMVs with different protein profiles may differ. It is possible that OMVs isolated from growth conditions different to the one used in this study (LB medium, 5% CO_2/air), may show increased OMV internalisation in cells, including T84 cells. OMVs from bacteria in close contact with the colonic epithelium are most likely to interact with host cells, therefore, it would be of interest to examine the interaction between OMVs isolated from EHEC-T84 cell co-cultures with colonic cells. To study the rate of OMV internalisation, previous studies have utilised fluorescently labelled OMVs to measure the rate of internalisation into host cells (Bielaszewska *et al.*, 2013, Bielaszewska *et al.*, 2017). This same method could be used to determine whether OMVs isolated from different conditions affects OMV uptake by host cells.

Another parameter which needs to be considered is the mucus layer which lines the colonic epithelium. The mucus layer protects the epithelium from bacteria and foreign antigens. Around 300µm thick, the mucus layer is made up of mucin glycoproteins which are secreted by goblet cells (Johansson *et al.*, 2008, McGuckin *et*

al., 2011, Johansson *et al.*, 2014). Due to its complex structure, the mucus layer may inhibit the ability of OMVs to interact with host cells. Here, the effect of the mucus layer was not taken into consideration when studying the interaction between OMVs and polarised Caco-2 cells which do not secrete mucus. In addition, despite the presence of MUC2-producing goblet cells in colonoid monolayers, a mucus layer was absent. It would be of interest to evaluate the ability of OMVs to be internalised by cells which are covered by a mucus layer. Furthermore, the ability of EHEC OMVs to penetrate and cross mucus complexes can be evaluated by preparing simulating mucus layers and loading them into make-shift columns or cell culture insert. Such penetration assays have been used to examine the ability of antibiotics and bacteria including enteroaggregative *E. coli* to penetrate through mucus (Saggers and Lawson, 1966, Sheikh *et al*., 2002, Kajikawa *et al*., 2018). The ability of OMVs from non-pathogenic *E. coli* strains to diffuse across the mucin layer produced by polarised mucus-producing HT29-MTX cells has been reported (Cañas *et al.*, 2016). However, this study reports the internalisation of fluorescently labelled OMVs by detecting fluorescence intensity changes in wells containing mucus-producing cells over time and no images are provided. Thus, this brings into question whether OMVs are being internalised or are trapped in the mucus layer, consequently trapping OMVs and increasing fluorescence intensity. Nevertheless, the relevance of a mucus layer during EHEC infections is debatable as previous studies on human colonic biopsies and colonoids have demonstrated that EHEC degrades and permeates the mucus layer (In *et al.*, 2016a, Hews *et al.*, 2017).

Another aspect which should be considered when examining how OMVs interact with human colonic epithelium, is the microaerobic environment at the mucosal surface (He *et al.*, 1999, Marteyn *et al.*, 2011, Kalantar-Zadeh *et al.*, 2018). Earlier work has determined that Stx translocation across polarised T84 monolayers can be enhanced during EHEC infection under microaerobic conditions compared to aerobic conditions (Tran *et al.*, 2014). Speculatively, this may be due to actions of the TTSS and its effectors, since the expression of the TTSS is enhanced under low oxygen levels (Schuller and Phillips, 2010, Müsken *et al.*, 2008). Likewise, it is possible that due to the presence of EHEC, the rate of OMV internalisation changes due to the ability of

adhered EHEC to alter host cell signalling and modulate actin-based host-cell cytoskeleton (Wong *et al.*, 2011, Alto *et al.*, 2007, In *et al.*, 2013). Previous studies have shown that secreted EHEC proteins are sufficient to manipulate host cell cytoskeleton and increase transcellular trafficking of Stx1 (In *et al*., 2013). This was achieved by incubating host cells with Stx1 and lysates of transformed *E. coli* K-12 cultures expressing EHEC EspP. Therefore, to test whether EHEC proteins can affect OMV internalisation, the same approach can be carried out using cell monolayers and evaluating OMV internalisation by microscopy. The endocytic abilities of host cells may also be influenced under microaerobic environments, therefore OMV internalisation may be affected by such conditions (Tran *et al.*, 2014).

In this investigation, the impact of EHEC OMVs on the innate immune response by colonic epithelial cells was not studied. EHEC OMVs are known to stimulate IL-8 secretion in Caco-2 cells, suggesting neutrophils recruitment and activation at the site of OMV internalisation (Bielaszewska *et al.*, 2018). Neutrophil recruitment will consequently lead to the disruption of the intestinal barrier, thus potentially permitting the paracellular transmigration of OMVs. To test this, colonic cells can be grown on inverted Transwells inserts. Upon reaching confluence, EHEC OMVs can be applied in the basolateral medium and neutrophils isolated from healthy volunteers can be applied in to apical medium. If paracellular migration of neutrophils arises due to OMVs, TEER reading will drop, and neutrophils can be isolated from basolateral medium. Moreover, to examine OMV translocation, apical medium can be collected and incubated with Vero cells, with immunostaining for EHEC OMVs subsequently performed.

The interaction between OMVs and immunological cells should also be evaluated in order to deduce whether or not OMVs are cleared. If OMVs are cleared, this would suggest that OMVs may not have a role in renal and neuronal damage during EHEC infection. Fluorescence microscopy can be used to analyse whether EHEC OMVs may be internalised and degraded by immune cells. However, if not degraded by immunological cells, such cells may provide a means of systemic spread within the host.

The effect of EHEC OMVs on the host response of T84 cells would also be of particular interest due to minimal OMV internalisation in this cell line. Previous work has shown induced secretion of the pro-inflammatory cytokines IL-6, IL-8 and TNF-α as well as the antimicrobial peptide β-defensin by T84 cells when incubated with OMVs from *C. jejuni* (Elmi *et al.*, 2012). In contrast, OMVs from *V. cholerae* dampen the expression of pro-inflammatory IL-8 and TNF-α in polarised T84 cells by increasing the expression of immunomodulatory microRNA (Bitar *et al.*, 2019). To test whether EHEC OMVs elicit an immune response in T84 cells, purified OMVs (using density gradient centrifugation) need to be used in order to exclude the effect of soluble LPS and flagella. After host incubation with OMVs, cell medium can be collected and cytokines can be quantified using ELISAs.

In this investigation, OMVs from non-Stx producing EHEC were demonstrated to translocate across polarised Caco-2 cells and colonoids. The precise route of transcellular trafficking has not been elucidated but it is speculated that recycling endosomes may be involved as they offer transcellular trafficking of toxins and antibodies (Müller *et al.*, 2017, Garcia-Castillo *et al.*, 2017, Saslowsky *et al.*, 2013, Brown *et al.*, 2000). To elucidate whether OMVs are trafficked via recycling endosomes, Transwell experiments similar to those in this investigation can be carried out. After different incubation periods, monolayer immunostaining for recycling endosome markers using Rab11 and OMV-LPS antibody should be made, in order to evaluate colocalisation through florescence microscopy.

In this study, widefield and confocal microscopy was utilised to determine the intracellular trafficking of EHEC OMVs and OMV-associated Stx. Even though colocalisation was quantified, the rate of overlap between different organelles (such as the Golgi apparatus and the ER) was not examined. It may be possible that colocalisation may be overemphasised due to the possibility of organelle overlap. Thus, the overlap between such organelles should be examined. Furthermore, in order to confirm the intracellular trafficking routes stated in this study, super-resolution microscopy could be applied as such microscopes have a higher resolution than the microscopes used in this study, thus giving detailed and clearer images.

It would also be of interest to examine the effect OMVs produced by Stx-producing EHEC strains would have on polarised monolayers. Investigations have shown that following internalisation of OMVs containing Stx, cell death occurs in Gb3 positive cells. Since Caco-2 cells express Gb3, it is possible that OMVs from Stx-producing EHEC strains will cause cell death and comprise the integrity of the cell barrier. As Gb3 is likely not expressed in the colon, the outcome of this experiment may be disputed (Schuller *et al*., 2004). The colonoid model may be a better model to elucidate the effects of OMV-associated Stx on the integrity of the colonic epithelium and to determine whether Stx disassociates from OMVs or whether Stxs are translocated with OMVs. Thus far it is not known whether colonocytes in colonoids express Gb3, therefore this would need to be elucidated in order to understand the possible outcomes of such experiments.

The ability of OMVs to damage renal cells has been demonstrated in this study. Indeed, it is likely that OMVs may damage Gb3-expressing endothelial cells, but it is not known whether OMVs can reach the kidneys. Intraperitoneal injected EHEC OMVs can cause HUS-like disease including kidney damage in mice, thus suggesting OMVs spread in host (Kim *et al*., 2011). The distribution of orally administrated OMVs isolated from *B. thetaiotaomicron* has also been demonstrated in mice (Jones *et al*., 2020). In Jones *et al*. (2020), after the administration of lipophilic-dyed OMVs, OMVs were detected in various organs such as the liver by excising organs and measuring fluorescence. By carrying out similar studies, results can be indicative of whether OMVs can distribute throughout the body.

5.3 Summary

This PhD project has demonstrated that different colonic conditions can affect EHEC OMV vesiculation in different ways. Abiotic conditions of the colonic milieu replicated by SCEM increase OMV vesiculation with bile salts further augmenting vesiculation. In contrast, the presence of colonic relevant levels of CO_2 and human cells resulted

in no significant changes. This project has also demonstrated that non-polarised and polarised Caco-2 cell monolayers and two-dimensional colonoids can internalise EHEC OMVs. Moreover, using polarised Caco-2 cells and colonoids, it was elucidated that OMVs can cross epithelial barriers via a transcellular route. This suggests that during infection, EHEC OMVs can cross the colonic epithelium and enter the vascular system. The cytotoxic ability of OMV-associated Stx2 was also verified using renal cells, therefore underlining the possible contribution of OMVs in the development of HUS.

References

ABDALHAMID, B., MCCUTCHEN, E. L., BOUSKA, A. C., WEIWEI, Z., LOECK, B., HINRICHS, S. H. & IWEN, P. C. 2019. Whole genome sequencing to characterize shiga toxin-producing *Escherichia coli* O26 in a public health setting. *J Infect Public Health*, 12, 884-889.

ABE, H., TATSUNO, I., TOBE, T., OKUTANI, A. & SASAKAWA, C. 2002. Bicarbonate ion stimulates the expression of locus of enterocyte effacement-encoded genes in enterohemorrhagic *Escherichia coli* O157:H7. *Infect Immun,* 70**,** 3500-9.

ACKERS, M. L., MAHON, B. E., LEAHY, E., GOODE, B., DAMROW, T., HAYES, P. S., BIBB, W. F., RICE, D. H., BARRETT, T. J., HUTWAGNER, L., GRIFFIN, P. M. & SLUTSKER, L. 1998. An outbreak of *Escherichia coli* O157:H7 infections associated with leaf lettuce consumption. *J Infect Dis,* 177**,** 1588-93.

ADLERBERTH, I. & WOLD, A. E. 2009. Establishment of the gut microbiota in Western infants. *Acta Paediatr*, 98, 229-38.

AERTSEN, A., FASTER, D. & MICHIELS, C. W. 2005. Induction of Shiga toxin-converting prophage in *Escherichia coli* by high hydrostatic pressure. *Appl Environ Microbiol,* 71**,** 1155-62.

AFOSHIN, A. S., KUDRYAKOVA, I. V., BOROVIKOVA, A. O., SUZINA, N. E., TOROPYGIN, I. Y., SHISHKOVA, N. A. & VASILYEVA, N. V. 2020. Lytic potential of *Lysobacter capsici* VKM B-2533(T): bacteriolytic enzymes and outer membrane vesicles. *Sci Rep,* 10**,** 9944.

AGGER, M., SCHEUTZ, F., VILLUMSEN, S., MOLBAK, K. & PETERSEN, A. M. 2015. Antibiotic treatment of verocytotoxin-producing *Escherichia coli* (VTEC) infection: a systematic review and a proposal. *J Antimicrob Chemother*, 70, 2440-6

AGIN, T. S., CANTEY, J. R., BOEDEKER, E. C. & WOLF, M. K. 1996. Characterization of the eaeA gene from rabbit enteropathogenic *Escherichia coli* strain RDEC-1 and comparison to other eaeA genes from bacteria that cause attaching-effacing lesions. *FEMS Microbiol Lett,* 144**,** 249-58.

ALBENBERG, L., ESIPOVA, T. V., JUDGE, C. P., BITTINGER, K., CHEN, J., LAUGHLIN, A., GRUNBERG, S., BALDASSANO, R. N., LEWIS, J. D., LI, H., THOM, S. R., BUSHMAN, F. D., VINOGRADOV, S. A. & WU, G. D. 2014. Correlation between intraluminal oxygen gradient and radial partitioning of intestinal microbiota. *Gastroenterology,* 147**,** 1055-63 e8.

ALBRIGHT, F. R., WHITE, D. A. & LENNARZ, W. J. 1973. Studies on enzymes involved in the catabolism of phospholipids in *Escherichia coli*. *J Biol Chem,* 248**,** 3968-77.

ALEXEEVA, S., HELLINGWERF, K. J. & TEIXEIRA DE MATTOS, M. J. 2003. Requirement of ArcA for redox regulation in *Escherichia coli* under microaerobic but not anaerobic or aerobic conditions. *J Bacteriol,* 185**,** 204-9.

ALLFORD, S. L., HUNT, B. J., ROSE, P. & MACHIN, S. J. 2003. Guidelines on the diagnosis and management of the thrombotic microangiopathic haemolytic anaemias. *Br J Haematol*, 120, 556-73.

ALTO, N. M., WEFLEN, A. W., RARDIN, M. J., YARAR, D., LAZAR, C. S., TONIKIAN, R., KOLLER, A., TAYLOR, S. S., BOONE, C., SIDHU, S. S., SCHMID, S. L., HECHT, G.

A. & DIXON, J. E. 2007. The type III effector EspF coordinates membrane trafficking by the spatiotemporal activation of two eukaryotic signaling pathways. *J Cell Biol,* 178**,** 1265-78.

ALVAREZ, C. S., BADIA, J., BOSCH, M., GIMÉNEZ, R. & BALDOMÀ, L. 2016. Outer Membrane Vesicles and Soluble Factors Released by Probiotic *Escherichia coli* Nissle 1917 and Commensal ECOR63 Enhance Barrier Function by Regulating Expression of Tight Junction Proteins in Intestinal Epithelial Cells. *Front Microbiol,* 7**,** 1981.

ALVAREZ, C. S., GIMÉNEZ, R., CAÑAS, M. A., VERA, R., DÍAZ-GARRIDO, N., BADIA, J. & BALDOMÀ, L. 2019. Extracellular vesicles and soluble factors secreted by *Escherichia coli* Nissle 1917 and ECOR63 protect against enteropathogenic *E. coli*-induced intestinal epithelial barrier dysfunction. *BMC Microbiol,* 19**,** 166.

ANDERSON, M., JAYKUS, L.-A., BEAULIEU, S. & DENNIS, S. 2011. Pathogen-produce pair attribution risk ranking tool to prioritize fresh produce commodity and pathogen combinations for further evaluation (P3ARRT). *Food Control,* 22**,** 1865-1872.

ANDO, H., ABE, H., SUGIMOTO, N. & TOBE, T. 2007. Maturation of functional type III secretion machinery by activation of anaerobic respiration in enterohaemorrhagic *Escherichia coli*. *Microbiology (Reading),* 153**,** 464-473.

ARBELOA, A., BULGIN, R. R., MACKENZIE, G., SHAW, R. K., PALLEN, M. J., CREPIN, V. F., BERGER, C. N. & FRANKEL, G. 2008. Subversion of actin dynamics by EspM effectors of attaching and effacing bacterial pathogens. *Cell Microbiol,* 10**,** 1429-41.

ARENAS-HERNANDEZ, M. M., ROJAS-LOPEZ, M., MEDRANO-LOPEZ, A., NUNEZ-REZA, K. J., PUENTE, J. L., MARTINEZ-LAGUNA, Y. & TORRES, A. G. 2014. Environmental regulation of the long polar fimbriae 2 of enterohemorrhagic *Escherichia coli* O157:H7. *FEMS Microbiol Lett,* 357**,** 105-14.

ARMSTRONG, G. L., HOLLINGSWORTH, J. & MORRIS, J. G., JR. 1996. Emerging foodborne pathogens: *Escherichia coli* O157:H7 as a model of entry of a new pathogen into the food supply of the developed world. *Epidemiol Rev,* 18**,** 29-51.

ARVIDSSON, I., STÅHL, A. L., HEDSTRÖM, M. M., KRISTOFFERSSON, A. C., RYLANDER, C., WESTMAN, J. S., STORRY, J. R., OLSSON, M. L. & KARPMAN, D. 2015. Shiga toxin-induced complement-mediated hemolysis and release of complement-coated red blood cell-derived microvesicles in hemolytic uremic syndrome. *J Immunol*, 194, 2309-18.

ASCHTGEN, M. S., LYNCH, J. B., KOCH, E., SCHWARTZMAN, J., MCFALL-NGAI, M. & RUBY, E. 2016. Rotation of *Vibrio fischeri* Flagella Produces Outer Membrane Vesicles That Induce Host Development. *J Bacteriol,* 198**,** 2156-65.

AUGUSTYNIAK, D., SEREDYŃSKI, R., MCCLEAN, S., ROSZKOWIAK, J., ROSZNIOWSKI, B., SMITH, D. L., DRULIS-KAWA, Z. & MACKIEWICZ, P. 2018. Virulence factors of *Moraxella catarrhalis* outer membrane vesicles are major targets for cross-reactive antibodies and have adapted during evolution. *Sci Rep,* 8**,** 4955.

BAI, L., SCHÜLLER, S., WHALE, A., MOUSNIER, A., MARCHES, O., WANG, L., OOKA, T., HEUSCHKEL, R., TORRENTE, F., KAPER, J. B., GOMES, T. A., XU, J., PHILLIPS, A. D. & FRANKEL, G. 2008. Enteropathogenic *Escherichia coli* O125:H6 triggers

attaching and effacing lesions on human intestinal biopsy specimens independently of Nck and TccP/TccP2. *Infect Immun,* 76**,** 361-8.

BARLOW, R. S., GOBIUS, K. S. & DESMARCHELIER, P. M. 2006. Shiga toxin-producing *Escherichia coli* in ground beef and lamb cuts: results of a one-year study. *Int J Food Microbiol*, 111, 1-5.

BASU, D., LI, X. P., KAHN, J. N., MAY, K. L., KAHN, P. C. & TUMER, N. E. 2016. The A1 Subunit of Shiga Toxin 2 Has Higher Affinity for Ribosomes and Higher Catalytic Activity than the A1 Subunit of Shiga Toxin 1. *Infect Immun,* 84**,** 149-61.

BAUMAN, S. J. & KUEHN, M. J. 2006. Purification of outer membrane vesicles from *Pseudomonas aeruginosa* and their activation of an IL-8 response. *Microbes Infect,* 8**,** 2400-8.

BAUMGARTEN, T., SPERLING, S., SEIFERT, J., VON BERGEN, M., STEINIGER, F., WICK, L. Y. & HEIPIEPER, H. J. 2012. Membrane vesicle formation as a multiple-stress response mechanism enhances *Pseudomonas putida* DOT-T1E cell surface hydrophobicity and biofilm formation. *Appl Environ Microbiol,* 78**,** 6217-24.

BAUWENS, A., KUNSMANN, L., KARCH, H., MELLMANN, A. & BIELASZEWSKA, M. 2017a. Antibiotic-Mediated Modulations of Outer Membrane Vesicles in Enterohemorrhagic *Escherichia coli* O104:H4 and O157:H7. *Antimicrob Agents Chemother,* 61.

BAUWENS, A., KUNSMANN, L., MAREJKOVA, M., ZHANG, W., KARCH, H., BIELASZEWSKA, M. & MELLMANN, A. 2017b. Intrahost milieu modulates production of outer membrane vesicles, vesicle-associated Shiga toxin 2a and cytotoxicity in *Escherichia coli* O157:H7 and O104:H4. *Environ Microbiol Rep,* 9**,** 626-634.

BEGLEY, M., GAHAN, C. G. & HILL, C. 2005. The interaction between bacteria and bile. *FEMS Microbiol Rev,* 29**,** 625-51.

BENJAMIN, M. M. & DATTA, A. R. 1995. Acid tolerance of enterohemorrhagic *Escherichia coli*. *Appl Environ Microbiol,* 61**,** 1669-72.

BENTANCOR, L. V., BILEN, M., BRANDO, R. J., RAMOS, M. V., FERREIRA, L. C., GHIRINGHELLI, P. D. & PALERMO, M. S. 2009. A DNA vaccine encoding the enterohemorragic *Escherichia coli* Shiga-like toxin 2 A2 and B subunits confers protective immunity to Shiga toxin challenge in the murine model. *Clin Vaccine Immunol,* 16**,** 712-8.

BERG, R. 1996. The indigenous gastrointestinal microflora. *Trends in Microbiology,* 4, 430-435.

BERGAN, J., DYVE LINGELEM, SU., SANDVIG, K. 2012. Shiga toxins. *Toxicon,* 60, 1085-1107.

BERNADAC, A., GAVIOLI, M., LAZZARONI, J. C., RAINA, S. & LLOUBES, R. 1998. *Escherichia coli* tol-pal mutants form outer membrane vesicles. *J Bacteriol,* 180**,** 4872-8.

BERNEDO-NAVARRO, R. A., MIYACHIRO, M. M., DA SILVA, M. J., REIS, C. F., CONCEICAO, R. A., GATTI, M. S. & YANO, T. 2014. Peptides derived from phage display libraries as potential neutralizers of Shiga toxin-induced cytotoxicity *in vitro* and *in vivo*. *J Appl Microbiol,* 116**,** 1322-33.

BERNET-CAMARD, M. F., COCONNIER, M. H., HUDAULT, S. & SERVIN, A. L. 1996. Differential expression of complement proteins and regulatory decay

accelerating factor in relation to differentiation of cultured human colon adenocarcinoma cell lines. *Gut,* 38**,** 248-53.

BERTIN, Y., GIRARDEAU, J. P., CHAUCHEYRAS-DURAND, F., LYAN, B., PUJOS-GUILLOT, E., HAREL, J. & MARTIN, C. 2011. Enterohaemorrhagic *Escherichia coli* gains a competitive advantage by using ethanolamine as a nitrogen source in the bovine intestinal content. *Environ Microbiol,* 13**,** 365-77.

BEUMER, R. R., DE VRIES, J. & ROMBOUTS, F. M. 1992. *Campylobacter jejuni* non-culturable coccoid cells. *Int J Food Microbiol,* 15, 153-63.

BEVERIDGE, T. J. 1999. Structures of gram-negative cell walls and their derived membrane vesicles. *J Bacteriol,* 181**,** 4725-33.

BIELASZEWSKA, M., DANIEL, O., KARCH, H. & MELLMANN, A. 2020. Dissemination of the blaCTX-M-15 gene among Enterobacteriaceae via outer membrane vesicles. *J Antimicrob Chemother,* 75, 2442-51.

BIELASZEWSKA, M. & KARCH, H. 2005. Consequences of enterohaemorrhagic *Escherichia coli* infection for the vascular endothelium. *Thromb Haemost,* 94, 312-8.

BIELASZEWSKA, M., MAREJKOVA, M., BAUWENS, A., KUNSMANN-PROKSCHA, L., MELLMANN, A. & KARCH, H. 2018. Enterohemorrhagic *Escherichia coli* O157 outer membrane vesicles induce interleukin 8 production in human intestinal epithelial cells by signaling via Toll-like receptors TLR4 and TLR5 and activation of the nuclear factor NF-kappaB. *Int J Med Microbiol,* 308**,** 882-889.

BIELASZEWSKA, M., RÜTER, C., BAUWENS, A., GREUNE, L., JAROSCH, K.-A., STEIL, D., ZHANG, W., HE, X., LLOUBES, R., FRUTH, A., KIM, K. S., SCHMIDT, M. A., DOBRINDT, U., MELLMANN, A. & KARCH, H. 2017. Host cell interactions of outer membrane vesicle-associated virulence factors of enterohemorrhagic *Escherichia coli* O157: Intracellular delivery, trafficking and mechanisms of cell injury. *PLOS Pathogens,* 13**,** e1006159.

BIELASZEWSKA, M., RÜTER, C., KUNSMANN, L., GREUNE, L., BAUWENS, A., ZHANG, W., KUCZIUS, T., KIM, K. S., MELLMANN, A., SCHMIDT, M. A. & KARCH, H. 2013. Enterohemorrhagic *Escherichia coli* Hemolysin Employs Outer Membrane Vesicles to Target Mitochondria and Cause Endothelial and Epithelial Apoptosis. *PLOS Pathogens,* 9**,** e1003797.

BISHOP, D. G. & WORK, E. 1965. An extracellular glycolipid produced by *Escherichia coli* grown under lysine-limiting conditions. *Biochemical Journal,* 96**,** 567-576.

BITAR, A., AUNG, K. M., WAI, S. N. & HAMMARSTROM, M. L. 2019. *Vibrio cholerae* derived outer membrane vesicles modulate the inflammatory response of human intestinal epithelial cells by inducing microRNA-146a. *Sci Rep,* 9**,** 7212.

BITZAN, M., RICHARDSON, S., HUANG, C., BOYD, B., PETRIC, M. & KARMALI, M. A. 1994. Evidence that verotoxins (Shiga-like toxins) from *Escherichia coli* bind to P blood group antigens of human erythrocytes in vitro. *Infect Immun,* 62**,** 3337-47.

BLACHIER, F., BOUTRY, C., BOS, C. & TOMÉ, D. 2009. Metabolism and functions of L-glutamate in the epithelial cells of the small and large intestines. *Am J Clin Nutr,* 90, 814S-821S.

BOLTE, S. & CORDELIÈRES, F. P. 2006. A guided tour into subcellular colocalization analysis in light microscopy. *J Microsc,* 224, 213-32.

BOMBERGER, J. M., MACEACHRAN, D. P., COUTERMARSH, B. A., YE, S., O'TOOLE, G. A. & STANTON, B. A. 2009. Long-distance delivery of bacterial virulence factors by *Pseudomonas aeruginosa* outer membrane vesicles. *PLoS Pathog,* 5**,** e1000382.

BONNINGTON, K. E. & KUEHN, M. J. 2016. Outer Membrane Vesicle Production Facilitates LPS Remodeling and Outer Membrane Maintenance in *Salmonella* during Environmental Transitions. *mBio,* 7.

BRADFORD, M. M. 1976. A rapid and sensitive method for the quantitation of microgram quantities of protein utilizing the principle of protein-dye binding. *Anal Biochem,* 72, 248-54.

BRAMEYER, S., PLENER, L., MULLER, A., KLINGL, A., WANNER, G. & JUNG, K. 2018. Outer Membrane Vesicles Facilitate Trafficking of the Hydrophobic Signaling Molecule CAI-1 between *Vibrio harveyi* Cells. *J Bacteriol,* 200, e00740-17.

BRAUN, V. & BOSCH, V. 1972. Sequence of the murein-lipoprotein and the attachment site of the lipid. *Eur J Biochem,* 28**,** 51-69.

BRAUN, V. & SIEGLIN, U. 1970. The covalent murein-lipoprotein structure of the *Escherichia coli* cell wall. The attachment site of the lipoprotein on the murein. *Eur J Biochem,* 13**,** 336-46.

BRAY, J. 1945. Isolation of antigenically homogeneous strains of *Bact. coli neapolitanum* from summer diarrhœa of infants. *The Journal of Pathology and Bacteriology,* 57**,** 239-247.

BRAY, J. & BEAVAN, T. E. D. 1948. Slide agglutination of *Bacterium coli* var. *neapolitanum* in summer diarrhæa. *The Journal of Pathology and Bacteriology,* 60**,** 395-401.

BRENNAN, C. A., HUNT, J. R., KREMER, N., KRASITY, B. C., APICELLA, M. A., MCFALL-NGAI, M. J. & RUBY, E. G. 2014. A model symbiosis reveals a role for sheathed-flagellum rotation in the release of immunogenic lipopolysaccharide. *Elife,* 3**,** e01579.

BRIGOTTI, M., CAPRIOLI, A., TOZZI, A. E., TAZZARI, P. L., RICCI, F., CONTE, R., CARNICELLI, D., PROCACCINO, M. A., MINELLI, F., FERRETTI, A. V., PAGLIALONGA, F., EDEFONTI, A. & RIZZONI, G. 2006. Shiga toxins present in the gut and in the polymorphonuclear leukocytes circulating in the blood of children with hemolytic-uremic syndrome. *J Clin Microbiol,* 44**,** 313-7.

BRIGOTTI, M., CARNICELLI, D., ARFILLI, V., PORCELLINI, E., GALASSI, E., VALERII, M. C. & SPISNI, E. 2018. Human monocytes stimulated by Shiga toxin 1a via globotriaosylceramide release proinflammatory molecules associated with hemolytic uremic syndrome. *Int J Med Microbiol,* 308, 940-946.

BRIGOTTI, M., CARNICELLI, D., ARFILLI, V., TAMASSIA, N., BORSETTI, F., FABBRI, E., TAZZARI, P. L., RICCI, F., PAGLIARO, P., SPISNI, E. & CASSATELLA, M. A. 2013. Identification of TLR4 as the receptor that recognizes Shiga toxins in human neutrophils. *J Immunol,* 191**,** 4748-58.

BRIGOTTI, M., ORTH-HÖLLER, D., CARNICELLI, D., PORCELLINI, E., GALASSI, E., TAZZARI, P. L., RICCI, F., MANOLI, F., MANET, I., TALASZ, H., LINDNER, H. H., SPETH, C., ERBEZNIK, T., FUCHS, S., POSCH, W., CHATTERJEE, S. & WÜRZNER, R. 2019. The structure of the Shiga toxin 2a A-subunit dictates the interactions of the toxin with blood components. *Cell Microbiol,* 21**,** e13000.

BRIGOTTI, M., TAZZARI, P. L., RAVANELLI, E., CARNICELLI, D., ROCCHI, L., ARFILLI, V., SCAVIA, G., MINELLI, F., RICCI, F., PAGLIARO, P., FERRETTI, A. V., PECORARO, C., PAGLIALONGA, F., EDEFONTI, A., PROCACCINO, M. A., TOZZI, A. E. & CAPRIOLI, A. 2011. Clinical relevance of shiga toxin concentrations in the blood of patients with hemolytic uremic syndrome. *Pediatr Infect Dis J,* 30**,** 486-90.

BROESDER, A., WOERDENBAG, H. J., PRINS, G. H., NGUYEN, D. N., FRIJLINK, H. W. & HINRICHS, W. L. J. 2020. pH-dependent ileocolonic drug delivery, part I: *in vitro* and clinical evaluation of novel systems. *Drug Discov Today,* 25, 1362-73.

BROOKS, J. T., SOWERS, E. G., WELLS, J. G., GREENE, K. D., GRIFFIN, P. M., HOEKSTRA, R. M. & STROCKBINE, N. A. 2005. Non-O157 Shiga toxin-producing *Escherichia coli* infections in the United States, 1983-2002. *J Infect Dis,* 192, 1422-9.

BROWN, L., WOLF, J. M., PRADOS-ROSALES, R. & CASADEVALL, A. 2015. Through the wall: extracellular vesicles in Gram-positive bacteria, mycobacteria and fungi. *Nature reviews. Microbiology,* 13**,** 620-630.

BROWN, P. S., WANG, E., AROETI, B., CHAPIN, S. J., MOSTOV, K. E. & DUNN, K. W. 2000. Definition of distinct compartments in polarized Madin-Darby canine kidney (MDCK) cells for membrane-volume sorting, polarized sorting and apical recycling. *Traffic,* 1, 124-40.

BRUNDER, W., SCHMIDT, H. & KARCH, H. 1996. KatP, a novel catalase-peroxidase encoded by the large plasmid of enterohaemorrhagic *Escherichia coli* O157:H7. *Microbiology,* 142 (Pt 11)**,** 3305-15.

BURLAND, V., SHAO, Y., PERNA, N. T., PLUNKETT, G., SOFIA, H. J. & BLATTNER, F. R. 1998. The complete DNA sequence and analysis of the large virulence plasmid of *Escherichia coli* O157:H7. *Nucleic Acids Res,* 26**,** 4196-204.

BUSTOS, A. Y., SAAVEDRA, L., DE VALDEZ, G. F., RAYA, R. R. & TARANTO, M. P. 2012. Relationship between bile salt hydrolase activity, changes in the internal pH and tolerance to bile acids in lactic acid bacteria. *Biotechnol Lett,* 34**,** 1511-8.

BYRNE, L., JENKINS, C., LAUNDERS, N., ELSON, R. & ADAK, G. K. 2015. The epidemiology, microbiology and clinical impact of Shiga toxin-producing *Escherichia coli* in England, 2009-2012. *Epidemiol Infect,* 143, 3475-87.

BYRNE, L., VANSTONE, G. L., PERRY, N. T., LAUNDERS, N., ADAK, G. K., GODBOLE, G., GRANT, K. A., SMITH, R. & JENKINS, C. 2014. Epidemiology and microbiology of Shiga toxin-producing *Escherichia coli* other than serogroup O157 in England, 2009-2013. *J Med Microbiol,* 63**,** 1181-8.

CAI, K., TU, W., LIU, Y., LI, T. & WANG, H. 2015. Novel fusion antigen displayed-bacterial ghosts vaccine candidate against infection of *Escherichia coli* O157:H7. *Sci Rep,* 5**,** 17479.

CALDERWOOD, S. B., AUCLAIR, F., DONOHUE-ROLFE, A., KEUSCH, G. T. & MEKALANOS, J. J. 1987. Nucleotide sequence of the Shiga-like toxin genes of *Escherichia coli*. *Proc Natl Acad Sci U S A,* 84**,** 4364-8.

CAMERON, P., SMITH, S. J., GIEMBYCZ, M. A., ROTONDO, D. & PLEVIN, R. 2003. Verotoxin activates mitogen-activated protein kinase in human peripheral blood monocytes: role in apoptosis and proinflammatory cytokine release. *Br J Pharmacol,* 140**,** 1320-30.

CAMPELLONE, K. G., GIESE, A., TIPPER, D. J. & LEONG, J. M. 2002. A tyrosine-phosphorylated 12-amino-acid sequence of enteropathogenic *Escherichia coli* Tir binds the host adaptor protein Nck and is required for Nck localization to actin pedestals. *Mol Microbiol,* 43, 1227-41.

CAMPELLONE, K. G., ROBBINS, D. & LEONG, J. M. 2004. EspFU is a translocated EHEC effector that interacts with Tir and N-WASP and promotes Nck-independent actin assembly. *Dev Cell,* 7**,** 217-28.

CAPASSO, C. & SUPURAN, C. T. 2015. An overview of the alpha-, beta- and gamma-carbonic anhydrases from Bacteria: can bacterial carbonic anhydrases shed new light on evolution of bacteria? *J Enzyme Inhib Med Chem,* 30**,** 325-32.

CARLSON-BANNING, K. M. & SPERANDIO, V. 2016. Catabolite and Oxygen Regulation of Enterohemorrhagic *Escherichia coli* Virulence. *mBio,* 7, e01852-16.

CASCALES, E., BERNADAC, A., GAVIOLI, M., LAZZARONI, J. C. & LLOUBES, R. 2002. Pal lipoprotein of *Escherichia coli* plays a major role in outer membrane integrity. *J Bacteriol,* 184**,** 754-9.

CASTANIE-CORNET, M. P., PENFOUND, T. A., SMITH, D., ELLIOTT, J. F. & FOSTER, J. W. 1999. Control of acid resistance in *Escherichia coli*. *J Bacteriol,* 181**,** 3525-35.

CAÑAS, M. A., GIMÉNEZ, R., FÁBREGA, M. J., TOLOZA, L., BALDOMÀ, L. & BADIA, J. 2016. Outer Membrane Vesicles from the Probiotic *Escherichia coli* Nissle 1917 and the Commensal ECOR12 Enter Intestinal Epithelial Cells via Clathrin-Dependent Endocytosis and Elicit Differential Effects on DNA Damage. *PLoS One,* 11**,** e0160374.

CECIL, J. D., O'BRIEN-SIMPSON, N. M., LENZO, J. C., HOLDEN, J. A., CHEN, Y. Y., SINGLETON, W., GAUSE, K. T., YAN, Y., CARUSO, F. & REYNOLDS, E. C. 2016. Differential Responses of Pattern Recognition Receptors to Outer Membrane Vesicles of Three Periodontal Pathogens. *PLoS One,* 11**,** e0151967.

CHAISRI, U., NAGATA, M., KURAZONO, H., HORIE, H., TONGTAWE, P., HAYASHI, H., WATANABE, T., TAPCHAISRI, P., CHONGSA-NGUAN, M. & CHAICUMPA, W. 2001. Localization of Shiga toxins of enterohaemorrhagic *Escherichia coli* in kidneys of paediatric and geriatric patients with fatal haemolytic uraemic syndrome. *Microb Pathog,* 31**,** 59-67.

CHANG, D. E., SMALLEY, D. J., TUCKER, D. L., LEATHAM, M. P., NORRIS, W. E., STEVENSON, S. J., ANDERSON, A. B., GRISSOM, J. E., LAUX, D. C., COHEN, P. S. & CONWAY, T. 2004. Carbon nutrition of *Escherichia coli* in the mouse intestine. *Proc Natl Acad Sci U S A,* 101**,** 7427-32.

CHAPMAN, P. A., CERDAN MALO, A. T., ELLIN, M., ASHTON, R. & HARKIN 2001. *Escherichia coli* O157 in cattle and sheep at slaughter, on beef and lamb carcasses and in raw beef and lamb products in South Yorkshire, UK. *Int J Food Microbiol,* 64, 139-50.

CHAPMAN, P. A., SIDDONS, C. A., CERDAN MALO, A. T. & HARKIN, M. A. 2000. A one year study of *Escherichia coli* O157 in raw beef and lamb products. *Epidemiol Infect,* 124**,** 207-13.

CHATTERJEE, D. & CHAUDHURI, K. 2011. Association of cholera toxin with *Vibrio cholerae* outer membrane vesicles which are internalized by human intestinal epithelial cells. *FEBS Lett,* 585**,** 1357-62.

CHERLA, R. P., LEE, S. Y., MEES, P. L. & TESH, V. L. 2006. Shiga toxin 1-induced cytokine production is mediated by MAP kinase pathways and translation initiation factor eIF4E in the macrophage-like THP-1 cell line. *J Leukoc Biol,* 79, 397-407.

CHIANG, J. Y. 2013. Bile acid metabolism and signaling. *Compr Physiol,* 3**,** 1191-212.

CHOI, C. W., PARK, E. C., YUN, S. H., LEE, S. Y., LEE, Y. G., HONG, Y., PARK, K. R., KIM, S. H., KIM, G. H. & KIM, S. I. 2014. Proteomic characterization of the outer membrane vesicle of Pseudomonas putida KT2440. *J Proteome Res,* 13**,** 4298-309.

CHONG, Y., FITZHENRY, R., HEUSCHKEL, R., TORRENTE, F., FRANKEL, G. & PHILLIPS, A. D. 2007. Human intestinal tissue tropism in *Escherichia coli* O157 : H7--initial colonization of terminal ileum and Peyer's patches and minimal colonic adhesion *ex vivo*. *Microbiology,* 153**,** 794-802.

CHUTKAN, H., MACDONALD, I., MANNING, A. & KUEHN, M. J. 2013. Quantitative and qualitative preparations of bacterial outer membrane vesicles. *Methods Mol Biol,* 966**,** 259-72.

CIOFU, O., BEVERIDGE, T. J., KADURUGAMUWA, J., WALTHER-RASMUSSEN, J. & HØIBY, N. 2000. Chromosomal beta-lactamase is packaged into membrane vesicles and secreted from *Pseudomonas aeruginosa*. *J Antimicrob Chemother,* 45**,** 9-13.

CLEVERS, H. 2013. The intestinal crypt, a prototype stem cell compartment. *Cell,* 154, 274-84.

COBBOLD, R. N., HANCOCK, D. D., RICE, D. H., BERG, J., STILBORN, R., HOVDE, C. J. & BESSER, T. E. 2007. Rectoanal junction colonization of feedlot cattle by *Escherichia coli* O157:H7 and its association with supershedders and excretion dynamics. *Appl Environ Microbiol,* 73**,** 1563-8.

CODEX ALIMENTARIUS COMMISSION. 2015. Report of the 47th Session of the Codex Committee on Food Hygiene. Rep 16/FH: Available at: http://www.fao.org/fao-who-codexalimentarius/meetings/detail/en/?meeting=CCFH&session=47.

CODY, S. H., GLYNN, M. K., FARRAR, J. A., CAIRNS, K. L., GRIFFIN, P. M., KOBAYASHI, J., FYFE, M., HOFFMAN, R., KING, A. S., LEWIS, J. H., SWAMINATHAN, B., BRYANT, R. G. & VUGIA, D. J. 1999. An outbreak of *Escherichia coli* O157:H7 infection from unpasteurized commercial apple juice. *Ann Intern Med,* 130**,** 202-9.

CONWAY, T. & COHEN, P. S. 2015. Commensal and Pathogenic *Escherichia coli* Metabolism in the Gut. *Microbiol Spectr,* 3.

COWDEN, J. M., AHMED, S., DONAGHY, M. & RILEY, A. 2001. Epidemiological investigation of the central Scotland outbreak of *Escherichia coli* O157 infection, November to December 1996. *Epidemiol Infect,* 126**,** 335-41.

CRAMM-BEHRENS, C. I., DIENST, M. & JACOB, R. 2008. Apical cargo traverses endosomal compartments on the passage to the cell surface. *Traffic.* England.

CROXEN, M. A. & FINLAY, B. B. 2010. Molecular mechanisms of *Escherichia coli* pathogenicity. *Nat Rev Microbiol,* 8, 26-38.

CROXEN, M. A., LAW, R. J., SCHOLZ, R., KEENEY, K. M., WLODARSKA, M. & FINLAY, B. B. 2013. Recent advances in understanding enteric pathogenic *Escherichia coli*. *Clin Microbiol Rev,* 26**,** 822-80.

DALLMAN, T. J., ASHTON, P. M., BYRNE, L., PERRY, N. T., PETROVSKA, L., ELLIS, R., ALLISON, L., HANSON, M., HOLMES, A., GUNN, G. J., CHASE-TOPPING, M. E., WOOLHOUSE, M. E. J., GRANT, K. A., GALLY, D. L., WAIN, J. & JENKINS, C. 2015. Applying phylogenomics to understand the emergence of Shiga-toxin-producing *Escherichia coli* O157:H7 strains causing severe human disease in the UK. *Microbial Genomics,* 1**,** e000029.

DAVIES, C., TAYLOR, A. J., ELMI, A., WINTER, J., LIAW, J., GRABOWSKA, A. D., GUNDOGDU, O., WREN, B. W., KELLY, D. J. & DORRELL, N. 2019. Sodium Taurocholate Stimulates *Campylobacter jejuni* Outer Membrane Vesicle Production via Down-Regulation of the Maintenance of Lipid Asymmetry Pathway. *Front Cell Infect Microbiol,* 9**,** 177.

DE BIASE, D., TRAMONTI, A., BOSSA, F. & VISCA, P. 1999. The response to stationary-phase stress conditions in *Escherichia coli*: role and regulation of the glutamic acid decarboxylase system. *Mol Microbiol,* 32, 1198-211.

DEAN-NYSTROM, E. A., BOSWORTH, B. T., MOON, H. W. & O'BRIEN, A. D. 1998. *Escherichia coli* O157:H7 requires intimin for enteropathogenicity in calves. *Infect Immun,* 66**,** 4560-3.

DEATHERAGE, B. L. & COOKSON, B. T. 2012. Membrane vesicle release in bacteria, eukaryotes, and archaea: a conserved yet underappreciated aspect of microbial life. *Infect Immun,* 80**,** 1948-57.

DEATHERAGE, B. L., LARA, J. C., BERGSBAKEN, T., RASSOULIAN BARRETT, S. L., LARA, S. & COOKSON, B. T. 2009. Biogenesis of bacterial membrane vesicles. *Mol Microbiol,* 72**,** 1395-407.

DEIBEL, C., KRAMER, S., CHAKRABORTY, T. & EBEL, F. 1998. EspE, a novel secreted protein of attaching and effacing bacteria, is directly translocated into infected host cells, where it appears as a tyrosine-phosphorylated 90 kDa protein. *Mol Microbiol,* 28**,** 463-74.

DEN BESTEN, G., VAN EUNEN, K., GROEN, A. K., VENEMA, K., REIJNGOUD, D. J. & BAKKER, B. M. 2013. The role of short-chain fatty acids in the interplay between diet, gut microbiota, and host energy metabolism. *J Lipid Res,* 54**,** 2325-40.

DENG, W., LI, Y., VALLANCE, B. A. & FINLAY, B. B. 2001. Locus of enterocyte effacement from *Citrobacter rodentium*: sequence analysis and evidence for horizontal transfer among attaching and effacing pathogens. *Infect Immun,* 69**,** 6323-35.

DERIU, E., LIU, J. Z., PEZESHKI, M., EDWARDS, R. A., OCHOA, R. J., CONTRERAS, H., LIBBY, S. J., FANG, F. C. & RAFFATELLU, M. 2013. Probiotic bacteria reduce *Salmonella* Typhimurium intestinal colonization by competing for iron. *Cell Host Microbe,* 14**,** 26-37.

DEVINNEY, R., STEIN, M., REINSCHEID, D., ABE, A., RUSCHKOWSKI, S. & FINLAY, B. B. 1999. Enterohemorrhagic *Escherichia coli* O157:H7 produces Tir, which is translocated to the host cell membrane but is not tyrosine phosphorylated. *Infect Immun,* 67**,** 2389-98.

DEVOS, S., VAN PUTTE, W., VITSE, J., VAN DRIESSCHE, G., STREMERSCH, S., VAN DEN BROEK, W., RAEMDONCK, K., BRAECKMANS, K., STAHLBERG, H., KUDRYASHEV, M., SAVVIDES, S. N. & DEVREESE, B. 2017. Membrane vesicle secretion and prophage induction in multidrug-resistant *Stenotrophomonas*

maltophilia in response to ciprofloxacin stress. *Environ Microbiol,* 19**,** 3930-3937.

DEVRIESE, S., VAN DEN BOSSCHE, L., VAN WELDEN, S., HOLVOET, T., PINHEIRO, I., HINDRYCKX, P., DE VOS, M. & LAUKENS, D. 2017. T84 monolayers are superior to Caco-2 as a model system of colonocytes. *Histochem Cell Biol,* 148**,** 85-93.

DIBDEN, D. P. & GREEN, J. 2005. In vivo cycling of the *Escherichia coli* transcription factor FNR between active and inactive states. *Microbiology (Reading),* 151**,** 4063-4070.

DONNENBERG, M. S., YU, J. & KAPER, J. B. 1993. A second chromosomal gene necessary for intimate attachment of enteropathogenic *Escherichia coli* to epithelial cells. *J Bacteriol,* 175**,** 4670-80.

DORWARD, D. W. & GARON, C. F. 1990. DNA Is Packaged within Membrane-Derived Vesicles of Gram-Negative but Not Gram-Positive Bacteria. *Appl Environ Microbiol,* 56**,** 1960-2.

DÉZIEL, E., GOPALAN, S., TAMPAKAKI, A. P., LÉPINE, F., PADFIELD, K. E., SAUCIER, M., XIAO, G. & RAHME, L. G. 2005. The contribution of MvfR to *Pseudomonas aeruginosa* pathogenesis and quorum sensing circuitry regulation: multiple quorum sensing-regulated genes are modulated without affecting *lasRI*, *rhlRI* or the production of N-acyl-L-homoserine lactones. *Mol Microbiol,* 55, 998-1014.

EISENHOFER, G., ANEMAN, A., FRIBERG, P., HOOPER, D., FÅNDRIKS, L., LONROTH, H., HUNYADY, B. & MEZEY, E. 1997. Substantial production of dopamine in the human gastrointestinal tract. *J Clin Endocrinol Metab,* 82**,** 3864-71.

EKLUND, T. 1984. The effect of carbon dioxide on bacterial growth and on uptake processes in bacterial membrane vesicles. *International Journal of Food Microbiology,* 1**,** 179-185.

ELDER, R. O., KEEN, J. E., SIRAGUSA, G. R., BARKOCY-GALLAGHER, G. A., KOOHMARAIE, M. & LAEGREID, W. W. 2000. Correlation of enterohemorrhagic *Escherichia coli* O157 prevalence in feces, hides and carcasses of beef cattle during processing. *Proc Natl Acad Sci U S A,* 97, 2999-3003.

ELLIOTT, S. J., SPERANDIO, V., GIRON, J. A., SHIN, S., MELLIES, J. L., WAINWRIGHT, L., HUTCHESON, S. W., MCDANIEL, T. K. & KAPER, J. B. 2000. The locus of enterocyte effacement (LEE)-encoded regulator controls expression of both LEE- and non-LEE-encoded virulence factors in enteropathogenic and enterohemorrhagic *Escherichia coli*. *Infect Immun,* 68**,** 6115-26.

ELLIS, S. J., CROSSMAN, L. C., MCGRATH, C. J., CHATTAWAY, M. A., HÖLKEN, J. M., BRETT, B., BUNDY, L., KAY, G. L., WAIN, J. & SCHÜLLER, S. 2020. Identification and characterisation of enteroaggregative *Escherichia coli* subtypes associated with human disease. *Sci Rep,* 10**,** 7475.

ELLURI, S., ENOW, C., VDOVIKOVA, S., ROMPIKUNTAL, P. K., DONGRE, M., CARLSSON, S., PAL, A., UHLIN, B. E. & WAI, S. N. 2014. Outer membrane vesicles mediate transport of biologically active *Vibrio cholerae* cytolysin (VCC) from *V. cholerae* strains. *PLoS One,* 9**,** e106731.

ELMI, A., DOREY, A., WATSON, E., JAGATIA, H., INGLIS, N. F., GUNDOGDU, O., BAJAJ-ELLIOTT, M., WREN, B. W., SMITH, D. G. E. & DORRELL, N. 2018. The bile salt sodium taurocholate induces *Campylobacter jejuni* outer membrane vesicle

production and increases OMV-associated proteolytic activity. *Cell Microbiol,* 20.

ELMI, A., NASHER, F., JAGATIA, H., GUNDOGDU, O., BAJAJ-ELLIOTT, M., WREN, B. & DORRELL, N. 2016. *Campylobacter jejuni* outer membrane vesicle-associated proteolytic activity promotes bacterial invasion by mediating cleavage of intestinal epithelial cell E-cadherin and occludin. *Cell Microbiol,* 18**,** 561-72.

ELMI, A., WATSON, E., SANDU, P., GUNDOGDU, O., MILLS, D. C., INGLIS, N. F., MANSON, E., IMRIE, L., BAJAJ-ELLIOTT, M., WREN, B. W., SMITH, D. G. & DORRELL, N. 2012. *Campylobacter jejuni* outer membrane vesicles play an important role in bacterial interactions with human intestinal epithelial cells. *Infect Immun,* 80**,** 4089-98.

ENDO, Y., TSURUGI, K., YUTSUDO, T., TAKEDA, Y., OGASAWARA, T. & IGARASHI, K. 1988. Site of action of a Vero toxin (VT2) from *Escherichia coli* O157:H7 and of Shiga toxin on eukaryotic ribosomes. RNA N-glycosidase activity of the toxins. *Eur J Biochem,* 171**,** 45-50.

ERDEM, A. L., AVELINO, F., XICOHTENCATL-CORTES, J. & GIRÓN, J. A. 2007. Host protein binding and adhesive properties of H6 and H7 flagella of attaching and effacing *Escherichia coli*. *J Bacteriol,* 189**,** 7426-35.

ESCHERICH, T. 1885. Die darmbakterien des neugeborenen und säuglings. *Fortsch der Med* 3**,** 547-554.

EVANS, A. G., DAVEY, H. M., COOKSON, A., CURRINN, H., COOKE-FOX, G., STANCZYK, P. J. & WHITWORTH, D. E. 2012. Predatory activity of *Myxococcus xanthus* outer-membrane vesicles and properties of their hydrolase cargo. *Microbiology,* 158**,** 2742-52.

EUROPEAN CENTRE FOR DISEASE PREVENTION AND CONTROL. 2020. Shiga toxin/ verocytotoxin-producing *Escherichia coli* (STEC/ VTEC) Infection- Annual Epidemiological Report for 2018. Available at: https://www.ecdc.europa.eu/ sites/default/files/documents/shiga-toxin-verocytototoxin-escherichia-coli-annual-epidemiological-report-2018.pdf

EUROPEAN FOOD SAFETY AUTHORITY. 2018. The European Union summary report on trends and sources of zoonoses, zoonotic agents and food-borne outbreaks in 2017. *EFSA Journal.* Available at: https://www.ecdc.europa.eu/ sites/default/files/documents/zoonoese-food-borne-outbreaks-surveillance-2017-updated.pdf

FALGUIERES, T., MALLARD, F., BARON, C., HANAU, D., LINGWOOD, C., GOUD, B., SALAMERO, J. & JOHANNES, L. 2001. Targeting of Shiga toxin B-subunit to retrograde transport route in association with detergent-resistant membranes. *Mol Biol Cell,* 12**,** 2453-68.

FALGUIERES, T., ROMER, W., AMESSOU, M., AFONSO, C., WOLF, C., TABET, J. C., LAMAZE, C. & JOHANNES, L. 2006. Functionally different pools of Shiga toxin receptor, globotriaosyl ceramide, in HeLa cells. *FEBS J,* 273, 5205-18.

FALLINGBORG, J. 1999. Intraluminal pH of the human gastrointestinal tract. *Dan Med Bull,* 46**,** 183-96.

FAN, R., SHAO, K., YANG, X., BAI, X., FU, S., SUN, H., XU, Y., WANG, H., LI, Q., HU, B., ZHANG, J. & XIONG, Y. 2019. High prevalence of non-O157 Shiga toxin-producing *Escherichia coli* in beef cattle detected by combining four selective agars. *BMC Microbiol,* 19**,** 213.

FARFAN, M. J., CANTERO, L., VIDAL, R., BOTKIN, D. J. & TORRES, A. G. 2011. Long Polar Fimbriae of Enterohemorrhagic *Escherichia coli* O157:H7 Bind to Extracellular Matrix Proteins. *Infection and Immunity,* 79**,** 3744-3750.

FARMER, J. J., 3RD, POTTER, M. E., RILEY, L. W., BARRETT, T. J., BLAKE, P. A., BOPP, C. A., COHEN, M. L., KAUFMANN, A., MORRIS, G. K., REMIS, R. S., THOMASON, B. M. & WELLS, J. G. 1983. Animal models to study *Escherichia coli* O157:H7 isolated from patients with haemorrhagic colitis. *Lancet,* 1**,** 702-3.

FENG, P., LAMPEL, K. A., KARCH, H. & WHITTAM, T. S. 1998. Genotypic and phenotypic changes in the emergence of *Escherichia coli* O157:H7. *J Infect Dis,* 177**,** 1750-3.

FEROCI, G., RODA, A. & FINI, A. 2007. Study of the interaction between oxygen and bile salts. *Bioelectrochemistry,* 70, 524-31.

FERRARI, G., GARAGUSO, I., ADU-BOBIE, J., DORO, F., TADDEI, A. R., BIOLCHI, A., BRUNELLI, B., GIULIANI, M. M., PIZZA, M., NORAIS, N. & GRANDI, G. 2006. Outer membrane vesicles from group B *Neisseria meningitidis* delta *gna33* mutant: proteomic and immunological comparison with detergent-derived outer membrane vesicles. *Proteomics,* 6**,** 1856-66.

FOSTER, G. H. & TESH, V. L. 2002. Shiga toxin 1-induced activation of c-Jun NH(2)-terminal kinase and p38 in the human monocytic cell line THP-1: possible involvement in the production of TNF-alpha. *J Leukoc Biol,* 71**,** 107-14.

FOULKE-ABEL, J., IN, J., YIN, J., ZACHOS, N. C., KOVBASNJUK, O., ESTES, M. K., DE JONGE, H. & DONOWITZ, M. 2016. Human Enteroids as a Model of Upper Small Intestinal Ion Transport Physiology and Pathophysiology. *Gastroenterology,* 150**,** 638-649 e8.

FRANCIS, D. H., COLLINS, J. E. & DUIMSTRA, J. R. 1986. Infection of gnotobiotic pigs with an *Escherichia coli* O157:H7 strain associated with an outbreak of hemorrhagic colitis. *Infect Immun,* 51**,** 953-6.

FRANKEL, G., PHILLIPS, A. D., TRABULSI, L. R., KNUTTON, S., DOUGAN, G. & MATTHEWS, S. 2001. Intimin and the host cell--is it bound to end in Tir(s)? *Trends Microbio,* 9, 214-8.

FRANZ, E., VAN HOEK, A. H., WUITE, M., VAN DER WAL, F. J., DE BOER, A. G., BOUW, E. I. & AARTS, H. J. 2015. Molecular hazard identification of non-O157 Shiga toxin-producing *Escherichia coli* (STEC). *PLoS One,* 10**,** e0120353.

FRASER, M. E., FUJINAGA, M., CHERNEY, M. M., MELTON-CELSA, A. R., TWIDDY, E. M., O'BRIEN, A. D. & JAMES, M. N. 2004. Structure of shiga toxin type 2 (Stx2) from *Escherichia coli* O157:H7. *J Biol Chem,* 279**,** 27511-7.

FRETIN, D., FAUCONNIER, A., KOHLER, S., HALLING, S., LEONARD, S., NIJSKENS, C., FEROOZ, J., LESTRATE, P., DELRUE, R. M., DANESE, I., VANDENHAUTE, J., TIBOR, A., DEBOLLE, X. & LETESSON, J. J. 2005. The sheathed flagellum of *Brucella melitensis* is involved in persistence in a murine model of infection. *Cell Microbiol,* 7, 687-98.

FRUTH, A., PRAGER, R., TIETZE, E., RABSCH, W. & FLIEGER, A. 2015. Molecular epidemiological view on Shiga toxin-producing *Escherichia coli* causing human disease in Germany: Diversity, prevalence, and outbreaks. *Int J Med Microbiol,* 305, 697-704.

FRYKLUND, B., TULLUS, K., BERGLUND, B. & BURMAN, L. G. 1992. Importance of the environment and the faecal flora of infants, nursing staff and parents as

sources of gram-negative bacteria colonizing newborns in three neonatal wards. *Infection,* 20**,** 253-7.

FUJII, J., NAITO, M., YUTSUDO, T., MATSUMOTO, S., HEATHERLY, D. P., YAMADA, T., KOBAYASHI, H., YOSHIDA, S. & OBRIG, T. 2012. Protection by a recombinant *Mycobacterium bovis* Bacillus Calmette-Guerin vaccine expressing Shiga toxin 2 B subunit against Shiga toxin-producing *Escherichia coli* in mice. *Clin Vaccine Immunol,* 19**,** 1932-7.

FULLER, C. A., PELLINO, C. A., FLAGLER, M. J., STRASSER, J. E. & WEISS, A. A. 2011. Shiga toxin subtypes display dramatic differences in potency. *Infect Immun,* 79**,** 1329-37.

FURNESS, J. B., KUNZE, W. A. & CLERC, N. 1999. Nutrient tasting and signaling mechanisms in the gut. II. The intestine as a sensory organ: neural, endocrine, and immune responses. *Am J Physiol,* 277**,** G922-8.

FURUTA, N., TSUDA, K., OMORI, H., YOSHIMORI, T., YOSHIMURA, F. & AMANO, A. 2009. *Porphyromonas gingivalis* outer membrane vesicles enter human epithelial cells via an endocytic pathway and are sorted to lysosomal compartments. *Infect Immun,* 77**,** 4187-96.

FÖRSTER, A. H. & GESCHER, J. 2014. Metabolic Engineering of *Escherichia coli* for Production of Mixed-Acid Fermentation End Products. *Front Bioeng Biotechnol,* 2**,** 16.

GAJIWALA, K. S. & BURLEY, S. K. 2000. HDEA, a periplasmic protein that supports acid resistance in pathogenic enteric bacteria. *J Mol Biol,* 295, 605-12.

GARCIA-CASTILLO, M. D., CHINNAPEN, D. J. & LENCER, W. I. 2017. Membrane Transport across Polarized Epithelia. *Cold Spring Harb Perspect Biol,* 9.

GARMENDIA, J., PHILLIPS, A. D., CARLIER, M. F., CHONG, Y., SCHULLER, S., MARCHES, O., DAHAN, S., OSWALD, E., SHAW, R. K., KNUTTON, S. & FRANKEL, G. 2004. TccP is an enterohaemorrhagic *Escherichia coli* O157:H7 type III effector protein that couples Tir to the actin-cytoskeleton. *Cell Microbiol,* 6**,** 1167-83.

GARRED, O., VAN DEURS, B. & SANDVIG, K. 1995. Furin-induced cleavage and activation of Shiga toxin. *J Biol Chem,* 270**,** 10817-21.

GASS, J., VORA, H., HOFMANN, A. F., GRAY, G. M. & KHOSLA, C. 2007. Enhancement of dietary protein digestion by conjugated bile acids. *Gastroenterology,* 113, 16-23.

GAYTAN, M. O., MARTINEZ-SANTOS, V. I., SOTO, E. & GONZALEZ-PEDRAJO, B. 2016. Type Three Secretion System in Attaching and Effacing Pathogens. *Front Cell Infect Microbiol,* 6**,** 129.

GELBERG, H. B. 2014. Comparative anatomy, physiology, and mechanisms of disease production of the esophagus, stomach, and small intestine. *Toxicol Pathol,* 42, 54-66.

GERRITZEN, M. J. H., MARTENS, D. E., WIJFFELS, R. H. & STORK, M. 2017. High throughput nanoparticle tracking analysis for monitoring outer membrane vesicle production. *J Extracell Vesicles,* 6**,** 1333883.

GEVA-ZATORSKY, N., SEFIK, E., KUA, L., PASMAN, L., TAN, T. G., ORTIZ-LOPEZ, A., YANORTSANG, T. B., YANG, L., JUPP, R., MATHIS, D., BENOIST, C. & KASPER, D. L. 2017. Mining the Human Gut Microbiota for Immunomodulatory Organisms. *Cell,* 168, 928-943.

GIEPMANS, B. N. & VAN IJZENDOORN, S. C. 2009. Epithelial cell-cell junctions and plasma membrane domains. *Biochim Biophys Acta,* 1788, 820-31.

GIRARD, F., DZIVA, F., VAN DIEMEN, P., PHILLIPS, A. D., STEVENS, M. P. & FRANKEL, G. 2007. Adherence of Enterohemorrhagic *Escherichia coli* O157, O26, and O111 Strains to Bovine Intestinal Explants Ex Vivo. *Applied and Environmental Microbiology,* 73**,** 3084-3090.

GITIAUX, C., KRUG, P., GREVENT, D., KOSSOROTOFF, M., PONCET, S., EISERMANN, M., OUALHA, M., BODDAERT, N., SALOMON, R. & DESGUERRE, I. 2013. Brain magnetic resonance imaging pattern and outcome in children with haemolytic-uraemic syndrome and neurological impairment treated with eculizumab. *Dev Med Child Neurol,* 55**,** 758-65.

GOBIN, M., HAWKER, J., CLEARY, P., INNS, T., GARDINER, D., MIKHAIL, A., MCCORMICK, J., ELSON, R., READY, D., DALLMAN, T., RODDICK, I., HALL, I., WILLIS, C., CROOK, P., GODBOLE, G., TUBIN-DELIC, D. & OLIVER, I. 2018. National outbreak of Shiga toxin-producing *Escherichia coli* O157:H7 linked to mixed salad leaves, United Kingdom, 2016. *Euro Surveill,* 23.

GONZÁLEZ-FLECHA, B. & DEMPLE, B. 1995. Metabolic sources of hydrogen peroxide in aerobically growing *Escherichia coli*. *J Biol Chem,* 270**,** 13681-7.

GRANT, J., WENDELBOE, A. M., WENDEL, A., JEPSON, B., TORRES, P., SMELSER, C. & ROLFS, R. T. 2008. Spinach-associated *Escherichia coli* O157:H7 outbreak, Utah and New Mexico, 2006. *Emerg Infect Dis,* 14**,** 1633-6.

GREIG, D. R., JENKINS, C., GHARBIA, S. & DALLMAN, T. J. 2019. Comparison of single-nucleotide variants identified by Illumina and Oxford Nanopore technologies in the context of a potential outbreak of Shiga toxin-producing *Escherichia coli*. *Gigascience,* 8.

GRENIER, D. & BÉLANGER, M. 1991. Protective effect of *Porphyromonas gingivalis* outer membrane vesicles against bactericidal activity of human serum. *Infect Immun,* 59**,** 3004-8.

GRIF, K., DIERICH, M. P., KARCH, H. & ALLERBERGER, F. 1998. Strain-specific differences in the amount of Shiga toxin released from enterohemorrhagic *Escherichia coli* O157 following exposure to subinhibitory concentrations of antimicrobial agents. *Eur J Clin Microbiol Infect Dis,* 17**,** 761-6.

GRIFFIN, P. M., OLMSTEAD, L. C. & PETRAS, R. E. 1990. *Escherichia coli* O157:H7-associated colitis. A clinical and histological study of 11 cases. *Gastroenterology,* 99**,** 142-9.

GRIFFIN, P. M., OSTROFF, S. M., TAUXE, R. V., GREENE, K. D., WELLS, J. G., LEWIS, J. H. & BLAKE, P. A. 1988. Illnesses associated with *Escherichia coli* O157:H7 infections. A broad clinical spectrum. *Ann Intern Med,* 109**,** 705-12.

GRISARU, S., MORGUNOV, M. A., SAMUEL, S. M., MIDGLEY, J. P., WADE, A. W., TEE, J. B. & HAMIWKA, L. A. 2011. Acute renal replacement therapy in children with diarrhea-associated hemolytic uremic syndrome: a single center 16 years of experience. *Int J Nephrol,* 2011**,** 930539.

GRÜN, D., LYUBIMOVA, A., KESTER, L., WIEBRANDS, K., BASAK, O., SASAKI, N., CLEVERS, H. & VAN OUDENAARDEN, A. 2015. Single-cell messenger RNA sequencing reveals rare intestinal cell types. *Nature,* 525, 251-5.

GUIDI, R., LEVI, L., ROUF, S. F., PUIAC, S., RHEN, M. & FRISAN, T. 2013. *Salmonella enterica* delivers its genotoxin through outer membrane vesicles secreted from infected cells. *Cell Microbiol,* 15**,** 2034-50.

GUIGNOT, J., HUDAULT, S., KANSAU, I., CHAU, I. & SERVIN, A. L. 2009. Human decay-accelerating factor and CEACAM receptor-mediated internalization and intracellular lifestyle of Afa/Dr diffusely adhering *Escherichia coli* in epithelial cells. *Infect Immun,* 77**,** 517-31.

GUNSALUS, R. P. & PARK, S. J. 1994. Aerobic-anaerobic gene regulation in *Escherichia coli*: control by the ArcAB and Fnr regulons. *Res Microbiol,* 145, 437-50.

GUNZER, F., HENNIG-PAUKA, I., WALDMANN, K. H., SANDHOFF, R., GRÖNE, H. J., KREIPE, H. H., MATUSSEK, A. & MENGEL, M. 2002. Gnotobiotic piglets develop thrombotic microangiopathy after oral infection with enterohemorrhagic *Escherichia coli*. *Am J Clin Pathol,* 118**,** 364-75.

HAGEL, C., KRASEMANN, S., LOFFLER, J., PUSCHEL, K., MAGNUS, T. & GLATZEL, M. 2015. Upregulation of Shiga toxin receptor CD77/Gb3 and interleukin-1beta expression in the brain of EHEC patients with hemolytic uremic syndrome and neurologic symptoms. *Brain Pathol,* 25**,** 146-56.

HALL-STOODLEY, L., COSTERTON, J. W. & STOODLEY, P. 2004. Bacterial biofilms: from the natural environment to infectious diseases. *Nat Rev Microbiol,* 2**,** 95-108.

HALLETT, F. R., WATTON, J. & KRYGSMAN, P. 1991. Vesicle sizing: Number distributions by dynamic light scattering. *Biophys J,* 59**,** 357-62.

HAMILTON, J. P., XIE, G., RAUFMAN, J. P., HOGAN, S., GRIFFIN, T. L., PACKARD, C. A., CHATFIELD, D. A., HAGEY, L. R., STEINBACH, J. H. & HOFMANN, A. F. 2007. Human cecal bile acids: concentration and spectrum. *Am J Physiol Gastrointest Liver Physiol,* 293, G256-63.

HAMNER, S., MCINNERNEY, K., WILLIAMSON, K., FRANKLIN, M. J. & FORD, T. E. 2013. Bile salts affect expression of *Escherichia coli* O157:H7 genes for virulence and iron acquisition, and promote growth under iron limiting conditions. *PLoS One,* 8**,** e74647.

HANSSON, G. C. 2019. Mucus and mucins in diseases of the intestinal and respiratory tracts. *J Intern Med,* 285**,** 479-490.

HAO, W., ALLEN, V. G., JAMIESON, F. B., LOW, D. E. & ALEXANDER, D. C. 2012. Phylogenetic incongruence in *E. coli* O104: understanding the evolutionary relationships of emerging pathogens in the face of homologous recombination. *PLoS One,* 7**,** e33971.

HE, B. & GUO, W. 2009. The exocyst complex in polarized exocytosis. *Curr Opin Cell Biol,* 21**,** 537-42.

HE, G., SHANKAR, R. A., CHZHAN, M., SAMOUILOV, A., KUPPUSAMY, P. & ZWEIER, J. L. 1999. Noninvasive measurement of anatomic structure and intraluminal oxygenation in the gastrointestinal tract of living mice with spatial and spectral EPR imaging. *Proc Natl Acad Sci U S A,* 96**,** 4586-91.

HE, Y., SHIOTSU, N., UCHIDA-FUKUHARA, Y., GUO, J., WENG, Y., IKEGAME, M., WANG, Z., ONO, K., KAMIOKA, H., TORII, Y., SASAKI, A., YOSHIDA, K. & OKAMURA, H. 2020. Outer membrane vesicles derived from *Porphyromonas gingivalis* induced cell death with disruption of tight junctions in human lung epithelial cells. *Arch Oral Biol,* 118, 104841.

HEIMESAAT, M. M., KUPZ, A., FISCHER, A., NIES, D. H., GRASS, G., GOBEL, U. B. & BERESWILL, S. 2013. Colonization resistance against genetically modified *Escherichia coli* K12 (W3110) strains is abrogated following broad-spectrum antibiotic treatment and acute ileitis. *Eur J Microbiol Immunol (Bp),* 3**,** 222-8.

HENTZER, M., WU, H., ANDERSEN, J. B., RIEDEL, K., RASMUSSEN, T. B., BAGGE, N., KUMAR, N., SCHEMBRI, M. A., SONG, Z., KRISTOFFERSEN, P., MANEFIELD, M., COSTERTON, J. W., MOLIN, S., EBERL, L., STEINBERG, P., KJELLEBERG, S., HØIBY, N. & GIVSKOV, M. 2003. Attenuation of *Pseudomonas aeruginosa* virulence by quorum sensing inhibitors. *EMBO J,* 22**,** 3803-15.

HEROLD, S., PATON, J. C. & PATON, A. W. 2009a. Sab, a novel autotransporter of locus of enterocyte effacement-negative shiga-toxigenic *Escherichia coli* O113:H21, contributes to adherence and biofilm formation. *Infect Immun,* 77**,** 3234-43.

HEROLD, S., PATON, J. C., SRIMANOTE, P. & PATON, A. W. 2009b. Differential effects of short-chain fatty acids and iron on expression of iha in Shiga-toxigenic *Escherichia coli*. *Microbiology (Reading),* 155**,** 3554-3563.

HERSH, B. M., FAROOQ, F. T., BARSTAD, D. N., BLANKENHORN, D. L. & SLONCZEWSKI, J. L. 1996. A glutamate-dependent acid resistance gene in *Escherichia coli*. *J Bacteriol,* 178**,** 3978-81.

HEWS, C. L., TRAN, S. L., WEGMANN, U., BRETT, B., WALSHAM, A. D., KAVANAUGH, D., WARD, N. J., JUGE, N. & SCHULLER, S. 2017. The StcE metalloprotease of enterohaemorrhagic *Escherichia coli* reduces the inner mucus layer and promotes adherence to human colonic epithelium *ex vivo*. *Cell Microbiol*, 19, e12717.

HICKEY, C. A., BEATTIE, T. J., COWIESON, J., MIYASHITA, Y., STRIFE, C. F., FREM, J. C., PETERSON, J. M., BUTANI, L., JONES, D. P., HAVENS, P. L., PATEL, H. P., WONG, C. S., ANDREOLI, S. P., ROTHBAUM, R. J., BECK, A. M. & TARR, P. I. 2011. Early volume expansion during diarrhea and relative nephroprotection during subsequent hemolytic uremic syndrome. *Arch Pediatr Adolesc Med,* 165**,** 884-9.

HOEKSTRA, D., VAN DER LAAN, J. W., DE LEIJ, L. & WITHOLT, B. 1976. Release of outer membrane fragments from normally growing *Escherichia coli*. *Biochim Biophys Acta,* 455**,** 889-99.

HOEY, D. E., SHARP, L., CURRIE, C., LINGWOOD, C. A., GALLY, D. L. & SMITH, D. G. 2003. Verotoxin 1 binding to intestinal crypt epithelial cells results in localization to lysosomes and abrogation of toxicity. *Cell Microbiol,* 5, 82-97.

HOFMANN, A. F. 1999. The continuing importance of bile acids in liver and intestinal disease. *Arch Intern Med,* 159**,** 2647-58.

HOFMANN, A. F. 2009. The enterohepatic circulation of bile acids in mammals: form and functions. *Front Biosci (Landmark Ed),* 14, 2584-98.

HOLMS, H. 1996. Flux analysis and control of the central metabolic pathways in *Escherichia coli*. *FEMS Microbiol Rev,* 19, 85-116.

HOLTZ, L. R., NEILL, M. A. & TARR, P. I. 2009. Acute bloody diarrhea: a medical emergency for patients of all ages. *Gastroenterology,* 136, 1887-98.

HONG, J., DAUROS-SINGORENKO, P., WHITCOMBE, A., PAYNE, L., BLENKIRON, C., PHILLIPS, A. & SWIFT, S. 2019. Analysis of the *Escherichia coli* extracellular vesicle proteome identifies markers of purity and culture conditions. *J Extracell Vesicles,* 8**,** 1632099.

HOOPER, L. V., XU, J., FALK, P. G., MIDTVEDT, T. & GORDON, J. I. 1999. A molecular sensor that allows a gut commensal to control its nutrient foundation in a competitive ecosystem. *Proc Natl Acad Sci U S A,* 96**,** 9833-8.

HORSTMAN, A. L. & KUEHN, M. J. 2000. Enterotoxigenic *Escherichia coli* secretes active heat-labile enterotoxin via outer membrane vesicles. *J Biol Chem,* 275**,** 12489-96.

HOUSE, B., KUS, J. V., PRAYITNO, N., MAIR, R., QUE, L., CHINGCUANCO, F., GANNON, V., CVITKOVITCH, D. G. & BARNETT FOSTER, D. 2009. Acid-stress-induced changes in enterohaemorrhagic *Escherichia coli* O157 : H7 virulence. *Microbiology,* 155**,** 2907-18.

HUANG, C. J., LIN, H. & YANG, X. 2012. Industrial production of recombinant therapeutics in *Escherichia coli* and its recent advancements. *J Ind Microbiol Biotechnol,* 39**,** 383-99.

HUGHES, D. T., CLARKE, M. B., YAMAMOTO, K., RASKO, D. A. & SPERANDIO, V. 2009. The QseC adrenergic signaling cascade in Enterohemorrhagic *E. coli* (EHEC). *PLoS Pathog,* 5**,** e1000553.

HURLEY, B. P., THORPE, C. M. & ACHESON, D. W. K. 2001. Shiga Toxin Translocation across Intestinal Epithelial Cells Is Enhanced by Neutrophil Transmigration. *Infection and Immunity,* 69**,** 6148-6155.

HUSSEIN, H. S. & SAKUMA, T. 2005. Prevalence of shiga toxin-producing *Escherichia coli* in dairy cattle and their products. *J Dairy Sci,* 88**,** 450-65.

IKEDA, M., GUNJI, Y., YAMASAKI, S. & TAKEDA, Y. 2000. Shiga toxin activates p38 MAP kinase through cellular Ca(2+) increase in Vero cells. *FEBS Lett,* 485**,** 94-8.

IN, J., FOULKE-ABEL, J., ZACHOS, N. C., HANSEN, A. M., KAPER, J. B., BERNSTEIN, H. D., HALUSHKA, M., BLUTT, S., ESTES, M. K., DONOWITZ, M. & KOVBASNJUK, O. 2016a. Enterohemorrhagic *Escherichia coli* reduce mucus and intermicrovillar bridges in human stem cell-derived colonoids. *Cell Mol Gastroenterol Hepatol,* 2**,** 48-62 e3.

IN, J., LUKYANENKO, V., FOULKE-ABEL, J., HUBBARD, A. L., DELANNOY, M., HANSEN, A. M., KAPER, J. B., BOISEN, N., NATARO, J. P., ZHU, C., BOEDEKER, E. C., GIRON, J. A. & KOVBASNJUK, O. 2013. Serine protease EspP from enterohemorrhagic *Escherichia coli* is sufficient to induce shiga toxin macropinocytosis in intestinal epithelium. *PLoS One,* 8**,** e69196.

IN, J. G., FOULKE-ABEL, J., CLARKE, E. & KOVBASNJUK, O. 2019. Human Colonoid Monolayers to Study Interactions Between Pathogens, Commensals, and Host Intestinal Epithelium. *J Vis Exp*, 146.

IN, J. G., FOULKE-ABEL, J., ESTES, M. K., ZACHOS, N. C., KOVBASNJUK, O. & DONOWITZ, M. 2016b. Human mini-guts: new insights into intestinal physiology and host-pathogen interactions. *Nat Rev Gastroenterol Hepatol,* 13**,** 633-642.

IORDANOV, M. S., PRIBNOW, D., MAGUN, J. L., DINH, T. H., PEARSON, J. A., CHEN, S. L. & MAGUN, B. E. 1997. Ribotoxic stress response: activation of the stress-activated protein kinase JNK1 by inhibitors of the peptidyl transferase reaction and by sequence-specific RNA damage to the alpha-sarcin/ricin loop in the 28S rRNA. *Mol Cell Biol,* 17**,** 3373-81.

ISHII, S., KSOLL, W. B., HICKS, R. E. & SADOWSKY, M. J. 2006. Presence and growth of naturalized *Escherichia coli* in temperate soils from Lake Superior watersheds. *Appl Environ Microbiol,* 72**,** 612-21.

ISHII, S. & SADOWSKY, M. J. 2008. *Escherichia coli* in the Environment: Implications for Water Quality and Human Health. *Microbes Environ,* 23, 101-8.

IYODA, S., KOIZUMI, N., SATOU, H., LU, Y., SAITOH, T., OHNISHI, M. & WATANABE, H. 2006. The GrlR-GrlA regulatory system coordinately controls the expression of flagellar and LEE-encoded type III protein secretion systems in enterohemorrhagic *Escherichia coli*. *J Bacteriol,* 188**,** 5682-92.

JACEWICZ, M. S., ACHESON, D. W., MOBASSALEH, M., DONOHUE-ROLFE, A., BALASUBRAMANIAN, K. A. & KEUSCH, G. T. 1995. Maturational regulation of globotriaosylceramide, the Shiga-like toxin 1 receptor, in cultured human gut epithelial cells. *J Clin Invest,* 96**,** 1328-35.

JACKSON, M. P., NEWLAND, J. W., HOLMES, R. K. & O'BRIEN, A. D. 1987. Nucleotide sequence analysis of the structural genes for Shiga-like toxin I encoded by bacteriophage 933J from *Escherichia coli*. *Microb Pathog,* 2, 147-53.

JAMES, B. W. & KEEVIL, C. W. 1999. Influence of oxygen availability on physiology, verocytotoxin expression and adherence of *Escherichia coli* O157. *J Appl Microbiol,* 86**,** 117-24.

JANG, J., HUR, H. G., SADOWSKY, M. J., BYAPPANAHALLI, M. N., YAN, T. & ISHII, S. 2017. Environmental *Escherichia coli*: ecology and public health implications-a review. *J Appl Microbiol,* 123**,** 570-581.

JENKINS, C., DALLMAN, T. J. & GRANT, K. A. 2019. Impact of whole genome sequencing on the investigation of food-borne outbreaks of Shiga toxin-producing *Escherichia coli* serogroup O157:H7, England, 2013 to 2017. *Euro Surveill,* 24.

JOHANNES, L. & ROMER, W. 2010. Shiga toxins--from cell biology to biomedical applications. *Nat Rev Microbiol,* 8**,** 105-16.

JOHANSSON, K., WILLYSSON, A., KRISTOFFERSSON, A. C., TONTANAHAL, A., GILLET, D., STÅHL, A. L. & KARPMAN, D. 2020. Shiga Toxin-Bearing Microvesicles Exert a Cytotoxic Effect on Recipient Cells Only When the Cells Express the Toxin Receptor. *Front Cell Infect Microbiol,* 10**,** 212.

JOHANSSON, M. E., GUSTAFSSON, J. K., HOLMÉN-LARSSON, J., JABBAR, K. S., XIA, L., XU, H., GHISHAN, F. K., CARVALHO, F. A., GEWIRTZ, A. T., SJÖVALL, H. & HANSSON, G. C. 2014. Bacteria penetrate the normally impenetrable inner colon mucus layer in both murine colitis models and patients with ulcerative colitis. *Gut,* 63**,** 281-91.

JOHANSSON, M. E., LARSSON, J. M. & HANSSON, G. C. 2011. The two mucus layers of colon are organized by the MUC2 mucin, whereas the outer layer is a legislator of host-microbial interactions. *Proc Natl Acad Sci U S A,* 108 Suppl 1**,** 4659-65.

JOHANSSON, M. E., PHILLIPSON, M., PETERSSON, J., VELCICH, A., HOLM, L. & HANSSON, G. C. 2008. The inner of the two Muc2 mucin-dependent mucus layers in colon is devoid of bacteria. *Proc Natl Acad Sci U S A,* 105**,** 15064-9.

JONES, E. J., BOOTH, C., FONSECA, S., PARKER, A., CROSS, K., MIQUEL-CLOPÉS, A., HAUTEFORT, I., MAYER, U., WILEMAN, T., STENTZ, R. & CARDING, S. R. 2020.

The Uptake, Trafficking, and Biodistribution of *Bacteroides thetaiotaomicron* Generated Outer Membrane Vesicles. *Front Microbiol,* 11**,** 57.

JONES, S. A., CHOWDHURY, F. Z., FABICH, A. J., ANDERSON, A., SCHREINER, D. M., HOUSE, A. L., AUTIERI, S. M., LEATHAM, M. P., LINS, J. J., JORGENSEN, M., COHEN, P. S. & CONWAY, T. 2007. Respiration of *Escherichia coli* in the mouse intestine. *Infect Immun,* 75**,** 4891-9.

JUDICIAL COMMISSION OF THE INTERNATIONAL COMMITTEE ON BACTERIOLOGICAL NOMENCLATURE. 1958. Conservation of the family name Enterobacteriaceae, of the name of the type genus, and designation of the type species. OPINION NO. 15.

KAILASAN VANAJA, S., BERGHOLZ, T. M. & WHITTAM, T. S. 2009. Characterization of the *Escherichia coli* O157:H7 Sakai GadE regulon. *J Bacteriol,* 191**,** 1868-77.

KAJIKAWA, A., SUZUKI, S. & IGIMI, S. 2018. The impact of motility on the localization of *Lactobacillus agilis* in the murine gastrointestinal tract. *BMC Microbiol,* 18**,** 68.

KALANTAR-ZADEH, K., BEREAN, K. J., HA, N., CHRIMES, A. F., XU, K., GRANDO, D., OU, J. Z., PILLAI, N., CAMPBELL, J. L., BRKLJAČA, R., TAYLOR, K. M., BURGELL, R. E., YAO, C. K., WARD, S. A., MCSWEENEY, C. S., MUIR, J. G. & GIBSON, P. R. 2018. A human pilot trial of ingestible electronic capsules capable of sensing different gases in the gut. *Nat Electron,* 1, 78-76.

KANDELL, R. L. & BERNSTEIN, C. 1991. Bile salt/acid induction of DNA damage in bacterial and mammalian cells: implications for colon cancer. *Nutr Cancer,* 16**,** 227-38.

KAPARAKIS, M., TURNBULL, L., CARNEIRO, L., FIRTH, S., COLEMAN, H. A., PARKINGTON, H. C., LE BOURHIS, L., KARRAR, A., VIALA, J., MAK, J., HUTTON, M. L., DAVIES, J. K., CRACK, P. J., HERTZOG, P. J., PHILPOTT, D. J., GIRARDIN, S. E., WHITCHURCH, C. B. & FERRERO, R. L. 2010. Bacterial membrane vesicles deliver peptidoglycan to NOD1 in epithelial cells. *Cell Microbiol,* 12**,** 372-85.

KAPER, J. B., NATARO, J. P. & MOBLEY, H. L. T. 2004. Pathogenic *Escherichia coli*. *Nat Rev Micro,* 2**,** 123-140.

KARCH, H., DENAMUR, E., DOBRINDT, U., FINLAY, B. B., HENGGE, R., JOHANNES, L., RON, E. Z., TØNJUM, T., SANSONETTI, P. J. & VICENTE, M. 2012. The enemy within us: lessons from the 2011 European *Escherichia coli* O104:H4 outbreak. *EMBO Mol Med,* 4**,** 841-8.

KARCH, H., FRIEDRICH, A. W., GERBER, A., ZIMMERHACKL, L. B., SCHMIDT, M. A. & BIELASZEWSKA, M. 2006. New aspects in the pathogenesis of enteropathic hemolytic uremic syndrome. *Semin Thromb Hemost,* 32**,** 105-12.

KARCH, H., MELLMANN, A. & BIELASZEWSKA, M. 2009. Epidemiology and pathogenesis of enterohaemorrhagic *Escherichia coil*. *Berl Munch Tierarztl Wochenschr,* 122**,** 417-24.

KARMALI, M. A., PETRIC, M., LIM, C., FLEMING, P. C. & STEELE, B. T. 1983a. *Escherichia coli* cytotoxin, haemolytic-uraemic syndrome, and haemorrhagic colitis. *Lancet,* 2, 1299-1300.

KARMALI, M. A., STEELE, B. T., PETRIC, M. & LIM, C. 1983b. Sporadic cases of haemolytic-uraemic syndrome associated with faecal cytotoxin and cytotoxin-producing *Escherichia coli* in stools. *Lancet,* 1**,** 619-20.

KARPMAN, D., STÅHL, A. L. & ARVIDSSON, I. 2017. Extracellular vesicles in renal disease. *Nat Rev Nephrol,* 13, 545-562.

KAWANO, K., OKADA, M., HAGA, T., MAEDA, K. & GOTO, Y. 2008. Relationship between pathogenicity for humans and stx genotype in Shiga toxin-producing *Escherichia coli* serotype O157. *Eur J Clin Microbiol Infect Dis,* 27**,** 227-32.

KEENAN, J. I. & ALLARDYCE, R. A. 2000. Iron influences the expression of *Helicobacter pylori* outer membrane vesicle-associated virulence factors. *Eur J Gastroenterol Hepatol,* 12**,** 1267-73.

KEENAN, K. P., SHARPNACK, D. D., COLLINS, H., FORMAL, S. B. & O'BRIEN, A. D. 1986. Morphologic evaluation of the effects of Shiga toxin and *E coli* Shiga-like toxin on the rabbit intestine. *Am J Pathol,* 125**,** 69-80.

KEENSWIJK, W., VANMASSENHOVE, J., RAES, A., DHONT, E. & VANDEWALLE, J. 2017. Epidemiology and outcome of acute kidney injury in children, a single center study. *Acta Clin Belg,* 72**,** 405-412.

KELLY, J. K., PAI, C. H., JADUSINGH, I. H., MACINNIS, M. L., SHAFFER, E. A. & HERSHFIELD, N. B. 1987. The histopathology of rectosigmoid biopsies from adults with bloody diarrhea due to verotoxin-producing *Escherichia coli*. *Am J Clin Pathol,* 88**,** 78-82.

KENDALL, M. M., GRUBER, C. C., PARKER, C. T. & SPERANDIO, V. 2012. Ethanolamine controls expression of genes encoding components involved in interkingdom signaling and virulence in enterohemorrhagic *Escherichia coli* O157:H7. *mBio,* 3.

KENNY, B. 1999. Phosphorylation of tyrosine 474 of the enteropathogenic *Escherichia coli* (EPEC) Tir receptor molecule is essential for actin nucleating activity and is preceded by additional host modifications. *Mol Microbiol,* 31**,** 1229-41.

KENNY, B., DEVINNEY, R., STEIN, M., REINSCHEID, D. J., FREY, E. A. & FINLAY, B. B. 1997. Enteropathogenic *E. coli* (EPEC) transfers its receptor for intimate adherence into mammalian cells. *Cell,* 91**,** 511-20.

KESTY, N. C., MASON, K. M., REEDY, M., MILLER, S. E. & KUEHN, M. J. 2004. Enterotoxigenic *Escherichia coli* vesicles target toxin delivery into mammalian cells. *Embo j,* 23**,** 4538-49.

KEUSCH, G. T., ACHESON, D. W., AALDERING, L., ERBAN, J. & JACEWICZ, M. S. 1996. Comparison of the effects of Shiga-like toxin 1 on cytokine- and butyrate-treated human umbilical and saphenous vein endothelial cells. *J Infect Dis,* 173**,** 1164-70.

KIELSTEIN, J. T., BEUTEL, G., FLEIG, S., STEINHOFF, J., MEYER, T. N., HAFER, C., KUHLMANN, U., BRAMSTEDT, J., PANZER, U., VISCHEDYK, M., BUSCH, V., RIES, W., MITZNER, S., MEES, S., STRACKE, S., NURNBERGER, J., GERKE, P., WIESNER, M., SUCKE, B., ABU-TAIR, M., KRIBBEN, A., KLAUSE, N., SCHINDLER, R., MERKEL, F., SCHNATTER, S., DORRESTEIJN, E. M., SAMUELSSON, O. & BRUNKHORST, R. 2012. Best supportive care and therapeutic plasma exchange with or without eculizumab in Shiga-toxin-producing *E. coli* O104:H4 induced haemolytic-uraemic syndrome: an analysis of the German STEC-HUS registry. *Nephrol Dial Transplant,* 27, 3807-15.

KIM, S. H., LEE, S. R., KIM, K. S., KO, A., KIM, E., KIM, Y. H. & CHANG, K. T. 2010. Shiga toxin A subunit mutant of *Escherichia coli* O157:H7 releases outer membrane

vesicles containing the B-pentameric complex. *FEMS Immunol Med Microbiol,* 58**,** 412-20.

KIM, S. H., LEE, Y. H., LEE, S. H., LEE, S. R., HUH, J. W., KIM, S. U. & CHANG, K. T. 2011. Mouse model for hemolytic uremic syndrome induced by outer membrane vesicles of *Escherichia coli* O157:H7. *FEMS Immunol Med Microbiol,* 63**,** 427-34.

KIM, S. W., LEE, J. S., PARK, S. B., LEE, A. R., JUNG, J. W., CHUN, J. H., LAZARTE, J. M. S., KIM, J., SEO, J. S., KIM, J. H., SONG, J. W., HA, M. W., THOMPSON, K. D., LEE, C. R., JUNG, M. & JUNG, T. S. 2020. The Importance of Porins and β-Lactamase in Outer Membrane Vesicles on the Hydrolysis of β-Lactam Antibiotics. *Int J Mol Sci,* 21.

KIM, S. W., PARK, S. B., IM, S. P., LEE, J. S., JUNG, J. W., GONG, T. W., LAZARTE, J. M. S., KIM, J., SEO, J. S., KIM, J. H., SONG, J. W., JUNG, H. S., KIM, G. J., LEE, Y. J., LIM, S. K. & JUNG, T. S. 2018. Outer membrane vesicles from β-lactam-resistant *Escherichia coli* enable the survival of β-lactam-susceptible *E. coli* in the presence of β-lactam antibiotics. *Sci Rep,* 8**,** 5402.

KIMMITT, P. T., HARWOOD, C. R. & BARER, M. R. 2000. Toxin gene expression by shiga toxin-producing *Escherichia coli*: the role of antibiotics and the bacterial SOS response. *Emerg Infect Dis,* 6**,** 458-65.

KING, L. A., NOGAREDA, F., WEILL, F. X., MARIANI-KURKDJIAN, P., LOUKIADIS, E., GAULT, G., JOURDAN-DASILVA, N., BINGEN, E., MACÉ, M., THEVENOT, D., ONG, N., CASTOR, C., NOËL, H., VAN CAUTEREN, D., CHARRON, M., VAILLANT, V., ALDABE, B., GOULET, V., DELMAS, G., COUTURIER, E., LE STRAT, Y., COMBE, C., DELMAS, Y., TERRIER, F., VENDRELY, B., ROLLAND, P. & DE VALK, H. 2012. Outbreak of Shiga toxin-producing *Escherichia coli* O104:H4 associated with organic fenugreek sprouts, France, June 2011. *Clin Infect Dis,* 54, 1588-94.

KINTZ, E., BRAINARD, J., HOOPER, L. & HUNTER, P. 2017. Transmission pathways for sporadic Shiga-toxin producing *E. coli* infections: A systematic review and meta-analysis. *Int J Hyg Environ Health,* 220, 57-67.

KINTZ, E., BYRNE, L., JENKINS, C., MC, C. N., VIVANCOS, R. & HUNTER, P. 2019. Outbreaks of Shiga Toxin-Producing *Escherichia coli* Linked to Sprouted Seeds, Salad, and Leafy Greens: A Systematic Review. *J Food Prot,* 82**,** 1950-1958.

KLEIN, E. J., STAPP, J. R., CLAUSEN, C. R., BOSTER, D. R., WELLS, J. G., QIN, X., SWERDLOW, D. L. & TARR, P. I. 2002. Shiga toxin-producing *Escherichia coli* in children with diarrhea: a prospective point-of-care study. *J Pediatr,* 141, 172-7.

KLIMENTOVÁ, J. & STULÍK, J. 2015. Methods of isolation and purification of outer membrane vesicles from gram-negative bacteria. *Microbiol Res,* 170, 1-9.

KNOX, K. W., VESK, M. & WORK, E. 1966. Relation between excreted lipopolysaccharide complexes and surface structures of a lysine-limited culture of *Escherichia coli*. *J Bacteriol,* 92**,** 1206-17.

KNUTTON, S., BALDWIN, T., WILLIAMS, P. H. & MCNEISH, A. S. 1989. Actin accumulation at sites of bacterial adhesion to tissue culture cells: basis of a new diagnostic test for enteropathogenic and enterohemorrhagic *Escherichia coli*. *Infect Immun,* 57**,** 1290-8.

KNUTTON, S., LLOYD, D. R. & MCNEISH, A. S. 1987. Adhesion of enteropathogenic *Escherichia coli* to human intestinal enterocytes and cultured human intestinal mucosa. *Infect Immun,* 55**,** 69-77.

KOEBNIK, R. 1995. Proposal for a peptidoglycan-associating alpha-helical motif in the C-terminal regions of some bacterial cell-surface proteins. *Mol Microbiol,* 16**,** 1269-70.

KOLLING, G. L. & MATTHEWS, K. R. 1999. Export of virulence genes and Shiga toxin by membrane vesicles of *Escherichia coli* O157:H7. *Appl Environ Microbiol,* 65**,** 1843-8.

KONOWALCHUK, J., SPEIRS, J. I. & STAVRIC, S. 1977. Vero response to a cytotoxin of *Escherichia coli*. *Infect Immun,* 18**,** 775-9.

KOVBASNJUK, O., MOURTAZINA, R., BAIBAKOV, B., WANG, T., ELOWSKY, C., CHOTI, M. A., KANE, A. & DONOWITZ, M. 2005. The glycosphingolipid globotriaosylceramide in the metastatic transformation of colon cancer. *Proc Natl Acad Sci U S A,* 102**,** 19087-92.

KULKARNI, A. A., FULLER, C., KORMAN, H., WEISS, A. A. & IYER, S. S. 2010. Glycan encapsulated gold nanoparticles selectively inhibit shiga toxins 1 and 2. *Bioconjug Chem,* 21**,** 1486-93.

KULKARNI, H. M., NAGARAJ, R. & JAGANNADHAM, M. V. 2015. Protective role of *E. coli* outer membrane vesicles against antibiotics. *Microbiol Res,* 181, 1-7.

KUNSMANN, L., RÜTER, C., BAUWENS, A., GREUNE, L., GLÜDER, M., KEMPER, B., FRUTH, A., WAI, S. N., HE, X., LLOUBES, R., SCHMIDT, M. A., DOBRINDT, U., MELLMANN, A., KARCH, H. & BIELASZEWSKA, M. 2015. Virulence from vesicles: Novel mechanisms of host cell injury by *Escherichia coli* O104:H4 outbreak strain. *Scientific Reports,* 5**,** 13252.

KURDI, P., KAWANISHI, K., MIZUTANI, K. & YOKOTA, A. 2006. Mechanism of growth inhibition by free bile acids in lactobacilli and bifidobacteria. *J Bacteriol,* 188**,** 1979-86.

KURMANOVA, A., LLORENTE, A., POLESSKAYA, A., GARRED, O., OLSNES, S., KOZLOV, J. & SANDVIG, K. 2007. Structural requirements for furin-induced cleavage and activation of Shiga toxin. *Biochem Biophys Res Commun,* 357, 144-9.

LAABERKI, M. H., JANABI, N., OSWALD, E. & REPOILA, F. 2006. Concert of regulators to switch on LEE expression in enterohemorrhagic *Escherichia coli* O157:H7: interplay between Ler, GrlA, HNS and RpoS. *Int J Med Microbiol,* 296, 197-210.

LACOURSIERE, A., THOMPSON, B. G., KOLE, M. M., WARD, D. & GERSON, D. F. 1986. Effects of carbon dioxide concentration on anaerobic fermentations of *Escherichia coli*. *Applied Microbiology and Biotechnology,* 23**,** 404-406.

LACY, B. E., GABBARD, S. L. & CROWELL, M. D. 2011. Pathophysiology, evaluation, and treatment of bloating: hope, hype, or hot air? *Gastroenterol Hepatol (N Y),* 7**,** 729-39.

LAI, Y., RILEY, K., CAI, A., LEONG, J. M. & HERMAN, I. M. 2011. Calpain mediates epithelial cell microvillar effacement by enterohemorrhagic *Escherichia coli*. *Front Microbiol,* 2**,** 222.

LANSBURY, L. E. & LUDLAM, H. 1997. *Escherichia coli* O157: lessons from the past 15 years. *J Infect,* 34, 189-93.

LAPEYRAQUE, A. L., MALINA, M., FREMEAUX-BACCHI, V., BOPPEL, T., KIRSCHFINK, M., OUALHA, M., PROULX, F., CLERMONT, M. J., LE DEIST, F., NIAUDET, P. &

SCHAEFER, F. 2011. Eculizumab in severe Shiga-toxin-associated HUS. *N Engl J Med,* 364**,** 2561-3.

LAPOINTE, P., WEI, X. & GARIEPY, J. 2005. A role for the protease-sensitive loop region of Shiga-like toxin 1 in the retrotranslocation of its A1 domain from the endoplasmic reticulum lumen. *J Biol Chem,* 280, 23310-8.

LAPPANN, M., OTTO, A., BECHER, D. & VOGEL, U. 2013. Comparative proteome analysis of spontaneous outer membrane vesicles and purified outer membranes of *Neisseria meningitidis*. *J Bacteriol,* 195**,** 4425-35.

LATHEM, W. W., GRYS, T. E., WITOWSKI, S. E., TORRES, A. G., KAPER, J. B., TARR, P. I. & WELCH, R. A. 2002. StcE, a metalloprotease secreted by *Escherichia coli* O157:H7, specifically cleaves C1 esterase inhibitor. *Mol Microbiol,* 45, 277-88.

LAUVRAK, S. U., TORGERSEN, M. L. & SANDVIG, K. 2004. Efficient endosome-to-Golgi transport of Shiga toxin is dependent on dynamin and clathrin. *J Cell Sci,* 117**,** 2321-31.

LEE, E. Y., BANG, J. Y., PARK, G. W., CHOI, D. S., KANG, J. S., KIM, H. J., PARK, K. S., LEE, J. O., KIM, Y. K., KWON, K. H., KIM, K. P. & GHO, Y. S. 2007. Global proteomic profiling of native outer membrane vesicles derived from *Escherichia coli*. *Proteomics,* 7**,** 3143-53.

LEKMEECHAI, S., SU, Y. C., BRANT, M., ALVARADO-KRISTENSSON, M., VALLSTRÖM, A., OBI, I., ARNQVIST, A. & RIESBECK, K. 2018. *Helicobacter pylori* Outer Membrane Vesicles Protect the Pathogen From Reactive Oxygen Species of the Respiratory Burst. *Front Microbiol,* 9**,** 1837.

LEVITT, M. D. & BOND, J. H., JR. 1970. Volume, composition, and source of intestinal gas. *Gastroenterology,* 59**,** 921-9.

LEWIS, S. B., COOK, V., TIGHE, R. & SCHULLER, S. 2015. Enterohemorrhagic *Escherichia coli* colonization of human colonic epithelium *in vitro* and *ex vivo*. *Infect Immun,* 83**,** 942-9.

LEWIS, S. B., PRIOR, A., ELLIS, S. J., COOK, V., CHAN, S. S., GELSON, W. & SCHÜLLER, S. 2016. Flagellin Induces β-Defensin 2 in Human Colonic Ex vivo Infection with Enterohemorrhagic *Escherichia coli*. *Front Cell Infect Microbiol,* 6**,** 68.

LI, T., TU, W., LIU, Y., ZHOU, P., CAI, K., LI, Z., LIU, X., NING, N., HUANG, J., WANG, S. & WANG, H. 2016. A potential therapeutic peptide-based neutralizer that potently inhibits Shiga toxin 2 *in vitro* and *in vivo*. *Sci Rep,* 6**,** 21837.

LI, Z., CLARKE, A. J. & BEVERIDGE, T. J. 1998. Gram-negative bacteria produce membrane vesicles which are capable of killing other bacteria. *J Bacteriol,* 180**,** 5478-83.

LIAO, Y. T., KUO, S. C., CHIANG, M. H., LEE, Y. T., SUNG, W. C., CHEN, Y. H., CHEN, T. L. & FUNG, C. P. 2015. *Acinetobacter baumannii* Extracellular OXA-58 Is Primarily and Selectively Released via Outer Membrane Vesicles after Sec-Dependent Periplasmic Translocation. *Antimicrob Agents Chemother,* 59**,** 7346-54.

LIH, A., HIBBERT, E., WONG, T., GIRGIS, C. M., GARG, N. & CARTER, J. N. 2010. The role of insulin glulisine to improve glycemic control in children with diabetes mellitus. *Diabetes Metab Syndr Obes,* 3**,** 403-12.

LIN, J., LEE, I. S., FREY, J., SLONCZEWSKI, J. L. & FOSTER, J. W. 1995. Comparative analysis of extreme acid survival in *Salmonella typhimurium*, *Shigella flexneri*, and *Escherichia coli*. *J Bacteriol,* 177**,** 4097-104.

LIN, J., SMITH, M. P., CHAPIN, K. C., BAIK, H. S., BENNETT, G. N. & FOSTER, J. W. 1996. Mechanisms of acid resistance in enterohemorrhagic *Escherichia coli*. *Appl Environ Microbiol,* 62**,** 3094-100.

LINDHOLM, M., METSÄNIITTY, M., GRANSTRÖM, E. & OSCARSSON, J. 2020. Outer membrane vesicle-mediated serum protection in *Aggregatibacter actinomycetemcomitans*. *J Oral Microbiol,* 12**,** 1747857.

LINDSEY, R. L., POUSEELE, H., CHEN, J. C., STROCKBINE, N. A. & CARLETON, H. A. 2016. Implementation of Whole Genome Sequencing (WGS) for Identification and Characterization of Shiga Toxin-Producing *Escherichia coli* (STEC) in the United States. *Front Microbiol,* 7**,** 766.

LING, H., BOODHOO, A., HAZES, B., CUMMINGS, M. D., ARMSTRONG, G. D., BRUNTON, J. L. & READ, R. J. 1998. Structure of the shiga-like toxin I B-pentamer complexed with an analogue of its receptor Gb3. *Biochemistry,* 37, 1777-88.

LING, Z., DAYONG, C., DENGGAO, Y., YITING, W., LIAOQIONG, F. & ZHIBIAO, W. 2019. *Escherichia coli* Outer Membrane Vesicles Induced DNA Double-Strand Breaks in Intestinal Epithelial Caco-2 Cells. *Med Sci Monit Basic Res,* 25**,** 45-52.

LINGWOOD, C. A., LAW, H., RICHARDSON, S., PETRIC, M., BRUNTON, J. L., DE GRANDIS, S. & KARMALI, M. 1987. Glycolipid binding of purified and recombinant *Escherichia coli* produced verotoxin in vitro. *J Biol Chem,* 262**,** 8834-9.

LIU, J., SUN, Y., FENG, S., ZHU, L., GUO, X. & QI, C. 2009. Towards an attenuated enterohemorrhagic *Escherichia coli* O157:H7 vaccine characterized by a deleted *ler* gene and containing apathogenic Shiga toxins. *Vaccine,* 27, 5929-35.

LOOS, S., AHLENSTIEL, T., KRANZ, B., STAUDE, H., PAPE, L., HÄRTEL, C., VESTER, U., BUCHTALA, L., BENZ, K., HOPPE, B., BERINGER, O., KRAUSE, M., MÜLLER, D., POHL, M., LEMKE, J., HILLEBRAND, G., KREUZER, M., KÖNIG, J., WIGGER, M., KONRAD, M., HAFFNER, D., OH, J. & KEMPER, M. J. 2012. An outbreak of Shiga toxin-producing *Escherichia coli* O104:H4 hemolytic uremic syndrome in Germany: presentation and short-term outcome in children. *Clin Infect Dis,* 55, 753-9.

LOOS, S., AULBERT, W., HOPPE, B., AHLENSTIEL-GRUNOW, T., KRANZ, B., WAHL, C., STAUDE, H., HUMBERG, A., BENZ, K., KRAUSE, M., POHL, M., LIEBAU, M. C., SCHILD, R., LEMKE, J., BERINGER, O., MÜLLER, D., HÄRTEL, C., WIGGER, M., VESTER, U., KONRAD, M., HAFFNER, D., PAPE, L., OH, J. & KEMPER, M. J. 2017. Intermediate Follow-up of Pediatric Patients With Hemolytic Uremic Syndrome During the 2011 Outbreak Caused by *E. coli* O104:H4. *Clin Infect Dis,* 64, 1637-1643.

LOPEZ, E. L., CONTRINI, M. M., GLATSTEIN, E., GONZALEZ AYALA, S., SANTORO, R., ALLENDE, D., EZCURRA, G., TEPLITZ, E., KOYAMA, T., MATSUMOTO, Y., SATO, H., SAKAI, K., HOSHIDE, S., KOMORIYA, K., MORITA, T., HARNING, R. & BROOKMAN, S. 2010. Safety and pharmacokinetics of urtoxazumab, a humanized monoclonal antibody, against Shiga-like toxin 2 in healthy adults and in pediatric patients infected with Shiga-like toxin-producing *Escherichia coli*. *Antimicrob Agents Chemother,* 54**,** 239-43.

LOUIS, P. & FLINT, H. J. 2009. Diversity, metabolism and microbial ecology of butyrate-producing bacteria from the human large intestine. *FEMS Microbiol Lett,* 294, 1-8.

LOUIS, P. & FLINT, H. J. 2017. Formation of propionate and butyrate by the human colonic microbiota. *Environ Microbiol,* 19**,** 29-41.

LOŚ, J. M., LOŚ, M., WEGRZYN, A. & WEGRZYN, G. 2010. Hydrogen peroxide-mediated induction of the Shiga toxin-converting lambdoid prophage ST2-8624 in *Escherichia coli* O157:H7. *FEMS Immunol Med Microbiol.* England.

LU, S., GOUGH, A. W., BOBROWSKI, W. F. & STEWART, B. H. 1996. Transport properties are not altered across Caco-2 cells with heightened TEER despite underlying physiological and ultrastructural changes. *J Pharm Sci,* 85, 270-3.

LUKE, C. J. & PENN, C. W. 1995. Identification of a 29 kDa flagellar sheath protein in *Helicobacter pylori* using a murine monoclonal antibody. *Microbiology,* 141 (Pt 3)**,** 597-604.

LUKJANCENKO, O., WASSENAAR, T. M. & USSERY, D. W. 2010. Comparison of 61 sequenced *Escherichia coli* genomes. *Microb Ecol,* 60**,** 708-20.

LUKYANENKO, V., MALYUKOVA, I., HUBBARD, A., DELANNOY, M., BOEDEKER, E., ZHU, C., CEBOTARU, L. & KOVBASNJUK, O. 2011. Enterohemorrhagic *Escherichia coli* infection stimulates Shiga toxin 1 macropinocytosis and transcytosis across intestinal epithelial cells. *Am J Physiol Cell Physiol,* 301**,** C1140-9.

LULEVICH, V., SHIH, Y. P., LO, S. H. & LIU, G. Y. 2009. Cell tracing dyes significantly change single cell mechanics. *J Phys Chem B,* 113**,** 6511-9.

LUND, P., TRAMONTI, A. & DE BIASE, D. 2014. Coping with low pH: molecular strategies in neutralophilic bacteria. *FEMS Microbiol Rev,* 38**,** 1091-125.

LUZADER, D. H., CLARK, D. E., GONYAR, L. A. & KENDALL, M. M. 2013. EutR is a direct regulator of genes that contribute to metabolism and virulence in enterohemorrhagic *Escherichia coli* O157:H7. *J Bacteriol,* 195**,** 4947-53.

LYTE, M., ARULANANDAM, B., NGUYEN, K., FRANK, C., ERICKSON, A. & FRANCIS, D. 1997. Norepinephrine induced growth and expression of virulence associated factors in enterotoxigenic and enterohemorrhagic strains of *Escherichia coli*. *Adv Exp Med Biol,* 412**,** 331-9.

LYTE, M. & BAILEY, M. T. 1997. Neuroendocrine-bacterial interactions in a neurotoxin-induced model of trauma. *J Surg Res,* 70, 195-201.

LYTE, M., FRANK, C. D. & GREEN, B. T. 1996. Production of an autoinducer of growth by norepinephrine cultured *Escherichia coli* O157:H7. *FEMS Microbiol Lett,* 139**,** 155-9.

MA, D., COOK, D. N., ALBERTI, M., PON, N. G., NIKAIDO, H. & HEARST, J. E. 1995. Genes *acrA* and *acrB* encode a stress-induced efflux system of *Escherichia coli*. *Mol Microbiol,* 16**,** 45-55.

MACDONALD, I. A. & KUEHN, M. J. 2013. Stress-Induced Outer Membrane Vesicle Production by *Pseudomonas aeruginosa*. *Journal of Bacteriology,* 195**,** 2971-2981.

MADARA, J. L., STAFFORD, J., DHARMSATHAPHORN, K. & CARLSON, S. 1987. Structural analysis of a human intestinal epithelial cell line. *Gastroenterology,* 95, 1133-45.

MAHAJAN, A., CURRIE, C. G., MACKIE, S., TREE, J., MCATEER, S., MCKENDRICK, I., MCNEILLY, T. N., ROE, A., LA RAGIONE, R. M., WOODWARD, M. J., GALLY, D.

L. & SMITH, D. G. 2009. An investigation of the expression and adhesin function of H7 flagella in the interaction of *Escherichia coli* O157 : H7 with bovine intestinal epithelium. *Cell Microbiol,* 11, 121-37.

MAJOWICZ, S. E., SCALLAN, E., JONES-BITTON, A., SARGEANT, J. M., STAPLETON, J., ANGULO, F. J., YEUNG, D. H. & KIRK, M. D. 2014. Global incidence of human Shiga toxin-producing *Escherichia coli* infections and deaths: a systematic review and knowledge synthesis. *Foodborne Pathog Dis,* 11**,** 447-55.

MALTBY, R., LEATHAM-JENSEN, M. P., GIBSON, T., COHEN, P. S. & CONWAY, T. 2013. Nutritional basis for colonization resistance by human commensal *Escherichia coli* strains HS and Nissle 1917 against *E. coli* O157:H7 in the mouse intestine. *PLoS One,* 8**,** e53957.

MALUYKOVA, I., GUTSAL, O., LAIKO, M., KANE, A., DONOWITZ, M. & KOVBASNJUK, O. 2008. Latrunculin B facilitates Shiga toxin 1 transcellular transcytosis across T84 intestinal epithelial cells. *Biochim Biophys Acta,* 1782**,** 370-7.

MALYUKOVA, I., MURRAY, K. F., ZHU, C., BOEDEKER, E., KANE, A., PATTERSON, K., PETERSON, J. R., DONOWITZ, M. & KOVBASNJUK, O. 2009. Macropinocytosis in Shiga toxin 1 uptake by human intestinal epithelial cells and transcellular transcytosis. *Am J Physiol Gastrointest Liver Physiol,* 296**,** G78-92.

MANABE, T., KATO, M., UENO, T. & KAWASAKI, K. 2013. Flagella proteins contribute to the production of outer membrane vesicles from *Escherichia coli* W3110. *Biochem Biophys Res Commun,* 441, 151-6.

MANNING, A. J. & KUEHN, M. J. 2011. Contribution of bacterial outer membrane vesicles to innate bacterial defense. *BMC Microbiol,* 11**,** 258.

MARCHIANDO, A. M., GRAHAM, W. V. & TURNER, J. R. 2010. Epithelial barriers in homeostasis and disease. *Annu Rev Pathol,* 5**,** 119-44.

MAREDIA, R., DEVINENI, N., LENTZ, P., DALLO, S. F., YU, J., GUENTZEL, N., CHAMBERS, J., ARULANANDAM, B., HASKINS, W. E. & WEITAO, T. 2012. Vesiculation from *Pseudomonas aeruginosa* under SOS. *ScientificWorldJournal,* 2012**,** 402919.

MARTEYN, B., SCORZA, F. B., SANSONETTI, P. J. & TANG, C. 2011. Breathing life into pathogens: the influence of oxygen on bacterial virulence and host responses in the gastrointestinal tract. *Cell Microbiol,* 13**,** 171-6.

MASHBURN, L. M. & WHITELEY, M. 2005. Membrane vesicles traffic signals and facilitate group activities in a prokaryote. *Nature,* 437, 422-5.

MASHBURN-WARREN, L. M. & WHITELEY, M. 2006. Special delivery: vesicle trafficking in prokaryotes. *Mol Microbiol,* 61**,** 839-46.

MATHEW, B. & NAGARAJ, R. 2017. Variations in the interaction of human defensins with *Escherichia coli*: Possible implications in bacterial killing. *PLoS One,* 12**,** e0175858.

MCBROOM, A. J., JOHNSON, A. P., VEMULAPALLI, S. & KUEHN, M. J. 2006. Outer membrane vesicle production by *Escherichia coli* is independent of membrane instability. *J Bacteriol,* 188**,** 5385-92.

MCBROOM, A. J. & KUEHN, M. J. 2007. Release of outer membrane vesicles by Gram-negative bacteria is a novel envelope stress response. *Mol Microbiol,* 63**,** 545-58.

MCCAIG, W. D., KOLLER, A. & THANASSI, D. G. 2013. Production of outer membrane vesicles and outer membrane tubes by *Francisella novicida*. *J Bacteriol,* 195**,** 1120-32.

MCDANIEL, T. K., JARVIS, K. G., DONNENBERG, M. S. & KAPER, J. B. 1995. A genetic locus of enterocyte effacement conserved among diverse enterobacterial pathogens. *Proc Natl Acad Sci U S A,* 92**,** 1664-8.

MCGANNON, C. M., FULLER, C. A. & WEISS, A. A. 2010. Different classes of antibiotics differentially influence shiga toxin production. *Antimicrob Agents Chemother,* 54**,** 3790-8.

MCGUCKIN, M. A., LINDÉN, S. K., SUTTON, P. & FLORIN, T. H. 2011. Mucin dynamics and enteric pathogens. *Nat Rev Microbiol,* 9, 265-78.

MELLIES, J. L., ELLIOTT, S. J., SPERANDIO, V., DONNENBERG, M. S. & KAPER, J. B. 1999. The Per regulon of enteropathogenic *Escherichia coli* : identification of a regulatory cascade and a novel transcriptional activator, the locus of enterocyte effacement (LEE)-encoded regulator (Ler). *Mol Microbiol,* 33, 296-306.

MELLOR, G. E., FEGAN, N., DUFFY, L. L., MC, M. K., JORDAN, D. & BARLOW, R. S. 2016. National Survey of Shiga Toxin-Producing *Escherichia coli* Serotypes O26, O45, O103, O111, O121, O145, and O157 in Australian Beef Cattle Feces. *J Food Prot,* 79**,** 1868-1874.

MELSON, E. M. & KENDALL, M. M. 2019. The sRNA DicF integrates oxygen sensing to enhance enterohemorrhagic *Escherichia coli* virulence via distinctive RNA control mechanisms. *Proc Natl Acad Sci U S A,* 116**,** 14210-14215.

MELTON-CELSA, A. R. 2014. Shiga Toxin (Stx) Classification, Structure, and Function. *Microbiol Spectr,* 2**,** EHEC-0024-2013.

MERLIN, C., MASTERS, M., MCATEER, S. & COULSON, A. 2003. Why is carbonic anhydrase essential to *Escherichia coli*? *J Bacteriol,* 185**,** 6415-24.

MERRITT, M. E. & DONALDSON, J. R. 2009. Effect of bile salts on the DNA and membrane integrity of enteric bacteria. *J Med Microbiol,* 58**,** 1533-1541.

MODY, R. K., GU, W., GRIFFIN, P. M., JONES, T. F., ROUNDS, J., SHIFERAW, B., TOBIN-D'ANGELO, M., SMITH, G., SPINA, N., HURD, S., LATHROP, S., PALMER, A., BOOTHE, E., LUNA-GIERKE, R. E. & HOEKSTRA, R. M. 2015. Postdiarrheal hemolytic uremic syndrome in United States children: clinical spectrum and predictors of in-hospital death. *J Pediatr,* 166, 1022-9.

MOON, H. W., WHIPP, S. C., ARGENZIO, R. A., LEVINE, M. M. & GIANNELLA, R. A. 1983. Attaching and effacing activities of rabbit and human enteropathogenic *Escherichia coli* in pig and rabbit intestines. *Infect Immun,* 41**,** 1340-51.

MOR, M. & ASHKENAZI, S. 2014. The dilemma of antimicrobial treatment of Shiga toxin-producing *Escherichia coli*. *Pediatr Infect Dis J,* 33, 979-81.

MORGAN, G. M., NEWMAN, C., PALMER, S. R., ALLEN, J. B., SHEPHERD, W., RAMPLING, A. M., WARREN, R. E., GROSS, R. J., SCOTLAND, S. M. & SMITH, H. R. 1988. First recognized community outbreak of haemorrhagic colitis due to verotoxin-producing *Escherichia coli* O 157.H7 in the UK. *Epidemiol Infect,* 101**,** 83-91.

MORGAN, J. K., CARROLL, R. K., HARRO, C. M., VENDURA, K. W., SHAW, L. N. & RIORDAN, J. T. 2016. Global Regulator of Virulence A (GrvA) Coordinates Expression of Discrete Pathogenic Mechanisms in Enterohemorrhagic *Escherichia coli* through Interactions with GadW-GadE. *J Bacteriol,* 198**,** 394-409.

MORGAN, J. K., VENDURA, K. W., STEVENS, S. M. & RIORDAN, J. T. 2013. RcsB determines the locus of enterocyte effacement (LEE) expression and adherence phenotype of *Escherichia coli* O157 : H7 spinach outbreak strain TW14359 and coordinates bicarbonate-dependent LEE activation with repression of motility. *Microbiology (Reading),* 159**,** 2342-2353.

MOXLEY, R. A., FRANCIS, D. H., TAMURA, M., MARX, D. B., SANTIAGO-MATEO, K. & ZHAO, M. 2017. Efficacy of Urtoxazumab (TMA-15 Humanized Monoclonal Antibody Specific for Shiga Toxin 2) Against Post-Diarrheal Neurological Sequelae Caused by *Escherichia coli* O157:H7 Infection in the Neonatal Gnotobiotic Piglet Model. *Toxins (Basel),* 9.

MULCAHY, L. A., PINK, R. C. & CARTER, D. R. 2014. Routes and mechanisms of extracellular vesicle uptake. *J Extracell Vesicles,* 3.

MUNIZ, L. R., KNOSP, C. & YERETSSIAN, G. 2012. Intestinal antimicrobial peptides during homeostasis, infection, and disease. *Front Immunol,* 3**,** 310.

MÜHLDORFER, I., HACKER, J., KEUSCH, G. T., ACHESON, D. W., TSCHÄPE, H., KANE, A. V., RITTER, A., OLSCHLÄGER, T. & DONOHUE-ROLFE, A. 1996. Regulation of the Shiga-like toxin II operon in *Escherichia coli*. *Infect Immun,* 64**,** 495-502.

MÜLLER, S. K., WILHELM, I., SCHUBERT, T., ZITTLAU, K., IMBERTY, A., MADL, J., EIERHOFF, T., THUENAUER, R. & RÖMER, W. 2017. Gb3-binding lectins as potential carriers for transcellular drug delivery. *Expert Opin Drug Deliv,* 14**,** 141-153.

MÜSKEN, A., BIELASZEWSKA, M., GREUNE, L., SCHWEPPE, C. H., MÜTHING, J., SCHMIDT, H., SCHMIDT, M. A., KARCH, H. & ZHANG, W. 2008. Anaerobic conditions promote expression of Sfp fimbriae and adherence of sorbitol-fermenting enterohemorrhagic *Escherichia coli* O157:NM to human intestinal epithelial cells. *Appl Environ Microbiol,* 74**,** 1087-93.

NAKAJIMA, H., KIYOKAWA, N., KATAGIRI, Y. U., TAGUCHI, T., SUZUKI, T., SEKINO, T., MIMORI, K., EBATA, T., SAITO, M., NAKAO, H., TAKEDA, T. & FUJIMOTO, J. 2001. Kinetic analysis of binding between Shiga toxin and receptor glycolipid Gb3Cer by surface plasmon resonance. *J Biol Chem,* 276, 42915-22.

NAKANISHI, N., TASHIRO, K., KUHARA, S., HAYASHI, T., SUGIMOTO, N. & TOBE, T. 2009. Regulation of virulence by butyrate sensing in enterohaemorrhagic *Escherichia coli*. *Microbiology (Reading),* 155**,** 521-530.

NAVARRO-GARCIA, F. 2014. *Escherichia coli* O104:H4 Pathogenesis: an Enteroaggregative *E. coli*/Shiga Toxin-Producing *E. coli* Explosive Cocktail of High Virulence. *Microbiol Spectr,* 2.

NAYLOR, S. W., LOW, J. C., BESSER, T. E., MAHAJAN, A., GUNN, G. J., PEARCE, M. C., MCKENDRICK, I. J., SMITH, D. G. & GALLY, D. L. 2003. Lymphoid follicle-dense mucosa at the terminal rectum is the principal site of colonization of enterohemorrhagic *Escherichia coli* O157:H7 in the bovine host. *Infect Immun,* 71**,** 1505-12.

NEELY, M. N. & FRIEDMAN, D. I. 1998. Functional and genetic analysis of regulatory regions of coliphage H-19B: location of shiga-like toxin and lysis genes suggest a role for phage functions in toxin release. *Mol Microbiol,* 28**,** 1255-67.

NEWTON, H. J., PEARSON, J. S., BADEA, L., KELLY, M., LUCAS, M., HOLLOWAY, G., WAGSTAFF, K. M., DUNSTONE, M. A., SLOAN, J., WHISSTOCK, J. C., KAPER, J. B., ROBINS-BROWNE, R. M., JANS, D. A., FRANKEL, G., PHILLIPS, A. D.,

COULSON, B. S. & HARTLAND, E. L. 2010. The type III effectors NleE and NleB from enteropathogenic *E. coli* and OspZ from *Shigella* block nuclear translocation of NF-kappaB p65. *PLoS Pathog,* 6**,** e1000898.

NGUYEN, Y. & SPERANDIO, V. 2012. Enterohemorrhagic *E. coli* (EHEC) pathogenesis. *Front Cell Infect Microbiol,* 2**,** 90.

NJOROGE, J. & SPERANDIO, V. 2012. Enterohemorrhagic *Escherichia coli* virulence regulation by two bacterial adrenergic kinases, QseC and QseE. *Infect Immun,* 80**,** 688-703.

NJOROGE, J. W., GRUBER, C. & SPERANDIO, V. 2013. The interacting Cra and KdpE regulators are involved in the expression of multiple virulence factors in enterohemorrhagic *Escherichia coli*. *J Bacteriol,* 195**,** 2499-508.

NJOROGE, J. W., NGUYEN, Y., CURTIS, M. M., MOREIRA, C. G. & SPERANDIO, V. 2012. Virulence meets metabolism: Cra and KdpE gene regulation in enterohemorrhagic *Escherichia coli*. *mBio,* 3**,** e00280-12.

O'BRIEN, A. D. & LAVECK, G. D. 1983. Purification and characterization of a *Shigella dysenteriae* 1-like toxin produced by *Escherichia coli*. *Infect Immun,* 40**,** 675-83.

O'BRIEN, A. D., LAVECK, G. D., THOMPSON, M. R. & FORMAL, S. B. 1982. Production of *Shigella dysenteriae* type 1-like cytotoxin by *Escherichia coli*. *J Infect Dis,* 146**,** 763-9.

O'BRIEN, A. D., NEWLAND, J. W., MILLER, S. F., HOLMES, R. K., SMITH, H. W. & FORMAL, S. B. 1984. Shiga-like toxin-converting phages from *Escherichia coli* strains that cause hemorrhagic colitis or infantile diarrhea. *Science,* 226**,** 694-6.

O'DONOGHUE, E. J. & KRACHLER, A. M. 2016. Mechanisms of outer membrane vesicle entry into host cells. *Cell Microbiol,* 18**,** 1508-1517.

O'NEIL, D. A., PORTER, E. M., ELEWAUT, D., ANDERSON, G. M., ECKMANN, L., GANZ, T. & KAGNOFF, M. F. 1999. Expression and regulation of the human beta-defensins hBD-1 and hBD-2 in intestinal epithelium. *J Immunol,* 163, 6718-24.

OBATA, F., TOHYAMA, K., BONEV, A. D., KOLLING, G. L., KEEPERS, T. R., GROSS, L. K., NELSON, M. T., SATO, S. & OBRIG, T. G. 2008. Shiga Toxin 2 Affects the Central Nervous System Through Receptor Gb(3) Localized to Neurons. *The Journal of infectious diseases,* 198**,** 1398-1406.

OBRIG, T. G. 2010. *Escherichia coli* Shiga Toxin Mechanisms of Action in Renal Disease. *Toxins (Basel),* 2**,** 2769-2794.

ODUMOSU, O., NICHOLAS, D., YANO, H. & LANGRIDGE, W. 2010. AB toxins: a paradigm switch from deadly to desirable. *Toxins (Basel),* 2**,** 1612-45.

OGASAWARA, T., ITO, K., IGARASHI, K., YUTSUDO, T., NAKABAYASHI, N. & TAKEDA, Y. 1988. Inhibition of protein synthesis by a Vero toxin (VT2 or Shiga-like toxin II) produced by *Escherichia coli* O157:H7 at the level of elongation factor 1-dependent aminoacyl-tRNA binding to ribosomes. *Microb Pathog,* 4, 127-35.

OLIVEIRA, A. F., CARDOSO, S. A., ALMEIDA, F. B., DE OLIVEIRA, L. L., PITONDO-SILVA, A., SOARES, S. G. & HANNA, E. S. 2012. Oral immunization with attenuated Salmonella vaccine expressing *Escherichia coli* O157:H7 intimin gamma triggers both systemic and mucosal humoral immunity in mice. *Microbiol Immunol,* 56**,** 513-22.

OLOFSSON, A., NYGÅRD SKALMAN, L., OBI, I., LUNDMARK, R. & ARNQVIST, A. 2014. Uptake of *Helicobacter pylori* vesicles is facilitated by clathrin-dependent and clathrin-independent endocytic pathways. *mBio,* 5**,** e00979-14.

OMISAKIN, F., MACRAE, M., OGDEN, I. D. & STRACHAN, N. J. 2003. Concentration and prevalence of *Escherichia coli* O157 in cattle feces at slaughter. *Appl Environ Microbiol,* 69**,** 2444-7.

ORENCH-RIVERA, N. & KUEHN, M. J. 2016. Environmentally controlled bacterial vesicle-mediated export. *Cell Microbiol,* 18**,** 1525-1536.

ORSKOV F., O. I. 1984. Serotyping of *Escherichia coli. Methods in Microbiology*, 43-113.

ORSKOV, I., ORSKOV, F., JANN, B. & JANN, K. 1977. Serology, chemistry, and genetics of O and K antigens of *Escherichia coli*. *Bacteriol Rev,* 41**,** 667-710.

ORTH, D., GRIF, K., KHAN, A. B., NAIM, A., DIERICH, M. P. & WURZNER, R. 2007. The Shiga toxin genotype rather than the amount of Shiga toxin or the cytotoxicity of Shiga toxin in vitro correlates with the appearance of the hemolytic uremic syndrome. *Diagn Microbiol Infect Dis,* 59**,** 235-42.

OSAWA, R. O., IYODA, S., NAKAYAMA, S. I., WADA, A., YAMAI, S. & WATANABE, H. 2000. Genotypic variations of Shiga toxin-converting phages from enterohaemorrhagic *Escherichia coli* O157: H7 isolates. *J Med Microbiol,* 49**,** 565-574.

OU, G., BARANOV, V., LUNDMARK, E., HAMMARSTRÖM, S. & HAMMARSTRÖM, M. L. 2009. Contribution of intestinal epithelial cells to innate immunity of the human gut--studies on polarized monolayers of colon carcinoma cells. *Scand J Immunol.* England.

PACHECO, A. R., CURTIS, M. M., RITCHIE, J. M., MUNERA, D., WALDOR, M. K., MOREIRA, C. G. & SPERANDIO, V. 2012. Fucose sensing regulates bacterial intestinal colonization. *Nature,* 492**,** 113-117.

PACHECO, A. R. & SPERANDIO, V. 2012. Shiga toxin in enterohemorrhagic *E.coli*: regulation and novel anti-virulence strategies. *Front Cell Infect Microbiol,* 2**,** 81.

PAI, C. H., KELLY, J. K. & MEYERS, G. L. 1986. Experimental infection of infant rabbits with verotoxin-producing *Escherichia coli*. *Infect Immun,* 51**,** 16-23.

PALMELA, C., CHEVARIN, C., XU, Z., TORRES, J., SEVRIN, G., HIRTEN, R., BARNICH, N., NG, S. C. & COLOMBEL, J. F. 2018. Adherent-invasive *Escherichia coli* in inflammatory bowel disease. *Gut,* 67, 574-587.

PANDA, A., TATAROV, I., MELTON-CELSA, A. R., KOLAPPASWAMY, K., KRIEL, E. H., PETKOV, D., COKSAYGAN, T., LIVIO, S., MCLEOD, C. G., NATARO, J. P., O'BRIEN, A. D. & DETOLLA, L. J. 2010. *Escherichia coli* O157:H7 infection in Dutch belted and New Zealand white rabbits. *Comp Med,* 60**,** 31-7.

PAPE, L., HARTMANN, H., BANGE, F. C., SUERBAUM, S., BUELTMANN, E. & AHLENSTIEL-GRUNOW, T. 2015. Eculizumab in Typical Hemolytic Uremic Syndrome (HUS) With Neurological Involvement. *Medicine,* 94**,** e1000.

PAPENFORT, K. & BASSLER, B. L. 2016. Quorum sensing signal-response systems in Gram-negative bacteria. *Nat Rev Microbiol,* 14**,** 576-88.

PARKER, H., CHITCHOLTAN, K., HAMPTON, M. B. & KEENAN, J. I. 2010. Uptake of *Helicobacter pylori* outer membrane vesicles by gastric epithelial cells. *Infect Immun,* 78**,** 5054-61.

PARSONS, L. M., LIN, F. & ORBAN, J. 2006. Peptidoglycan recognition by Pal, an outer membrane lipoprotein. *Biochemistry,* 45**,** 2122-8.

PELEMAN, C., CAMILLERI, M., BUSCIGLIO, I., BURTON, D., DONATO, L. & ZINSMEISTER, A. R. 2017. Colonic Transit and Bile Acid Synthesis or Excretion in Patients With Irritable Bowel Syndrome-Diarrhea Without Bile Acid Malabsorption. *Clin Gastroenterol Hepatol,* 15**,** 720-727 e1.

PENADÉS, J. R., CHEN, J., QUILES-PUCHALT, N., CARPENA, N. & NOVICK, R. P. 2015. Bacteriophage-mediated spread of bacterial virulence genes. *Curr Opin Microbiol,* 23, 171-8.

PENDERS, J., THIJS, C., VINK, C., STELMA, F. F., SNIJDERS, B., KUMMELING, I., VAN DEN BRANDT, P. A. & STOBBERINGH, E. E. 2006. Factors influencing the composition of the intestinal microbiota in early infancy. *Pediatrics,* 118, 511-21.

PERNA, N. T., MAYHEW, G. F., POSFAI, G., ELLIOTT, S., DONNENBERG, M. S., KAPER, J. B. & BLATTNER, F. R. 1998. Molecular evolution of a pathogenicity island from enterohemorrhagic *Escherichia coli* O157:H7. *Infect Immun,* 66**,** 3810-7.

PETTIT, R. K. & JUDD, R. C. 1992. The interaction of naturally elaborated blebs from serum-susceptible and serum-resistant strains of *Neisseria gonorrhoeae* with normal human serum. *Mol Microbiol,* 6**,** 729-34.

PETTY, N. K., BULGIN, R., CREPIN, V. F., CERDENO-TARRAGA, A. M., SCHROEDER, G. N., QUAIL, M. A., LENNARD, N., CORTON, C., BARRON, A., CLARK, L., TORIBIO, A. L., PARKHILL, J., DOUGAN, G., FRANKEL, G. & THOMSON, N. R. 2010. The *Citrobacter rodentium* genome sequence reveals convergent evolution with human pathogenic *Escherichia coli*. *J Bacteriol,* 192**,** 525-38.

PHILLIPS, A., NAVABPOUR, S., HICKS, S., DOUGAN, G., WALLIS, T. & FRANKEL, G. 2000. Enterohaemorrhagic *Escherichia coli* O157:H7 target Peyer's patches in humans and cause attaching/effacing lesions in both human and bovine intestine. *Gut,* 47**,** 377-381.

PHILPOTT, D. J., ACKERLEY, C. A., KILIAAN, A. J., KARMALI, M. A., PERDUE, M. H. & SHERMAN, P. M. 1997. Translocation of verotoxin-1 across T84 monolayers: mechanism of bacterial toxin penetration of epithelium. *Am J Physiol,* 273**,** G1349-58.

PHILPOTT, D. J., MCKAY, D. M., MAK, W., PERDUE, M. H. & SHERMAN, P. M. 1998. Signal transduction pathways involved in enterohemorrhagic *Escherichia coli*-induced alterations in T84 epithelial permeability. *Infect Immun,* 66**,** 1680-7.

PINAUD, L., SANSONETTI, P. J & PHALIPON, A. 2018. Host cell targeting by enteropathogenic bacteria TT3SS effectors. *Trends Microbiol*, 26, 266-283.

PLUZNICK, J. L. 2016. Gut microbiota in renal physiology: focus on short-chain fatty acids and their receptors. *Kidney Int,* 90**,** 1191-1198.

POHLENZ, J. F., WINTER, K. R. & DEAN-NYSTROM, E. A. 2005. Shiga-toxigenic *Escherichia coli*-inoculated neonatal piglets develop kidney lesions that are comparable to those in humans with hemolytic-uremic syndrome. *Infect Immun,* 73**,** 612-6.

POLLAK, C. N., DELPINO, M. V., FOSSATI, C. A. & BALDI, P. C. 2012. Outer membrane vesicles from *Brucella abortus* promote bacterial internalization by human monocytes and modulate their innate immune response. *PLoS One,* 7**,** e50214.

POLZIN, S., HUBER, C., EYLERT, E., ELSENHANS, I., EISENREICH, W. & SCHMIDT, H. 2013. Growth media simulating ileal and colonic environments affect the intracellular proteome and carbon fluxes of enterohemorrhagic *Escherichia coli* O157:H7 strain EDL933. *Appl Environ Microbiol,* 79**,** 3703-15.

POTTER, M. E., KAUFMANN, A. F., THOMASON, B. M., BLAKE, P. A. & FARMER, J. J., 3RD 1985. Diarrhea due to *Escherichia coli* O157:H7 in the infant rabbit. *J Infect Dis,* 152**,** 1341-3.

PRETA, G., CRONIN, J. G. & SHELDON, I. M. 2015. Dynasore - not just a dynamin inhibitor. *Cell Commun Signal,* 13**,** 24.

PRIETO, A. I., RAMOS-MORALES, F. & CASADESUS, J. 2004. Bile-induced DNA damage in *Salmonella enterica*. *Genetics,* 168**,** 1787-94.

PRUIMBOOM-BREES, I. M., MORGAN, T. W., ACKERMANN, M. R., NYSTROM, E. D., SAMUEL, J. E., CORNICK, N. A. & MOON, H. W. 2000. Cattle lack vascular receptors for *Escherichia coli* O157:H7 Shiga toxins. *Proc Natl Acad Sci U S A,* 97**,** 10325-9.

PÉREZ-CRUZ, C., CARRIÓN, O., DELGADO, L., MARTINEZ, G., LÓPEZ-IGLESIAS, C. & MERCADE, E. 2013. New type of outer membrane vesicle produced by the Gram-negative bacterium *Shewanella vesiculosa* M7T: implications for DNA content. *Appl Environ Microbiol,* 79**,** 1874-81.

PUBLIC HEALTH ENGLAND. 2020. Research and analysis: Shiga toxin-producing *Escherchia coli* (STEC) data: 2018. Available at: https://www.gov.uk/government/publications/escherichia-coli-e-coli-o157-annual-totals/shiga-toxin-producing-escherichia-coli-stec-data-2018

RAKOFF-NAHOUM, S., COYNE, M. J. & COMSTOCK, L. E. 2014. An ecological network of polysaccharide utilization among human intestinal symbionts. *Curr Biol,* 24**,** 40-49.

READING, N. C., RASKO, D. A., TORRES, A. G. & SPERANDIO, V. 2009. The two-component system QseEF and the membrane protein QseG link adrenergic and stress sensing to bacterial pathogenesis. *Proc Natl Acad Sci U S A,* 106**,** 5889-94.

RENDON, M. A., SALDANA, Z., ERDEM, A. L., MONTEIRO-NETO, V., VAZQUEZ, A., KAPER, J. B., PUENTE, J. L. & GIRON, J. A. 2007. Commensal and pathogenic *Escherichia coli* use a common pilus adherence factor for epithelial cell colonization. *Proc Natl Acad Sci U S A,* 104**,** 10637-42.

REPASKE, R. & CLAYTON, M. A. 1978. Control of *Escherichia coli* growth by CO2. *J Bacteriol,* 135**,** 1162-4.

REWATKAR, P. V., PARTON, R. G., PAREKH, H. S. & PARAT, M. O. 2015. Are caveolae a cellular entry route for non-viral therapeutic delivery systems? *Adv Drug Deliv Rev,* 91, 92-108.

RICCI, V., CHIOZZI, V., NECCHI, V., OLDANI, A., ROMANO, M., SOLCIA, E. & VENTURA, U. 2005. Free-soluble and outer membrane vesicle-associated VacA from Helicobacter pylori: Two forms of release, a different activity. *Biochem Biophys Res Commun,* 337, 173-8.

RICHARD, H. & FOSTER, J. W. 2004. *Escherichia coli* glutamate- and arginine-dependent acid resistance systems increase internal pH and reverse transmembrane potential. *J Bacteriol,* 186**,** 6032-41.

RIDLON, J. M., KANG, D. J. & HYLEMON, P. B. 2006. Bile salt biotransformations by human intestinal bacteria. *J Lipid Res,* 47**,** 241-59.

RIETHORST, D., MOLS, R., DUCHATEAU, G., TACK, J., BROUWERS, J. & AUGUSTIJNS, P. 2016. Characterization of Human Duodenal Fluids in Fasted and Fed State Conditions. *J Pharm Sci,* 105, 673-681.

RILEY, L. W., REMIS, R. S., HELGERSON, S. D., MCGEE, H. B., WELLS, J. G., DAVIS, B. R., HEBERT, R. J., OLCOTT, E. S., JOHNSON, L. M., HARGRETT, N. T., BLAKE, P. A. & COHEN, M. L. 1983. Hemorrhagic colitis associated with a rare *Escherichia coli* serotype. *N Engl J Med,* 308**,** 681-5.

RIQUELME-NEIRA, R., RIVERA, A., SAEZ, D., FERNANDEZ, P., OSORIO, G., DEL CANTO, F., SALAZAR, J. C., VIDAL, R. M. & ONATE, A. 2015. Vaccination with DNA Encoding Truncated Enterohemorrhagic *Escherichia coli* (EHEC) Factor for Adherence-1 Gene (efa-1') Confers Protective Immunity to Mice Infected with *E. coli* O157:H7. *Front Cell Infect Microbiol,* 5**,** 104.

RITCHIE, J. M., BRADY, M. J., RILEY, K. N., HO, T. D., CAMPELLONE, K. G., HERMAN, I. M., DONOHUE-ROLFE, A., TZIPORI, S., WALDOR, M. K. & LEONG, J. M. 2008. EspF(U), a type III-translocated effector of actin assembly, fosters epithelial association and late-stage intestinal colonization by *E. coli* O157:H7. *Cellular microbiology,* 10**,** 836-847.

RITCHIE, J. M., THORPE, C. M., ROGERS, A. B. & WALDOR, M. K. 2003. Critical Roles for *stx(2)*, *eae*, and *tir* in Enterohemorrhagic *Escherichia coli*-Induced Diarrhea and Intestinal Inflammation in Infant Rabbits. *Infection and Immunity,* 71**,** 7129-7139.

RITCHIE, J. M. & WALDOR, M. K. 2005. The locus of enterocyte effacement-encoded effector proteins all promote enterohemorrhagic *Escherichia coli* pathogenicity in infant rabbits. *Infect Immun,* 73**,** 1466-74.

RIZZONI, G., CLARIS-APPIANI, A., EDEFONTI, A., FACCHIN, P., FRANCHINI, F., GUSMANO, R., IMBASCIATI, E., PAVANELLO, L., PERFUMO, F. & REMUZZI, G. 1988. Plasma infusion for hemolytic-uremic syndrome in children: results of a multicenter controlled trial. *J Pediatr,* 112, 284-90.

ROBINS-BROWNE, R. M., HOLT, K. E., INGLE, D. J., HOCKING, D. M., YANG, J. & TAUSCHEK, M. 2016. Are *Escherichia coli* Pathotypes Still Relevant in the Era of Whole-Genome Sequencing? *Front Cell Infect Microbiol,* 6**,** 141.

RODRIGUEZ-BELTRAN, J., RODRIGUEZ-ROJAS, A., GUELFO, J. R., COUCE, A. & BLAZQUEZ, J. 2012. The *Escherichia coli* SOS gene dinF protects against oxidative stress and bile salts. *PLoS One,* 7**,** e34791.

ROHATGI, R., NOLLAU, P., HO, H. Y., KIRSCHNER, M. W. & MAYER, B. J. 2001. Nck and phosphatidylinositol 4,5-bisphosphate synergistically activate actin polymerization through the N-WASP-Arp2/3 pathway. *J Biol Chem,* 276**,** 26448-52.

ROIER, S., ZINGL, F. G., CAKAR, F., DURAKOVIC, S., KOHL, P., EICHMANN, T. O., KLUG, L., GADERMAIER, B., WEINZERL, K., PRASSL, R., LASS, A., DAUM, G., REIDL, J., FELDMAN, M. F. & SCHILD, S. 2016. A novel mechanism for the biogenesis of outer membrane vesicles in Gram-negative bacteria. *Nat Commun,* 7**,** 10515.

ROJAS-LOPEZ, M., MARTINELLI, M., BRANDI, V., JUBELIN, G., POLTICELLI, F., SORIANI, M., PIZZA, M., DESVAUX, M. & ROSINI, R. 2019. Identification of lipid A

deacylase as a novel, highly conserved and protective antigen against enterohemorrhagic *Escherichia coli*. *Sci Rep,* 9**,** 17014.

ROMPIKUNTAL, P. K., THAY, B., KHAN, M. K., ALANKO, J., PENTTINEN, A. M., ASIKAINEN, S., WAI, S. N. & OSCARSSON, J. 2012. Perinuclear localization of internalized outer membrane vesicles carrying active cytolethal distending toxin from *Aggregatibacter actinomycetemcomitans*. *Infect Immun,* 80**,** 31-42.

ROMPIKUNTAL, P. K., VDOVIKOVA, S., DUPERTHUY, M., JOHNSON, T. L., ÅHLUND, M., LUNDMARK, R., OSCARSSON, J., SANDKVIST, M., UHLIN, B. E. & WAI, S. N. 2015. Outer Membrane Vesicle-Mediated Export of Processed PrtV Protease from *Vibrio cholerae*. *PLoS One,* 10**,** e0134098.

ROSENBERG, E. Y., BERTENTHAL, D., NILLES, M. L., BERTRAND, K. P. & NIKAIDO, H. 2003. Bile salts and fatty acids induce the expression of *Escherichia coli* AcrAB multidrug efflux pump through their interaction with Rob regulatory protein. *Mol Microbiol,* 48, 1609-19.

ROSENSHINE, I., DONNENBERG, M. S., KAPER, J. B. & FINLAY, B. B. 1992. Signal transduction between enteropathogenic *Escherichia coli* (EPEC) and epithelial cells: EPEC induces tyrosine phosphorylation of host cell proteins to initiate cytoskeletal rearrangement and bacterial uptake. *EMBO J,* 11**,** 3551-60.

ROSENSHINE, I., RUSCHKOWSKI, S., STEIN, M., REINSCHEID, D. J., MILLS, S. D. & FINLAY, B. B. 1996. A pathogenic bacterium triggers epithelial signals to form a functional bacterial receptor that mediates actin pseudopod formation. *EMBO J,* 15**,** 2613-24.

ROSZKOWIAK, J., JAJOR, P., GUŁA, G., GUBERNATOR, J., ŻAK, A., DRULIS-KAWA, Z. & AUGUSTYNIAK, D. 2019. Interspecies Outer Membrane Vesicles (OMVs) Modulate the Sensitivity of Pathogenic Bacteria and Pathogenic Yeasts to Cationic Peptides and Serum Complement. *Int J Mol Sci,* 20.

ROWLAND, I., GIBSON, G., HEINKEN, A., SCOTT, K., SWANN, J., THIELE, I. & TUOHY, K. 2018. Gut microbiota functions: metabolism of nutrients and other food components. *Eur J Nutr,* 57**,** 1-24.

ROY, K., HAMILTON, D. J., MUNSON, G. P. & FLECKENSTEIN, J. M. 2011. Outer membrane vesicles induce immune responses to virulence proteins and protect against colonization by enterotoxigenic *Escherichia coli*. *Clin Vaccine Immunol,* 18**,** 1803-8.

RUMBO, C., FERNÁNDEZ-MOREIRA, E., MERINO, M., POZA, M., MENDEZ, J. A., SOARES, N. C., MOSQUERA, A., CHAVES, F. & BOU, G. 2011. Horizontal transfer of the OXA-24 carbapenemase gene via outer membrane vesicles: a new mechanism of dissemination of carbapenem resistance genes in *Acinetobacter baumannii*. *Antimicrob Agents Chemother,* 55**,** 3084-90.

SAGGERS, B. A. & LAWSON, D. 1966. Some observations on the penetration of antibiotics through mucus in vitro. *J Clin Pathol,* 19**,** 313-7.

SALLEE, N. A., RIVERA, G. M., DUEBER, J. E., VASILESCU, D., MULLINS, R. D., MAYER, B. J. & LIM, W. A. 2008. The pathogen protein EspFU hijacks actin polymerization using mimicry and multivalency. *Nature,* 454**,** 1005-1008.

SAMPATH, V., MCCAIG, W. D. & THANASSI, D. G. 2018. Amino acid deprivation and central carbon metabolism regulate the production of outer membrane vesicles and tubes by Francisella. *Mol Microbiol,* 107**,** 523-541.

SANDVIG, K., GARRED, O., PRYDZ, K., KOZLOV, J. V., HANSEN, S. H. & VAN DEURS, B. 1992. Retrograde transport of endocytosed Shiga toxin to the endoplasmic reticulum. *Nature,* 358**,** 510-2.

SANDVIG, K., TORGERSEN, M. L., RAA, H. A. & VAN DEURS, B. 2008. Clathrin-independent endocytosis: from nonexisting to an extreme degree of complexity. *Histochem Cell Biol,* 129**,** 267-76.

SARAFIAN, M. H., LEWIS, M. R., PECHLIVANIS, A., RALPHS, S., MCPHAIL, M. J., PATEL, V. C., DUMAS, M. E., HOLMES, E. & NICHOLSON, J. K. 2015. Bile acid profiling and quantification in biofluids using ultra-performance liquid chromatography tandem mass spectrometry. *Anal Chem,* 87**,** 9662-70.

SASLOWSKY, D. E., TE WELSCHER, Y. M., CHINNAPEN, D. J., WAGNER, J. S., WAN, J., KERN, E. & LENCER, W. I. 2013. Ganglioside GM1-mediated transcytosis of cholera toxin bypasses the retrograde pathway and depends on the structure of the ceramide domain. *J Biol Chem,* 288**,** 25804-9.

SATO, T. & CLEVERS, H. 2013. Growing self-organizing mini-guts from a single intestinal stem cell: mechanism and applications. *Science,* 340, 1190-4.

SATO, T., VRIES, R. G., SNIPPERT, H. J., VAN DE WETERING, M., BARKER, N., STANGE, D. E., VAN ES, J. H., ABO, A., KUJALA, P., PETERS, P. J. & CLEVERS, H. 2009. Single Lgr5 stem cells build crypt-villus structures *in vitro* without a mesenchymal niche. *Nature,* 459, 262-5.

SAVEYN, H., DE BAETS, B., THAS, O., HOLE, P., SMITH, J. & VAN DER MEEREN, P. 2010. Accurate particle size distribution determination by nanoparticle tracking analysis based on 2-D Brownian dynamics simulation. *J Colloid Interface Sci,* 352, 593-600.

SCALLAN, E., HOEKSTRA, R. M., ANGULO, F. J., TAUXE, R. V., WIDDOWSON, M. A., ROY, S. L., JONES, J. L. & GRIFFIN, P. M. 2011. Foodborne illness acquired in the United States--major pathogens. *Emerg Infect Dis,* 17**,** 7-15.

SCHAAR, V., NORDSTROM, T., MORGELIN, M. & RIESBECK, K. 2011. *Moraxella catarrhalis* outer membrane vesicles carry beta-lactamase and promote survival of *Streptococcus pneumoniae* and *Haemophilus influenzae* by inactivating amoxicillin. *Antimicrob Agents Chemother,* 55**,** 3845-53.

SCHAAR, V., UDDBÄCK, I., NORDSTRÖM, T. & RIESBECK, K. 2014. Group A streptococci are protected from amoxicillin-mediated killing by vesicles containing β-lactamase derived from *Haemophilus influenzae*. *J Antimicrob Chemother,* 69, 117-20.

SCHERTZER, J. W., BROWN, S. A. & WHITELEY, M. 2010. Oxygen levels rapidly modulate *Pseudomonas aeruginosa* social behaviours via substrate limitation of PqsH. *Mol Microbiol,* 77**,** 1527-38.

SCHERTZER, J. W. & WHITELEY, M. 2012. A bilayer-couple model of bacterial outer membrane vesicle biogenesis. *MBio,* 3.

SCHMIDT, H. 2001. Shiga-toxin-converting bacteriophages. *Res Microbiol,* 152, 687-95.

SCHMIDT, H., BEUTIN, L. & KARCH, H. 1995. Molecular analysis of the plasmid-encoded hemolysin of *Escherichia coli* O157:H7 strain EDL 933. *Infect Immun,* 63**,** 1055-61.

SCHMIDT, H., HENKEL, B. & KARCH, H. 1997. A gene cluster closely related to type II secretion pathway operons of gram-negative bacteria is located on the large

plasmid of enterohemorrhagic *Escherichia coli* O157 strains. *FEMS Microbiol Lett,* 148, 265-72.

SCHMIDT, H. & HENSEL, M. 2004. Pathogenicity islands in bacterial pathogenesis. *Clin Microbiol Rev,* 17**,** 14-56.

SCHNEEBERGER, K., ROTH, S., NIEUWENHUIS, E. E. S. & MIDDENDORP, S. 2018. Intestinal epithelial cell polarity defects in disease: lessons from microvillus inclusion disease. *Dis Model Mech,* 11.

SCHOOLING, S. R. & BEVERIDGE, T. J. 2006. Membrane vesicles: an overlooked component of the matrices of biofilms. *J Bacteriol,* 188**,** 5945-57.

SCHULLER, S., FRANKEL, G. & PHILLIPS, A. D. 2004. Interaction of Shiga toxin from *Escherichia coli* with human intestinal epithelial cell lines and explants: Stx2 induces epithelial damage in organ culture. *Cell Microbiol,* 6**,** 289-301.

SCHÜLLER, S., CHONG, Y., LEWIN, J., KENNY, B., FRANKEL, G. & PHILLIPS, A. D. 2007. Tir phosphorylation and Nck/N-WASP recruitment by enteropathogenic and enterohaemorrhagic *Escherichia coli* during *ex vivo* colonization of human intestinal mucosa is different to cell culture models. *Cell Microbiol,* 9, 1352-64.

SCHULLER, S. & PHILLIPS, A. D. 2010. Microaerobic conditions enhance type III secretion and adherence of enterohaemorrhagic *Escherichia coli* to polarized human intestinal epithelial cells. *Environ Microbiol,* 12**,** 2426-35.

SCHÜLLER, S. 2011. Shiga toxin interaction with human intestinal epithelium. *Toxins (Basel),* 3**,** 626-39.

SCHULZ, E., GOES, A., GARCIA, R., PANTER, F., KOCH, M., MÜLLER, R., FUHRMANN, K. & FUHRMANN, G. 2018. Biocompatible bacteria-derived vesicles show inherent antimicrobial activity. *J Control Release,* 290, 46-55.

SCHUSTER, M., LOSTROH, C. P., OGI, T. & GREENBERG, E. P. 2003. Identification, timing, and signal specificity of *Pseudomonas aeruginosa* quorum-controlled genes: a transcriptome analysis. *J Bacteriol,* 185**,** 2066-79.

SCHWECHHEIMER, C. & KUEHN, M. J. 2015. Outer-membrane vesicles from Gram-negative bacteria: biogenesis and functions. *Nat Rev Microbiol,* 13**,** 605-19.

SCHWECHHEIMER, C., KULP, A. & KUEHN, M. J. 2014. Modulation of bacterial outer membrane vesicle production by envelope structure and content. *BMC Microbiol,* 14**,** 324.

SCHWECHHEIMER, C., RODRIGUEZ, D. L. & KUEHN, M. J. 2015. NlpI-mediated modulation of outer membrane vesicle production through peptidoglycan dynamics in *Escherichia coli*. *Microbiologyopen,* 4**,** 375-89.

SCHWECHHEIMER, C., SULLIVAN, C. J. & KUEHN, M. J. 2013. Envelope control of outer membrane vesicle production in Gram-negative bacteria. *Biochemistry,* 52**,** 3031-40.

SEZONOV, G., JOSELEAU-PETIT, D. & D'ARI, R. 2007. *Escherichia coli* physiology in Luria-Bertani broth. *J Bacteriol,* 189**,** 8746-9.

SHARMA, J. N., AL-OMRAN, A. & PARVATHY, S. S. 2007. Role of nitric oxide in inflammatory diseases. *Inflammopharmacology,* 15**,** 252-9.

SHEIKH, J., CZECZULIN, J. R., HARRINGTON, S., HICKS, S., HENDERSON, I. R., LE BOUGUÉNEC, C., GOUNON, P., PHILLIPS, A. & NATARO, J. P. 2002. A novel dispersin protein in enteroaggregative *Escherichia coli*. *J Clin Invest,* 110**,** 1329-37.

SHIGA, K. 1898. Ueber den Disenteriebacillus (*Bacillus dysenteriae*). *Zentralblat fuer Bakteriologie, Parasitenkunde und Infektionskrankheiten Erste Abteilung,* 24**,** 913-918.

SHIGENO, T., AKAMATSU, T., FUJIMORI, K., NAKATSUJI, Y. & NAGATA, A. 2002. The clinical significance of colonoscopy in hemorrhagic colitis due to enterohemorrhagic *Escherichia coli* O157:H7 infection. *Endoscopy,* 34**,** 311-4.

SHIMADA, T., YAMAMOTO, K. & ISHIHAMA, A. 2011. Novel members of the Cra regulon involved in carbon metabolism in *Escherichia coli*. *J Bacteriol,* 193**,** 649-59.

SIEGLER, R. L., OBRIG, T. G., PYSHER, T. J., TESH, V. L., DENKERS, N. D. & TAYLOR, F. B. 2003. Response to Shiga toxin 1 and 2 in a baboon model of hemolytic uremic syndrome. *Pediatr Nephrol,* 18**,** 92-6.

SIMONS, K. & SAMPAIO, J. L. 2011. Membrane organization and lipid rafts. *Cold Spring Harb Perspect Biol,* 3**,** a004697.

SIMOVITCH, M., SASON, H., COHEN, S., ZAHAVI, E. E., MELAMED-BOOK, N., WEISS, A., AROETI, B. & ROSENSHINE, I. 2010. EspM inhibits pedestal formation by enterohaemorrhagic *Escherichia coli* and enteropathogenic *E. coli* and disrupts the architecture of a polarized epithelial monolayer. *Cell Microbiol,* 12**,** 489-505.

SLATER, S. L., SAGFORS, A. M., POLLARD, D. J., RUANO-GALLEGO, D. & FRANKEL, G. 2018. The Type III Secretion System of Pathogenic *Escherichia coli*. *Curr Top Microbiol Immunol,* 416**,** 51-72.

SLAVICEK, J., PURETIC, Z., NOVAK, M., SARNAVKA, V., BENJAK, V., GLAVAS-BORAS, S. & THUNE, S. 1995. The role of plasma exchange in the treatment of severe forms of hemolytic-uremic syndrome in childhood. *Artif Organs,* 19**,** 506-10.

SLUTSKER, L., RIES, A. A., GREENE, K. D., WELLS, J. G., HUTWAGNER, L. & GRIFFIN, P. M. 1997. *Escherichia coli* O157:H7 diarrhea in the United States: clinical and epidemiologic features. *Ann Intern Med,* 126**,** 505-13.

SMATI, M., CLERMONT, O., BLEIBTREU, A., FOURREAU, F., DAVID, A., DAUBIE, A. S., HIGNARD, C., LOISON, O., PICARD, B. & DENAMUR, E. 2015. Quantitative analysis of commensal *Escherichia coli* populations reveals host-specific enterotypes at the intra-species level. *Microbiologyopen,* 4**,** 604-15.

SMITH, K. E., WILKER, P. R., REITER, P. L., HEDICAN, E. B., BENDER, J. B. & HEDBERG, C. W. 2012. Antibiotic treatment of *Escherichia coli* O157 infection and the risk of hemolytic uremic syndrome, Minnesota. *Pediatr Infect Dis J,* 31**,** 37-41.

SMITH, W. E., KANE, A. V., CAMPBELL, S. T., ACHESON, D. W., COCHRAN, B. H. & THORPE, C. M. 2003. Shiga toxin 1 triggers a ribotoxic stress response leading to p38 and JNK activation and induction of apoptosis in intestinal epithelial cells. *Infect Immun,* 71**,** 1497-504.

SPERANDIO, V., TORRES, A. G., JARVIS, B., NATARO, J. P. & KAPER, J. B. 2003. Bacteria-host communication: the language of hormones. *Proc Natl Acad Sci U S A,* 100**,** 8951-6.

SPERANDIO, V., TORRES, A. G. & KAPER, J. B. 2002. Quorum sensing *Escherichia coli* regulators B and C (QseBC): a novel two-component regulatory system involved in the regulation of flagella and motility by quorum sensing in *E. coli*. *Mol Microbiol,* 43, 809-21.

STAHL, A. L., SARTZ, L., NELSSON, A., BEKASSY, Z. D. & KARPMAN, D. 2009. Shiga toxin and lipopolysaccharide induce platelet-leukocyte aggregates and tissue factor release, a thrombotic mechanism in hemolytic uremic syndrome. *PLoS One,* 4**,** e6990.

STALEY, T. E., JONES, E. W. & CORLEY, L. D. 1969. Attachment and penetration of *Escherichia coli* into intestinal epithelium of the ileum in newborn pigs. *Am J Pathol,* 56**,** 371-92.

STEARNS-KUROSAWA, D. J., COLLINS, V., FREEMAN, S., TESH, V. L. & KUROSAWA, S. 2010. Distinct physiologic and inflammatory responses elicited in baboons after challenge with Shiga toxin type 1 or 2 from enterohemorrhagic *Escherichia coli*. *Infect Immun,* 78**,** 2497-504.

STEIN, P. E., BOODHOO, A., TYRRELL, G. J., BRUNTON, J. L. & READ, R. J. 1992. Crystal structure of the cell-binding B oligomer of verotoxin-1 from *E. coli*. *Nature,* 355**,** 748-50.

STENTZ, R., HORN, N., CROSS, K., SALT, L., BREARLEY, C., LIVERMORE, D. M. & CARDING, S. R. 2015. Cephalosporinases associated with outer membrane vesicles released by Bacteroides spp. protect gut pathogens and commensals against beta-lactam antibiotics. *J Antimicrob Chemother,* 70**,** 701-9.

STEPHENS, D. S., EDWARDS, K. M., MORRIS, F. & MCGEE, Z. A. 1982. Pili and outer membrane appendages on *Neisseria meningitidis* in the cerebrospinal fluid of an infant. *J Infect Dis,* 146**,** 568.

STETEFELD, J., MCKENNA, S. A. & PATEL, T. R. 2016. Dynamic light scattering: a practical guide and applications in biomedical sciences. *Biophys Rev,* 8**,** 409-427.

STEWART, J. C. 1980. Colorimetric determination of phospholipids with ammonium ferrothiocyanate. *Anal Biochem,* 104, 10-4.

STOLPER, D. A., REVSBECH, N. P. & CANFIELD, D. E. 2010. Aerobic growth at nanomolar oxygen concentrations. *Proc Natl Acad Sci U S A,* 107**,** 18755-60.

STOOPS, E. H. & CAPLAN, M. J. 2014. Trafficking to the apical and basolateral membranes in polarized epithelial cells. *J Am Soc Nephrol,* 25**,** 1375-86.

STROCKBINE, N. A., JACKSON, M. P., SUNG, L. M., HOLMES, R. K. & O'BRIEN, A. D. 1988. Cloning and sequencing of the genes for Shiga toxin from *Shigella dysenteriae* type 1. *J Bacteriol,* 170**,** 1116-22.

STROCKBINE, N. A., MARQUES, L. R., NEWLAND, J. W., SMITH, H. W., HOLMES, R. K. & O'BRIEN, A. D. 1986. Two toxin-converting phages from *Escherichia coli* O157:H7 strain 933 encode antigenically distinct toxins with similar biologic activities. *Infect Immun,* 53**,** 135-40.

STÅHL, A.-L., ARVIDSSON, I., JOHANSSON, K. E., CHROMEK, M., REBETZ, J., LOOS, S., KRISTOFFERSSON, A.-C., BÉKÁSSY, Z. D., MÖRGELIN, M. & KARPMAN, D. 2015. A Novel Mechanism of Bacterial Toxin Transfer within Host Blood Cell-Derived Microvesicles. *PLOS Pathogens,* 11**,** e1004619.

STÅHL, A. L., SARTZ, L. & KARPMAN, D. 2011. Complement activation on platelet-leukocyte complexes and microparticles in enterohemorrhagic *Escherichia coli*-induced hemolytic uremic syndrome. *Blood,* 117, 5503-13.

SVENNERHOLM, K., PARK, K. S., WIKSTRÖM, J., LÄSSER, C., CRESCITELLI, R., SHELKE, G. V., JANG, S. C., SUZUKI, S., BANDEIRA, E., OLOFSSON, C. S. & LÖTVALL, J.

2017. *Escherichia coli* outer membrane vesicles can contribute to sepsis induced cardiac dysfunction. *Sci Rep,* 7**,** 17434.

TAKAO, T., TANABE, T., HONG, Y. M., SHIMONISHI, Y., KURAZONO, H., YUTSUDO, T., SASAKAWA, C., YOSHIKAWA, M. & TAKEDA, Y. 1988. Identity of molecular structure of Shiga-like toxin I (VT1) from *Escherichia coli* O157:H7 with that of Shiga toxin. *Microb Pathog,* 5**,** 57-69.

TAKEUCHI, H., FURUTA, N., MORISAKI, I. & AMANO, A. 2011. Exit of intracellular *Porphyromonas gingivalis* from gingival epithelial cells is mediated by endocytic recycling pathway. *Cell Microbiol,* 13**,** 677-91.

TAM, P. J. & LINGWOOD, C. A. 2007. Membrane cytosolic translocation of verotoxin A1 subunit in target cells. *Microbiology,* 153**,** 2700-2710.

TARR, P. I., GORDON, C. A. & CHANDLER, W. L. 2005. Shiga-toxin-producing *Escherichia coli* and haemolytic uraemic syndrome. *Lancet,* 365**,** 1073-86.

TASHIRO, Y., ICHIKAWA, S., SHIMIZU, M., TOYOFUKU, M., TAKAYA, N., NAKAJIMA-KAMBE, T., UCHIYAMA, H. & NOMURA, N. 2010. Variation of physiochemical properties and cell association activity of membrane vesicles with growth phase in *Pseudomonas aeruginosa*. *Appl Environ Microbiol,* 76**,** 3732-9.

TATSUNO, I., HORIE, M., ABE, H., MIKI, T., MAKINO, K., SHINAGAWA, H., TAGUCHI, H., KAMIYA, S., HAYASHI, T. & SASAKAWA, C. 2001. toxB gene on pO157 of enterohemorrhagic *Escherichia coli* O157:H7 is required for full epithelial cell adherence phenotype. *Infect Immun,* 69**,** 6660-9.

TAYLOR, C. M., WHITE, R. H., WINTERBORN, M. H. & ROWE, B. 1986. Haemolytic-uraemic syndrome: clinical experience of an outbreak in the West Midlands. *Br Med J (Clin Res Ed),* 292**,** 1513-6.

TE LOO, D. M., MONNENS, L. A., VAN DER VELDEN, T. J., VERMEER, M. A., PREYERS, F., DEMACKER, P. N., VAN DEN HEUVEL, L. P. & VAN HINSBERGH, V. W. 2000. Binding and transfer of verocytotoxin by polymorphonuclear leukocytes in hemolytic uremic syndrome. *Blood,* 95, 3396-402.

TE LOO, D. M., VAN HINSBERGH, V. W., VAN DEN HEUVEL, L. P. & MONNENS, L. A. 2001. Detection of verocytotoxin bound to circulating polymorphonuclear leukocytes of patients with hemolytic uremic syndrome. *J Am Soc Nephrol,* 12**,** 800-6.

TENAILLON, O., SKURNIK, D., PICARD, B. & DENAMUR, E. 2010. The population genetics of commensal *Escherichia coli*. *Nat Rev Microbiol.* England.

TESH, V. L. 2012. The induction of apoptosis by Shiga toxins and ricin. *Curr Top Microbiol Immunol,* 357**,** 137-78.

TESH, V. L., BURRIS, J. A., OWENS, J. W., GORDON, V. M., WADOLKOWSKI, E. A., O'BRIEN, A. D. & SAMUEL, J. E. 1993. Comparison of the relative toxicities of Shiga-like toxins type I and type II for mice. *Infect Immun,* 61**,** 3392-402.

THANASSI, D. G., CHENG, L. W. & NIKAIDO, H. 1997. Active efflux of bile salts by *Escherichia coli*. *J Bacteriol,* 179**,** 2512-8.

THOMAS, C. M. & NIELSEN, K. M. 2005. Mechanisms of, and barriers to, horizontal gene transfer between bacteria. *Nat Rev Microbio,* 3, 711-21.

THORPE, C. M., HURLEY, B. P., LINCICOME, L. L., JACEWICZ, M. S., KEUSCH, G. T. & ACHESON, D. W. 1999. Shiga toxins stimulate secretion of interleukin-8 from intestinal epithelial cells. *Infect Immun,* 67**,** 5985-93.

TOBE, T., BEATSON, S. A., TANIGUCHI, H., ABE, H., BAILEY, C. M., FIVIAN, A., YOUNIS, R., MATTHEWS, S., MARCHES, O., FRANKEL, G., HAYASHI, T. & PALLEN, M. J. 2006. An extensive repertoire of type III secretion effectors in *Escherichia coli* O157 and the role of lambdoid phages in their dissemination. *Proc Natl Acad Sci U S A,* 103**,** 14941-6.

TOBE, T., NAKANISHI, N. & SUGIMOTO, N. 2011. Activation of motility by sensing short-chain fatty acids via two steps in a flagellar gene regulatory cascade in enterohemorrhagic *Escherichia coli*. *Infect Immun,* 79**,** 1016-24.

TOLEDO, A., COLEMAN, J. L., KUHLOW, C. J., CROWLEY, J. T. & BENACH, J. L. 2012. The enolase of *Borrelia burgdorferi* is a plasminogen receptor released in outer membrane vesicles. *Infect Immun,* 80**,** 359-68.

TORGERSEN, M. L., LAUVRAK, S. U. & SANDVIG, K. 2005. The A-subunit of surface-bound Shiga toxin stimulates clathrin-dependent uptake of the toxin. *FEBS J,* 272, 4103-13.

TOUCHON, M., HOEDE, C., TENAILLON, O., BARBE, V., BAERISWYL, S., BIDET, P., BINGEN, E., BONACORSI, S., BOUCHIER, C., BOUVET, O., CALTEAU, A., CHIAPELLO, H., CLERMONT, O., CRUVEILLER, S., DANCHIN, A., DIARD, M., DOSSAT, C., KAROUI, M. E., FRAPY, E., GARRY, L., GHIGO, J. M., GILLES, A. M., JOHNSON, J., LE BOUGUENEC, C., LESCAT, M., MANGENOT, S., MARTINEZ-JEHANNE, V., MATIC, I., NASSIF, X., OZTAS, S., PETIT, M. A., PICHON, C., ROUY, Z., RUF, C. S., SCHNEIDER, D., TOURRET, J., VACHERIE, B., VALLENET, D., MEDIGUE, C., ROCHA, E. P. & DENAMUR, E. 2009. Organised genome dynamics in the *Escherichia coli* species results in highly diverse adaptive paths. *PLoS Genet,* 5**,** e1000344.

TRACHTMAN, H., AUSTIN, C., LEWINSKI, M. & STAHL, R. A. K. 2012. Renal and neurological involvement in typical Shiga toxin-associated HUS. *Nat Rev Nephrol,* 8**,** 658-669.

TRAN, S. L., BILLOUD, L., LEWIS, S. B., PHILLIPS, A. D. & SCHULLER, S. 2014. Shiga toxin production and translocation during microaerobic human colonic infection with Shiga toxin-producing *E. coli* O157:H7 and O104:H4. *Cell Microbiol,* 16**,** 1255-66.

TRAN, S. L., JENKINS, C., LIVRELLI, V. & SCHÜLLER, S. 2018. Shiga toxin 2 translocation across intestinal epithelium is linked to virulence of Shiga toxin-producing *Escherichia coli* in humans. *Microbiology,* 164**,** 509-516.

TURNBULL, L., TOYOFUKU, M., HYNEN, A. L., KUROSAWA, M., PESSI, G., PETTY, N. K., OSVATH, S. R., CARCAMO-OYARCE, G., GLOAG, E. S., SHIMONI, R., OMASITS, U., ITO, S., YAP, X., MONAHAN, L. G., CAVALIERE, R., AHRENS, C. H., CHARLES, I. G., NOMURA, N., EBERL, L. & WHITCHURCH, C. B. 2016. Explosive cell lysis as a mechanism for the biogenesis of bacterial membrane vesicles and biofilms. *Nat Commun,* 7**,** 11220.

TURNER, L., BITTO, N. J., STEER, D. L., LO, C., D'COSTA, K., RAMM, G., SHAMBROOK, M., HILL, A. F., FERRERO, R. L. & KAPARAKIS-LIASKOS, M. 2018. *Helicobacter pylori* Outer Membrane Vesicle Size Determines Their Mechanisms of Host Cell Entry and Protein Content. *Front Immunol,* 9**,** 1466.

TURNER, L., PRASZKIER, J., HUTTON, M. L., STEER, D., RAMM, G., KAPARAKIS-LIASKOS, M. & FERRERO, R. L. 2015. Increased Outer Membrane Vesicle Formation in a *Helicobacter pylori tolB* Mutant. *Helicobacter,* 20**,** 269-83.

TUTTLE, J., GOMEZ, T., DOYLE, M. P., WELLS, J. G., ZHAO, T., TAUXE, R. V. & GRIFFIN, P. M. 1999. Lessons from a large outbreak of *Escherichia coli* O157:H7 infections: insights into the infectious dose and method of widespread contamination of hamburger patties. *Epidemiol Infect,* 122**,** 185-92.

TYRER, P. C., FRIZELLE, F. A. & KEENAN, J. I. 2014. *Escherichia coli*-derived outer membrane vesicles are genotoxic to human enterocyte-like cells. *Infect Agent Cancer,* 9**,** 2.

TZIPORI, S., GIBSON, R. & MONTANARO, J. 1989. Nature and distribution of mucosal lesions associated with enteropathogenic and enterohemorrhagic *Escherichia coli* in piglets and the role of plasmid-mediated factors. *Infect Immun,* 57**,** 1142-50.

TZIPORI, S., GUNZER, F., DONNENBERG, M. S., DE MONTIGNY, L., KAPER, J. B. & DONOHUE-ROLFE, A. 1995. The role of the eaeA gene in diarrhea and neurological complications in a gnotobiotic piglet model of enterohemorrhagic *Escherichia coli* infection. *Infection and Immunity,* 63**,** 3621-3627.

TZIPORI, S., KARCH, H., WACHSMUTH, K. I., ROBINS-BROWNE, R. M., O'BRIEN, A. D., LIOR, H., COHEN, M. L., SMITHERS, J. & LEVINE, M. M. 1987. Role of a 60-megadalton plasmid and Shiga-like toxins in the pathogenesis of infection caused by enterohemorrhagic *Escherichia coli* O157:H7 in gnotobiotic piglets. *Infect Immun,* 55**,** 3117-25.

TZIPORI, S., WACHSMUTH, I. K., CHAPMAN, C., BIRDEN, R., BRITTINGHAM, J., JACKSON, C. & HOGG, J. 1986. The pathogenesis of hemorrhagic colitis caused by *Escherichia coli* O157:H7 in gnotobiotic piglets. *J Infect Dis,* 154**,** 712-6.

UM, M. M., BRUGERE, H., KEROUREDAN, M., OSWALD, E. & BIBBAL, D. 2018. Antimicrobial Resistance Profiles of Enterohemorrhagic and Enteropathogenic *Escherichia coli* of Serotypes O157:H7, O26:H11, O103:H2, O111:H8, O145:H28 Compared to *Escherichia coli* Isolated from the Same Adult Cattle. *Microb Drug Resist,* 24**,** 852-859.

URASHIMA, A., SANOU, A., YEN, H. & TOBE, T. 2017. Enterohaemorrhagic *Escherichia coli* produces outer membrane vesicles as an active defence system against antimicrobial peptide LL-37. *Cell Microbiol,* 19.

VALILIS, E., RAMSEY, A., SIDIQ, S. & DUPONT, H. L. 2018. Non-O157 Shiga toxin-producing *Escherichia coli*-A poorly appreciated enteric pathogen: Systematic review. *Int J Infect Dis,* 76, 82-87.

VAN DE WATERBEEMD, B., STREEFLAND, M., VAN DER LEY, P., ZOMER, B., VAN DIJKEN, H., MARTENS, D., WIJFFELS, R. & VAN DER POL, L. 2010. Improved OMV vaccine against *Neisseria meningitidis* using genetically engineered strains and a detergent-free purification process. *Vaccine,* 28, 4810-6.

VAN DER VLIST, E. J., NOLTE-'T HOEN, E. N., STOORVOGEL, W., ARKESTEIJN, G. J. & WAUBEN, M. H. 2012. Fluorescent labeling of nano-sized vesicles released by cells and subsequent quantitative and qualitative analysis by high-resolution flow cytometry. *Nat Protoc,* 7, 1311-26.

VAN DER WOUDEN, J. M., MAIER, O., VAN, I. S. C. & HOEKSTRA, D. 2003. Membrane dynamics and the regulation of epithelial cell polarity. *Int Rev Cytol,* 226**,** 127-64.

VAN DYCK, M. & PROESMANS, W. 2004. Renoprotection by ACE inhibitors after severe hemolytic uremic syndrome. *Pediatr Nephrol,* 19**,** 688-90.

VAN SETTEN, P. A., MONNENS, L. A., VERSTRATEN, R. G., VAN DEN HEUVEL, L. P. & VAN HINSBERGH, V. W. 1996. Effects of verocytotoxin-1 on nonadherent human monocytes: binding characteristics, protein synthesis, and induction of cytokine release. *Blood,* 88**,** 174-83.

VASILYEVA, N. V., TSFASMAN, I. M., SUZINA, N. E., STEPNAYA, O. A. & KULAEV, I. S. 2009. Outer membrane vesicles of *Lysobacter* sp. *Dokl Biochem Biophys,* 426**,** 139-42.

VEITH, P. D., CHEN, Y. Y., GORASIA, D. G., CHEN, D., GLEW, M. D., O'BRIEN-SIMPSON, N. M., CECIL, J. D., HOLDEN, J. A. & REYNOLDS, E. C. 2014. *Porphyromonas gingivalis* outer membrane vesicles exclusively contain outer membrane and periplasmic proteins and carry a cargo enriched with virulence factors. *J Proteome Res,* 13**,** 2420-32.

VERCAUTEREN, D., VANDENBROUCKE, R. E., JONES, A. T., REJMAN, J., DEMEESTER, J., DE SMEDT, S. C., SANDERS, N. N. & BRAECKMANS, K. 2010. The use of inhibitors to study endocytic pathways of gene carriers: optimization and pitfalls. *Mol Ther,* 18**,** 561-9.

VESTAD, B., LLORENTE, A., NEURAUTER, A., PHUYAL, S., KIERULF, B., KIERULF, P., SKOTLAND, T., SANDVIG, K., HAUG, K. B. F. & ØVSTEBØ, R. 2017. Size and concentration analyses of extracellular vesicles by nanoparticle tracking analysis: a variation study. *J Extracell Vesicles,* 6**,** 1344087.

VINGADASSALOM, D., KAZLAUSKAS, A., SKEHAN, B., CHENG, H. C., MAGOUN, L., ROBBINS, D., ROSEN, M. K., SAKSELA, K. & LEONG, J. M. 2009. Insulin receptor tyrosine kinase substrate links the *E. coli* O157:H7 actin assembly effectors Tir and EspF(U) during pedestal formation. *Proc Natl Acad Sci U S A,* 106**,** 6754-9.

VISWANATHAN, V. K., KOUTSOURIS, A., LUKIC, S., PILKINTON, M., SIMONOVIC, I., SIMONOVIC, M. & HECHT, G. 2004. Comparative analysis of EspF from enteropathogenic and enterohemorrhagic *Escherichia coli* in alteration of epithelial barrier function. *Infect Immun,* 72**,** 3218-27.

WADDELL, T., COHEN, A. & LINGWOOD, C. A. 1990. Induction of verotoxin sensitivity in receptor-deficient cell lines using the receptor glycolipid globotriosylceramide. *Proc Natl Acad Sci U S A,* 87**,** 7898-901.

WADDELL, T., HEAD, S., PETRIC, M., COHEN, A. & LINGWOOD, C. 1988. Globotriosyl ceramide is specifically recognized by the *Escherichia coli* verocytotoxin 2. *Biochem Biophys Res Commun,* 152**,** 674-9.

WAGNER, P. L., ACHESON, D. W. & WALDOR, M. K. 2001. Human neutrophils and their products induce Shiga toxin production by enterohemorrhagic *Escherichia coli*. *Infect Immun,* 69**,** 1934-7.

WAGNER, P. L., LIVNY, J., NEELY, M. N., ACHESON, D. W., FRIEDMAN, D. I. & WALDOR, M. K. 2002. Bacteriophage control of Shiga toxin 1 production and release by *Escherichia coli*. *Mol Microbiol,* 44**,** 957-70.

WAGNER, V. E., BUSHNELL, D., PASSADOR, L., BROOKS, A. I. & IGLEWSKI, B. H. 2003. Microarray analysis of *Pseudomonas aeruginosa* quorum-sensing regulons: effects of growth phase and environment. *J Bacteriol,* 185**,** 2080-95.

WALDOR, M. K. & FRIEDMAN, D. I. 2005. Phage regulatory circuits and virulence gene expression. *Curr Opin Microbiol,* 8, 459-65.

WANG, Y. 2002. The function of OmpA in *Escherichia coli*. *Biochem Biophys Res Commun,* 292**,** 396-401.

WEISZ, O. A. & RODRIGUEZ-BOULAN, E. 2009. Apical trafficking in epithelial cells: signals, clusters and motors. *J Cell Sci,* 122**,** 4253-66.

WENDEL, A. M., JOHNSON, D. H., SHARAPOV, U., GRANT, J., ARCHER, J. R., MONSON, T., KOSCHMANN, C. & DAVIS, J. P. 2009. Multistate outbreak of *Escherichia coli* O157:H7 infection associated with consumption of packaged spinach, August-September 2006: the Wisconsin investigation. *Clin Infect Dis,* 48**,** 1079-86.

WERBER, D., FRUTH, A., BUCHHOLZ, U., PRAGER, R., KRAMER, M. H., AMMON, A. & TSCHAPE, H. 2003. Strong association between shiga toxin-producing *Escherichia coli* O157 and virulence genes *stx2* and *eae* as possible explanation for predominance of serogroup O157 in patients with haemolytic uraemic syndrome. *Eur J Clin Microbiol Infect Dis,* 22**,** 726-30.

WESSEL, A. K., LIEW, J., KWON, T., MARCOTTE, E. M. & WHITELEY, M. 2013. Role of *Pseudomonas aeruginosa* peptidoglycan-associated outer membrane proteins in vesicle formation. *J Bacteriol,* 195**,** 213-9.

WHITWORTH, D. E. 2011. Myxobacterial vesicles death at a distance? *Adv Appl Microbiol,* 75**,** 1-31.

WORLD HEALTH ORGANIZATION & FOOD AND AGRICULTURE ORGANIZATION OF THE UNITED NATIONS. 2018. Shiga toxin-producing *Escherichia coli* (STEC) and food: attribution, characterization, and monitoring: Microbiological Risk Assessment Series 31, report. Available at: https://www.who.int/foodsafety/publications/mra_31/en/

WORLD HEALTH ORGANIZATION. 2011. Outbreaks of E*. coli* O104: H4 infection: update 30. Available at: http://www.euro.who.int/en.what-we-do/health-topics/emergencies.internation-health-regulation/news/news/2011/07/outbreak-of-e.-coli-o104h4-infection-update-30

WINFIELD, M. D. & GROISMAN, E. A. 2003. Role of nonhost environments in the lifestyles of *Salmonella* and *Escherichia coli*. *Appl Environ Microbiol,* 69**,** 3687-94.

WONG, A. R., PEARSON, J. S., BRIGHT, M. D., MUNERA, D., ROBINSON, K. S., LEE, S. F., FRANKEL, G. & HARTLAND, E. L. 2011. Enteropathogenic and enterohaemorrhagic *Escherichia coli*: even more subversive elements. *Mol Microbiol,* 80**,** 1420-38.

WONG, C. S., JELACIC, S., HABEEB, R. L., WATKINS, S. L. & TARR, P. I. 2000. The risk of the hemolytic-uremic syndrome after antibiotic treatment of *Escherichia coli* O157:H7 infections. *N Engl J Med,* 342**,** 1930-6.

WORK, E., KNOX, K. W. & VESK, M. 1966. The chemistry and electron microscopy of an extracellular lipopolysaccharide from *Escherichia coli*. *Ann N Y Acad Sci,* 133**,** 438-49.

WU, C. J., HSUEH, P. R. & KO, W. C. 2011. A new health threat in Europe: Shiga toxin-producing *Escherichia coli* O104:H4 infections. *J Microbiol Immunol Infect*, 44, 390-3.

XICOHTENCATL-CORTES, J., MONTEIRO-NETO, V., LEDESMA, M. A., JORDAN, D. M., FRANCETIC, O., KAPER, J. B., PUENTE, J. L. & GIRON, J. A. 2007. Intestinal

adherence associated with type IV pili of enterohemorrhagic *Escherichia coli* O157:H7. *J Clin Invest,* 117**,** 3519-29.

XU, H. & REN, D. 2015. Lysosomal physiology. *Annu Rev Physiol,* 77**,** 57-80.

XU, Y., ZHAO, Z., TONG, W., DING, Y., LIU, B., SHI, Y., WANG, J., SUN, S., LIU, M., WANG, Y., QI, Q., XIAN, M. & ZHAO, G. 2020. An acid-tolerance response system protecting exponentially growing *Escherichia coli*. *Nat Commun,* 11**,** 1496.

YARON, S., KOLLING, G. L., SIMON, L. & MATTHEWS, K. R. 2000. Vesicle-mediated transfer of virulence genes from *Escherichia coli* O157:H7 to other enteric bacteria. *Appl Environ Microbiol,* 66**,** 4414-20.

YASID, N. A., ROLFE, M. D., GREEN, J. & WILLIAMSON, M. P. 2016. Homeostasis of metabolites in *Escherichia coli* on transition from anaerobic to aerobic conditions and the transient secretion of pyruvate. *R Soc Open Sci,* 3**,** 160187.

YOKOYAMA, K., HORII, T., YAMASHINO, T., HASHIKAWA, S., BARUA, S., HASEGAWA, T., WATANABE, H. & OHTA, M. 2000. Production of shiga toxin by *Escherichia coli* measured with reference to the membrane vesicle-associated toxins. *FEMS Microbiol Lett,* 192**,** 139-44.

YONEZAWA, H., OSAKI, T., KURATA, S., FUKUDA, M., KAWAKAMI, H., OCHIAI, K., HANAWA, T. & KAMIYA, S. 2009. Outer membrane vesicles of *Helicobacter pylori* TK1402 are involved in biofilm formation. *BMC Microbiol,* 9**,** 197.

YONEZAWA, H., OSAKI, T., WOO, T., KURATA, S., ZAMAN, C., HOJO, F., HANAWA, T., KATO, S. & KAMIYA, S. 2011. Analysis of outer membrane vesicle protein involved in biofilm formation of *Helicobacter pylori*. *Anaerobe,* 17**,** 388-90.

YU, M. & HASLAM, D. B. 2005. Shiga toxin is transported from the endoplasmic reticulum following interaction with the luminal chaperone HEDJ/ERdj3. *Infect Immun,* 73**,** 2524-32.

YUK, H. G. & MARSHALL, D. L. 2004. Adaptation of *Escherichia coli* O157:H7 to pH alters membrane lipid composition, verotoxin secretion, and resistance to simulated gastric fluid acid. *Appl Environ Microbiol,* 70**,** 3500-5.

ZHANG, X., MCDANIEL, A. D., WOLF, L. E., KEUSCH, G. T., WALDOR, M. K. & ACHESON, D. W. 2000. Quinolone antibiotics induce Shiga toxin-encoding bacteriophages, toxin production, and death in mice. *J Infect Dis,* 181, 664-70.

ZHANG, Y., LIAO, Y. T., SALVADOR, A., SUN, X. & WU, V. C. H. 2019. Prediction, Diversity, and Genomic Analysis of Temperate Phages Induced From Shiga Toxin-Producing *Escherichia coli* Strains. *Front Microbiol,* 10**,** 3093.

ZHOU, J., XIONG, X., WANG, K., ZOU, L., LV, D. & YIN, Y. 2017. Ethanolamine Metabolism in the Mammalian Gastrointestinal Tract: Mechanisms, Patterns, and Importance. *Curr Mol Med,* 17, 92-99.

ZHU, J., SÁNCHEZ, A., BENNETT, G. N. & SAN, K. Y. 2011. Manipulating respiratory levels in *Escherichia coli* for aerobic formation of reduced chemical products. *Metab Eng,* 13**,** 704-12.

ZIHNI, C., MILLS, C., MATTER, K. & BALDA, M. S. 2016. Tight junctions: from simple barriers to multifunctional molecular gates. *Nat Rev Mol Cell Biol,* 17, 564-80.

ZOJA, C., CORNA, D., FARINA, C., SACCHI, G., LINGWOOD, C., DOYLE, M. P., PADHYE, V. V., ABBATE, M. & REMUZZI, G. 1992. Verotoxin glycolipid receptors determine the localization of microangiopathic process in rabbits given verotoxin-1. *J Lab Clin Med,* 120, 229-38.

ZUMBRUN, S. D., MELTON-CELSA, A. R., SMITH, M. A., GILBREATH, J. J., MERRELL, D. S. & O'BRIEN, A. D. 2013. Dietary choice affects Shiga toxin-producing *Escherichia coli* (STEC) O157:H7 colonization and disease. *Proc Natl Acad Sci U S A,* 110**,** E2126-33.

Appendix: Supplementary Data

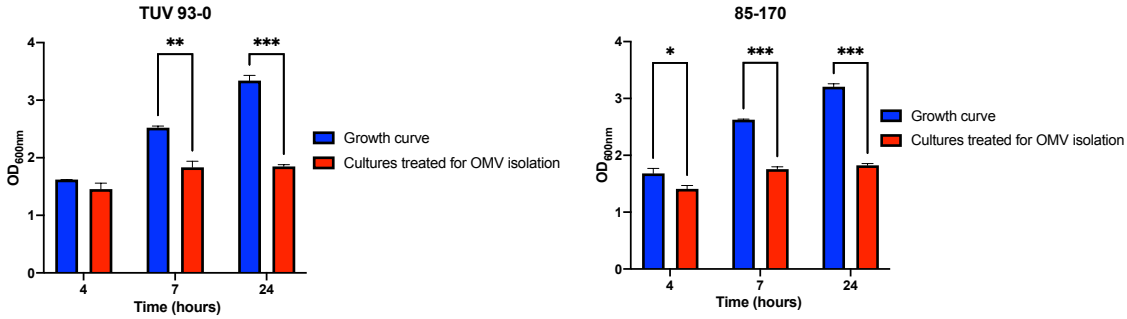

Figure S1: Significantly lower OD_{600} measurements are attained from EHEC cultures when grown for OMV isolation compared to measurements attained from EHEC growth curves. Overnight cultures of EHEC strains TUV 93-0 and 85-170 were inoculated in LB medium (1:100) and grown shaking at 37°C for 4, 7 and 24 hours. Data is shown as means ± SD of three independent experiments, performed in duplicates. Statistical tests were only made between OD_{600} measurements of EHEC cultures attained after growing for the same amount of time. * = $P < 0.05$, ** = $P < 0.01$, *** = $P < 0.001$.

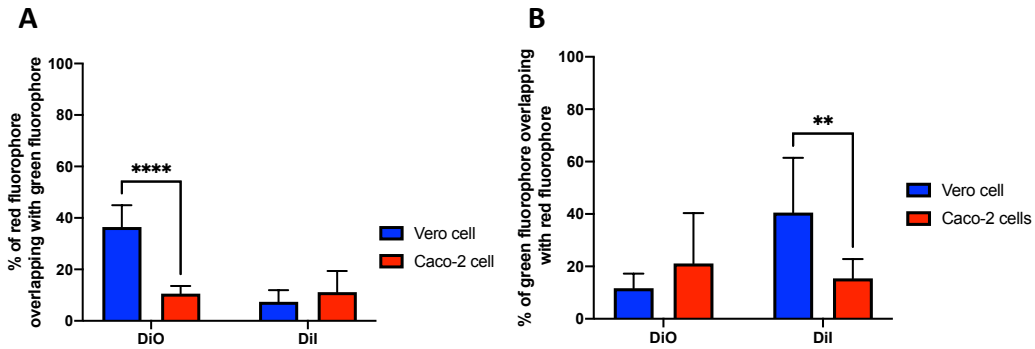

Figure S2: Quantification and statistical analysis of signal colocalisation between DiO or DiI signals and OMV-LPS signal in Vero cells and non-polarised Caco-2 cells. A) Graphical presentation of the mean percentage of red fluorophores which colocalised with green fluorophores ± SD of five or ten representative cells (Vero cells and Caco-2 cells, respectively; M1). B) Graphical presentation of the mean percentage of green fluorophores which colocalised with red fluorophores. Data is shown as the means of colocalisation ± SD of five or ten representative cells (Vero cells and Caco-2 cells, respectively; M2). Statistical tests were only made between colocalisation measurements with the same lipophilic dye between Vero cells and Caco-2 cells. ** = $P < 0.01$, **** = $P < 0.0001$.

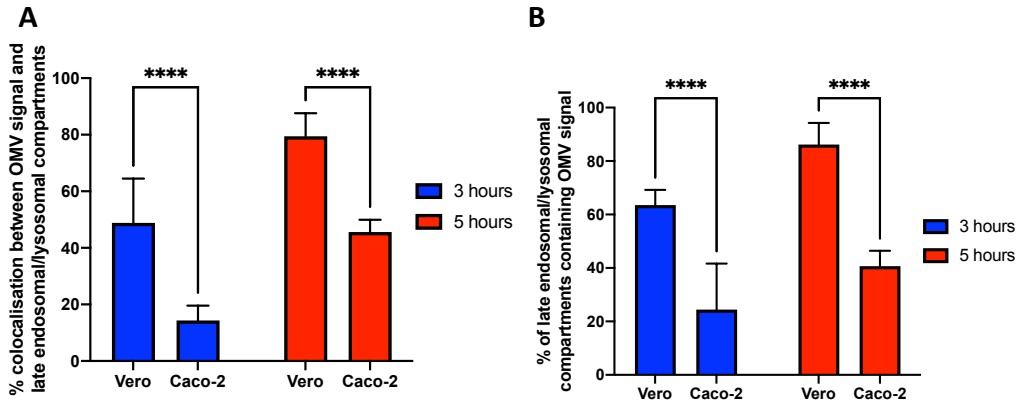

Figure S3: Quantification and statistical analysis of signal colocalisation between OMVs isolated from EHEC strains 85-170 and late endosomal/lysosomal compartments in Vero and non-polarised Caco-2 cells. A) Graphical presentation of the mean percentage of OMV signal colocalising with late endosomal/lysosomal compartment signal ± SD of five representative cells (M1). B) Graphical presentation of the mean percentage of late endosomal/lysosomal compartment signal colocalising with OMV signal ± SD of five representative cells (M2). Statistical tests were only made between colocalisation measurements attained for Vero cells and Caco-2 cells after incubating with EHEC OMVs for the same time periods. **** = $P < 0.0001$.

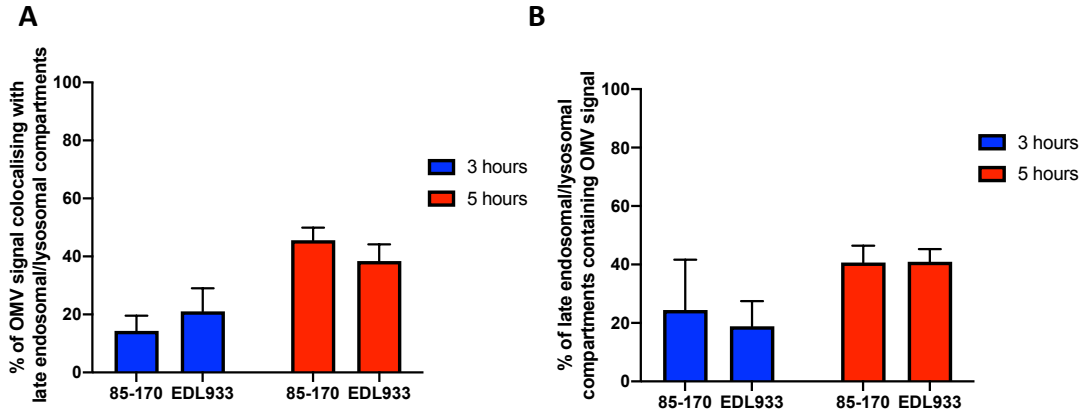

Figure S4: Quantification and statistical analysis of signal colocalisation between OMVs isolated from EHEC strains 85-170 or EDL933 and late endosomal/lysosomal compartments in non-polarised Caco-2 cells. A) Graphical presentation of the mean percentage of OMV signal colocalising with late endosomal/lysosomal compartment signal ± SD of five representative cells (M1). B) Graphical presentation of the mean percentage of late endosomal/lysosomal compartment signal colocalising with OMV signal ± SD of five representative cells (M2). Statistical tests were only made between colocalisation measurements attained between EHEC OMVs isolated from EHEC strain 85-170 or EDL933 and late endosomal/lysosomal compartments after similar incubation periods.

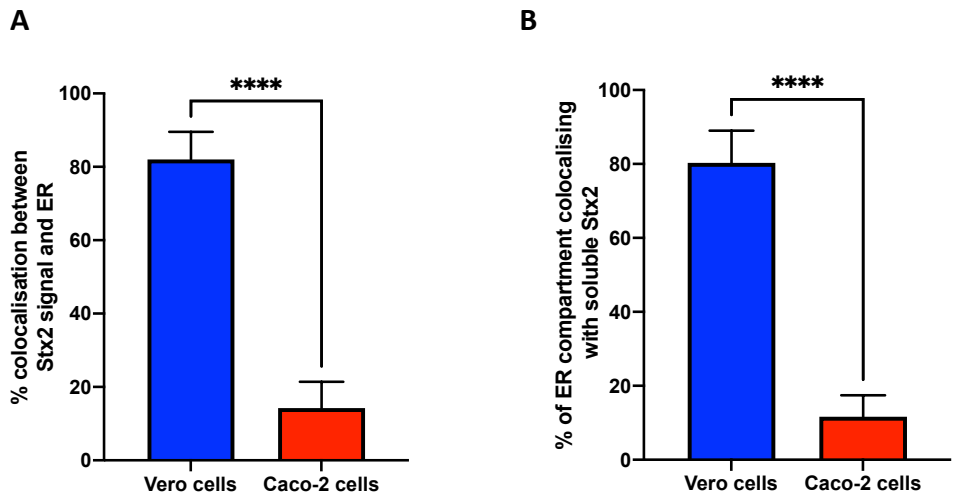

Figure S5: Quantification and statistical analysis of colocalisation between Stx2 and ER in Vero cells and non-polarised Caco-2 cells. A) Graphical presentation of the mean percentage of Stx2 signal colocalising with organelle compartment signal ± SD of five representative cells (M1). B) Graphical presentation of the mean percentage of organelle compartment signal containing Stx2 signal ± SD of five representative cells (M2). **** = $P < 0.0001$.

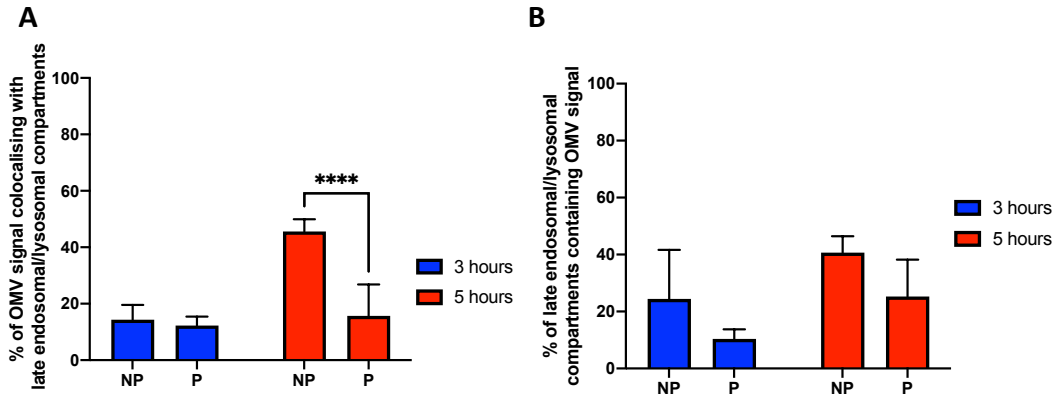

Figure S6: Quantification and statistical analysis of signal colocalisation between OMVs isolated from EHEC strains 85-170 and late endosomal/lysosomal compartments in non-polarised (NP) and polarised (P) Caco-2 cells. A) Graphical presentation of the mean percentage of OMV signal colocalising with late endosomal/lysosomal compartment signal ± SD of five representative cells (M1). B) Graphical presentation of the mean percentage of late endosomal/lysosomal compartment signal colocalising with OMV signal ± SD of five representative cells (M2). Statistical tests were only made between colocalisation measurements attained for non-polarised and polarised Caco-2 cells after incubating with EHEC OMVs for the same time periods. **** = $P < 0.001$.